8-2018

Multidentate Ligand Design for the F-Elements

Ashleigh Kirstin Smith Sockwell
Clemson University, aksockwell@gmail.com

MULTIDENTATE LIGAND DESIGN FOR THE *F*-ELEMENTS

A Dissertation
Presented to
the Graduate School of
Clemson University

In Partial Fulfillment
of the Requirements for the Degree
Doctor of Philosophy
Chemistry

---

by
Ashleigh Kirstin Smith Sockwell
August 2018

Accepted by:
Brian Powell, Committee Chair
Modi Wetzler
Bill Pennington
Shiou-Jyh Hwu
Lindsay Shuller-Nickles

ABSTRACT

The wide use of the *f*-elements, including nuclear weapons, nuclear energy and radiopharmaceuticals, has led to the growing unwanted accumulation of the lanthanides and actinides in the environment. The removal of these metals requires the design of highly selective ligands that take advantage of their complex chemistry (wide degree of covalency and high coordination numbers). Additionally, the environments these metals are typically being removed from involve a complicated mixture of other metals and strong counterions. Ligand design for the *f*-elements requires high selectivity and the formation of stable complexes in a wide range of environments.

Ethylene diamine tetraacetic acid (EDTA) is one of the most well-known and widely utilized ligands in coordination chemistry, and hydroxamate-containing ligands are some of the most common in biological chemistry, suggesting a natural combination of EDTA-like backbones with hydroxamate arms. Specifically, the increase from the hexadentate EDTA to the decadentate hydroxamate analog would address the larger coordination numbers of the *f*-elements. EDTA, however, is too small even for Fe(III), leaving a coordinated water on the Fe, and is far too small for Ln/An(III) ions. Consequently, I synthesized a hydroxamate EDTA analog where the arms are longer by one carbon (ethylenediamine tetrapropionyl hydroxamic acid, EDTPHA). Potentiometric titrations of EDTPHA with La(III), Eu(III), and Lu(III), and a comparison with a synthetic all-carboxylate analog (EDTP) reveal that EDTPHA is powerful ligand for lanthanides competitive with EDTA.

During the course of the work I developed a new protecting group for use in hydroxamate synthesis, and the straightforward synthesis of the EDTPHA ligand (utilizing highly pure aza-Michael chemistry) enables future work with additional ligands including EDTA-like ligands as well as siderophore-like peptide ligands to optimize their selectivity for *f*-element chemistry.

DEDICATION

This work is dedicated to the many teachers who sparked my interest in pursuing knowledge throughout my academic career.

Without the support of the many friends and colleagues I have met at Clemson, I would not have survived this degree. I also truly appreciate the many discussions shared with my group members (past and present).

The never-ending support of my parents has been instrumental in my growth as a person and scientist. Without their constant pushing, I would never have realized the type of person I could become.

Finally, I cannot express enough appreciation for my husband, who deserves this degree as much as I do.

ACKNOWLEDGMENTS

I would like to thank Dr. Modi Wetzler, for his direction and encouragement throughout the course of this work. Without his mentoring, I would not have become the scientist I am today.

I would also like to than Dr. Brian Powell for his role in my graduate work. His support for all things engineering allowed me to expand outside of a strictly chemistry world.

I would also like to thank all members of my committee for their input and time. Lastly, I want to express thanks to the many undergraduate students who worked on various parts of this project.

TABLE OF CONTENTS

Page

Table of Contents (Continued) Page

LIST OF TABLES

LIST OF FIGURES

List of Figures (Continued)

Figure Page

List of Figures (Continued)

List of Figures (Continued)

LIST OF SCHEMES

List of Schemes (Continued)

Scheme Page

List of Schemes (Continued)

CHAPTER ONE

BEYOND BIOLOGICAL CHELATION: *F*-ELEMENT COORDINATION BY POLYHYDROXAMATE LIGANDS

Abstract: The promise of polyhydroxamic acid ligands for the selective chelation of the *f*-elements is becoming increasingly more apparent. The initial studies of polyhydroxamic acid siderophores showed the formation of highly stable complexes with Pu(IV), but a higher preference for Fe(III) hindered effective applications. The development of synthetic routes toward highly pure and customizable ligands containing multiple hydroxamic acids allowed for the growth of new classes of compounds. While the first round of these ligands focused on the incorporation of siderophore-like frameworks, the new synthetic strategies led to small molecules of various frameworks and even resins for applications in the field of *f*-element separations and biological desorption. Unfortunately, a lack of consistent stability constant data makes direct comparisons across this body of work difficult. More studies into the stability constants and separations of the *f*-elements in a variety of pH ranges is necessary to truly realize the potential for polyhydroxamic acid ligands.

Introduction

The *f*-elements are utilized in a variety of applications, including nuclear weapons, nuclear energy and radiopharmaceuticals.[1–4] These applications, as well as the unwanted accumulation of lanthanides and actinides in the environment, necessitate advances in understanding and exploitation of their basic coordination chemistry. The *f*-elements display a broad range of oxidation states, wide degree of covalency, high coordination numbers, and variable coordination environments which make the area ripe for advances in ligand design.[1–3,5] Increased exposure of

the public to these metals, along with a growing demand for their availability by the technology and energy industries, require the design of highly selective ligands capable of the formation of stable complexes with the *f*-elements.[5–9]

Siderophores, biological scavengers primarily of iron(III), are strongly chelating polydentate ligands, often with preorganized binding pockets tuned for metal selectivity. Siderophores have often been used as the basis for actinide ligand design due to the similar charge/ionic radius ratio between iron(III) (4.2 *e*/Å) and plutonium(IV) (4.6 *e*/Å).[1,2,10,11] Ferrichrome (Figure 1.1), the first isolated and characterized siderophore, contains three bidentate hydroxamic acid moieties, making it a strong chelator of the ferric ion. Consequently, hydroxamic acids have long been investigated as potent actinide ligands.[2,11,12]

Siderophores provide high affinity and selectivity, enabling separation of metal ions from other metals or coordinating ions, as well as the removal of metals from complex environments, such as groundwater or biological systems. Such selectivity could prove highly advantageous in controlling the complicated chemistry of the *f*-elements in their array of applications. This article introduces the hydroxamic acid functional group and the naturally-occurring polyhydroxamic acid-containing siderophores, then reviews some of the polyhydroxamic ligands that have been reported and their uses with the *f*-elements.

Hydroxamic acids

The hydroxamic acid (HA) class of compounds was discovered in 1869 by H. Lossen's study of the reaction between ethyl oxalate and hydroxylamine, producing oxalohydroxamic acid (Scheme 1).[13] Hydroxamic acids (HA), with the structure -RC(O)NHOH, are bidentate analogs of the biologically/environmentally ubiquitous monodentate carboxylates (-RC(O)OH). However, a

lack of understanding of the structure of hydroxamic acids in solution hindered developmental research until the mid-20th century, when multiple HA-containing siderophores were isolated.[14] Two siderophores of note, the linear desferrioxamine (DFOB, Figure 1.1) and the cyclic ferrichrome, both contain three HA residues, making them powerful iron chelators.[15–18]

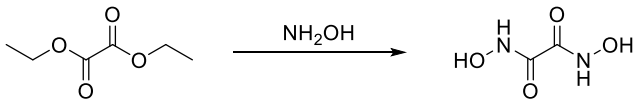

Scheme 1.1. Reaction of ethyl oxalate and hydroxylamine to form oxalohydroxamic acid.[19]

N-acylated hydroxylamines, more commonly called hydroxamic acids, are known to exist in two distinct tautomeric forms, the keto and enol form (Scheme 2). The keto form is believed to predominate in solid and solution state.[13,20–22] Hydroxamic acids are weakly acidic, primarily due to the -OH group (pKa 8-9). They are weaker acids than their corresponding carboxylic acids (pKa 4-5), but more acidic than the amides (pKa 20-22).[23,24]

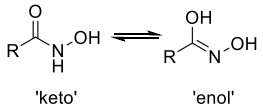

Scheme 1.2. Possible protonated forms of hydroxamic acid.

Hydroxamic acids are capable of acting as mono- or bidentate ligands through the oxygen atoms, but can more rarely also act as monodentate ligands through the nitrogen atom, if unsubstituted.[18,25] The loss of a proton from the hydroxy group, followed by a ring closing by the carbonyl allows for the formation of a stable five-membered metallacycle during metal coordination.[26] Some metal-HA complexes are highly colored and have been used in the spectrophotometric and gravimetric analysis of the involved metals.[25–27] Due to the neutral charge

of many hydroxamate-metal complexes, they can be extracted from aqueous systems by many immiscible organic solvents.[26,28,29]

Siderophores

Siderophores are low molecular weight, iron(III) chelators synthesized by microorganisms in low-iron environments, containing, most commonly, catecholate or hydroxamate groups. They help solubilize iron oxides and transport the resultant iron ions into microorganism cells. The high stability of the Fe(III)-siderophore complexes complicates the dissociation of the Fe(III) for use in the cell. There are several known pathways, which are typically specific to the siderophore involved. These pathways typically involve membrane-recognition of the complex and subsequent transport into the cell, where a change in environment is involved in the dissociation of the Fe(III) ion, or reductive actions at the cell membranes.[30–34]

The coordination of Fe(III) by hydroxamic acid-containing siderophores leads to similar coordination properties as when Fe(III) is bound by three unlinked hydroxamates. In both cases, the Fe(III) core is bound in an octahedral geometry and is high-spin, thermodynamically stable, and labile. The hydroxamic acid moieties form stable, five-membered rings with the Fe(III) ion through primarily electrostatic interactions.

Ferrichrome binds Fe(III) with a stability constant about ten times that of EDTA and is highly selective for the Fe(III) ion.[17] Synthetic analogs of ferrichrome and DFO have been heavily studied for possible medicinal applications.[35–38] Desferal, desferrioxamine mesylate (DFOM), was approved by the FDA in the mid-20th century for the treatment of iron overload and thalassemia. Desferal helps solubilize biological iron(III), which is then excreted from the body. However,

Desferal is not orally active and requires prolonged intravenous delivery, drastically decreasing its efficacy at the removal of iron(III) from the body.[39–42]

The difficulty of cyclizing peptides has hindered the synthesis of peptide analogs of ferrichrome. Another major roadblock was the difficult synthesis of high purity hydroxamate-containing building blocks due to incomplete conversion of starting materials, such as carboxylic acids and subsequent characterization difficulties. One attempt at circumscribing this issue was performed by Maurer *et al.*, who utilized *O*-benzylhydroxylamines and subsequent alkylation of the amine in the hydroxamic acid to prevent unwanted side products from forming.[43,44]

New approaches to the treatment of iron overload diseases were realized through the use of synthetic siderophores.[45,46] Traditionally, these synthetic compounds were designed around the common subunits found in the naturally occurring siderophores. For example, several synthetic ferrichrome analogues have been reported.[32,35,36,47–49] The analogues are related by the inclusion of three hydroxamic acid groups bridging from a central backbone. Compounds such as BAMTPH[50] and MEDROX[46] utilize a rigid tri-substituted benzene backbone, while others, such as TRENDROX[46], TAGP, and TAGE[51,52] utilize a more flexible TREN anchor. Recent work by Crumbliss and coworkers showed a saccharide backbone was effective in the synthesis of ferrichrome mimics.[32,53] Control of the backbone or anchor allows for direct control over the tuning of the binding pocket of the hydroxamic acid groups.[35,51] Many studies have shown that the backbone does not directly affect the chelation ability of these siderophore analogues, so much research has focused more on the hydroxamate arms and the terminal groups (*e.g.* substituted versus unsubstituted hydroxamate units).[35–37,54–57]

Siderophore analogues

The development of synthetic siderophores allowed for a wide variety of well-studied ligand scaffolds to be tuned for the coordination of specific metals, such as Pu(IV). DFOM was an early attempt for chelation therapy in case of Pu(IV) contamination (Figure 1.1).[2] However, DFOM removal of Pu(IV) from plasma proteins *in vivo* proved to be similarly as effective as DTPA. Metabolic destruction and rapid renal clearance prevented DFOM from being more effective.[58–60] Further investigation showed DFOM to be an ineffective chelator of trivalent actinides and lanthanides.[59,60]

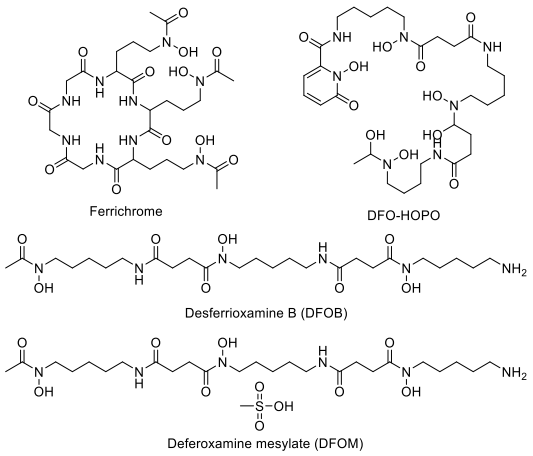

Figure 1.1. Structures of naturally occurring trihydroxamate-containing siderophores, ferrichrome, desferrioxamine E (DFOE), desferrioxamine B (DFOB), and deferoxamine mesylate (DFOM).

Flow-injection ESI-MS (FI-ESI-MS) was used to investigate the affinity of ferrichrome and DFOB for Th(IV). Ferrichrome was five times more effective at Th(IV) coordination than DFOB. The inverse was measured for Fe(III). More interestingly, when in the presence of Fe(III) or a cation-exchange method, the Th(IV) core was rapidly exchanged. Desporption of the Th(IV) in the presence of anionic binding sites suggests a possible route toward Th(IV) impediment in

environmental conditions through adsorption onto anionic binding sites, such as anionic minerals. This finding demonstrated that the presence of siderophores in soil conditions does not necessarily lead to increased mobility of Th(IV) ions due to its preference for interaction with anionic sorbents over the siderophore framework, specifically DFO in this case.[61]

The presence of siderophores with affinity for Pu(IV) or other potentially toxic metals can drastically affect their bioavailability, solubility and accumulation in soil and groundwater.[9,62,63] Siderophores, ferrioxamines in particular, are estimated to be found in soils at concentrations from 0.01-0.1 μM.[62,63] The Pu(IV)-DFOB complex was shown to be taken up into the bacteria *Microbacterium flavenscens* by the same recognition mechanism as the Fe(III)-DFOB complex. The two metals were also shown to be in competition for binding sites in the uptake proteins.[64] DFOM and pyoverdine siderophore, a mixed catechol/hydroxamic acid siderophore, were shown to bind Th(IV), U(VI) and Pu(IV) through the dissolution of spent nuclear fuel pellets.[65] DFOB and the tetrahydroxamate analogue DFO-HOPO (Figure 1.1) were investigated for their ability to prevent the adsorption of Pb(II) and Eu(III) onto goethite and boehmite through the solubilization of the metal ions. The high specificity of DFOB for Th(IV) (logK=30.6) and Pu(IV) (logK=38.8) combats the coordination of competitive metals (e.g. Ca^{2+}).[66]

Small molecules

The larger radii of the *f*-elements allow for higher coordination numbers (8-12) than are seen with the transition metals. For this reason, the bidentate hydroxamic acid moiety shows high affinity for the *f*-elements, as seen through the studies of naturally-occurring siderophores and Pu(IV). However, the structural limitations of natural siderophores (e.g. ferrichrome and desferrioxamine), combined with difficult synthesis of direct analogues, led researchers to focus investigation on the incorporation of HA binding moieties into various commercially available

backbones. Both aliphatic and aromatic (1,2-HOPO, Figure 1.2) hydroxamic acids in a multitude of backbones have been heavily studied with the lanthanides and actinides.

Motekaitis, Murase and Martell published the synthesis of *N,N'*-ethylenediaminediacetic-*N,N'*-diacethydroxamic acid (EDTA-DX, **I**) and potentiometric titrations with Mg(II), Fe(III), Co(II), Ni(II), Cu(II) and Zn(II).[67] Later, Martell *et al*. published work with a trihydroxamate ligand, *N,N',N''*-tris[2-*N*-hydroxycarbamoyl)ethyl]-1,3,5-benzenetricarboxamide (BAMPTH, **XII**). This ligand featured three hydroxamic acid residues on a benzene backbone. Potentiometric titrations with Fe(III), Co(II), Ni(II), Cu(II), Zn(II), Ga(III) and Al(III) showed that with trivalent metals, all three arms interacted during bonding, but with divalent metals, only two arms interacted.[50] The lack of chelate effect with these polyhydroxamic acids was also noted, in agreement with previous work by Raymond and Schwarzenbach.[31,57] The tetrahydroxamate derivative of EDTA **(II)** was reported by Karlicek and Majer in 1972. This ligand was shown to preferentially form a 1:1 complex with Cu(II) and Fe(III) despite variations of ligand:metal ratios, also demonstrating the lack of chelate effect noted by Schwarzenbach.[68]

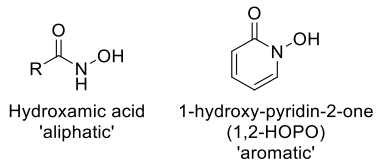

Figure 1.2. Structure of aliphatic and aromatic hydroxamic acid moiety.

Table 1.1. Stability constant data for ligands XI and III (n=4,6,7,8).[69]

			III			
	Reaction	**XI**	n=4	n=6	n=7	n=8
H^+	$[HL]/[H^+][L]$	10.04	9.38	9.61	9.65	9.52
	$[H_2L]/[HL][H^+]$	9.33	8.81	8.92	9.02	8.82
	$[H_3L]/[H_2L^+][H^+]$	8.48				
Fe(III)	[ML]/[M][L]	26.32	17.60	18.01	20.08	20.30
La(III)	[ML]/[M][L]	14.42	9.01	9.59	9.98	10.33
Nd(III)	[ML]/[M][L]	16.70				
Yb(III)	[ML]/[M][L]	18.08				
Th(IV)	[ML]/[M][L]		16.36			18.44
UO_2^{2+}	[ML]/[M][L]		13.27	12.95	13.07	13.28
	[MHL]/[ML][H]		17.50	17.50	17.48	16.92
Pu(IV)	[ML]/[M][L]	30.0[b]				

[a] All data reported at 25°C and μ=0.1 $NaNO_3$. [b] Ref 70, this data did not keep constant ionic strength, preventing it from being added to the NIST database; however, it allows for extrapolation of the general trend discussed by Evers *et al*.[69]

Martell *et al.* suggested a linear relationship between the logK of ligands containing only negative oxygen atoms and the logK(OH) of the metal ions could be used to predict the affinity of metal ions for *O*-donor ligands. This linear relationship was shown to hold true for DFOB, BAMPTH, and a series of dihydroxamic acids with varying linker chains (C_nDHA, **III**). The study found that the stability of these complexes with only negative oxygen donors was closely linked to the affinity of metal ions for the hydroxide ion, leading to difficulty in altering observed selectivity of naturally occurring siderophores, other than through the introduction of sterically constrained groups or different donor groups, for example DFO-HOPO. They also reported that the maximum complex stability with DHA was reached with a chain length of eight methylene

groups (C_8DHA).[69] A subsequent study suggested the same relationship existed for the coordination of Pu(IV) by **IX**; however, lower standards of experimental design (for example, the ionic strength was not kept constant) require further study for accurate reporting of the calculated data. Despite these problems, the reported **IX**-Pu(IV) stability constant is listed in Table 1, reflecting an agreement with the original trend studied by Evers *et al*.[69,70]

While Martell did not expressly focus on coordination of the *f*-elements, the synthetic considerations developed through the synthesis of EDTA-DX and BAMPTH were applied to subsequent ligand development and study of the *f*-element complexes. Gopalan *et al.*[71,72] and Koshti *et al.*[73,74] investigated a new series of cost-effective tetrahydroxamic acid ligand, which utilized the straightforward aza-Michael reaction to produce a wide variety of ligands, with the goal of designing Pu(IV) selective ligands for waste extraction. An early ligand design utilized a meta- or para-substituted xylylenediamine backbone and four propyl hydroxamic acid residues **(IV and V)**. These ligands were designed with the goal of prearranging hydroxamic acid groups for optimal octadentate coordination of actinide ions, on an easily tunable backbone which incorporated amines for water solubility. Th(IV) and Nd(III) were studied as surrogates for Pu(IV) and Am(III) complexation. Both ligands showed similar affinity for Fe(III) and Th(IV) and lower affinity for Nd(III). However, **V** formed slightly stronger complexes with Fe(III) and Th(IV), most likely due to better preorganization for the formation of strong complexes (Table 2).[71] This line of research produced the CYTROX ligand **(VII)**, a cyclam-based ligand with much potential for actinide selectivity.[73] However, the stability of this ligand with a variety of metals was not studied. In 2000, Santos *et al*. published a similar ligand with aliphatic hydroxamic acids on a cyclohexane backbone, cyclohexane-1,2-diyldinitrilotetra(*N*-methylacetohydroxamic acid) (H_4CDTMAHA, **VI**) . This ligand was shown to form stronger complexes with Th(IV) and Fe(III) than the corresponding carboxylate analog, cyclohexane-1,2-diyl-dinitriletetraacetic acid

(H_4CDTA).[75] The authors also compared their data to **IV**. As can be seen in Table 2, **VI** formed slightly stronger complexes with Fe(III) and Th(IV) than **IV**, though they were comparable in selectivity.[71]

The aromatic 1,2-HOPO (Figure 1.2) based ligands were more heavily studied. Raymond *et al.* published the first Pu(IV)-HOPO crystal structure in 2005. However, this complex utilized the 3,2-HOPO (technically not a hydroxamate) binding moiety on either a TREN or LICAM-type backbone.[76] Previously, Raymond *et al*. had shown the effectiveness of 1,2-HOPO as a Pu(IV) extractant from nitric acid solutions.[77] In 2011, the same group published the synthesis of a mixed donor ligand consisting of a TAM (2,3-dihydroxyterephthalamide) backbone and two terminal HOPO groups **(X).** This TAM$(HOPO)_2$ ligand was capable of fully coordinating the equatorial plane of the actinyl ($AnO_2^{+/2+}$) ion in a distorted octadentate geometry. The first two protonation constants (Table 2) represent the deprotonation of the 1,2-HOPO moieties, followed by the deprotonation of the TAM group. At pH 3, the 1,2-HOPO groups had fully coordinated with the uranyl ion.[78]

Dasaradhi *et al*. investigated a tetrahydroxamic acid derivative of calixarenes, assuming the highly preorganized backbone would lend the ligand toward high stability with metal ions **(IX)** and provide an effective method for solvent extraction of Pu(IV). Solvent extraction studies using Th(IV) as a Pu(IV) surrogate, Fe(III), Cu(II) and UO_2^{2+} showed **IX** was capable of extracting Th(IV) (95-100%) and Fe(III) (98-99%) into a chloroform layer at low pH (1-2) and unable to extract Cu(II) and UO_2^{2+} until higher pH (4-6). The hydroxamate and *N*-substituted hydroxamate ligands were slightly more efficient in the extraction of Th(IV) than the corresponding carboxylate ligand. Despite a lack of selectivity toward Th(IV) in the presence of Fe(III), these

ligands hold potential as extractants for Th(IV) and Pu(IV) in the presence of UO_2^{2+} at low pH (1-2), typical of reprocessing of nuclear fuel.[79]

Table 1.2. Stability constant data for ligands IV, V, and VI.

Compound	Reaction	Fe(III) Logβ	Nd(III) Logβ	Th(IV) Logβ
IV[b]	[MLH]/[M][L][H]		25.54	39.65
	$[MLH_2]/[M][L][H]^2$		32.40	43.16
	$[MLH_3]/[M][L][H]^3$	43.41	37.04	45.92
	$[MLH_4]/[M][L][H]^4$	47.43		
V[b]	[MLH]/[M][L][H]		26.28	36.85
	$[MLH_2]/[M][L][H]^2$	40.50	32.78	42.13
	$[MLH_3]/[M][L][H]^3$	45.21	37.03	45.18
	$[MLH_4]/[M][L][H]^4$	48.70		48.28
VI[c]	[MLH]/[M][L][H]			30.0
	$[MLH_2]/[M][L][H]^2$			36.23
	$[MLH_3]/[M][L][H]^3$	46.39		41.99
	$[MLH_4]/[M][L][H]^4$	48.2		46.37

[a] All data reported at 25°C and μ=0.1 KNO_3. [b] Ref. 71. [c] Ref. 75. [d] Only stability constants with data for comparison were reported.

The 1,2-HOPO group has also been incorporated into siderophore analogues, such as DFO-HOPO.[80] This compound was compared with other multidentate hydroxamic acid ligands, such as 3,4,3-LI(1,2-HOPO) **(VIII)** and the dihydroxamate DTPA derivative, DTPA-DX.[81–83] All of these ligands were studied for their effectiveness at the removal of Pu-238 and Am-241 after inhalation and injection contamination routes. These ligands were also directly compared with the effectiveness of DTPA, the standard treatment for the removal of Pu(IV) and Am(III). **VIII** has been shown to be more effective in enhancing the excretion of Pu(IV) after exposure through injection and inhalation. For the removal of Pu(IV) from the lungs, a repeated dose of 30 $\mu mol/kg^{-1}$ of the ligand was capable of lowering the Pu(IV) content in the lungs and total body to

2% and 4% of the untreated controls, respectively. When treated with the same dosage of DTPA, the Pu content of the lungs and body were six times and three times more than with **VIII**.[81] Similar results were observed with the treatment of simulated contaminated wounds,[82] and the early treatment of Pu(IV) and Am(III) contamination (1 hour).[83] The 3,4,3-LI(1,2-HOPO) ligand has shown high promise as a decorporation agent for the removal of actinides from the body.

Table 1.3. Protonation constants of some polyhydroxamic acid ligands.

Compound	$\log K_{101}$	$\log K_{102}$	$\log K_{103}$	$\log K_{104}$	$\log K_{105}$	$\log K_{106}$
I	9.93[b]	9.00[b]	6.67[b]	3.48[b]	1.6[b]	
II	11.1[c]	10.6[c]	7.23[c]	6.05[c]	5.55[c]	1.55[c]
IV	10.18[d]	9.64[d]	8.99[d]	8.17[d]	6.38[d]	5.36[d]
V	10.22[d]	9.60[d]	9.05[d]	8.31[d]	6.40[d]	5.35[d]
VI	9.91[e]	8.88[e]	8.52[e]	7.80[e]	7.56[e]	6.42[e]
VIII	6.64[f]	5.68[f]	5.01[f]	3.87[f]		
X	4.91[g][h]	6.56[g][h]	8.7[g][h]	10.2[g][h]		
XI	10.04[i]	9.33[i]	8.48[i]	10.04[i]		

[a] All data reported at 25°C and μ=0.1 KNO_3. [b] Ref. 67. [c] Ref. 68. [d] Ref. 71. [e] Ref. 75 [f] Ref. 85. [g] R=ethylene, X=1,2-HOPO. [h] Ref. 78. [i] Ref. 50; Ref. 69.

The protonation constants of several polyhydroxamic acid ligands are listed in Table 3. This data shows how the reported ligands are deprotonated and thus, capable of interacting with metals at the typical desired pH range of environmental and biological conditions. Further comparison of the effectiveness of these ligands as *f*-element chelators is difficult, due to a lack of consistent data. While some stability constants have been published for these ligands (*e.g.* Table 2), Fe(III) and Cu(II) are typically the metals of choice. However, the affinity simple hydroxamic acids show for the *f*-elements is similarly demonstrated by the polyhydroxamic acid ligands which have

been reported. The ligands **IV, V, and VI** each demonstrate the ability to form strong complexes with Nd(III) and Th(IV), despite a lack of selectivity over Fe(III).

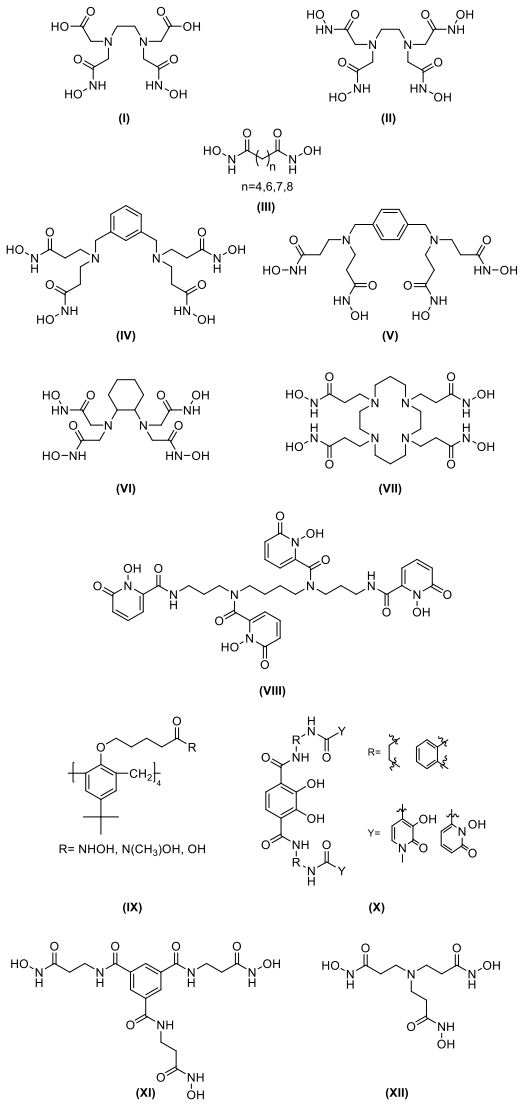

Figure 1.3. Structures of polyHA small molecules. (I) EDTA-DX,[84], (II) EDTPHA,[68] (III) DHA, [69] (IV) no abbreviation provided by the authors,[71] (V) no abbreviation provided by the authors,[71] (VI) H_4CDTMAHA,[75] (VII) CYTROX,[73] (VIII) 3,4,3-LI(1,2-HOPO),[81–83,85] (IX) Calix(HYD)$_4$,[79] (X) TAM(HOPO)$_2$,[78] (XI) BAMPTH,[50,69,70] (XII) no abbreviation provided by the authors.[86]

Polyhydroxamic acid resins

The desire to remove select metals from aqueous environments, along with the need for metal separations has driven the design of chelating polymers. Vernon published the necessary qualities of a chelating polymer, which include high capacity, high selectivity and high durability.[87] The high affinity of hydroxamic acids toward Pu(IV) as seen with siderophores demonstrated a promising group for functionalization of resins designed toward chelation of the *f*-elements. The initial driving force for the development of polymeric hydroxamic acids was to investigate potent iron(III) chelators for removal from the body and aqueous environments. The initial reported example was published by Deuel *et al* in 1954 and utilized a reaction between an acid chloride and hydroxylamine.[88,89]

Charles Fetscher published the synthesis of a polyhydroxamic acid-containing radioactive fuel source from a polyacrylonitrile through the hydrolysis of the amidoxime intermediate. The low molecular weight of the hydroxamic acid unit allowed for a high chelating capacity and could be formed into a strong, flexible fabric for use as a radioactive source. Fetscher suggested that the chelating ability of the polyhydroxamic acid would occur on the surface, allowing for control of the amount of metal chelation, up to about 50% by weight of the material.[95]

Petrie, Locke, and Meloan reported the synthesis of a polyhydroxamic acid-functionalized ion-exchange resin for metal separations, including V(V), Fe(II), Fe(III), Mo(VI), Ti(IV), Hg(II), Cu(II), UO_2^{2+}, and Ca(II). The authors theorized the inclusion of hydroxamic acids would allow for a gain of advantages over the corresponding resins functionalized with carboxylic acids, including higher selectivity and better separation of metal ions. A preliminary comparison of the carboxylic acid and hydroxamic acid funtionalized resins showed an increased elution volume for

several metals, including Fe(III) (1.5 mL), Cu(II) (0.5-1 mL), UO_2^{2+} (1 mL), and Ce(IV) (5 mL), demonstrating more interaction of certain metals with the hydroxamic acid resin than others.[90]

The conversion of poly(methyl methacrylate) to the corresponding polyhydroxamic acid product was reported in *N,N'*-dimethylformamide with an 80% conversion yield. This resin was modeled after the structure of DFOB. The authors determined that the spacing of the hydroxamic acid units was instrumental in the formation of strong iron(III) chelates, with the optimal spacing of nine atoms between units.[94,96] The DFOB framework was further investigated by Winston *et al*, who further investigated the effects of spacing of the hydroxamic acid units and their chelation efficiency for iron(III). A polymer containing hydroxamic acids side by side, HAP-1 (Figure 1.4), had a poor performance compared to DFOB due to the inability for units so close to keep iron(III) chelated in an octahedral geometry. However, the use of β-alanine in place of alanine allowed for 11-atom spacing between the units, HAP-II (Figure 1.4). The larger spacing allowed for similar chelating efficiency as DFOB. A smaller, more crowded polymer, HAP-III (Figure 1.4), showed a much lower affinity for Fe(III) consistent with the lack of the 8-9 atom spacers.[97] These results further confirm the importance of spacing between hydroxamic acid groups for metal chelation that was previously reported by Evers *et al.*[69]

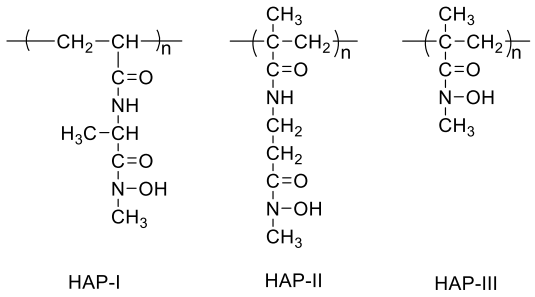

Figure 1.4. Structures of DFOB-inspired polyhydroxamic acid resins with varying spacing between hydroxamic acid units.[97]

The polymerization of an acrylonitrile-divinylbenzene copolymer, followed by hydrolysis and subsequent reaction of the polyamide with hydroxylamine, led to a promising polyhydroxamic acid ion-exchange resin which was investigated for removal of uranium from seawater. The authors were able to remove Fe(III) and U(VI) from seawater with 97-99% efficiency.[98] Selective absorption and desorption of metals through strict control of the pH allowed for the separation of U(VI) from a variety of trace metals utilizing a PHA resin bead system. The authors found the optimum pH for U(VI) adsorption to be 4 with a U(VI) capacity of 2.9 mmol/g, however at the relevant pH of seawater, 7.8, the resin had a capacity of 0.9 mmol/g. They were also able to discern that a contact time of 10-20 minutes between seawater samples and the resin was necessary for >50% extraction of the U(VI).[96]

Phillips and Fritz compared the efficiency of resins functionalized by hydroxamic acid, *N*-methylhydroxamic acid, and *N*-phenylhydroxamic acid with the extraction of nineteen metal ions as a function of pH and found the *N*-methyl resin had the highest metal capacity. This resin was shown to be effective at the removal of U(VI) (99-101%) from synthetic seawater samples at pH 7-8. They were also able to separate Th(IV) from U(VI) through the elution of the former by 3M HCl and the latter by 3M HCl and the addition of 0.1M oxalic acid.[99]

More recently, Agrawal and coworkers have explored a series of *N*-substituted polyacryloylhydroxamic acid ion-exchange resins (including *N*-phenyl, *N*-*p*-tolyl, *N*-*m*-tolyl, *N*-*o*-tolyl, *N*-*p*-chlorophenyl, *N*-*m*-chlorophenyl, *N*-*p*-bromophenyl and *N*-*p*-iodophenyl) which were synthesized from a reaction of polyacryloyl chloride and *N*-arylhydroxylamines to give 80-95% yields and strong coordination of divalent metals (Pb(II), Cu(II), Ni(II)).[91,92] Subsequent development of a synthetic route toward poly(β-sytryl)hydroxamic acids led to the study of a

series of new poly(styrene)hydroxamic acid resins (A and B, Figure 1.5) and their use in U(VI) and Ln(III) determination in rock and seawater samples (1-10 ppm).[93,100,101]

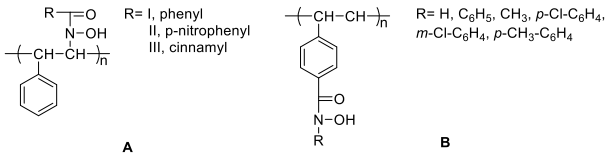

Figure 1.5. Structures of (A) poly(β-styrene)hydroxamic acid[100] and (B) poly(styrene-*p*-hydroxamic acid) resins.[101]

Mendez *et al* attached *N*-phenylhydroxamic acid to poly(styrene-co-maleic acid) cross-linked with divinylbenzene and studied the effects on extraction of ten metals, including Fe(III), Zn(II), and U(VI). The maximum sorption of U(VI) occurred at pH 4.5 with a capacity of 0.13 mmol/g resin and 50% maximum sorption after three minutes exposure time.[102] Rahman and coworkers developed a polyhydroxamic acid resin with a poly(methyl acrylate) grafted on a sago starch backbone and studied the chelation behavior with the trivalent lanthanides. The resin had a capacity for La(III) of 2.3 mmol/g resin at an optimal pH of 6. The resin selectivity toward the lanthanide metals followed the trend La(III) > Dy(III) > Pr(III) > Ce(III) > Nd(III) > Gd(III) > Eu(III) > Tb(III).[103,104]

The chelation effect of poly(amidoxime-hydroxamic acid) and poly(*N*-methyl amidoxime-*N*-methyl hydroxamic acid) resins toward the trivalent lanthanides was studied by Alakhras and coworkers. The authors noted that 90% of the metal uptake occurred after 2-3 hours and the resin capacity increased with decreasing ionic radii (Tb(III) > Gd(III) > Sm(III) > Nd(III) > La(III)), in agreement with previous literature involving simple hydroxamic acids and Ln(III), however the trend was opposite of that published by Rahman *et al*.[103,105] The authors did note that the inclusion

of the *N*-methyl group appeared to be beneficial to metal uptake, possibly due to higher stability constants of the hydroxamic acid-metal complexes.[105]

Polyhydroxamic acid resins show promise for the chelation of *f*-elements in aqueous systems. Although most studies have focused on the uptake of uranium from seawater or nuclear waste environments, these resins also hold potential as decorporation agents. Each system is dependent on the separation of different metals and different pH ranges, further complicating the overall comparison of work due to the lack of consistent studies and stability constants of the hydroxamic acid groups.

Conclusion

The research presented here covers a broad spectrum of the development of polyhydroxamic acid ligands and their potential as *f*-element chelators. Early hydroxamate chemistry involved several studies of the use of monohydroxamic acids for actinide chelation,[28,106,107] however the use of polyhydroxamic acid ligands grew in popularity with the discovery of siderophores such as ferrichrome and desferrioxamine due to the similarities of Fe(III) and Pu(IV) chemistries.[1,2,18]

Early attempts of siderophore analogs, such as DFOM, provided little advantage over traditional ligands (*e.g.* DTPA) when applied to Pu(IV) decorporation studies, due to a lack of selectivity and degradation *in vivo*.[58–60] The deviation from siderophore backbones and the consequent development of polyhydroxamic acid ligands with a variety of backbones has led to a variety of promising polydentate ligands for the coordination of *f*-elements.

Research into polyhydroxamic acid resins has also recently come to the limelight. Early work with these resins was hindered by the incomplete conversion to the desired hydroxamic acid unit

and the consequent by-products poisoning the chelate efficiency of the resin.[88–90,94,96] However, new methods have been developed utilizing acrylamides and amidoxime-hydroxamic acid combinations, providing higher conversion yields and promising methods for Ln(III)-Ln(III), Ln(III)-An(IV), and Ln(III)-transition metal separations.[91,100,101] Current efforts have focused on the development of resins for removal of Pu(IV) from carbonate solutions, such as those produced from the alkali washes of the PUREX process.[108]

While the field has far to go, the development of polyhydroxamic acids has produced many promising ligands for coordination of the *f*-elements. These ligands have potential for use in a variety of fields, including environmental remediation, biological decorporation and nuclear waste reprocessing.

Note: This chapter reflects an article accepted to *Chemistry-A European Journal* (July 2018).

This chapter discusses a narrow focus of f-element ligand design, hydroxamic acid ligands. However, it serves as an introduction to the overall goal of this dissertation, the development of highly selective ligands for the f-elements with the ability to form stable metal complexes in competitive environments. Three approaches toward this goal were taken, including azamacrocycles, cyclopeptoids and polyhydroxamate EDTA derivatives. Each approach utilized the same considerations discussed above for the design of f-element ligands, ligand topology, multidentate binding capability, and strong coordination of the target metals.

(1) Kaltsoyannis, N.; Scott, P. *The F Elements*; Oxford University Press, 1999.

(2) Gorden, A. E. V.; Xu, J.; Raymond, K. N.; Durbin, P. Rational Design of Sequestering Agents for Plutonium and Other Actinides. *Chemical Reviews* **2003**, *103*, 4207–4282.

(3) Silverio, L. B.; Lamas, W. de Q. An Analysis of Development and Research on Spent Nuclear Fuel Reprocessing. *Energy Policy* **2011**, *39*, 281–289.

(4) Silva, R. J.; Nitsche, H. Actinide Environmental Chemistry. *Radiochimica Acta* **1995**, *70–71* (Supplement), 377–396.

(5) Hirano, S.; Suzuki, K. T. Exposure, Metabolism, and Toxicity of Rare Earths and Related Compounds. *Environmental Health Perspectives* **1996**, *104*, 85–95.

(6) Deblonde, G. J.-P.; Sturzbecher-Hoehne, M.; Mason, A. B.; Abergel, R. J. Receptor Recognition of Transferrin Bound to Lanthanides and Actinides: A Discriminating Step in Cellular Acquisition of f-Block Metals. *Metallomics* **2013**, *5* (6), 619–626.

(7) Tian, G.; Teat, S. J.; Zhang, Z.; Rao, L. Sequestering Uranium from Seawater: Binding Strength and Modes of Uranyl Complexes with Glutarimidedioxime. *Dalton Transactions* **2012**, *41*, 11579–11586.

(8) Davies, R. V.; Kennedy, J.; McIlroy, R. W.; Spence, R. Extraction of Uranium from Sea Water. *Nature* **1964**, *203*, 1110–1115.

(9) Maher, K.; Bargar, J. R.; Brown Jr, G. E. Environmental Speciation of Actinides. *Inorganic Chemistry* **2012**, *52* (7), 3510–3532.

(10) Gopalan, A. S.; Jacobs, H.; Koshti, N. M.; Stark, P.; Huber, V.; Dasaradhi, L.; Caswell, W.; Smith, P. H.; Jarvinen, G. Synthesis and Evaluation of Polyhydroxamate Chelators for Selective Actinide Ion Sequestration. In *5th Annual WERC Technology Development Conference*; Las Cruces, NM, 1995; pp 77–98.

(11) O'Boyle, N. C.; Nicholson, G. P.; Piper, T. J.; Taylor, D. M.; Williams, D. R.; Williams, G. A Review of Plutonium(IV) Selective Ligands. *Applied Radiation and Isotopes* **1997**, *48* (2), 183–200.

(12) Whisenhunt, D. W.; Neu, M. P.; Hou, Z.; Xu, J.; Hoffman, D. C.; Raymond, K. N. Specific Sequestering Agents for the Actinides. 29. Stability of the Thorium(IV) Complexes of Desferrioxamine B (DFO) and Three Octadentate Catecholate or Hydroxypyridinonate DFO Derivatives: DFOMTA, DFOCAMC, and DFO-1,2-HOPO. Comparative Stability of The. *Inorganic Chemistry* **1996**, *35* (14), 4128–4136.

(13) Yale, H. L. The Hydroxamic Acids. *Chemical Reviews* **1943**, *33* (1), 209–256.

(14) Sandler, S. R.; Karo, W. Hydroxamic Acids. In *Organic Functional Groups Preparations Volume III*; Blomquist, A. T., Wasserman, H., Eds.; Academic Press: New York, 1989; pp 482–522.

(15) Hider, R. C.; Kong, X. Chemistry and Biology of Siderophores. *Natural Product Reports* **2010**, *27* (5), 637.

(16) Neilands, J. B. A Crystalline Organo-Iron Pigment from a Rust Fungus (Ustilago Sphaerogena). *Journal of the American Chemical Society* **1952**, *74*, 4846–4847.

(17) Neilands, J. B. Some Aspects of Microbial Iron Metabolism. *Bacteriological Reviews* **1957**, *21* (2), 101–111.

(18) Neilands, J. B. Hydroxamic Acids in Nature. *Science* **1967**, *156* (3781), 1443–1447.

(19) Lossen, H. Ueber Die Oxalohydroxamsaure. *Justus Liebigs Ann. Chem.* **1869**, *150*, 314–322.

(20) Plapinger, R. E. Ultraviolet Absorption Spectra of Some Hydroxamic Acids and Hydroxamic Acid Derivatives. *Journal of Organic Chemistry* **1958**, *24*, 802–804.

(21) Bauer, L.; Exner, O. The Chemistry of Hydroxamic Acids and N-Hydroxyimides. *Angewandte Chemie* **1974**, *13* (6), 376–384.

(22) Steinberg, G. M.; Swidler, R. The Benzohydroxamate Anion. *Journal of Organic Chemistry* **1965**, *30*, 2362–2365.

(23) Knapp, D. R. Nitrogen Functional Groups Other than the Amino Group. In *Handbook of Analytical Derivatization Reactions*; Wiley: New York, 1979; pp 350–372.

(24) Abualreish, M. J. A.; Abdein, M. A. The Analytical Applications And Biological Activity of Hydroxamic Acids. *Journal of Advances in Chemistry* **2014**, *10* (1), 2117–2125.

(25) Kakkar, R. Theoretical Studies on Hydroxamic Acids. In *Hydroxamic Acids: A Unique Family of Chemicals with Multiple Biological Activities*; Gupta, S. P., Ed.; Springer-Verlag: Berlin, 2013; pp 19–53.

(26) Agrawal, Y. K. Hydroxamic Acids and Their Metal Complexes. *Russian Chemical Reviews* **1979**, *48* (10), 948–963.

(27) Chatterjee, B. Donor Properties of Hydroxamic Acids. *Coordination Chemistry Reviews* **1978**, *26* (3), 281–303.

(28) Barocas, A.; Baroncelli, F.; Biondi, G. B.; Grossi, G. The Complexing Power of Hydroxamic Acids and Its Effect on Behaviour of Organic Extractants in the Reprocessing of Irradiated Fuels II: The Complexes Between Benzohydroxamic Acid and Thorium,

Uranium(IV) and Plutonium(IV). *Journal of Inorganic and Nuclear Chemistry* **1966**, *28*, 2961–2967.

(29) Baroncelli, F.; Grossi, G. The Complexing Power of Hydroxamic Acids and Its Effect on the Behaviour of Organic Extractants in the Reprocessing of Irradiated Fuels I: The Complexes Between Benzohydroxamic Acid and Zirconium, Iron(III) and Uranium(VI). *Journal of Inorganic and Nuclear Chemistry* **1965**, *27*, 1085–1092.

(30) Renshaw, J. C.; Robson, G. D.; Trinci, A. P. J.; Wiebe, M. G.; Livens, F. R.; Collison, D.; Taylor, R. J. Fungal Siderophores: Structures, Functions and Applications. *Mycological Research* **2002**, *106* (10), 1123–1142.

(31) Raymond, K. N.; Carrano, C. J. Coordination Chemistry and Microbial Iron Transport. *Accounts of Chemical Research* **1979**, *12*, 183–190.

(32) Dhungana, S.; Heggemann, S.; Gebhardt, P.; Möllmann, U.; Crumbliss, A. L. Fe(III) Coordination Properties of a New Saccharide-Based Exocyclic Trihydroxamate Analogue of Ferrichrome. *Inorganic Chemistry* **2003**, *42* (1), 42–50.

(33) Kuma, K.; Tanaka, J.; Matsunaga, K. Effect of Natural and Synthetic Organic-Fe(III) Complexes in an Esturaine Mixing Model on Iron Uptake and Growth of a Coastal Marine Diatom, Chaetoceros Sociale. *Marine Biology* **1999**, *134* (6), 761–769.

(34) Hartmann, A.; Braun, V. Iron Transport in Escherichia Coli: Uptake and Modification of Ferrichrome. *Journal of Bacteriology* **1980**, *143* (1), 246–255.

(35) Tor, Y.; Libman, J.; Shanzer, A. Biomimetic Ferric Ion Carriers. Chiral Ferrichrome Analogs. *Journal of the American Chemical Society* **1987**, *109* (21), 6518–6519.

(36) Shanzer, A.; Libman, J.; Lazar, R.; Tor, Y.; Emery, T. Synthetic Ferrichrome Analogues with Growth Promotion Activity for Arthrobacter Flavescens. *Biochemical and Biophysical Research Communications* **1988**, *157* (1), 389–394.

(37) Shanzer, A.; Libman, J. Synthetic Siderophores as Biological Probes. *Biology of Metals* **1989**, *2* (3), 129–134.

(38) Johnstone, T. C.; Nolan, E. M. Beyond Iron: Non-Classical Biological Functions of Bacterial Siderophores. *Dalton Transactions* **2015**, *44* (14), 6320–6339.

(39) Halliwell, B. Protection against Tissue Damage in Vivo by Desferrioxamine: What Is Its Mechanism of Action? *Free Radical Biology and Medicine* **1989**, *7* (6), 645–651.

(40) Modell, B.; Letsky, E. A.; Flynn, D. M.; Peto, R.; Weatherall, D. J. Survival and Desferrioxamine in Thalassaemia Major. *British Medical Journal* **1982**, *284* (6322),

1081–1084.

(41) Mclaren, G. D.; Muir, W. A.; Kellermeyer, R. W.; Jacobs, A. Iron Overload Disorders: Natural History, Pathogenesis, Diagnosis, and Therapy. *Critical Reviews in Clinical Laboratory Sciences* **1983**, *19* (3), 205–266.

(42) Liu, Z. D.; Hider, R. C. Design of Iron Chelators with Therapeutic Application. *Coordination Chemistry Reviews* **2002**, *232* (1–2), 151–171.

(43) Maurer, P. J.; Miller, M. J. Microbial Iron Chelators: Total Synthesis of Aerobactin and Its Constituent Amino Acid, N6-Acetyl-N6-Hydroxylysine. *Journal of the American Chemical Society* **1982**, *104* (11), 3096–3101.

(44) Maurer, P. J.; Miller, M. J. Total Synthesis of a Mycobactin: Mycobactin S2. *Journal of the American Chemical Society* **1983**, *105* (2), 240–245.

(45) Rodgers, S. J.; Lee, C. W.; Ng, C. Y.; Raymond, K. N. Ferric Ion Sequestering Agents. 15. Synthesis, Solution Chemistry, and Electrochemistry of a New Cationic Analogue of Enterobactin. *Inorganic Chemistry* **1987**, *26* (10), 1622–1625.

(46) Ng, C. Y.; Rodgers, S. J.; Raymond, K. N. Ferric Ion Sequestering Agents. 21. Synthesis and Spectrophotometric and Potentiometric Evaluation of Trihydroxamate Analogues of Ferrichrome. *Inorganic Chemistry* **1989**, *28* (11), 2062–2066.

(47) Ramasamy, K.; Olsen, R. K.; Emery, T. Synthesis of a Retrohydroxamate Analogue of the Iron-Binding Ionophoric Peptide Ferrichrome. In *Peptides, structure and function: Eighth American Peptide Symposium*; 1983; pp 187–190.

(48) Emery, T.; Emery, L.; Olsen, R. K. Retrohydroxamate Ferrichrome, A Biomimetic Analogue of Ferrichrome. *Biochemical and Biophysical Research Communications* **1984**, *119* (3), 1191–1197.

(49) Olsen, R. K.; Ramasamy, K. Synthesis of Retrohydroxamate Analogues of the Microbial Iron-Transport Agent Ferrichrome. *Journal of Organic Chemistry* **1985**, *50*, 2264–2271.

(50) Yoshida, I.; Murase, I.; Motekaitis, R. J.; Martell, A. E. New Multidentate Ligands. XXI. Synthesis, Proton, and Metal Ion Binding Affinities of N,N′,N″-Tris[2-(N-Hydroxycarbamoyl)Ethyl]-1,3,5-Benzenetricarboxamide (BAMTPH). *Canadian Journal of Chemistry* **1983**, *61* (12), 2740–2744.

(51) Matsumoto, K.; Suzuki, N.; Ozawa, T.; Jitsukawa, K.; Masuda, H. Crystal Structure and Solution Behavior of the Iron(III) Complex of the Artificial Trihydroxamate Siderophore with a Tris(3-Aminopropyl)Amine Backbone. *European Journal of Inorganic Chemistry*

2001, *6*, 2481–2484.

(52) Matsumoto, K.; Ozawa, T.; Jitsukawa, K.; Einaga, H.; Masuda, H. Crystal Structure and Redox Behavior of a Novel Siderophore Model System: A Trihydroxamato-Iron(III) Complex with Intra- and Interstrand Hydrogen Bonding Networks. *Inorganic Chemistry* **2001**, *40* (2), 190–191.

(53) Dhungana, S.; Harrington, J. M.; Gebhardt, P.; Möllmann, U.; Crumbliss, A. L. Iron Chelation Equilibria, Redox, and Siderophore Activity of a Saccharide Platform Ferrichrome Analogue. *Inorganic Chemistry* **2007**, *46* (20), 8362–8371.

(54) Monzyk, B.; Crumbliss, A. L. Mechanism of Ligand Substitution on High Spin Iron(III) by Hydroxamic Acid Chelators. Thermodynamic and Kinetic Studies on the Formation and Dissociation of a Series of Monohydroxamatoiron (III) Complexes. *Journal of the American Chemical Society* **1979**, *101* (21), 6203–6213.

(55) Crumbliss, A. L. Iron Bioavailability and the Coordination Chemistry of Hydroxamic Acids. *Coordination Chemistry Reviews* **1990**, *105*, 155–179.

(56) Crumbliss, A. L.; Harrington, J. M. *Iron Sequestration by Small Molecules: Thermodynamic and Kinetic Studies of Natural Siderophores and Synthetic Model Compounds*; Elsevier, 2009; Vol. 61.

(57) Schwarzenbach, G.; Schwarzenbach, K. Hydroxamate Complexes. I. The Stabilities of the Iron(LlI) Complexes of Simple Hydroxamic Acids and Desferriferrioxamin B. *Helvetica Chimica Acta* **1963**, *46* (4), 1390–1400.

(58) Rosenthal, M. W.; Lindenbaum, A. Effect of Deferrioxamine B Methanesulfonate on Removal of Plutonium in Vitro and in Vivo. In *Proceedings of the Society for Experimental Biology and Medicine*; New York, 1964; Vol. 117, pp 749–750.

(59) Taylor, D. M. The Effects of Desferrioxamine on the Retention of Actinide Elements in the Rat. *Health Physics* **1967**, *13*, 135–140.

(60) Nigrovic, V.; Catsch, A. Incorporation of Radionuclides. Comparative Investigation of Deferrioxamine B and Diethylenetriaminopentaacetic Acid. *Strahlentherapie* **1965**, *128* (2), 283–287.

(61) Keith-Roach, M. J.; Buratti, M. V.; Worsfold, P. J. Thorium Complexation by Hydroxamate Siderophores in Perturbed Multicomponent Systems Using Flow Injection Electrospray Ionization Mass Spectrometry. *Analytical Chemistry* **2005**, *77* (22), 7335–7341.

(62) Neu, M. P.; Matonic, J. H.; Ruggiero, C. E.; Scott, B. L. Structural Characterization of a Plutonium(IV) Siderophore Complex: Single-Crystal Structure of Pu-Desferrioxamine E. *Angewandte Chemie - International Edition* **2000**, *39* (8), 1442–1444.

(63) Boukhalfa, H.; Reilly, S. D.; Neu, M. P. Complexation of Pu(IV) with the Natural Siderophore Desferrioxamine B and the Redox Properties of Pu(IV)(Siderophore) Complexes. *Inorganic Chemistry* **2007**, *46* (3), 1018–1026.

(64) John, S. G.; Ruggiero, C. E.; Hersman, L. E.; Tung, C. S.; Neu, M. P. Siderophore Mediated Plutonium Accumulation by Microbacterium Flavescens (JG-9). *Environmental Science and Technology* **2001**, *35* (14), 2942–2948.

(65) Johnsson, A.; Ödegaard-Jensen, A.; Skarnemark, G.; Pedersen, K. Leaching of Spent Nuclear Fuel in the Presence of Siderophores. *Journal of Radioanalytical and Nuclear Chemistry* **2009**, *279* (2), 619–626.

(66) Kraemer, S. M.; Xu, J.; Raymond, K. N.; Sposito, G. Adsorption of Pb(II) and Eu(III) by Oxide Minerals in the Presence of Natural and Synthetic Hydroxamate Siderophores. *Environmental Science and Technology* **2002**, *36* (6), 1287–1291.

(67) Motekaitis, R. J.; Murase, I.; Martell, A. E. New Multidentate Ligands XII: Chelating Tendencies of N,N'-Ethylenediaminediacetic-N,N'-Diacethydroxamic Acid. *Journal of Coordination Chemistry* **1971**, *1*, 77–87.

(68) Karlicek, R.; Majer, J. Neue Komplexane XXIII. Athylediamin-N,N,N',N'-Tetraacethydroxamsaure. *Collection of Czechoslovak Chemical Collections* **1972**, *37*, 805–818.

(69) Evers, A.; Hancock, R. D.; Martell, A. E.; Motekaitis, R. J. Metal Ion Recognition in Ligands with Negatively Charged Oxygen Donor Groups. Complexation of Fe(III), Ga(III), In(III), Al(III), and Other Highly Charged Metal Ions. *Inorganic Chemistry* **1989**, *28* (11), 2189–2195.

(70) Jarvis, N. V.; Hancock, R. D. Some Correlations Involving the Stability of Complexes of Transuranium Metal Ions and Ligands with Negatively Charged Oxygen Donors. *Inorganica Chimica Acta*. 1991, pp 229–232.

(71) Gopalan, A. S.; Huber, V. J.; Zincircioglu, O.; Smith, P. H. Novel Tetrahydroxamate Chelators for Actinide Complexation: Synthesis and Binding Studies. *Journal of the Chemical Society, Chemical Communications* **1992**, No. 17, 1266–1268.

(72) Gopalan, A. S.; Zincircioglu, O.; Smith, P. Minimization and Remediation of DOE

Nuclear Waste Problems Using High Selectivity Actinde Chelators. *Radioactive Waste Management and the Nuclear Fuel Cycle*. 1993, pp 161–175.

(73) Koshti, N.; Huber, V.; Smith, P.; Gopalan, A. S. Design and Synthesis of Actinide Specific Chelators: Synthesis of New Cyclam Tetrahydroxamate (CYTROX) and Cyclam Tetraacetonylacetone (CYTAC) Chelators. *Tetrahedron* **1994**, *50* (9), 2657–2664.

(74) Koshti, N. M.; Jacobs, H. K.; Martin, P. A.; Smith, P. H.; Gopalan, A. S. Convenient Method for the Preparation of Some Polyhydroxamic Acids: Michael Addition of Amines to Acrylohydroxamic Acid Derivatives. *Tetrahedron Letters* **1994**, *35* (29), 5157–5160.

(75) Santos, M. A.; Rodrigues, E.; Gaspar, M. A Cyclohexane-1,2-Diyldinitrilotetraacetate Tetrahydroxamate Derivative for Actinide Complexation: Synthesis and Complexation Studies. *Dalton Transactions* **2000**, 4398–4402.

(76) Gorden, A. E. V.; Shuh, D. K.; Tiedemann, B. E. F.; Wilson, R. E.; Xu, J.; Raymond, K. N. Sequestered Plutonium: [PuIV{5LIO(Me-3,2-HOPO)}2] - The First Structurally Characterized Plutonium Hydroxypyridonate Complex. *Chemistry - A European Journal* **2005**, *11* (9), 2842–2848.

(77) Veeck, A. C.; White, D. J.; Whisenhunt, D. W.; Xu, J.; Gorden, A. E. V.; Romanovski, V.; Hoffman, D. C.; Raymond, K. N. Hydroxypyridinone Extraction Agents for Pu(IV). *Solvent Extraction and Ion Exchange* **2004**, *22*, 1037–1068.

(78) Szigethy, G.; Raymond, K. N. Hexadentate Terephthalamide(Bis-Hydroxypyridinone) Ligands for Uranyl Chelation: Structural and Thermodynamic Consequences of Ligand Variation. *Journal of the American Chemical Society* **2011**, *133*, 7942–7956.

(79) Dasaradhi, L.; Stark, Peter, C.; Huber, Vincent, J.; Smith, Paul, H.; Jarvinen, Gordon, D.; Gopalan, A. S. 4-Tert-Butylcalix[4]Arene Tetrahydroxamate Chelators for the Selective Extraction of Actinide Ions: Synthesis and Preliminary Metal Ion Extraction Studies. *Journal of the Chemical Society, Perkin Transactions 2* **1997**, No. 6, 1187–1192.

(80) White, D. L.; Durbin, P. W.; Jeung, N.; Raymond, K. N. Specific Sequestering Agents for the Actinides. 16. Synthesis and Initial Biological Testing of Polydentate Oxohydroxypyridinecarboxylate Ligands. *Journal of Medicinal Chemistry* **1988**, *31* (1), 11–18.

(81) Stradling, G. N.; Gray, S. A.; Ellender, M.; Moody, J. C.; Hodgson, A.; Pearce, M. J.; Wilson, I.; Burgada, R.; Bailly, T.; Leroux, Y. G. P.; El Manouni, D.; Raymond, K. N.; Durbin, P. W. The Efficacies of 3,4,3-LIHOPO and DTPA for Enhancing the Excretion of

Plutonium and Americium from the Rat: Comparison with Other Siderophore Analogues. *International Journal of Radiation Biology* **1992**, *62* (4), 487–497.

(82) Stradling, G. N.; Gray, S. A.; Moody, J. C.; Pearce, M. J.; Wilson, I.; Burgada, R.; Bailly, T.; Leroux, Y.; Raymond, K. N.; Durbin, P. W. Comparative Efficacies of 3,4,3-LIHOPO and DTPA for Enhancing the Excretion of Plutonium and Americium from the Rat after Simulated Wound Contamination as Nitrates. *International Journal of Radiation Biology* **1993**, *64*, 133–140.

(83) Volf, V.; Burgada, R.; Raymond, K. N.; Durbin, P. W. Early Chelation Therapy for Injected Pu-238 and Am-241 in the Rat: Comparison of 3,4,3-LIHOPO, DFO-HOPO, DTPA-DX, DTPA and DFOA. *International Journal of Radiation Biology* **1993**, *63* (6), 785–793.

(84) Courtney, R. C.; Chaberek, S.; Martell, A. E. Metal Chelates. VII. N,N'-Ethylenediaminedipropionic Acid and N,N'-Ethylenediaminetetrapropionic Acid. *Journal of the American Chemical Society* **1953**, *75* (19), 4814–4818.

(85) Sturzbecher-Hoehne, M.; Ng Pak Leung, C.; D'Aléo, A.; Kullgren, B.; Prigent, A.-L.; Shuh, D. K.; Raymond, K. N.; Abergel, R. J. 3,4,3-LI(1,2-HOPO): In Vitro Formation of Highly Stable Lanthanide Complexes Translates into Efficacious in Vivo Europium Decorporation. *Dalton Transactions* **2011**, *40* (33), 8340–8346.

(86) Karunaratne, V.; Hoveyda, H. R.; Orvig, C. General Method for the Synthesis of Trishydroxamic Acids. *Tetrahedron Letters*. 1992, pp 1827–1830.

(87) Vernon, F. The Preparation and Properties of Chelating Ion Exchange Resins. *Chemistry & Industry* **1977**, No. 15, 634–637.

(88) Cornaz, J. P.; Deuel, H. Selective Ion-Exchangers for Ferric Ions. *Experientia* **1954**, *10*, 137–138.

(89) Cornaz, J. P.; Hutschneker, K.; Deuel, H. Ion Exchanges. X. Acid Chlorides and Hydroxamic Acids of Carboxyl Ion Exchangers. *Helvetica Chimica Acta* **1957**, *40*, 2015–2019.

(90) Petrie, G.; Locke, D.; Meloan, C. E. Hydroxamic Acid Chelate Ion Exchange Resin. *Analytical Chemistry* **1965**, *37* (7), 919–920.

(91) Agrawal, Y. K.; Rao, K. V. Polyhydroxamic Acids: Synthesis, Ion Exchange Separation and Atomic Absorption Spectrophotometric Determination of Divalent Metal Ions. *Reactive Polymers* **1995**, *25* (1), 79–87.

(92) Agrawal, Y. K.; Rao, K. V. Synthesis, Complexation and Ion-Exchange Reactivity of Polymethacrylohydroxamic Acid. *Reactive and Functional Polymers* **1996**, *31* (3), 225–235.

(93) Agrawal, Y. K.; Kaur, H. Polhydroxamic Acids for the Chromatographic Separation of Metal Ions. *Reviews in Analytical Chemistry* **2001**, *20* (3), 183–206.

(94) Winston, A.; Mazza, E. T.; Virginia, W. Hydroxamic Acid Polymers. *Journal of Polymer Science, Polymer Chemistry Edition* **1975**, *13*, 2019–2030.

(95) Fetscher, C. A. Radioactive Source Comprising a Polyamidoxime or a Polyhydroxamic Acid Complexed with a Radioactive Metal. US3154499, 1961.

(96) Vernon, F. Chelating Ion Exchangers - The Synthesis and Uses of Poly(Hydroxamic Acid) Resins. *Pure and Applied Chemistry* **1982**, *54* (11), 2151–2158.

(97) Winston, A.; Mclaughlin, G. R. Hydroxamic Acid Polymers. II. Design of a Polymeric Chelating Agent for Iron. *Journal of Polymer Science, Polymer Chemistry Edition* **1976**, *14*, 2155–2165.

(98) Vernon, F.; Eccles, H. Chelating Ion-Exchanges Containing N-Susbstituted Hydroxylamine Functional Groups Part III. Hydroxamic Acids. *Analytica Chimica Acta*. 1976, pp 369–375.

(99) Phillips, R. J.; Fritz, J. S. Extraction of Metal Ions by N-Phenyl-, N-Methyl-, and N-Unsubstituted Hydroxamic Acid Resins. *Analytica Chimica Acta* **1982**, *139*, 237–246.

(100) Agrawal, Y. K.; Kaur, H. Synthesis, Characterization and Applications of Poly(Beta-Styryl) Hydroxamic Acids. *Reactive & Functional Polymers* **1999**, *42* (1), 1–9.

(101) Agrawal, Y. K.; Kaur, H.; Menon, S. K. Poly(Styrene-p-Hydroxamic Acids): Synthesis, and Ion Exchange Separation of Rare Earths. *Reactive and Functional Polymers* **1999**, *39* (2), 155–164.

(102) Mendez, R.; Pillai, V. N. S. Pre-Concentration and Separation of Metal Ions on an N-Phenylhydroxamic Acid Resin. *The Analyst* **1990**, *115* (2), 213.

(103) Rahman, L.; Silong, S.; Md Zin, W.; Ab Rahman, M. Z.; Ahmad, M.; Haron, J. Graft Copolymerization of Methyl Acrylate onto Sago Starch Using Ceric Ammonium Nitrate as an Initiator. *Journal of Applied Polymer Science* **2000**, *76* (4), 516–523.

(104) Mohamad Zaki Ab Rahman; Md Lutfor Rahman; Md Jelas Haron; Sidik Silong; Wan Md Zin Wan Yunus; Mansor B. Ahmad. Preliminary Study on Application of Sago Starch Based Poly (Hydroxamic Acid) Resin for Extraction of Lanthanide Group Elements from

Aqueous Media. *Malaysian Journal of Analytical Sciences* **2001**, *7* (2), 453–456.

(105) Alakhras, F. A.; Dari, K. A.; Mubarak, M. S. Synthesis and Chelating Properties of Some Poly(Amidoxime-Hydroxamic Acid) Resins toward Some Trivalent Lanthanide Metal Ions. *Journal of Applied Polymer Science* **2005**, *97* (2), 691–696.

(106) Huggard, A. J.; Warner, B. F. Investigations to Determine the Extent of Degradation of TBP/Oderless Kerosene Solvent in the New Separation Plant, Windscale. *Nuclear Science and Engineering* **1963**, *17* (4), 638–650.

(107) Taylor, R. J.; May, I.; Wallwork, A. L.; Denniss, I. S.; Hill, N. J.; Galkin, B. Y.; Zilberman, B. Y.; Fedorov, Y. S. The Applications of Formo- and Aceto-Hydroxamic Acids in Nuclear Fuel Reprocessing. *Journal of Alloys and Compounds* **1998**, *271–273*, 534–537.

(108) Pathak, S. S.; Pius, I. C.; Mukerjee, S. K.; Pal, S.; Tewari, P. K. Studies on Sorption of Plutonium from Carbonate Medium on Polyacrylhydroxamic Acid Resin. *Journal of Radioanalytical and Nuclear Chemistry* **2012**, *293* (2), 483–488.

CHAPTER TWO

AZAMACROCYCLIC LIGANDS FOR SELECTIVE ACTINYL COORDINATION

2.1 Introduction

Actinides (An) are known to exist in a wide variety of oxidation states, from An^{2+} to An^{7+}. The early actinides, Th-Pu, are more similar to the early transition metals than the later actinides, marked by higher stable oxidation states and the formation of covalent bonds with ligands. The late actinides, Am-Lr, exist primarily in a stable An^{3+} oxidation state and form ionic bonds, similar to the lanthanides.[1,2] The 5f orbitals are more available for bond interactions than the 4f orbitals due to the presence of a radial node that places the electron density further from the nucleus and less "buried" by other orbitals.[2]

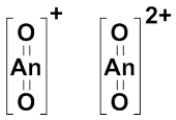

Figure 2.1: General actinyl ion structures

Uranium, neptunium, plutonium and americium exist as stable actinyl ions, where the metal ion forms double bonds to two oxygen atoms in a near-linear structure, shown in Figure 2.1. In aqueous solutions, these complexes form through the hydrolysis of aquo ligands. These unique actinide ions provide excellent targets for ligand design. The UO_2^{2+} ion is the most stable form of uranium in aqueous solutions and is often targeted in the design of uranium-specific ligands.[3,4] Most reported uranyl-binding ligands only interact with the equatorial plane, with few examples of interaction with the oxygen atoms.[5–7] Figure 2.2 is representative of the general design followed for actinide ligands. It is comprised of a bulky, organic macrocyclic molecule with hard donors that interact with the uranium ion in the center of the macrocycle.[8] Despite the formation

of stable uranium complexes with the aforementioned ligands, actinide selectivity remains an issue in complex environments.[9]

The radioactive properties of actinides have led to many industrial needs for actinide-specific ligands. The mitigation of the continuously increasing volume of nuclear waste is at the forefront of actinide research.[2,3] Nuclear waste is comprised of three types of radioactive waste: low, intermediate, and high level. High level waste, accounting for 95% of the radioactivity of nuclear waste, consists of depleted uranium (96%), plutonium (1%), and fission products, such as lanthanides (3%).[10] Reprocessing of the high level waste not only decreases the amount of radiation present, but also allows for the recycling of the uranium and plutonium collected. The most widely commercially used method for reprocessing nuclear waste is the Plutonium and Uranium Extraction (PUREX) method. This solvent extraction method was designed during the Manhattan Project and has experienced only minor modifications since, focused on decreasing the amount of additional waste produced and preventing the production of pure plutonium.[2]

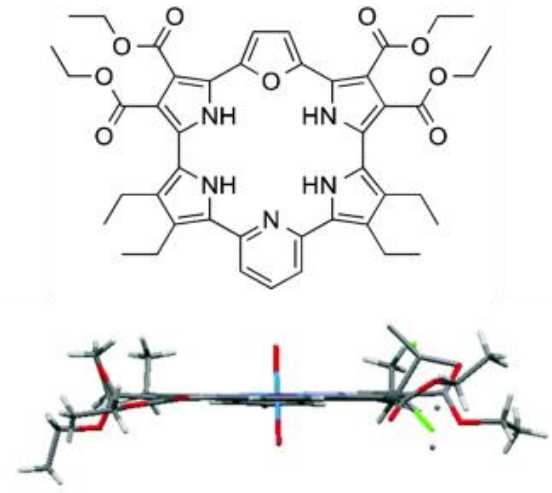

Figure 2.2: Top and side views of an expanded-porphorin uranyl complex[8]

The increased demand for nuclear power has also increased the demand for uranium fuel. The current demand for uranium ore is 67 kton/year and is expected to double by 2030.[10] Seawater contains four gigatons of uranium, 1000 times more than the uranium in land.[11–13] This source is mostly untapped due to the low concentration of uranium (3 ppb) in comparison to other competitive metal ions (Na^+, K^+, Ca^{2+}, Mg^{2+}) and the formation of stable carbonate-uranium species. Other important areas of actinide-ligand research are the need for environmental remediation of actinides after spills or use of nuclear weapons and chelation therapy following actinide exposure.[9]

Crown ethers and aza-crown ethers have been shown to form stable complexes with the uranyl ion. The most well characterized complex is that of UO_2^{2+} and 18-crown-6. A crystal structure of this complex has been solved and shows the macrocycle interacting with the uranium ion, which sits in the middle of the ligand.[14–16] However, other metals ions, such as potassium, could easily displace the uranyl ion. We hypothesize that selectivity and the stability of the actinide complex can be increased by utilizing the crown ether backbone and incorporating sidearms that can interact with the two actinyl oxygen atoms. Although there are no current examples of ligands that can bind both actinyl oxygen atoms, modest gains in selectivity have been observed using ligands designed to bind one actinyl oxygen.[17]

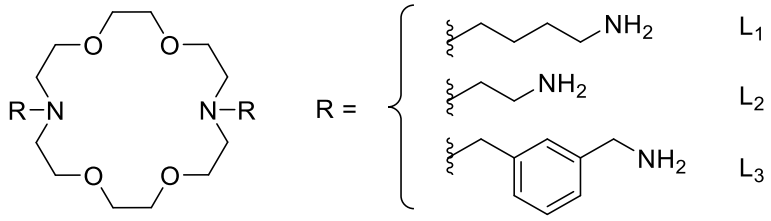

Figure 2.3: TEG-based ligand structure of L_1, L_2, and L_3.

This chapter discusses the design and characterization of a macrocyclic diazacrown ether ligand for coordination of the uranyl ion. The original goal of this project was to synthesize a series of ligands incorporating the diazacrown ether backbone and amine sidearms of varying lengths for selective control of the ligand topology. The final goal was to study the solution thermodynamics of the uranyl complexes of these ligands to gain a better understanding of the necessary structural restraints for high selectivity and coordination of the uranyl ion. However, as will be discussed, problems arose from the flexibility of the diazacrown ether backbone which prevented this project from progressing past its infancy.

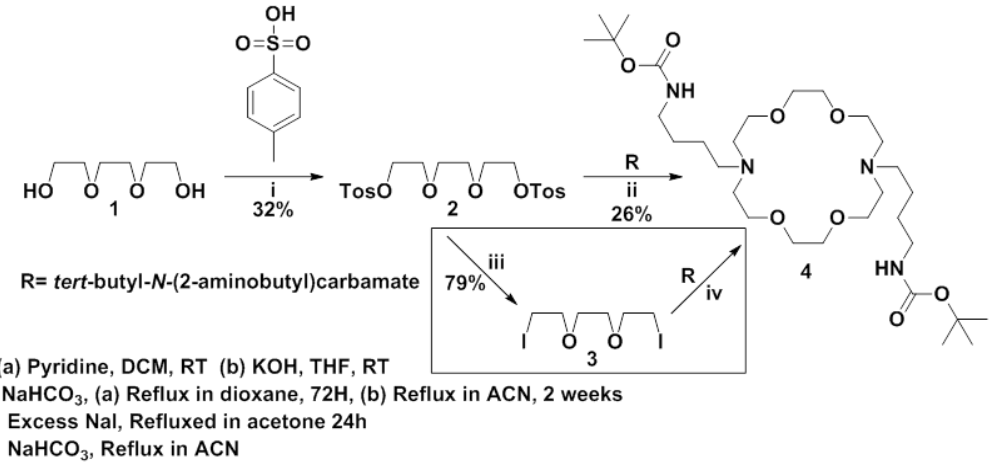

Scheme 2.1: The synthesis route for diaza-crown ether ligands containing diamine sidearms. Triethylene glycol is activated through tosylation and then cyclized through a substitution reaction with the diamine sidearms. An alternate route is shown in a box where the tosyl group is replaced by iodine before cyclization.

2.2 Results and Discussion

Ligand Synthesis

The initial synthetic route was focused on allowing for straightforward manipulation of the backbone size as well as the sidearms. Due to this requirement, we began by activating triethylene glycol (TEG) through tosylation. This reaction initially produced a low yield, due to

the necessity of multiple columns for purification. However, using potassium hydroxide in place of the pyridine allowed for purification through recrystallization due to easier removal of excess base, which could potentially increase yield and decrease the time required for purification.[18–20] The tosyl group was then displaced in a 2+2 cyclization reaction with a Boc-protected diamine, as shown in Scheme 2.1. The Boc-protecting group was thermally unstable above 80°C, which required the change from dioxane to acetonitrile as our solvent. It also increased the time of reaction from four days to over two weeks. Column chromatography was used for purification of the final ligand. Once a pure product was obtained, the Boc-protecting groups were removed in 80% trifluoroacetic acid/methanol.

An alternative route to avoid the presence of the tosyl counterion was attempted by substituting iodine for the toluenesulfonyl groups (iii, Scheme 2.1). This reaction proceeded quickly and required minor purification. The diiodinated product was not stable, so it was quickly used in the cyclization step. However, the final cyclized product was not isolated through this method. It is possible that the tosyl counterion is instrumental in the cyclization step through a template effect.

The top route in Scheme 2.1 was used to successfully synthesize L_1 and L_2 (Figure 2.3). Both syntheses were low yield (<10%). Only L_1 was subsequently used in complexation studies with uranyl nitrate.

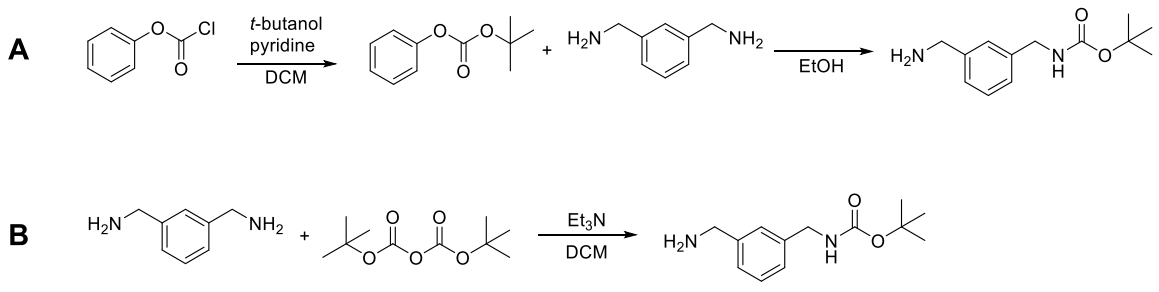

Scheme 2.2: Routes toward mono-*N*-Boc protection of m-xylylenediamine.

The synthesis of L_3 required a preliminary mono-Boc protection of the m-xylylenediamine starting material, before moving forward with the ligand synthesis in Scheme 2.1. Two methods of *N*-Bocylation were attempted. Route 1 (A, Scheme 2.2) followed a literature procedure for the esterification of phenyl chloroformate with *tert*-butanol.[21] This product was isolated through extraction to give 50% yield. However, the subsequent *N*-Boc protection of m-xylylenediamine did not lead to a clean product. An alternative literature produce utilizing Boc anhydride was attempted (B, Scheme 2.2).[22] The mono-Boc protected product was purified through column chromatography before being used in the synthesis of L_3 (Figure 2.3). The route in Scheme 2.1 was used for the synthesis of L_3. Unfortunately, L_3 was not successfully isolated.

Ligand Characterization

The ligands were characterized through MALDI-TOF (Figure 2.4), ^{1}H NMR and ^{13}C NMR. The MALDI-TOF spectra of the ditosylated TEG backbone, Boc-protected L_1, and deprotected L_1 are shown in Figure 2.4. The ^{1}H NMR and ^{13}C NMR both show a pure product with tosylate and trifluoroacetic acid counterions. In the ^{1}H NMR, a tosylate counterion can be assigned to the singlet at 2.2 ppm as well as the aromatic peaks (7.2, 7.3, 7.4, 7.6 ppm). The remaining peaks correspond to the macrocyclic product. The ^{13} C NMR not only shows evidence of a tosylate counterion (19, 125, 129, 139 and 142 ppm), but also the presence of a trifluoroacetic acid counterion from the deprotection of the Boc-protecting group (112-119, 162 ppm). The remaining seven peaks correspond to the cyclic macrocycle. The L_1-uranyl complexation products were characterized with ATR-FTIR and UV-vis (below).

L_2 was never fully isolated. MALDI of the crude reaction showed the presence of the desired product, however, once extraction or a column was performed, the product peak disappeared. It is

possible that degradation of the Boc-protecting groups occurred during purification of the crude reaction.

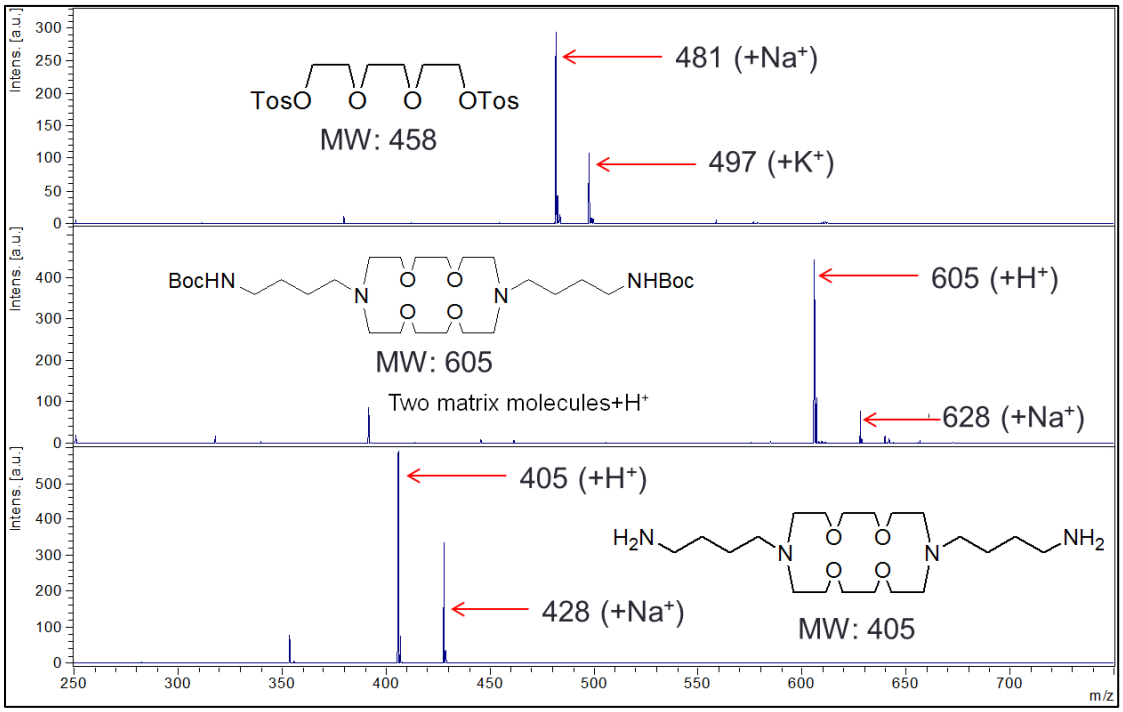

Figure 2.4: MALDI-TOF of crown-ether ligand synthesis using HCCA/TFA matrix

Ligand-Actinide Complexation

Complexation with uranyl nitrate hexahydrate was initially carried out at 1 mmol scale. Due to the nature of the metals being studied (U(VI), Np(V), Pu(V)), validation of the synthesis was necessary before moving to potentially larger scales. A second complexation at 60 mmol scale was carried out to validate complexation at a higher concentration. In both cases an equimolar solution of L_1 and uranyl nitrate hexahydrate in Milli-Q water was heated at 80°C for 120 hours. No further purification was performed prior to characterization.

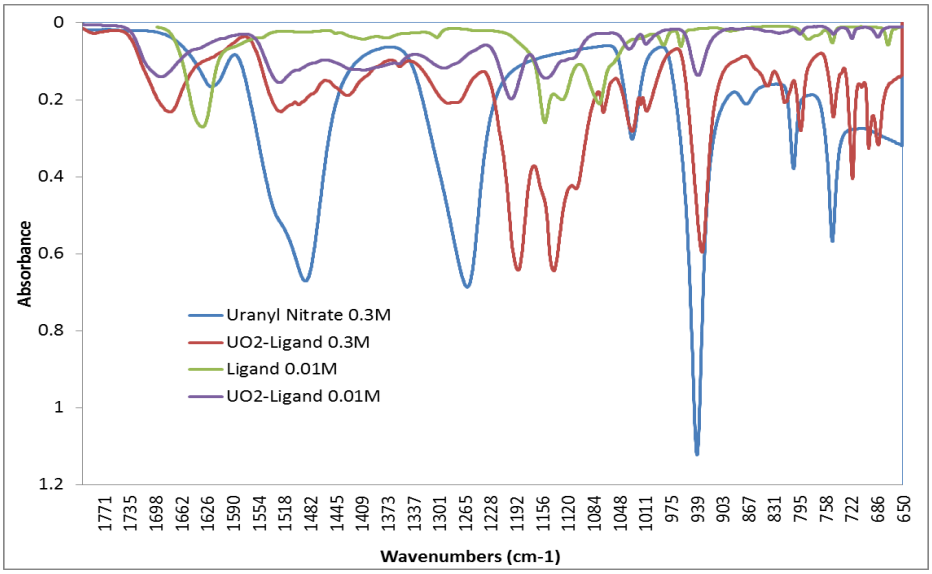

Figure 2.5: ATR-FTIR spectra of uranyl-L_3 complex (red, 0.3 M), uranyl nitrate (blue, 0.3 M), and L_3 (green, 0.01 M).

Attenuated total reflection-infrared spectroscopy (ATR-FTIR)

Samples were spotted on a diamond crystal and evaporated *in situ* with nitrogen. Each spectrum was then collected in triplicate and averaged. Spectra were collected for: 0.3 M uranyl nitrate stock, 0.3 M UO_2^{2+}-ligand, and 0.01 M ligand, all dried from Milli-Q water. A diluted sample of the UO_2^{2+}-ligand (0.01 M) was also run to further investigate the presence of changes in the spectra at lower concentrations. The spectra are shown in Figure 2.5.

The peaks at 940 cm^{-1} and 800 cm^{-1} are indicative of the uranyl antisymmetric and symmetric stretches, respectively. Upon complexation, there was a notable shift in both peaks, giving evidence toward a change in the ligand geometry of the uranyl ion. Further evidence toward this change is seen in the two broad peaks at 1480 cm^{-1} and 1265 cm^{-1}, which are characteristic of the nitrate groups complexed with uranyl. Complexation leads to a drastic decrease of these peaks, consistent with the loss of these nitrates. However, studies of the various hydrates of uranyl nitrate (di-, tri-, and hexa-) have shown that the hexahydrate does not typically produce these

nitrate peaks and appears more like an ionic nitrate ion. Our peaks are more similar to those seen with the uranyl trihydrate compound, suggesting a possible dehydration of the sample occurred during drying.[23,24] Both trends were noted for both concentrations (0.01 M and 0.3 M), giving more evidence toward a successful ligand exchange occurring.

Ultraviolet-visible spectroscopy (UV-vis)

Samples were diluted to 60 mM and UV-vis spectra were collected in triplicate in matching quartz cuvettes on a Cary-300 spectrometer. The spectrum (Figure 2.6) shows the uranyl nitrate stock solution as well as the uranyl-ligand complex. The characteristic peak pattern of the uranyl ion experiences a change in absorbance as well as a slight blue-shift in wavelength upon complexation, again consistent with a change in the uranyl's ligand environment in the presence of our ligand. The addition of a strong ligand, such as a carbonate or amine, to the uranyl ion has been shown to induce an increase in absorption. Meanwhile, hydrolysis products produce a low absorbance, so the change in the spectrum suggests no hydrolysis of the uranyl ion occurred.[25]

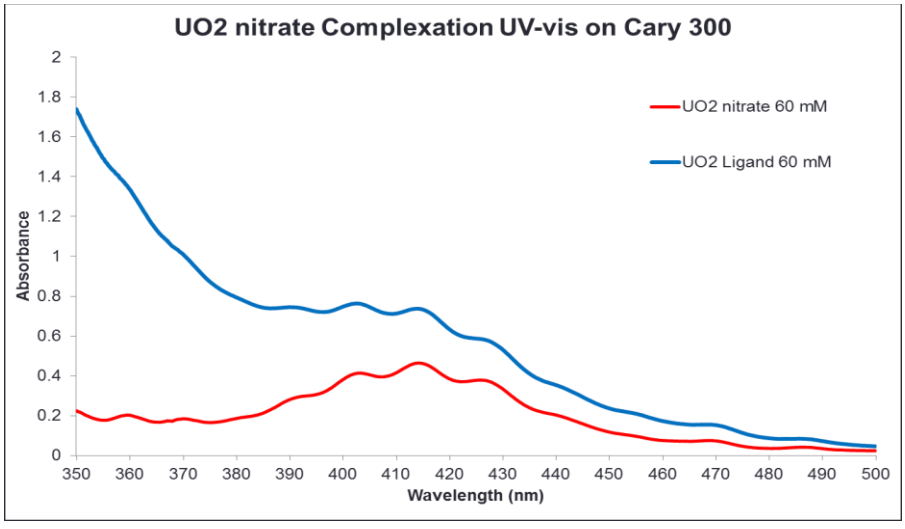

Figure 2.6: UV-vis spectrum of uranyl-ligand complex.

2.3 Conclusion

L_1 and L_2 were both successfully synthesized, however only L_1 was purified and subsequently used. The synthetic route that was used was inefficient and produced an overall yield <10%. Attempts of utilizing a better leaving group than tosylate (iii, Scheme 2.1) gave evidence that a template effect with the tosyl counterion is necessary for the final cyclization step of the ligand synthesis (ii, Scheme 2.1). Extensive purification of each step drastically diminished the yields of the reactions. Despite this, L_1 was isolated and used in a complexation study with uranyl nitrate.

Initial evidence suggested the successful complexation of uranyl with L_1. A shift in the symmetric and antisymmetric FTIR peaks for the UO_2^{2+} ion as well as the loss of the nitrate peaks suggested the formation of a complex. UV-vis results also suggested the formation of a uranyl complex due to the slight shift of peaks. Nierlich and coworkers showed the coordination of the uranyl ion by the parent azamacrocycle in organic solvents when a non-coordinating triflate counterion.[15] However, the presence of the more strongly coordinating nitrate anion prevents the inclusion of the uranyl ion into 18-crown-6 (instead the uranyl was present as a counterion, uncoordinated by the macrocycle).[26] Consequently, although FTIR and UV-vis were consistent with at least some interaction of L_1 with uranyl in water, it was decided that an alternative, more strongly-coordinating macrocycle, could provide a better framework for a second-generation approach.

Additionally, preliminary computational work showed the preference of the 18-diazacrown-6 backbone for collapsing inward, which would prevent the coordination of a metal ion. With this information in mind, reviewing the FTIR and UV-vis data suggests no more than partial change of the coordination environment around the uranyl ion. Specifically, it is possible that the shifts seen in FTIR are only due to dehydration of the samples during sample preparation, which

involved the drying of the samples with nitrogen and the UV-vis data could be showing the hydrolysis of the uranyl ion rather than complex formation.

2.4 Future Directions

The ultimate goal of this project was to determine the structural requirements for the coordination of both uranyl oxo-atoms by studying the solution thermodynamics of three azamacrocyclic-based ligands. The synthesis of L_1 successfully provided a ligand for complexation with uranyl. However, literature precedence, preliminary computational modeling and the FTIR and UV-vis data suggest no formation of a complex.

Initial computational geometry optimization by Dr. Shuller-Nickles of only the macrocyclic portion of the ligand backbone showed a possible preference of the backbone for geometries not conducive to metal coordination. A possible way to combat this issue would be the incorporation of rigidity into the backbone, creating a preorganized structure designed for metal coordination. This could be achieved by integrating 2,3-dihydroxyterepthalic acid, a well-known actinide ligand[27]. The incorporation of the terepthalic acid would be performed using NHS-activation of the carboxylic acids, and subsequent reaction with a corresponding amine (*e.g.* diethylenetriamine). The preorganization of the backbone toward cyclization could also potentially allow for higher reaction yields by circumventing the high energy of cyclization.

To further increase selectivity for the uranyl ion, rigidified sidearms can be incorporated into the ligand. This can be done through the use of xylylenediamine rather than the alkyl diamine sidearms. Reducing the number of free, rotatable bonds in the sidearm would decrease the entropy loss upon binding of the uranyl oxygen atoms. This strategy was employed with the TEG-based ligands (L_3). Unfortunately, mono-*N*-Boc protection of m-xylylenediamine was not

successful. However, further investigation into this reaction could lead to a new strategy that would allow for incorporation into the diazacrown backbone.

The initial attempts to coordinate L_1 with uranyl nitrate proved unsuccessful due to the flexibility of the diazacrown backbone and its preference for collapse in solution. This conclusion led to the termination of the development of L_1, L_2 and L_3. However, understanding the issues with the original 18-diazacrown-6 backbone provides some evidence toward the ultimate goal of investigating the structural requirements for the full coordination of the uranyl ion. Future investigations into this project should incorporate this finding through implementation of more rigidity into the backbone.

2.5 Materials and Methods

Chemicals. Triethylene glycol, pyridine, and tosyl chloride were obtained from Alfa Aesar. Dichloromethane, acetonitrile, dichloromethane, di-tert-butyl dicarbonate, and sodium bicarbonate were received from BDH. TFA was obtained from Oakwood Chemicals. *Tert*-butyl-*N*-(2-aminoethyl)carbamate and *tert*-butyl-*N*-(2-aminobutyl)carbamate were obtained from AK Scientific. 1,4-dioxane was obtained from Beantown Chemicals. α-Cyano-4-hydroxycinnamic acid and *m*-xylylenediamine were obtained from Acros. All chemicals were used without further purification.

General. ^{1}H NMR and ^{13}C NMR were collected on a Bruker 500 MHz FT-NMR spectrometer using deuterated solvents ($CDCl_3$, D_2O, DMSO). All NMR data is reported in ppm. MALDI-TOF data was collected on a Bruker Onmiflex MALDI-TOF mass spectrometer using a stainless steel plate and HCCA matrix in acetone/formic acid. UV-vis spectra were collected with a quartz cuvette and a Cary-300 spectrometer.

General Procedure for Deprotection of Boc groups: Ligands were stirred overnight in a mixture of 80% TFA/MeOH. The solvent was removed *in vacuo* to give quantitative yield.

Synthesis of 1,2-ethanediylbis(oxy-2,1-ethanedyl) bis(4-methylbenzenesulfonate) **(2)**: Triethylene glycol (4.077 g, 27.1 mmol) was cooled to 0°C in dichloromethane (25 mL). Pyridine (3 eq, 81.3 mmol) was slowly added. Last, tosyl chloride (2.2 eq, 59.6 mmol) was added and the reaction immediately changed from colorless to yellow. After the tosyl chloride addition, the reaction was removed from ice and stirred at room temperature for 18 hours. The product was cooled to 0°C and purified by column chromatography (0-10% MeOH/DCM). The product was isolated as a white powder (35% yield), (R_f: 0.575, 2% MeOH/DCM), ^{1}H NMR (500 MHz, DMSO): 7.78-7.77 δ (d, *J* = 8.23 Hz, 2H), 7.47-7.46 δ (d, *J* = 8.23, 2H), 3.38 δ (s, 2H), 2.41 δ (s, 3H), ^{13}C NMR (500 MHz, DMSO): 144.9 δ, 132.4 δ, 130.1 δ, 127.6 δ, 69.9 δ, 69.6 δ, 67.9 δ, 21.1 δ, m/z: 458.2 (calc), 481.4 (+ Na^+, obsd), 497.3 (+ K^+, obsd).

Synthesis of **(4): (2)** (5.84 g, 12.7 mmol) was dissolved in acetonitrile, then 2-methyl-2-popanyl(4-aminobutyl)carbamate (1 eq, 12.7 mmol) and sodium bicarbonate (2 eq, 25.4 mmol) were added and the reaction was refluxed for 120 hours without exceeding 80°C to prevent deprotection of the Boc-group. The solvent was removed *in vacuo* and the product was purified by column chromatography (0-20% MeOH/DCM). The product was isolated as a white solid (26% yield), ^{1}H NMR (500 MHz, DMSO): 7.53-7.51 δ (d, *J* = 8.14 Hz, 10H), 7.15-7.14 δ (d, *J* = 8.14, 10H), 3.72-3.67 δ (m, 2H), 3.58-3.57 δ (m, 2H), 3.42 δ (s, 14H), m/z: 605.1 (calc), 605.8 (+ H^+, obsd), 628.3 (+ Na^+). This product was deprotected using the *General procedure for deprotection of Boc groups.*

L_1 (1,10-dibutane diamine-1,10-diaza-18-crown-6): The product was an oil. ^{1}H NMR (500 MHz, D_2O): 7.62-7.61 δ (d, *J* = 8.35 Hz, 3H), 7.31-7.29 δ (d, *J* = 8.35 Hz, 3H), 3.81-3.77 δ (m, 9H),

3.67 δ (s, 10H), 3.41-3.39 δ (m, 8H), 3.23-3.20 δ (t, *J* = 7.99 Hz, 4H) 2.99-2.96 δ (t, *J* = 7.61 Hz, 4H), 2.32 δ (s, 4H), 1.75-1.66 δ (m, 8H), ^{13}C NMR (500 MHz, D_2O): 163.2 δ, 162.9 δ, 162.3 δ, 142.6 δ, 139.8 δ, 129.6 δ, 125.5 δ, 119.9 δ, 117.6 δ, 115.3 δ, 112.9 δ, 70.9 δ, 70.0 δ, 69.9 δ, 69.87 δ, 69.83 δ, 69.8 δ, 69.6 δ, 64.4 δ, 64.2 δ, 63.9 δ, 53.5 δ, 53.1 δ, 52.9 δ, 43.6 δ, 38.9 δ, 24.0 δ, 20.6 δ, 20.4 δ, 19.8, m/z: 405.1 (calc), 405.8 (+ H^+, obsd), 428 (+ Na^+, obsd).

L_2 (1,10-diethane diamine-1,10-diaza-18-crown-6): The same method was used as for L_1. The product was an oil.

(1) Kaltsoyannis, N.; Scott, P. *The F Elements*; Oxford University Press, 1999.

(2) Gorden, A. E. V.; Devore II, M. A.; Maynard, B. A. Coordination Chemistry with F-Element Complexes for an Improved Understanding of Factors That Contribute to Extraction Selectivity. *Inorganic Chemistry* **2013**, *52*, 3445–3458.

(3) Altmaier, M.; Gaona, X.; Fanghänel, T. Recent Advances in Aqueous Actinide Chemistry and Thermodynamics. *Chemical Reviews* **2013**, *113* (2), 901–943.

(4) Meinrath, G. *Aquatic Chemistry of Uranium: A Review Focusing on Aspects of Environmental Chemistry*; 1998; Vol. 1.

(5) Franczyk, T. S.; Czerwinski, K. R.; Raymond, K. N. Stereognostic Coordination Chemistry. 1. The Design and Synthesis of Chelators for the Uranyl Ion. *Journal of the American Chemical Society* **1992**, *114*, 8138–8146.

(6) Arnold, P. L.; Patel, D.; Wilson, C.; Love, J. B. Reduction and Selective Oxo Group Silylation of the Uranyl Dication. *Nature* **2008**, *451*, 315–317.

(7) Sather, A. C.; Berryman, O. B.; Rebek Jr., J. Selective Recognition and Extraction of the Uranyl Ion. *Journal of the American Chemical Society* **2010**, *132*, 13572–13574.

(8) Davis, C. M.; Ohkubo, K.; Ho, I.-T.; Zhang, Z.; Ishida, M.; Fang, Y.; Lynch, V. M.; Kadish, K. M.; Sessler, J. L.; Fukuzumi, S. Near-Infrared-Induced Electron Transfer of an Uranyl Macrocyclic Complex without Energy Transfer to Dioxygen. *Chemical Communications* **2015**, *51*, 6757–6760.

(9) Gorden, A. E. V.; Xu, J.; Raymond, K. N.; Durbin, P. Rational Design of Sequestering Agents for Plutonium and Other Actinides. *Chemical Reviews* **2003**, *103*, 4207–4282.

(10) Silverio, L. B.; Lamas, W. de Q. An Analysis of Development and Research on Spent Nuclear Fuel Reprocessing. *Energy Policy* **2011**, *39*, 281–289.

(11) Tian, G.; Teat, S. J.; Zhang, Z.; Rao, L. Sequestering Uranium from Seawater: Binding Strength and Modes of Uranyl Complexes with Glutarimidedioxime. *Dalton Transactions* **2012**, *41*, 11579–11586.

(12) Tian, G.; Teat, S. J.; Rao, L. Thermodynamic Studies of U(VI) Complexation with Glutardiamidoxime for Sequestration of Uranium from Seawater. *Dalton Transactions* **2013**, *42*, 5690–5696.

(13) Davies, R. V.; Kennedy, J.; McIlroy, R. W.; Spence, R. Extraction of Uranium from Sea Water. *Nature* **1964**, *203*, 1110–1115.

(14) Rogers, R. D.; Bond, A. H.; Hipple, W. G.; Rollins, A. N.; Henry, R. F. Synthesis and

Structural Elucidation of Novel Uranyl-Crown Ether Compounds Isolated from Nitric, Hydrochloric, Sulfuric, and Acetic Acids. *Inorganic Chemistry* **1991**, *30* (12), 2671–2679.

(15) Thuéry, P.; Keller, N.; Lance, M.; Sabattié, J.-M.; Vigner, J.-D.; Nierlich, M. An Inclusion Complex of Uranyl in a Diazacrown: (Diaza-18-Crown-6)2+.-2CF3SO3− and [UO2(Diaza-18-Crown-6)]+.-CF3SO3−. *Acta Crystallographica* **1995**, *C51*, 801–805.

(16) Shamov, G. A.; Schreckenbach, G.; Martin, R. L.; Hay, P. J. Crown Ether Inclusion Complexes of the Early Actinide Elements, [AnO2(18-Crown-6)]N+, An = U, Np, Pu, and n = 1, 2: A Relativistic Density Functional Study. *Inorganic Chemistry* **2008**, *47*, 1465–1475.

(17) Sinkov, S. I.; Lumetta, G. J.; Warner, M. G.; Pittman, J. W. Binding of Stereognostically Designed Ligands to Trivalent, Pentavalent, and Hexavalent f -Block Elements. *Radiochimica Acta* **2012**, *100*, 349–357.

(18) Marshall, A.; Mobbs, R. H.; Booth, C. Preparation of Ethylene Glycol Oligomers. *European Polymer Journal* **1980**, *16*, 881–885.

(19) Ogawa, M.; Nagashima, M.; Sogawa, H.; Kuwata, S.; Takata, T. Synthesis and Cavity Size Effect of Pd-Containing Macrocycle Catalyst for Efficient Intramolecular Hydroamination of Allylurethane. *Organic Letters* **2015**, *17*, 1664–1667.

(20) Caicedo, C.; Rivera, E.; Valdez-Hernández, Y.; Carreón-Castro, M. del P. Synthesis and Characterization of Novel Liquid-Crystalline Azo-Dyes Bearing Two Amino-Nitro Substituted Azobenzene Units and a Well-Defined, Oligo(Ethylene Glycol) Spacer. *Materials Chemistry and Physics* **2011**, *130*, 471–480.

(21) Collins, D.; Mayo, J.; Thatte, S. D.; Tibbetts, F. T-Butyl Carbazate. *Organic Syntheses* **1964**, *44*, 20.

(22) Goodyer, C. L. M.; Chinje, E. C.; Jaffar, M.; Stratford, I. J.; Threadgill, M. D. Synthesis of N-Benzyl- and N-Phenyl-2-Amino-4,5-Dihydrothiazoles and Thioureas and Evaluation as Modulators of the Isoforms of Nitric Oxide Synthase. *Bioorganic and Medicinal Chemistry* **2003**, *11* (19), 4189–4206.

(23) Gatehouse, B. M.; Comyns, A. E. Infrared Spectra of Uranyl Nitrate Hydrates and Rubidium Uranyl Nitrate. *Journal of the Chemical Society* **1958**, 3965–3971.

(24) Johnson, T. J.; Sweet, L. E.; Meier, D. E.; Mausolf, E. J.; Kim, E.; Weck, P. F.; Buck, E. C.; McNamara, B. K. Time-Resolved Infrared Reflectance Studies of the Dehydration-Induced Transformation of Uranyl Nitrate Hexahydrate to the Trihydrate Form. *The*

Journal of Physical Chemistry A **2015**, *119*, 9996–10006.

(25) Natrajan, L. S.; Swinburne, A. N.; Andrews, M. B.; Randall, S.; Heath, S. L. Redox and Environmentally Relevant Aspects of Actinide(IV) Coordination Chemistry. *Coordination Chemistry Reviews* **2014**, *266–267*, 171–193.

(26) Belomestnykh, V. I.; Sveshnikova, L. B.; Mikhailov, Y. N.; Kanishcheva, A. S.; Gorbunova, Y. E. The Synthesis and Crystal and Molecular Structure of a Diazaonia-18-Crown-6 Tetranitratodioxouranate [C12H28O4N2][UO2(NO3)3]. *Zhurnal Neorganicheskoi Khimii* **2004**, *49* (7), 1110–1116.

(27) Szigethy, G.; Raymond, K. N. Hexadentate Terephthalamide(Bis-Hydroxypyridinone) Ligands for Uranyl Chelation: Structural and Thermodynamic Consequences of Ligand Variation. *Journal of the American Chemical Society* **2011**, *133*, 7942–7956.

CHAPTER THREE

CYCLIC PEPTOIDS AS SIDEROPHORE ANALOGUES FOR TETRAVALENT ACTINIDE COORDINATION

3.1 Introduction

Tetravalent actinides form stable, insoluble hydroxides which pose a major environmental hazard. The preference for these ions to hydrolyze into the insoluble hydroxides can lead to accumulation of radioactivity in unwanted areas.[1–3] Additionally, the similar chemistries of Fe(III) and Pu(IV) make Pu(IV) an exceptional target for biological Fe(III) chelators, such as transferrin, allowing for the internal transportation and amassing of this toxic metal.[4–8] The design of ligands to target the tetravalent actinides is heavily influenced by naturally-occurring Fe(III) chelators known as siderophores. These small molecules are produced by bacteria and fungi to aid the solubilization and transportation of Fe(III) from soil into their biological systems.[9–12] The coordination of the actinides by the trishydroxamate siderophore desferrioxamine (DFO)[13–16] and the triscatecholate siderophore enterobactin[17] have demonstrated the extraordinary potential that the siderophore framework has for coordination of these metals.

Peptoids, *N*-substituted glycine oligomers, hold advantages over peptide analogues due to synthetic benefits gained from the *N*-substituted glycine monomers they are comprised of. The movement of the sidearm from the α-carbon to the nitrogen allows for more flexibility of the glycine backbone and consequently, more straightforward cyclization of the backbone.[18–21] Additonally, peptoid synthesis is not limited to the natural amino acids, allowing for more customization through the use of any primary amine as the source of the peptoid side chain.[18,22]

For these reasons, cyclic peptoids offer a synthetic route toward peptidomimetics of peptide siderophores for tetravalent actinide coordination.

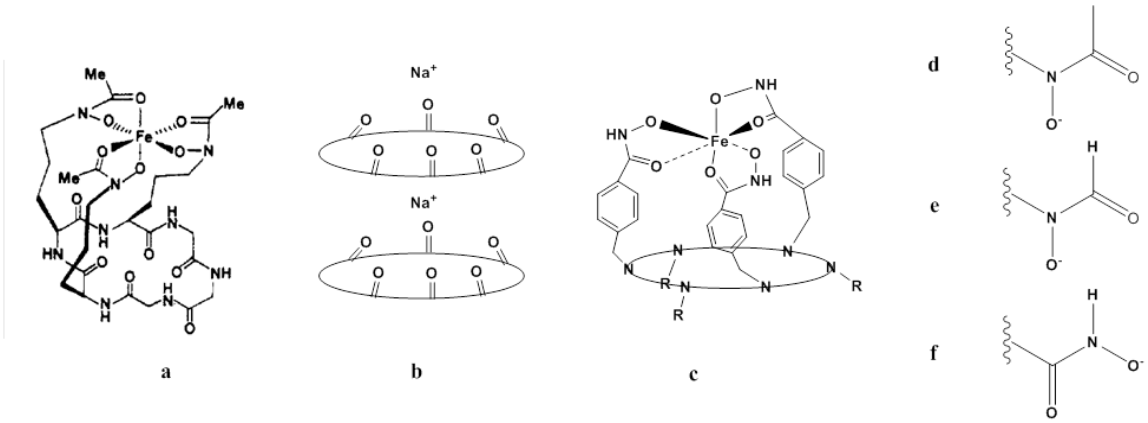

Figure 3.1: Macrocyclic ligands interacting with various metal ions (a-c) and different configurations of the chelating hydroxamate utilized in ferrichrome analogs (d-f). The pink box highlights the macrocyclic backbone. a) Interaction between ferrichrome and iron(III),[23] b) cartoon showing interaction between cyclic hexapeptoid backbone carbyonyls and sodium, c) illustration of potential coordination by a peptoid hydroxamate siderophore, d) ferrichrome hydroxamate moiety, f) desmethylhydroxamate ferrichrome moiety, f) retrohydroxamate

Two siderophores, ferrichrome (Figure 3.1)[23] and enterobactin, are comprised of a cyclic backbone and three metal-chelating arms, including three hydroxamic acid or catechol moieties, respectively. Alternatively, most literature concerning metal-peptoid complexation shows weak interaction between the carbonyls in the cyclic backbone with Group 1 or II metals.[20,24,25] Figure 3.1 shows the coordination mode this work hopes to effect by combining the cyclic-peptoid backbone with sidearms similar to those found in siderophores. Since most metal-peptoid interactions occur via weak carbonyl interactions[25] or sidechains in a helical structure[26], this work represents a new approach toward peptoid coordination chemistry. As seen in Figure 3.1, by

incorporating metal chelators into the sidearms, the coordination of metals in a similar fashion to the highly efficacious design of siderophores such as ferrichrome is possible.

Peptoids

Peptoids (*N*-substituted glycine oligomers) were first reported in 1992.[18,22] The advantages of peptoids stem from the structural difference between peptoids and peptides, where the side chain has been moved from the alpha carbon to the nitrogen. The sidechains therefore arise from primary amines used in the synthesis rather than requiring asymmetric synthesis to make new amino acids.[18] The modular synthesis allows for each residue to be installed separately and a wide variety of sidechains to be incorporated.[27] Peptoids are also resistant to proteolytic degradation[28] and flexible, allowing for simple cyclization and distinct secondary structure formation.[21,29,30] They have been investigated for many applications, including antimicrobial agents,[31,32] phase-transfer catalysts,[33] MRI contrast agents,[34] and other peptidomimetic applications.[20,22,35–38]

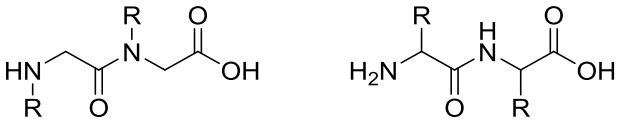

Figure 3.2. Structure of (left) peptoid and (right) peptide dimer.

Peptoids can be synthesized similarly to peptides using Fmoc-protected *N*-substituted glycine monomersFmoc,[39] although are more commonly synthesized using the submonomer synthesis as described later in the chapter. The macrocyclization of peptoids has been shown to provide rigid, distinct secondary structures capable of selectivity toward target molecules.[21,24,40] Peptoids exhibit a rapid *cis-trans* tertiary amide conversion which allows for cyclization without high-dilution

conditions.[21,40] A variety of side chains can be introduced into the peptoid-backbone through the use of primary amines in the submonomer synthesis. This allows for the introduction of properties, such as metal selectivity, *e.g.* hydroxamate and catecholate units.

Siderophores

In 1952, Neilands, *et al* reported the isolation of a non-protein crystalline compound from the rust fungus, *Ustilago sphaerogena*, which had been grown in a yeast-containing medium in an attempt to study the increased cytochrome-c production. This compound was shown to contain iron through the use of UV-vis and was subsequently labeled ferrichrome.[9,41,42] In the same year, Hesseltine *et al* reported the isolation of a red, crystalline, biologically active non-protein compound from the fungi, *Pilobolus*, while studying new growth media. This compound was also shown to contain iron, but was labeled coprogen.[43,44] Over a decade later, in 1967 a third compound of similar properties was isolated and shown to break down into the monohydroxamic acid fusarinine. This was labeled fusagen, later acknowledged as part of the fusarinine siderophore family.[45,46]

Fungi predominately produce hydroxamic acid-containing siderophores, which fall into three categories, fusarinine, coprogen, and ferrichrome. The fusarinine family includes both linear and cyclic mono-, di- and trimers of acylated ornithinine groups. Coprogens contain di- or trihydroxamic acids composed of *trans*-fusarinine subunits. Ferrichromes, the most common fungal siderophore, are nearly all cyclic, trishydroxamic acid, hexapeptides derived from N^5-hydroxyornithine.[10] The commonalities among the fungal siderophores include the incorporation of hydroxamic acids and the derivation from L-ornithine. The only polyhydroxamic acid siderophores derived from N^6-hydroxylysine are aerobactins, mycobactins, and exochelins.[47]

The hydroxamic acid moieties form stable, five-membered rings with the Fe(III) ion through primarily electrostatic interactions. The L-ornithine units of siderophores allow for a large distance to exist between the multiple hydroxamic acid residues. For this reason, despite being attached to one molecule, the siderophore hydroxamic acids do not benefit from the chelate effect.[48–50] Instead, their Fe(III) complex stability is due to the concentration effect, where they are able to more effectively bind Fe(III) at lower concentrations than monohydroxamic acids.[10] This is due to the need for fewer moles of the compound to be present for a higher ratio of complex:uncomplexed metal ions. This same lack of chelate effect is noted in the desferrioxamine B system.[51] The lack of chelate effect was later confirmed by Yoshida *et al* with their work with the synthetic ferrichrome analogue, BAMTPH.[52]

In general, bacterial siderophores have been investigated for medicinal applications, such as antitumor[10,53], antimalarial,[54,55] and antibiotic agents[56–58]. Desferrioxamine (DFO) has been the most heavily studied siderophore for these applications. Similar to the fungal siderophores, DFOB, a linear bacterial siderophore produced by *Streptomyces pilosus*, contains hydroxamic acid moieties, which increase the effectiveness as an iron chelator.[59] Desferal, desferrioxamine mesylate, was approved by the FDA in the mid-20th century for the treatment of iron overload and thalassemia. Desferal helps solubilize biological iron(III), which is then excreted from the body. However, Desferal is not orally active and requires prolonged intravenous delivery.[55,59–61] Desferrioxamine is cleared from the body with a $t_{1/2}$ of 5-10 minutes. Therefore, for necessary iron excretion levels to be maintained, the intravenous delivery must be 8-12 h/day and 5-7 d/week.[59,61]

An additional application of DFO was investigated due to its potential antioxidant properties. Reactive oxygen species (ROS) are created through the oxidation of Fe(II) to Fe(III) by O_2^- or

H_2O_2 in the body. These ROS can lead to DNA damage and subsequent diseases. The rate-limiting step for this catalytic ROS production *in vivo* is the reduction of Fe(III) back to Fe(II), and DFO has been investigated for its ability to prevent Fe(III) from being reduced. The DFO fully protects the Fe(III) core from reduction by forming a octahedral binding pocket.[62] EDTA differs because it is too small to fully protect the Fe(III) core, allowing one labile water molecule to interact with the Fe(III). This water molecule is capable of exchanging with oxygen or hydrogen peroxide, leading to possible radical formation.[55,59] Additionally, the possible synthesis of an enzyme-damaging nitroxide radical upon reduction has been investigated for its potential for some of the unwanted side effects caused by long-term Desferal usage.[62] DFO has also been used to treat Al(III) overload and with ^{68}Ga(III) as an agent for radiography.[63]

The linear DFOB is a well-studied, strong chelator of Fe(III). However, the cyclic DFOE has been shown to form a more stable complex with Fe(III). As the complex forms, the three hydroxamate groups must form stable five-membered rings with the Fe(III) ion. The preorganization of the cyclic DFOE allows for this to happen with a lower change in entropy relative to linear DFOB, allowing for a more stable complex to form.[51] The cyclic siderophores, such as DFOE and ferrichrome, offer more opportunities for highly stable metal complexes.

Ferrichrome binds Fe(III) with a stability constant ~10x that of EDTA and is highly selective for the Fe(III) ion. In the presence of Cu(II) and Zn(II), the iron complex remains stable.[9] The acid hydrolysis of the complex leads to desorption of the iron ion and loss of the characteristic red complex color. However, the complex is easily reformed at higher pH and remains stable up to pH 11-12. The hydroxamic acid residues were not positively identified for several years due to a lack of literature focus on that functional group. The well-known purple color produced by Fe(III)-monohydroxamic acid complexes is not replicated by Fe(III)-ferrichrome complexes.

Instead, a yellow color is produced, indicative of a 3:1 ligand:metal complex. This is due to the presence of three hydroxamic acid residues in the ferrichrome structure.[64]

Ferrichromes are produced by nearly all known families of fungi.[10] Synthetic analogs of ferrichrome have been heavily studied for possible medicinal applications.[65–68] For example, retrohydroxamate ferrichrome (side chain reversed from typical, as shown in Figure 3.1d, to an inverted configuration, as shown in Figure 3.1f) was synthesized and shown to have little effect on Fe(III) binding affinity, but desferriretrohydroxamate ferrichrome led to the complete loss of iron transport and uptake by the cells, suggesting the necessity of structural recognition of the ferrichrome-Fe(III) complex for cellular iron uptake.[23,65,69–72] The difficulty of cyclizing peptides has hindered the synthesis of peptide analogs. In 1982, only rhodotorulic acid,[73] dimerum acid and ferrichrome[74] had been fully synthesized.[47] In contrast to the handful of peptide analogs, a large spectrum of non-peptide analogs have been synthesized by Crumbliss, Shanzer, and others.[65,66,75–79] Another major roadblock was the difficulty of synthesis of high purity hydroxamate-containing building blocks. Maurer *et al* utilized O-benzylhydroxylamines and subsequent alkylation of the open amine in the hydroxamic acid to prevent unwanted side products from forming. Using this method, they reported the synthesis of mycobactin in 1983.[47,80]

Many analogs of ferrichrome have been synthesized that incorporate hydroxamate sidechains on non-peptide scaffolds due to the difficulty of cyclizing peptides[81], leaving many fundamental questions about the coordination environment in ferrichrome unanswered. For example, why are all three chelating sidechains sequential in the peptide hexamer (AAABBB) instead of alternating with the non-coordinating residues (ABABAB)? The only two cyclic peptide analogues are retrohydroxamate ferrichrome, where the hydroxamic acid residue was inverted (i.e., Figure 3.1f instead of the natural 3.1d), and desmethylhydroxamate ferrichrome, where the methyl groups

were replaced with hydrogen atoms (Figure 3.1e instead of the natural 3.1d).[23,69,71] Retrohydroxamate ferrichrome was shown to be an indistinguishable ionophore of ferrichrome in activity toward iron-transport and bacteria growth. However, the substitution of the methyl group for a hydrogen resulted in a complete loss of iron-transport.[70,71]

The development of synthetic siderophores allowed for new approaches to the treatment of iron overload diseases.[82,83] Traditionally, these synthetic compounds were designed around the common subunits found in the naturally occurring siderophores. Several examples exist, where the structures were designed to mimic ferrichrome,[69–71,84] desferrioxamine,[15,17,53,57] or rhodotoluric acid.[73] Due to the oral inactivity and high doses needed for effectiveness of Desferal, many studies focused on the design of more efficient iron chelators. For example, several synthetic analogues of rhodotoluric acid were developed. The naturally occurring rhodotoluric acid is a dihydroxamic acid compound, which forms 3:2 complexes with iron(III) and is toxic due to water insolubility. However, the analogues that were developed were more soluble in water and had three hydroxamic acid groups, allowing for 1:1 complexes to form, thus requiring lower concentrations for effective iron binding. These compounds were shown to be active as *E. coli* growth factors through the ferrichrome mechanism, where the complex was taken into the cell and the iron(III) released through reduction to iron(II).[84,85] Several di- and trihydroxamate synthetic siderophores have been developed.[52,86–89]

Several synthetic ferrichrome analogues have been reported. The analogues are related by the inclusion of three hydroxamic acid groups bridging from a central backbone. Compounds such as BAMTPH[52] and MEDROX[83] utilize a rigid tri-substituted benzene backbone, while others, such as TRENDROX[83], TAGP, and TAGE[90,91] utilize a more flexible TREN anchor. Control of the backbone or anchor allows for direct control over the tuning of the binding pocket of the

hydroxamic acid groups.[90] Additionally, peptide analogues, such as peptoids, have the advantage of inherent biocompatibility and enable straightforward conjugation to proteins and antibodies as drug imaging agents.[31,32,34,36] These properties make peptoids an excellent target for the development of ligands for the *f*-elements, specifically the tetravalent actinides. Incorporating common chelation units found in siderophores, catechols and hydroxamic acids, into cyclic peptoid backbones allows for straightforward synthesis of siderophore analogues. Initial synthesis of hexameric cyclopeptoids with monomers allowing for incorporation of these chelation groups was performed. Ultimately, octameric cyclopeptoids, which would allowed for coordination of the larger coordination numbers of the tetravalent actinides would be synthesized.

3.2 Results and Discussion

Solid-phase peptide synthesis (SPPS) allows for straightforward synthesis of siderophore analogues through the customization of both sidechain properties (chelation units, length, flexibility, solubility) and the cyclic backbone size (hexamer, octamer). Through this route, it is possible to investigate the structural importance of side-by-side versus alternating chelating sidechains (*e.g.* AAABBB vs ABABAB). Manipulation of the sidechain and backbone length enables investigating previous claims that the atomic spacing between chelating units (specifically hydroxamic acids) plays an important role in complex stability.[86] The lack of chelate effect in polyhydroxamic acids with large spacer groups would also be easily investigated.[50,52] Finally, the solubility of peptoids is easily controlled through the incorporation of hydrophobic or hydrophilic side chains in the non-chelating residues. This property easily broadens the possible applications of these ligands from use in aqueous systems (biological/environmental) to organic systems (fuel reprocessing).

The initial consideration for the development of siderophore-inspired cyclopeptoids was how to incorporate the siderophore metal chelating units into the peptoid backbone. This was done through the synthesis of monomers which either contained the desired moieties, in this case, catechols and hydroxamic acids, or allowed for later addition or conversion to the desired moieties through off-resin chemistry after synthesis of the peptoid backbone. Protecting groups were necessary to prevent any undesired reactions of the chelating groups during synthesis of the peptoid backbone. Finally, deprotection of the protected groups needed to be achievable without destroying the rest of the ligand.

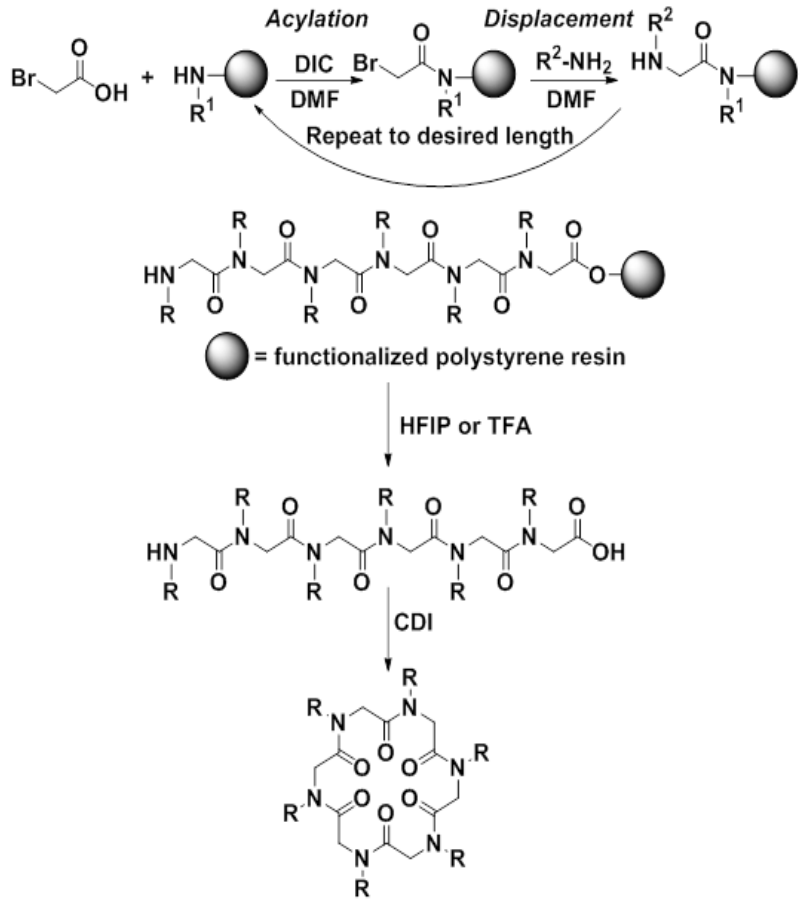

Scheme 3.1: Solid-phase synthesis followed by cleavage and cyclization of peptoids.

Peptoid backbone (SPPS and cyclization)

The submonomer method: a repeating two-step modular solid-phase peptoid synthesis (SPPS) was used for the synthesis of linear peptoids, as shown in Scheme 3.1. The two steps, acylation and halogen displacement (an S_N2 reaction), were repeated until the desired length peptoid was synthesized. The first step, acylation of the resin or peptoid chain by a haloacetic acid, used bromoacetic acid (BrAA). For all of the reported peptoids BrAA at a concentration of 0.4-1.2M was used. The BrAA was activated with *N,N'*-diisopropylcarbodiimide (DIC) and then reacted with the resin or *N*-terminus of the peptoid. This reaction was carried out for 1-5 minutes, depending on the amine residue being acylated. The second step then consisted of the displacement of the bromine with a primary amine monomer. Amine solutions at 0.25-0.75M in DMF or DMSO were used and reacted for 1-30 minutes. Each step was repeated twice to ensure complete reaction and was followed by washes with dichloromethane (DCM) and dimethylformamide (DMF). The peptoids were synthesized on chlorotrityl chloride resin (CTC, Figure 3.3), which resulted in a carboxylic acid at the *C*-terminus after cleavage, a necessity for cyclization of the peptoid chain. The peptoids were cleaved from the resin with hexafluoroisopropanol (HFIP) or trifluoroacetic acid (TFA), depending on the presence of acid-sensitive side groups. Once cleaved, the linear peptoids were cyclized with carbonyldiimidazole (CDI) in acetonitrile though an intramolecular condensation between the *C*- and *N*-termini. Subsequent off-resin chemistry was performed when necessary (see catechol and hydroxamic acid addition). The peptoids were characterized by MALDI-TOF mass spectrometry, which allowed for the identification of the desired product.

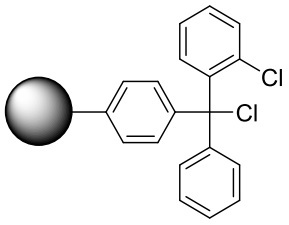

Figure 3.3: Structure of resin-bound chlorotrityl chloride.

The modular nature of SPPS allows for straightforward customization of the peptoid through the inclusion of desired properties by the monomers. For example, water-solubility may be controlled through the use of hydrophilic sidearms, such as pegylated primary amines (*e.g.* methoxypropylamine), or hydrophobic sidearms such as phenylethylamine. However, this method does suffer from several downfalls. The on-resin chemistry is limited to reactions and functional groups that will not interact with the two SPPS steps. For this reason, off-resin chemistry (pre-resin monomer synthesis, post-resin cyclization, post-resin monomer conversion/sidearm addition) is required. More detrimental is the characteristic low yield of resin cleavage. Peptoids are cleaved from resin through an acid-catalyzed cleavage. In the case of Rink Amide Resin, this cleavage is performed with trifluoroacetic acid (TFA) and produces an amide at the *C*-terminus.[22,92] CTC can be cleaved with TFA or hexafluoroisopropanol (HFIP). Cleavage with the very mild HFIP leads to retention of the side chain protecting groups, which is necessary if, for example, some of the side chains contain amines which must remain protected so that cyclization only happens with the *N*-terminus amine. Unfortunately, HFIP cleavage does not lead to good recovery of peptoid from the resin (<10%). Attempts to optimize cleavage conditions through changing the acid concentration (5-95%) and time of cleavage (5 min – 24 h) were inconclusive. A similar study utilizing TFA led to the same inconclusive results. Additionally, the CTC resin is capable of exchanging the reactive chloride residues for a less reactive hydroxide through

interaction with water in the air, drastically decreasing the loading capacity of the resin. The CTC resin can be regenerated through reaction with a reactive chloride, such as thionyl chloride and will potentially increase loading capacity and yield.

Catecholates

Incorporation of catechols into a peptoid backbone was accomplished by first synthesizing peptoids with mono-*N*-Boc-protected diamine sidechains. The diamine monomers were varied to investigate the effect of changing flexibility and the binding pocket of the chelating units. The Boc-protection group prevented reaction between the free amine and the bromoacetic acid used during peptoid synthesis. Cleavage of the peptoid from the resin was performed with hexafluoro-2-propanol (HFIP, pKa=9.3), rather than trifluoroacetic acid (TFA, pKa=0.25), to prevent the premature cleavage of the Boc-groups. After cyclization of the backbone with CDI, the Boc-group was removed with TFA.

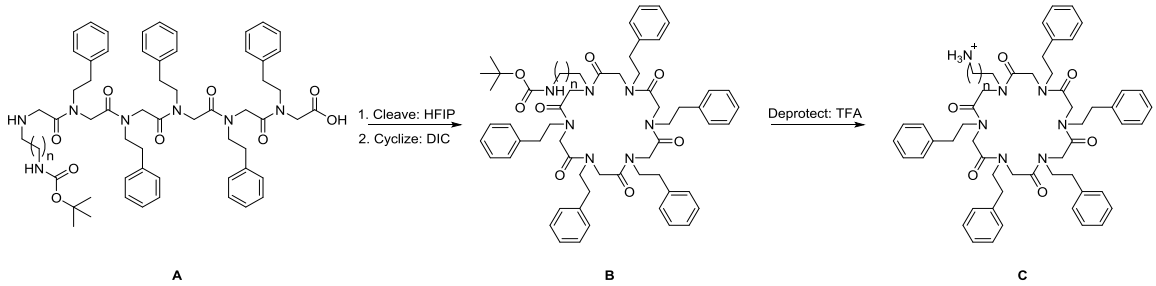

Scheme 3.2: Structure of a hexameric peptoid containing five phenylethylamine (Phe) residues and one diamine residue (n = 2, 3, 4). A) The diamine is mono-*N*-Boc protected when added to the peptoid on resin. B) The peptoid is cleaved from the resin with HFIP, leaving the Boc-group intact. The peptoid is then cyclized with CDI. C) The Boc-group is removed by TFA.

The catechol unit was incorporated by reaction of 2,3-dihydroxybenzoic acid with the liberated amine groups on the previously-cyclized peptoid. First, the carboxylic acid on 2,3-

dihydroxybenzoic acid was activated using *N*-hydroxysuccinamide (NHS) and dicyclohexylcarbodiimide (DCC), as shown in Scheme 3.3.[93] This activation allowed for the coupling of the catechol to the deprotected amine residues in the cyclic peptoid backbone, while avoiding the laborious protection and deprotection of the phenolic oxygens typically practiced in the field. The NHS-protecting group suffered low stability and consequently required immediate use once synthesized.

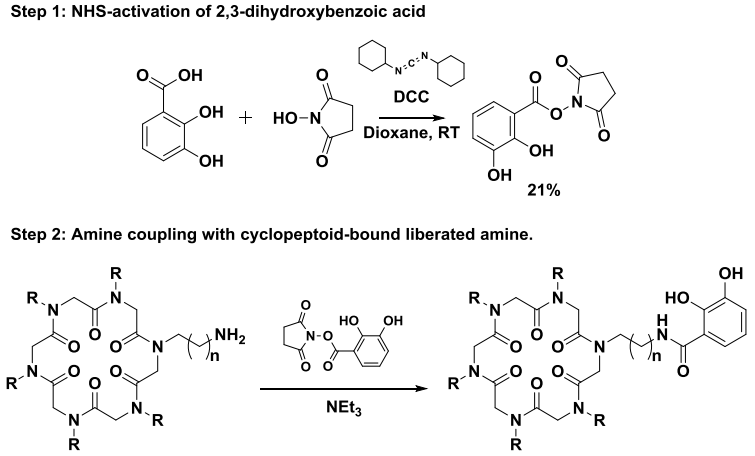

Scheme 3.3: Off-resin chemistry for catechol incorporation into peptoids. Step 1: NHS-activation of catechol for subsequent addition to amine residue (n = 2, 3, 4) on cyclic peptoid backbone, Step 2.

Two Boc-protected diamines were added to a cyclic peptoid backbone, *tert*-butyl-*N*-(2-aminobutyl)carbamate (4CDiamine) and *tert*-butyl-*N*-(2-aminoethyl)carbamate (2CDiamine). The synthesized ligands can be seen in Table 3.1 and Figure 3.4. All peptoids in this series were synthesized with phenylethylamine residues to increase organic solubility, allowing straightforward purification after cyclization with CDI by liquid-liquid extraction. NHS-dihydroxybenzoic acid was successfully added to one peptoid, (4CDiamine)-Phe_5 (Figure 3.5). This peptoid was characterized by MALDI-TOF (Figure 3.4). The small quantity did not allow for further testing of the product.

Table 3.1. Peptoid hexamers and octamers containing catecholate precursors synthesized, cyclized, and converted to final ligand forms to date. Phe = phenylethylamine, 4CDiamine = *tert*-butyl-*N*-(4-aminobutyl)carbamate, and 2CDiamine = *tert*-butyl-*N*-(2-aminoethyl)carbamate.

Peptoid	Linear	Cyclic	Catechol
(4CDiamine)-Phe_5	Yes	Yes	Yes
$(4CDiamine)_3$-Phe_3	Yes	Yes	No
$(4CDiamine\text{-}Phe)_3$	Yes	Yes	No
$(4CDiamine)_6$	Yes	Yes	No
$(4CDiamine)_8$	Yes	Yes	No
$(4CDiamine)_4$-Phe_4	Yes	Yes	No
$(4CDiamine\text{-}Phe)_4$	Yes	Yes	No
$(2CDiamine)_6$	Yes	Yes	No
(2CDiamine)-Phe_5	Yes	Yes	No
$(2CDiamine)_3$-Phe_3	Yes	Yes	No
$(2CDiamine\text{-}Phe)_3$	Yes	Yes	No

Table 3.2. MALDI-TOF results for peptoids containing catecholate precursor residues. All data collected with HCCA matrix and is reported as m/z. All data presented as m/z in positive mode. Values indicate the product + H^+ and + Na^+.

	Linear		Cyclic		Deprotected	
Peptoid	Calc	Obsd	Calc	Obsd	Calc	Obsd
(4CDiamine)-Phe_5	1051.6	1052, 1074	1033.6	1033, 1056	933.5	934, 956
$(4CDiamine)_3$-Phe_3	1185.7	1186, 1208	1167.7	1169, 1191	867.5	868, 890
$(4CDiamine\text{-}Phe)_3$	1185.7	1186, 1208	1167.7	1169, 1191	867.5	868, 890
$(4CDiamine)_6$	1386.9	1388, 1410	1368.9	1370, 1392	768.6	770, 792
$(4CDiamine)_8$	1814.3	1815, 1837	1796.3	1797, 1819	995.5	996, 1018
$(4CDiamine)_4$-Phe_4	1643.1	1644, 1666	1625.1	1626, 1648	1324.8	1326, 1348
$(4CDiamine\text{-}Phe)_4$	1643.1	1644, 1666	1625.1	1626, 1648	1324.8	1326, 1348
$(2CDiamine)_6$	1219.4	1220, 1242	1201.4	1202, 1224	600.8	602, 624
(2CDiamine)-Phe_5	1023.5	1024, 1046	1005.5	1006, 1028	905.5	907, 928
$(2CDiamine)_3$-Phe_3	1101.6	1102, 1124	801.5	802, 824	783.4	784, 807
$(2CDiamine\text{-}Phe)_3$	1101.6	1102, 1124	801.5	802, 824	783.4	784, 807

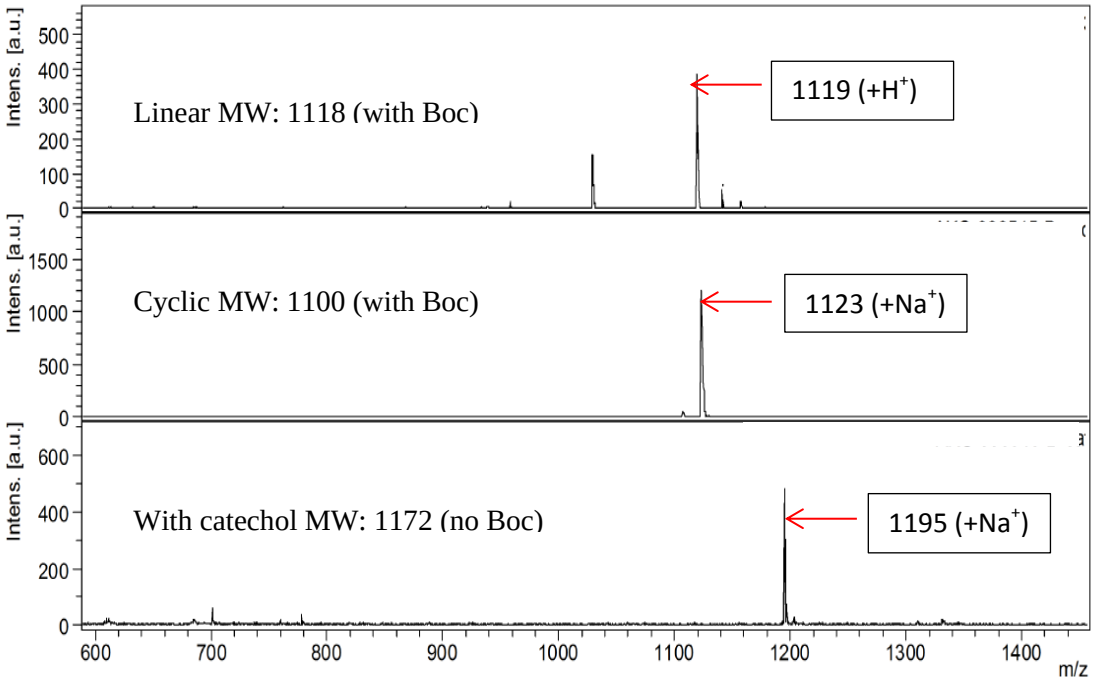

Figure 3.4: MALDI-TOF spectra of (top): linear (4CDiamine)-$(Phe)_5$, (middle) cyclized (4CDiamine)-$(Phe)_5$, and (bottom) cat-(4CDiamine)-$(Phe)_5$.

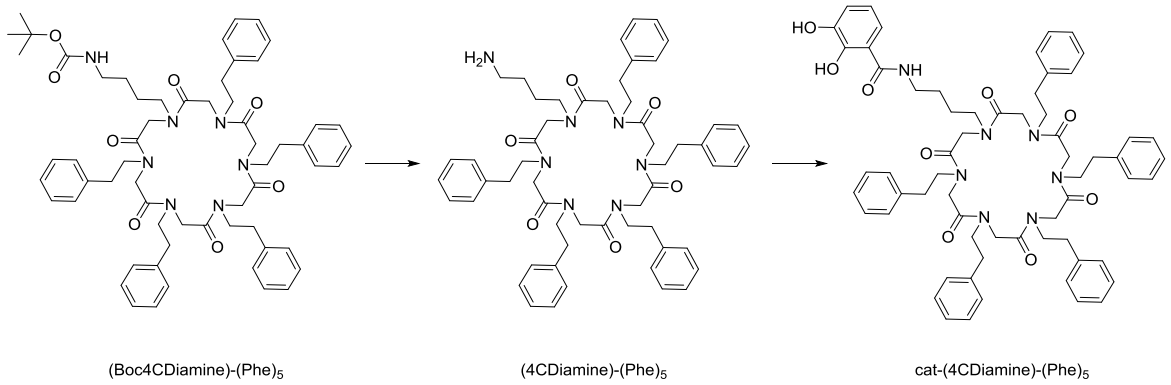

Scheme 3.4: Conversion from Boc-protected sidearm (left) to primary amine (middle) to catechol.

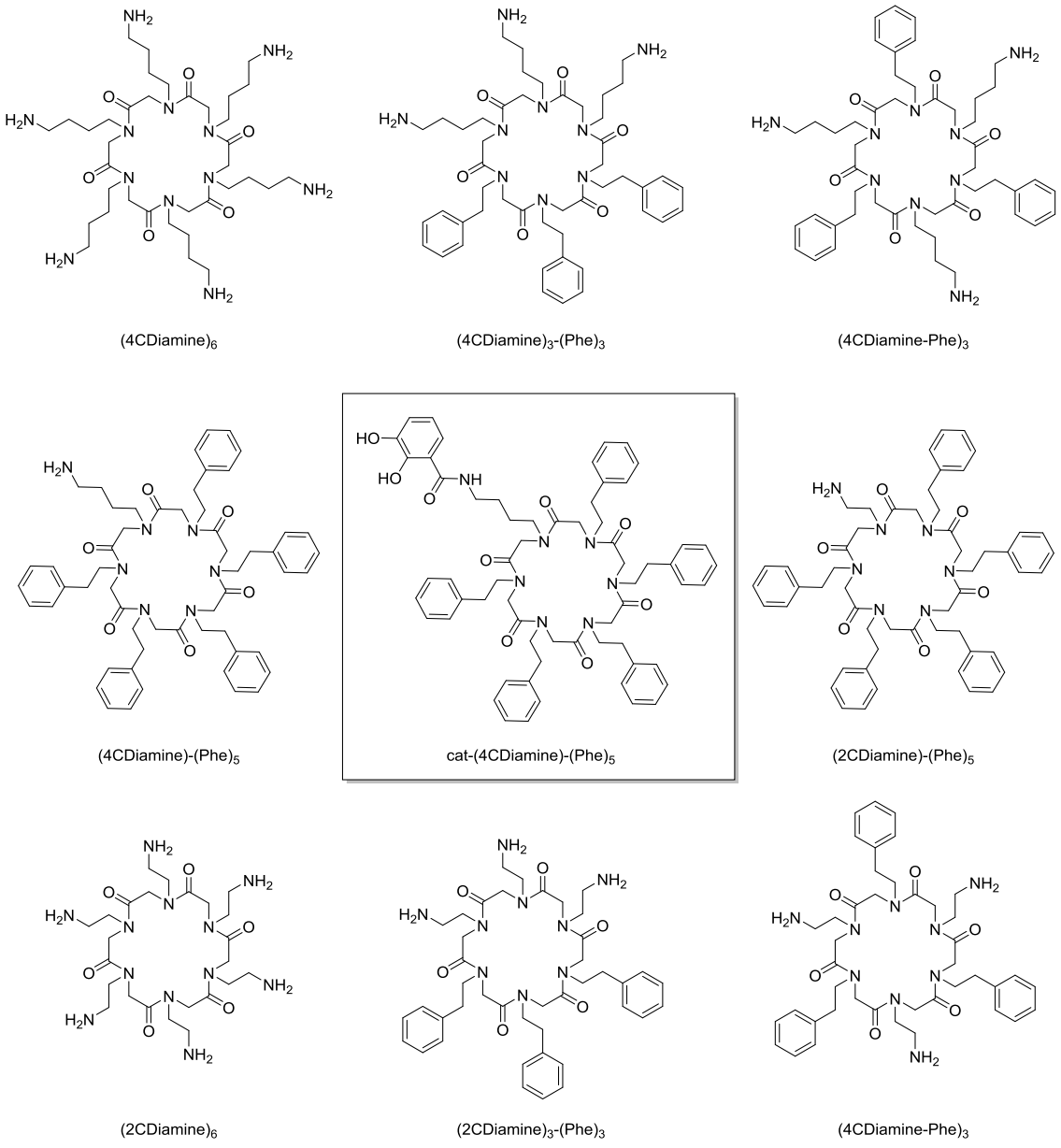

Figure 3.5: Successfully synthesized cyclopeptoids containing catechol-precursors, or catechol residues. Octamers are not shown.

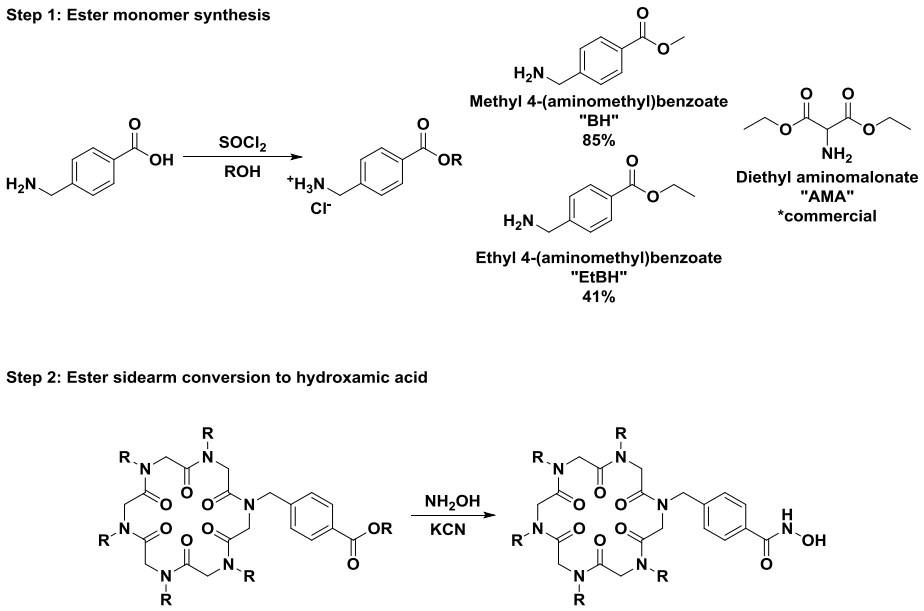

Scheme 3.5: Off-resin chemistry for hydroxamate-containing peptoids. Step 1: synthesis of hydroxamate precursor monomers through conversion of carboxylic acids to esters with thionyl chloride. Step 2: conversion of ester to hydroxamate on a cyclic peptoid backbone.

Hydroxamates

Two methods were investigated for the incorporation of hydroxamic acids into cyclic peptoid backbones. The first attempt involved utilizing monomers containing esters, which were then reacted with hydroxylamine after the peptoid had been cyclized, to give the hydroxamic acid. Such ester-to-hydroxamic acid conversions are common in the hydroxamate literature, albeit most commonly with monohydroxamates where low conversion yields are not problematic. Substituted benzoic acid precursors were converted from carboxylic acids to esters using thionyl chloride, as shown in Scheme 3.5.[94] 4-(aminomethyl)benzoic acid was converted into the methyl ester (BH) and ethyl ester (EtBH) through reactions with the corresponding alcohol. A third hydroxamate precursor, diethyl aminomalonate hydrochloride salt (AMA) was bought commercially and used without further purification. The BH and EtBH amines were obtained as

HCl salts after synthesis. The presence of the chloride counterion resulted in the conversion of the reactive bromoacetyl to a more inert chloroacetyl. This inactivation was countered using catalytic potassium iodide and longer reaction times during the SPPS acylation step (30 min).

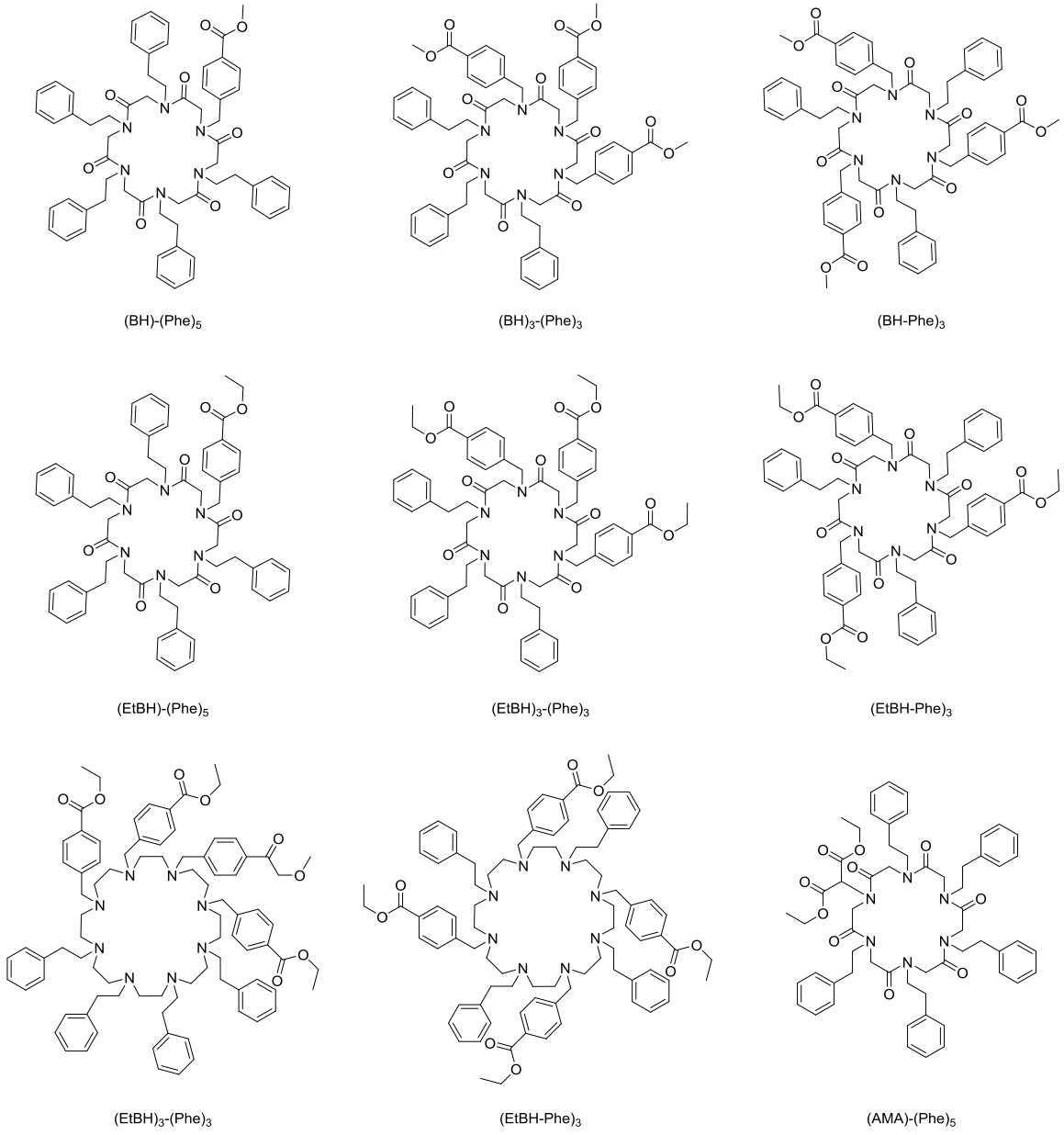

Figure 3.6: Successfully synthesized hexa- and octa-cyclopeptoids containing ester monomers.

The monomer synthesis was hindered by nearly-intractable solubility issues with aminomethyl benzoic acid, due to its ability to exist in a zwitterionic state that is difficult to solubilize. The ester product (BH, EtBH) also had low solubility in DMF, the solvent used for SPPS. A mixture of DMF/dimethylsulfoxide (DMSO) was used to dissolve the monomer, catalytic iodide and sodium carbonate, for deprotection of the ammonium salt formed during ester formation. The solubility issues limited peptoid loading efficiency, along with the issues mentioned above.

Once the peptoid was cyclized, the esters were converted to hydroxamic acids through a reaction with hydroxylamine and catalytic potassium cyanide (KCN), as shown in Scheme 3.5. The catalytic KCN supposedly led to an acyl-cyanide intermediate, followed by nucleophilic substitution by an amine.[94] This method was followed, after several trials with the traditional hydroxamic acid synthesis from esters, which involved the reaction with hydroxylamine hydrochloride, due to the low efficiency of this conversion.[95,96] The need to convert multiple residues on one molecule required the highest possible efficiency, due to difficult purification and low yields of the final product. Unfortunately, the use of KCN still led to a mixture of the hydroxamate and carboxylate products, a recognized, but understated issue in the literature when it comes to polyhydroxamic acids.

An additional monomer, diethyl aminomalonate (AMA) was investigated (Scheme 3.5). When this amine was used as the terminal residue during synthesis, an AMA-$(Phe)_5$ peptoid was successfully synthesized, cleaved and cyclized (Figure 3.6). When AMA was used in any position other than the terminal amine, the desired product did not form. The formation of a diketopiperazine (DKP) occurred through reaction between subsequent amine residues and the ester arm of the AMA residue (Scheme 3.6). The formation of a DKP prevents any subsequent

addition of amines or cyclization of the peptoid, severely limiting the use of AMA for peptoid design.

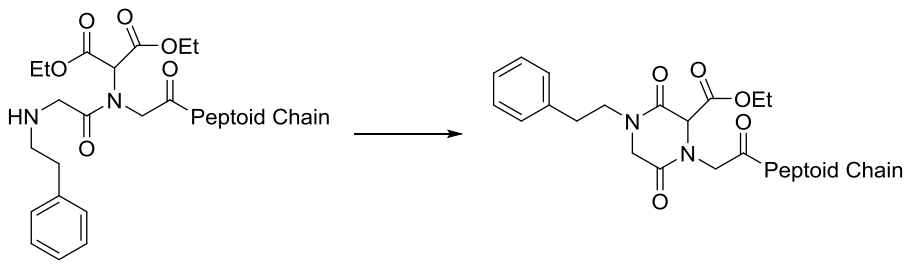

Scheme 3.6. Diketopiperazine formation by AMA during SPPS.

Table 3.3: Peptoid hexamers and octamers containing ester monomers for conversion to hydroxamic acid moieties. BH = methyl 4-(aminomethyl)benzoate, EtBH = ethyl 4-(aminomethyl)beozoate, AMA = diethyl aminomalonate, Phe = phenylethylamine, MPA = methoxypropylamine.

Peptoid	Linear	Cyclic	Hydroxamate
BH-Phe_5	Yes	Yes	Yes*
$(BH)_3$-$(Phe)_3$	Yes	Yes	No
$(BH\text{-}Phe)_3$	Yes	Yes	No
EtBH-Phe_5	Yes	Yes	No
$(EtBH)_3$-$(Phe)_3$	Yes	Yes	Yes*
$(EtBH\text{-}Phe)_3$	Yes	Yes	No
$(EtBH)_4$-$(Phe)_4$	Yes	Yes	Yes*
$(EtBH\text{-}Phe)_4$	Yes	Yes	No
(AMA)-$(Phe)_5$	Yes	Yes	No

*The final product was an impure mixture of compounds (-C(O)OH, -C(O)NHOH, etc)

Table 3.3 and Figure 3.6 show the ester-containing peptoid oligomers that were synthesized and cyclized. Along with hexamers, several octamer peptoids have been synthesized to

incorporate four bidentate ligand arms for actinide coordination as well as hexamers designed for aqueous solubility through the presence of methoxypropylamine (MPA) sidechains rather than phenylethylamine.

Table 3.4. MALDI-TOF results for peptoid hexamers and octamers containing ester monomers for conversion to hydroxamic acid moieties. All data presented as m/z in positive mode. Values indicate the product + H^+ and + Na^+.

	Linear		Cyclic		Hydroxamate	
Peptoid	Calc	Obsd	Calc	Obsd	Calc	Obsd
BH-Phe_5	1029.5	1029, 1051	1010.5	1033, 1049	1011.5	1012, 1034*
$(BH)_3$-$(Phe)_3$	1116.5	1117, 1139	1098.5	1100, 1122	1102.4	No
$(BH\text{-}Phe)_3$	1116.5	1117, 1139	1098.5	1100, 1122	1102.4	No
EtBH-Phe_5	1042.5	1043, 1065	1024.5	1026, 1048	1011.5	No
$(EtBH)_3$-$(Phe)_3$	1117.3	1118, 1140	1099.3	1100, 1122	1102.2	1103, 1125*
$(EtBH\text{-}Phe)_3$	1117.3	1118, 1140	1099.3	1100, 1122	1102.2	No
$(EtBH)_4$-$(Phe)_4$	1538.7	1540, 1562	1520.7	1522, 1544	1468.6	1470, 1492*
$(EtBH\text{-}Phe)_4$	1538.7	1540, 1562	1520.7	1522, 1544	1468.6	No
(AMA)-$(Phe)_5$	1038.5	1061, 1077	1020.5	1043, 1077	994.5	No

*The final product was an impure mixture of compounds (-C(O)OH, -C(O)NHOH, etc). Only C(O)NHOH listed.

A second route was investigated, in an attempt to avoid conversion issues of polyhydroxamic acids, along with solubility issues. This method involved the synthesis of amino acid-based monomers with *O*-tert-butylbenzyl hydroxamic acid. The use of the *O*-protected hydroxamic acid prevented decomposition of the hydroxamic acid into carboxylic acid, and interaction of the unit

in sub sequent chemistry and allowed for more straightforward characterization and purification of the product.[89,97,98] *O*-tert-butylbenzyl hydroxylamine was synthesized through a reaction of tert-butylbenzyl bromide and *N*-hydroxyphthalimide (Scheme 3.7, 1), followed by deprotection of the phthalimide group with excess hydrazine (Scheme 3.7, 2; see further discussion of this route in the subsequent chapter).[99–102]

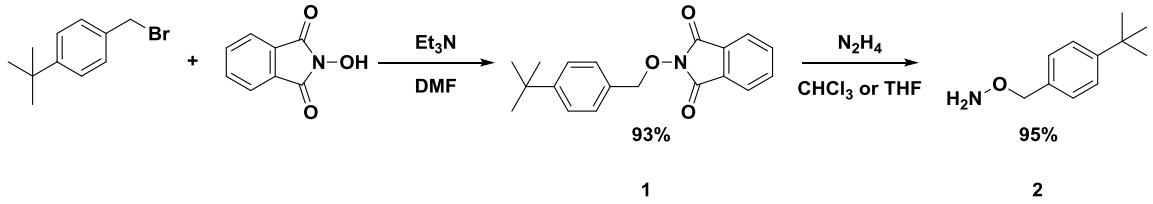

Scheme 3.7. Synthesis of *O*-tert-butylbenzyl hydroxylamine.

Amino acids were used due to the presence of a primary amine, for incorporation into a peptoid, and a carboxylic acid for conversion to the hydroxamic acid. The target amino acids were glycine (Gly), β-alanine (β-Ala), and γ-aminobutyric acid (GABA) (Figure 3.7). In order to convert the carboxylic acid into an *O*-protected hydroxamic acid, protection of the nitrogen was required. The use of three amino-protecting groups was attempted, including phthalimide, Boc, and Fmoc.

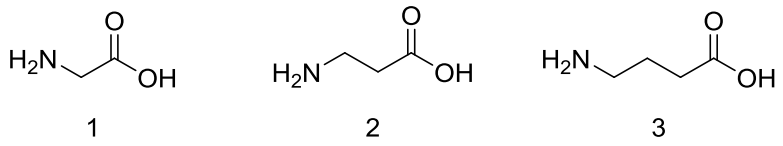

Figure 3.7. Structures of 1) glycine, 2) β-alanine, and 3) γ-aminobutyric acid.

Due to the success with using the phthalimide protecting group during the synthesis of protected hydroxylamines, this group was initially investigated. The target amino acid and phthalic anhydride were melted and refluxed gently for four hours. Upon cooling, a white solid

was formed, which was purified through recrystallization with water (Scheme 3.8, Step 1).[103] This reaction was successfully carried out with β-Ala and GABA. The *N*-phthalic amino acids were then converted to their corresponding acid chlorides through reflux with thionyl chloride in dichloromethane, followed by nucleophilic acyl substitution with the *O*-tert-butylbenzyl hydroxylamine (Scheme 3.8, Step 2). The final step required deprotection of the phthalimide group to give a primary amine group, which would allow for use in SPPS. Unfortunately, the hydroxamic acid unit was susceptible to acid- and base-catalyzed deprotection and/or decomposition into carboxylic acids. The hydrazine deprotection conditions used for the *O-tert-butyl hydroxylamine* synthesis were too harsh for the hydroxamic acid group. NMR and TLC showed evidence of removal of the hydroxamic acid group along with deprotection of the phthalimide group. Conditions were altered to use stoichiometric hydrazine, rather than excess, but this method still led to a mixture of products (Scheme 3.8, Step 3).

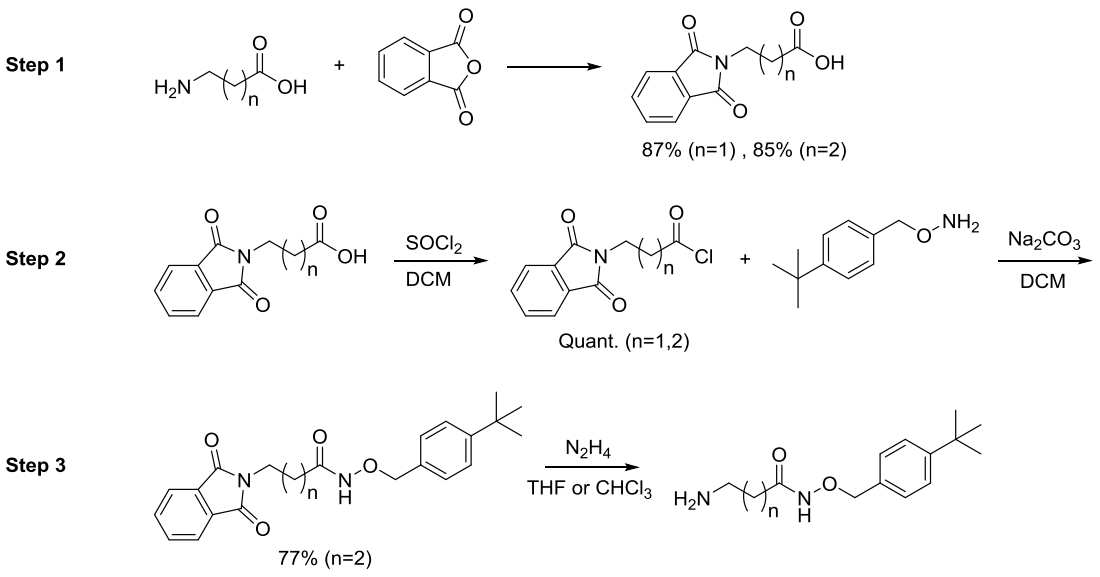

Scheme 3.8: Hydroxamate-amino acid derivative synthesis through phthalimide protection of the amine group.

The Boc protecting group can be removed in mildly acidic conditions, which would possibly allow for deprotection without removing the hydroxamic acid. Di-tert-butyl dicarbonate was reacted with the amino acid and a mild base to protect the amine terminus (Scheme 3.9, Step 1). Once the Boc group was present, the carboxylic acid was converted to an acid chloride, the *O*-protected hydroxylamine added to form a hydroxamic acid, and the Boc group removed by TFA (Scheme 3.9, Step 2). Unfortunately, the acylation of the carboxylic acid by thionyl chloride resulted in the premature removal of the Boc group. In an attempt to circumvent the issue, efforts to activate the carboxylic acid through reaction with a carbodiimide, dicyclohexylcarbodiimide (DCC) or 1-ethyl-3-(3-dimethylaminopropyl)carbodiimide (EDC) (Scheme 3.9, Step 3). The activation by carbodiimide produces a urea sideproduct. DCC produces a solid urea, which is removed by filtration. However, trace amounts of DCC can remain in the product and are difficult to fully remove. EDC produces a water-soluble urea, which could be removed by extraction. Neither activating group led to clean addition of the *O*-tert-butyl hydroxylamine. Removal of the urea sideproduct by filtration or extraction was not successful.

The use of the Fmoc and Boc protecting groups is common in peptide and peptoid synthesis. Once the Boc group was ruled out as a possibility, the Fmoc group was investigated. Initial attempts to synthesize Fmoc-GABA required purification through column chromatography and proved difficult,[104] but fortunately unnecessary because both Fmoc-GABA-OH and Fmoc-β-Ala are commercially available, making this route more attractive than the phthalimide and Boc routes. The Fmoc-amino acids were acylated by thionyl chloride, followed by substituted by the *O*-tert-butyl hydroxylamine.[105] The final step required the deprotection of the Fmoc group by 4-methylpiperidine followed by purification by column chromatography. While the final step was successful, optimization is necessary for large scale synthesis and subsequent use in SPPS.

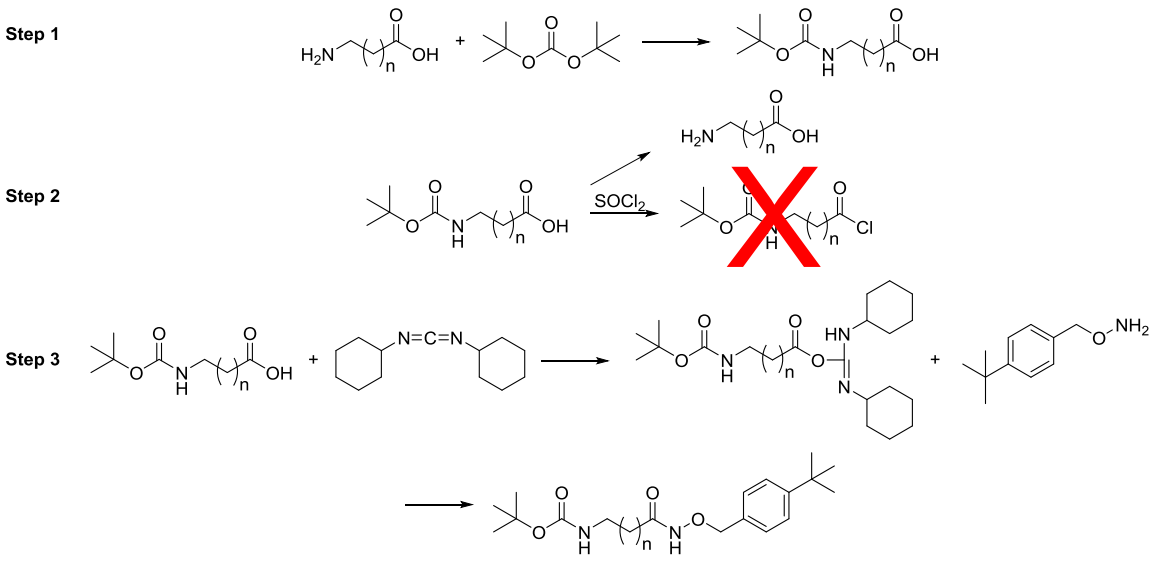

Scheme 3.9: Boc-protected amino acid synthesis of hydroxamic acid monomers. Step 1: *N*-Boc protection of amino acid, Step 2: Acylation of the carboxylic acid led to deprotection of the Boc group instead of acylation, Step 3: Activation of the carboxylic acid by carbodiimide (DCC is shown) and *O*-tert-butyl hydroxylamine.

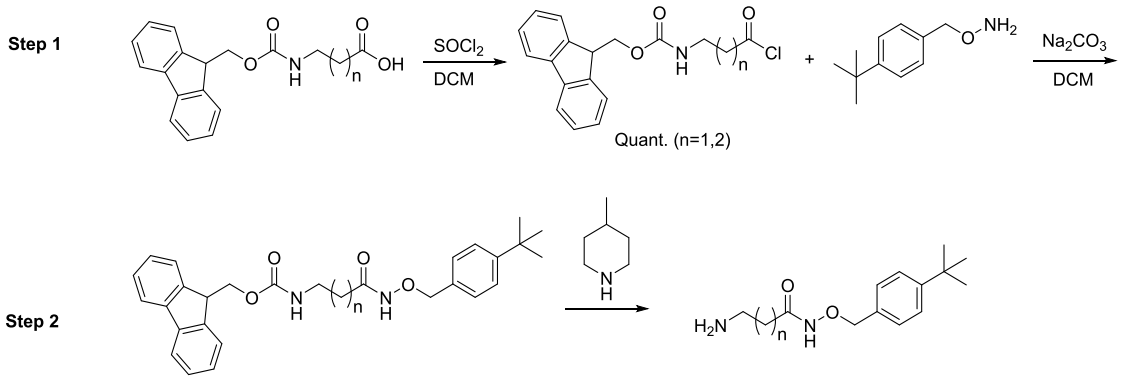

Scheme 3.10: Fmoc-amino acid synthesis of hydroxamic acid monomers. Step 1: Conversion of Fmoc-AA-OH to Fmoc-AA-Cl and reaction with *O*-protected hydroxylamine . Step 2: Deprotection of Fmoc group with 4-methylpiperidine.

The most promising route toward amino acids containing an *O*-protected hydroxamic acid group is shown in Scheme 3.10. The Fmoc protected amino acids are commercially available, obviating a step which was necessary for the phthalimide and Boc routes. The Fmoc group is

stable to the acidic conditions necessary for conversion of the carboxylic acid into an acyl chloride, which is necessary for addition of the hydroxylamine and formation of the hydroxamic acid. The Fmoc group also allows for straightforward purification through chromatography. However, the final step, deprotection of the Fmoc group, requires optimization. Large scale synthesis of the amino acid monomers would allow for use in SPPS.

3.3 Conclusions

Peptoids offer a unique opportunity for straightforward customization of large macrocyclic molecules with biological relevance. Inspiration taken from natural siderophores, such as ferrichrome and enterobactin, was the driving force for the design of cyclopeptoids containing catechol and hydroxamic acid chelating groups. By incorporating these units into a cyclic peptoid backbone, not only could a new class of ligands be developed, but several structural properties could be investigated. Peptoid synthesis utilizes primary amines, allowing for manipulation of properties, such as the order of chelating residues (AAABBB versus ABABAB), size of the backbone (hexamer versus octamer), length of the sidechains, and solubility. Through manipulation of these properties, strict control over the topology of the binding pocket is possible, allowing for the targeting of specific metals, specifically the tetravalent actinides.

A catechol monomer cannot be directly used in SPPS without extremely laborious orthogonal protecting groups due to interaction with the reagents during the backbone synthesis. However, by using a mono-*N*-Boc protected diamine, it was possible to synthesize and cyclize a peptoid chain with available sites for subsequent catechol conjugation. NHS-activated 2,3-dihydroxybenzoic acid was successfully added to the peptoid through reaction with the previously Boc protected amine—a hexamer containing one catechol group was successfully synthesized, as shown by MALDI-TOF. Optimization of the NHS-activation is necessary to push this route

forward. However, the initial step of synthesizing cyclopeptoids with open amines has been successful, as shown in Table 3.1 and Figure 3.5.

The incorporation of multiple hydroxamic acids into a peptoid required investigation of multiple synthetic approaches. The synthesis of hydroxamic acids from various functional groups, such as carboxylic acids and esters is well-known, with low-to-moderate yields, particularly for monohydroxamic acids. However, the conversion of multiple esters into hydroxamic acids, Scheme 3.5, did not prove successful. The ester monomer derivative of aminomethyl benzoic acid was plagued by solubility issues, which lowered the synthetic efficiency. Additionally, the conversion from ester to hydroxamic acid did not proceed cleanly and led to a mixture of products, including the ester staring material, hydroxamic acid product and carboxylic acid. Purification of resulting peptoids of molecular weights ~1000-2000 with a mixture of carboxylic and hydroxamic acids is quite complicated. Coupled with the low yield of peptoid cleavage from resin, this problem was not easily resolved.

In response, a new method was devised, which aimed to incorporate the hydroxamic acid group into the synthesis of the cyclopeptoid by use of an *O*-protected hydroxylamine. The conversion of an amino acid to the corresponding hydroxamic acid derivative required protection of the amine residue. Several protecting groups were attempted, phthalimide, Boc and Fmoc. Each protecting group was successfully used to protect the amino acids β-alanine and γ-aminobutyric acid. The phthalimide-amino acids and Fmoc-amino acids were subsequently converted to their corresponding acid chlorides, followed by addition of the *O*-protected hydroxylamine. The Boc group was removed upon attempts to convert the amino acids to the acid chloride. Deprotection of the phthalimide group removed the hydroxamic acid instead. The most promising route was through the use of the Fmoc amino acids, as shown in Scheme 3.10.

Optimization of the final deprotection of the Fmoc amine will allow for direct use in SPPS. Once the peptoid has been synthesized and cyclized, removal of the benzyl groups through hydrogenation will lead to hydroxamic acids.

3.4 Future Directions

Two promising routes toward siderophore-inspired cyclopeptoids were developed. Once the routes are optimized, forward progress will involve study of the stability constants of complex formation with various metals, primarily Fe(III) for the hexameric peptoids, and Ln(III) and/or An(IV) for the octameric peptoids.

Complex formation with transition metals and tetravalent actinides

Initially, complexes should be synthesized with the peptoids and first row transition metals, Fe(III), Cu(II) and Co(II). These non-radioactive complexes will be easier to characterize and can be compared to a wide body of literature on metal-hydroxamate and –catecholate complexes. Fe(III) is especially well known for forming various colored complexes with both hydroxamates and catecholates, which will allow for rapid visual validation of coordination by the peptoids which is particularly important given the small scales of peptoid chemistry.[106,107] Complexes will be formed through equimolar reactions of the metal and peptoid. The use of hydroxamate- and catecholate-containing sidearms will likely lead to interaction between the peptoid and metal ions, similar to those seen with siderophores such as ferrichrome and enterobactin (Figure 3.1). Actinide complexes using Th(IV) and U(IV) will be synthesized in aqueous conditions using water-soluble peptoids with methoxypropylamine sidechains using standard literature methods.[108,109]

Selectivity for various metal ions can be achieved by tuning the length of the cyclic backbone and controlling the placement and number of metal-binding residues. For the higher coordination numbers of the actinides, octamers will be used, which will allow for the incorporation of more hydroxamate or catecholate residues. The solubility will also be controlled through the use of phenylethylamine or methoxypropylamine residues.

Characterization of peptoid complexes

The peptoid-metal complexes can be characterized by UV-vis, FTIR, and NMR. Ultimately, diffraction quality crystals will be studied, if they can be grown. Once the interaction of the peptoids with the early transition metals is understood, complexation with tetravalent actinides, Th(IV) and U(IV), will be performed. The solution thermodynamics will be studied through potentiometric titrations, which will also allow for study of the complexation in complex environments, similar to those that actinides are often found in, such as ocean water or nuclear waste. Computational geometry optimization will further enhance understanding of how to best control selectivity in ligand design.

3.5 Experimental

Chemicals: 2-Chlorotrityl chloride resin was obtained from Aapptec. Bromoacetic acid, DIEA, 4-(aminomethyl)benzoic acid, *N*-hydroxyphthalimide, triethylamine, *N*,*N*'-carbonyldiimidazole (CDI), and γ-GABA were obtained from Chem-Impex. DMF was from BDH Chemicals. DCM was from Fisher Scientific. DIC, HFIP, TFA, p-tert-butylbenzyl bromide and β-alanine were obtained from Oakwood Chemicals. 2-Phenylethylamine was from Alfa Aesar. Hydrazine monohydrate was from Beantown Chemicals. Fmoc-β-Ala and fmoc-γ-GABA were from AK Scientific.

Solid-phase peptoid synthesis. All peptoids were synthesized manually with SPPS methods on chlorotrityl chloride (CTC) resin with 0.51 mmol/g. CTC resin (1 gram) was swollen in DCM (10 mL, 5 min) with stirring. The resin was activated through the addition of bromoacetic acid (BrAA, 0.13 M, 10 mL) and diisopropylethylamine (DIEA, 0.9 mL) for 60 minutes. This was performed two times. The resin was washed with DCM x3, DMF x3, DCM x3, MeOH x3 to remove unreacted BrAA and to cap unreacted sites on the resin. The resin was swelled again (DCM, 10 mL, 5 min) before addition of an amine. Amine solution concentrations were varied depending on the amine (0.25 – 1.5 M) and the amines were stirred with the activated resin for various times (1 – 30 min). This step was performed twice to ensure optimal reaction. Following the amine step, the resin was washed with DMF (3x). The amine was then acylated through reaction with BrAA (0.5 M, 10 mL, 1 – 30 min) and DIC (0.640 mL). The acylation step was dependent on the amine. The peptoid was built to a desired length by repeating the addition of amine, followed by acylation by BrAA and DIC activation. Each step was repeated twice to increase yield and purity. Each step was followed by washing with DMF (3x). The synthetic scheme is shown in Scheme 3.1. The specific reaction conditions are listed in Table 3.5.

Table 3.5. Synthetic conditions of various amines for SPPS.

Amine	BrAA (M)	BrAA (min)	Amine (M)	Amine (min)
Phe	0.4	1	0.5	1
AMA	0.4	1	0.75	30
BH	0.4	1	0.75	30
EtBH	0.4	1	0.75	30
4CDiamine	0.4	1	0.25	30
2CDiamine	0.4	1	0.25	30

Peptoid cleavage. A test cleavage of each peptoid was performed for preliminary identification by MALDI. A small amount of resin was stirred in a mixture of 80% HFIP/DCM for 10 min. The solvent was dried down by nitrogen and the resin was resuspended in 90% ACN/water and filtered for testing. Full cleavage was carried out by stirring the resin in 10 mL of 80%

HFIP/DCM or 5% TFA/DCM for 1 hour. This was performed twice. The solution was removed from the resin and dried down. The cleavage conditions were changed depending on the presence of acid-sensitive protecting groups (Boc).

Peptoid cyclization. The cleaved peptoid was dissolved in DCM and stirred for 18 hours with excess CDI (3 eq). The product was purified by washing with water (3x) and dried over sodium sulfate. The solvent was removed *in vacuo.*

Monomer synthesis.

Methyl- and ethyl-4(aminomethyl)benzoate (BH and EtBH): 4-(aminomethyl)benzoic acid (AMBA) (1 eq) was dissolved in the corresponding alcohol (methanol or ethanol) and excess thionyl chloride. The reaction was refluxed overnight. The solvent was removed *in vacuo* to give a white solid product.

BH: ^{1}H NMR (500 MHz, D_2O): 8.04-8.02 δ (d, *J* = 8.30 Hz, 2H), 7.54-7.52 δ (d, *J* = 8.30 Hz, 2H), 4.23 δ (s, 2H), 3.90 δ (s, 3H). ^{13}C NMR (500 MHz, D_2O): 138.0 δ, 130.2 δ, 129.0 δ, 52.8 δ, 42.7 δ. 85% yield.

EtBH: ^{1}H NMR (500 MHz, D_2O): 8.07-8.05 δ (d, *J* = 8.30 Hz, 2H), 7.55-7.54 δ (d, *J* = 8.30 Hz, 2H), 4.40-4.36 δ (m, *J* = 7.13 Hz, 2H), 4.25 δ (s, 2H), 1.38-1.35 δ (t, *J* = 7.17 Hz, 3H). 41% yield.

Hydroxamate synthesis

BH/EtBH Residues: The cyclized peptoid containing BH or EtBH residues was reacted with excess hydroxylamine hydrochloride and catalytic potassium cyanide in dichloromethane overnight at room temperature.

***O*-tert-butyl hydrodroxylamine**: Step 1: Minimal N,N-dimethylformamide (300 mL) was used to dissolve *N*-hydroxylphthalimide (1 eq, 24.4 g) in a round-bottom flask, resulting in a yellow solution. Slowly, triethylamine (1 eq, 20.9 mL) was added to the reaction, which turned the reaction mixture dark red. 4-t-butylbenzyl bromide (1 eq, 27.5 mL) was then added. After less than a minute, the reaction began to lighten, as solid began to form. The reaction was stirred at room temperature under ambient conditions. After 48 hours, enough solid was present to give the reaction an orange hue. The volume was doubled with deionized water, precipitating the product as a white solid, which was collected by vacuum and dried (43.4 g, 94%). ^{1}H NMR (500 MHz, DMSO): 7.19-7.17 δ (d, *J* = 10.25 Hz, 2 H), 6.86-6.84 δ (d, *J* = 10.25, 2 H), 3.73 δ (s, 2 H), 1.50 δ (s, 9 H). ^{13}C NMR (500 MHz, DMSO): 156.6 δ, 156.3 δ, 129.5 δ, 129.4 δ, 129.0 δ, 128.9 δ, 126.4 δ, 126.3 δ, 115.5 δ, 67.0 δ, 45.9 δ, 44.6 δ, 28.4 δ, 27.7 δ.

Step 2: Hydrazine monohydrate (10 eq, 130 mL) was slowly added to a solution of **1** (1 eq, 41.4 g) in chloroform (400 mL). The reaction mixture was stirred under reflux. Hydrazine was added every eight hours, three times for a total of 30 eq. After 24 hours, the reaction was cooled and the product extracted into dichloromethane three times, then dried over anhydrous sodium sulfate. The solvent was removed under reduced pressure, resulting in a viscous, colorless liquid (23.5 g, 98%). ^{1}H NMR (500 MHz, DMSO): 7.37-7.33 δ (t, *J* = 8.31 Hz, 2H), 7.26-7.22 δ (t, *J* = 8.31), 4.53 δ (s, 2H), 1.28 δ (s, 9H). ^{13}C NMR (500 MHz, DMSO): 150.28 δ, 135.71 δ, 128.31 δ, 125.35 δ, 77.18 δ, 34.69 δ, 31.63 δ.

Phthalimide-protected amino acids: The target amino acid (1 eq) and phthalic anhydride (1 eq) were refluxed for 4 hours. Once cooled, a colorless solid formed. This solid was recrystallized in hot water, to produce a white solid. Yield: β-alanine (87%) and γ-GABA (85%).

β-Alanine: ^{1}H NMR (500 MHz, $CDCl_3$): 7.86-7.84 δ (m, *J* = 3.11 Hz, 2H), 7.73-7.71 δ (m, *J* = 3.11 Hz, 2H), 4.01-3.98 δ (t, *J* = 6.12 Hz, 2H), 2.81-2.78 δ (t, *J* = 6.12 Hz, 2H).

γ-GABA: ^{1}H NMR (500 MHz, $CDCl_3$): 7.86-7.84 δ (m, *J* = 3.03 Hz, 2H), 7.73-7.71 δ (m, *J* = 3.03 Hz, 2H), 3.77-3.75 δ (t, *J* = 7.44 Hz, 2H), 2.43-2.40 δ (t, *J* = 7.44 Hz, 2H), 2.03-2.00 δ (m, *J* = 7.44 Hz, 2H).

General acylation of amino acids: Protected amino acids (β-Ala, γ-GABA) (1 eq) were refluxed in excess thionyl chloride (5-10 eq) in minimal DCM overnight. The solvent was removed *in vacuo*. The products were not isolated before moving to the next step. Quantitative yields were assumed for the subsequent reactions.

Fmoc-AA-Cl + *O*-*t*-bu-hydroxylamine: The acylated fmoc-amino acid (1 eq), sodium carbonate (2 eq) and *O*-t-bu-hydroxylamine were stirred at room temperature overnight in DCM. A white solid immediately formed with the addition of the hydroxylamine. The solid was removed by filtration and the solvent was removed *in vacuo*. The final product was not cleanly isolated.

Catechol synthesis

2,3-dihydroxybenzoic acid (1 eq) was reacted with DCC (1 eq) and N-hydroxysuccinimide (1 eq) in 1,4-dioxane at room temperature. The reaction was stirred overnight. The solvent was removed *in vacuo* and the product was purified by column chromatography (MeOH/DCM) to give a pure, final product, 21% yield. ^{1}H NMR (500 MHz, DMSO): 10.06 δ (s, 2H), 9.62 δ (s, 2H), 7.30-7.28 δ (d, *J* = 8.34 Hz, 2H), 7.14-7.11 δ (d, *J* = 8.34 Hz, 2H), 6.83-6.78 (t, *J* = 8.34 Hz, 2H), 2.87 δ (s, 8H).

Boc deprotection: The cyclized peptoids containing boc-protected amine residues were stirred at room temperature in 95% TFA/DCM overnight. The solvent was removed by nitrogen.

The NHS-activated 2,3-dihydroxybenzoic acid (1 eq/amine) and triethylamine (2 eq/amine) were stirred at room temperature in DCM with the deprotected cyclized peptoid overnight.

(1) Maher, K.; Bargar, J. R.; Brown Jr, G. E. Environmental Speciation of Actinides. *Inorg. Chem.* **2012**, *52* (7), 3510–3532.

(2) Powell, B. A.; Rao, L.; Nash, K. L. Effect of 1-Hydroxyethane-1,1-Diphosphonic Acid (HEDPA) on Partitioning of Np and Pu to Synthetic Boehmite. *Sep. Sci. Technol.* **2010**, *45* (6), 721–731.

(3) Neck, V.; Kim, J. I. Solubility and Hydrolysis of Tetravalent Actinides. *Radiochim. Acta* **2001**, *89* (1), 1–16.

(4) Li, H.; Sadler, P. J.; Sun, H. Rationalization of the Strength of Metal Binding to Human Serum Transferrin. *European Journal of Biochemistry*. 1996, pp 387–393.

(5) Harris, W. R. Binding and Transport of Nonferrous Metals by Serum Transferrin. *Less Common Metals in Proteins and Nucleic Acid Probes* **1998**, *92*, 121–162.

(6) Jeanson, A.; Ferrand, M.; Funke, H.; Hennig, C.; Moisy, P.; Solari, P. L.; Vidaud, C.; Auwer, C. Den. The Role of Transferrin in Actinide(IV) Uptake: Comparison with Iron (III). *Chem. - Eur. J.* **2010**, *16*, 1378–1387.

(7) Jensen, M. P.; Gorman-Lewis, D.; Aryal, B.; Paunesku, T.; Vogt, S.; Rickert, P. G.; Seifert, S.; Lai, B.; Woloschak, G. E.; Soderholm, L. An Iron-Dependent and Transferrin-Mediated Cellular Uptake Pathway for Plutonium. *Nat. Chem. Biol.* **2011**, *7* (8), 560–565.

(8) Deblonde, G. J.-P.; Sturzbecher-Hoehne, M.; Mason, A. B.; Abergel, R. J. Receptor Recognition of Transferrin Bound to Lanthanides and Actinides: A Discriminating Step in Cellular Acquisition of f-Block Metals. *Metallomics* **2013**, *5* (6), 619–626.

(9) Neilands, J. B. Some Aspects of Microbial Iron Metabolism. *Bacteriol. Rev.* **1957**, *21* (2), 101–111.

(10) Renshaw, J. C.; Robson, G. D.; Trinci, A. P. J.; Wiebe, M. G.; Livens, F. R.; Collison, D.; Taylor, R. J. Fungal Siderophores: Structures, Functions and Applications. *Mycol. Res.* **2002**, *106* (10), 1123–1142.

(11) Tufano, T. P.; Raymond, K. N. Coordination Chemistry of Microbial Iron Transport Compounds. 21. Kinetics and Mechanism of Iron Exchange in Hydroxamate Siderophore Complexes. *J. Am. Chem. Soc.* **1981**, *103* (22), 6617–6624.

(12) Budzikiewicz, H. Microbial Siderophores. In *Progress in the Chemistry of Organic Natural Products, Vol 92*; Kinghorn, A. D., Ed.; Springer-Verlag: Wien, 2010; pp 1–75.

(13) Boukhalfa, H.; Reilly, S. D.; Neu, M. P. Complexation of Pu(IV) with the Natural Siderophore Desferrioxamine B and the Redox Properties of Pu(IV)(Siderophore)

Complexes. *Inorg. Chem.* **2007**, *46* (3), 1018–1026.

(14) Taylor, D. M. The Effects of Desferrioxamine on the Retention of Actinide Elements in the Rat. *Health Phys.* **1967**, *13*, 135–140.

(15) Whisenhunt, D. W.; Neu, M. P.; Hou, Z.; Xu, J.; Hoffman, D. C.; Raymond, K. N. Specific Sequestering Agents for the Actinides. 29. Stability of the Thorium(IV) Complexes of Desferrioxamine B (DFO) and Three Octadentate Catecholate or Hydroxypyridinonate DFO Derivatives: DFOMTA, DFOCAMC, and DFO-1,2-HOPO. Comparative Stability of The. *Inorg. Chem.* **1996**, *35* (14), 4128–4136.

(16) Neu, M. P.; Matonic, J. H.; Ruggiero, C. E.; Scott, B. L. Structural Characterization of a Plutonium(IV) Siderophore Complex: Single-Crystal Structure of Pu-Desferrioxamine E. *Angew. Chem., Int. Ed.* **2000**, *39* (8), 1442–1444.

(17) White, D. L.; Durbin, P. W.; Jeung, N.; Raymond, K. N. Specific Sequestering Agents for the Actinides. 16. Synthesis and Initial Biological Testing of Polydentate Oxohydroxypyridinecarboxylate Ligands. *J. Med. Chem.* **1988**, *31* (1), 11–18.

(18) Zuckermann, R. N.; Kerr, J. M.; Kent, S. B. H.; Moos, W. H. Efficient Method for the Preparation of Peptoids [Oligo(N-Substituted Glycines)] by Submonomer Solid-Phase Synthesis. *J. Am. Chem. Soc.* **1992**, *114*, 10646–10647.

(19) Zuckermann, R. N. Peptoid Origins. *Biopolymers* **2011**, *96* (5), 545–555.

(20) De Cola, C. Synthesis and Properties of Linear and Cyclic Peptoids, University of Salerno, 2011.

(21) Shin, S. B. Y.; Yoo, B.; Todaro, L. J.; Kirshenbaum, K. Cyclic Peptoids. *J. Am. Chem. Soc.* **2007**, *129*, 3218–3225.

(22) Simon, R. J.; Kania, R. S.; Zuckermann, R. N.; Huebner, V. D.; Jewell, D. A.; Banville, S.; Ng, S.; Wang, L.; Rosenberg, S.; Marlowe, C. K.; Spellmeyer, D. C.; Tan, R.; Frankel, A. D.; Santi, D. V; Cohen, F. E.; Bartlett, P. A. Peptoids: A Modular Approach to Drug Discovery. *Proceedings of the National Academy of Sciences of the United States of America* **1992**, *89*, 9367–9371.

(23) Olsen, R. K.; Ramasamy, K. Synthesis of Retrohydroxamate Analogues of the Microbial Iron-Transport Agent Ferrichrome. *J. Org. Chem.* **1985**, *50*, 2264–2271.

(24) Maulucci, N.; Izzo, I.; Bifulco, G.; Aliberti, A.; De Cola, C.; Comegna, D.; Gaeta, C.; Napolitano, A.; Pizza, C.; Tedesco, C.; Flot, D.; De Riccardis, F. Synthesis, Structures, and Properties of Nine-, Twelve-, and Eighteen-Membered N-Benzyloxyethyl Cyclic

Alpha-Peptoids. *Chem. Commun.* **2008**, 3927–3929.

(25) Izzo, I.; Ianniello, G.; De Cola, C.; Nardone, B.; Erra, L.; Vaughan, G.; Tedesco, C.; De Riccardis, F. Structural Effects of Proline Substitution and Metal Binding on Hexameric Cyclic Peptoids. *Org. Lett.* **2013**, *15* (3), 598–601.

(26) Maayan, G.; Yoo, B.; Kirshenbaum, K. Heterocyclic Amines for the Construction of Peptoid Oligomers Bearing Multi-Dentate Ligands. *Tetrahedron Lett.* **2008**, *49*, 335–338.

(27) Culf, A. S.; Ouellette, R. J. Solid-Phase Synthesis of N-Substituted Glycine Oligomers (Alpha-Peptoids) and Derivatives. *Molecules* **2010**, *15*, 5282–5335.

(28) Miller, S. M.; Simon, R. J.; Ng, S.; Zuckermann, R. N.; Kerr, J. M.; Moos, W. H. Comparison of the Proteolytic Susceptibilities of Homologous L-Amino Acid, D-Amino Acid, and N-Substituted Glycine Peptide and Peptoid Oligomers. *Drug Dev. Res.* **1995**, *35*, 20–32.

(29) Shah, N. H.; Butterfoss, G. L.; Nguyen, K.; Yoo, B.; Bonneau, R.; Rabenstein, D. L.; Kirshenbaum, K. Oligo(N-Aryl Glycines): A New Twist on Structured Peptoids. *J. Am. Chem. Soc.* **2008**, *130* (49), 16622–16632.

(30) Baskin, M.; Maayan, G. Water-Soluble Chiral Metallopeptoids. *Biopolymers* **2015**, *104* (5), 577–584.

(31) Andreev, K.; Martynowycz, M. W.; Ivankin, A.; Huang, M. L.; Kuzmenko, I.; Meron, M.; Lin, B.; Kirshenbaum, K.; Gidalevitz, D. Cyclization Improves Membrane Permeation by Antimicrobial Peptoids. *Langmuir* **2016**, *32* (48), 12905–12913.

(32) Huang, M. L.; Benson, M. A.; Shin, S. B. Y.; Torres, V. J.; Kirshenbaum, K. Amphiphilic Cyclic Peptoids That Exhibit Antimicrobial Activity by Disrupting Staphylococcus Aureus Membranes. *European J. Org. Chem.* **2013**, No. 17, 3560–3566.

(33) Sala, G. Della; Nardone, B.; De Riccardis, F.; Izzo, I. Cyclopeptoids: A Novel Class of Phase-Transfer Catalysts. *Org. Biomol. Chem.* **2013**, *11* (5), 726–731.

(34) De Cola, C.; Fiorillo, G.; Meli, A.; Aime, S.; Gianolio, E.; Izzo, I.; De Riccardis, F. Gadolinium-Binding Cyclic Hexapeptoids: Synthesis and Relaxometric Properties. *Org. Biomol. Chem.* **2014**, *12* (3), 424–431.

(35) Knight, A. S.; Zhou, E. Y.; Pelton, J. G.; Francis, M. B. Selective Chromium(VI) Ligands Identified Using Combinatorial Peptoid Libraries. *J. Am. Chem. Soc.* **2013**, *135* (46), 17488–17493.

(36) De Cola, C.; Licen, S.; Comegna, D.; Cafaro, E.; Bifulco, G.; Izzo, I.; Tecilla, P.; De

Riccardis, F.; Cola, C. De; Licen, S.; Comegna, D.; Cafaro, E.; Bifulco, G.; Izzo, I.; Tecilla, P.; Riccardis, F. De. Size-Dependent Cation Transport by Cyclic Alpha-Peptoid Ion Carriers. *Org. Biomol. Chem.* **2009**, *7* (14), 2851–2854.

(37) Sun, J.; Zuckermann, R. N. Peptoid Polymers: A Highly Designable Bioinspired Material. *ACS Nano* **2013**, *7* (6), 4715–4732.

(38) Webster, A. M.; Cobb, S. L. Recent Advances in the Synthesis of Peptoid Macrocycles. *Chem. - Eur. J.* **2018**, *24*, 7560–7573.

(39) Zuckermann, R. N.; Kerr, J. M.; Kent, S. B. H.; Moos, W. H. Efficient Method for the Preparation of Peptoids [Oligo(N-Substituted Glycines)]. *J. Am. Chem. Soc.* **1992**, *114*, 10646–10647.

(40) Yoo, B.; Shin, S. B. Y.; Huang, M. L.; Kirshenbaum, K. Peptoid Macrocycles: Making the Rounds with Peptidomimetic Oligomers. *Chem. - Eur. J.* **2010**, *16* (19), 5528–5537.

(41) Neilands, J. B. A Crystalline Organo-Iron Pigment from a Rust Fungus (Ustilago Sphaerogena). *J. Am. Chem. Soc.* **1952**, *74*, 4846–4847.

(42) Emery, T.; Neilands, J. B. The Iron-Binding Centre of Ferrichrome Compounds. *Nature* **1959**, *183*, 1813–1814.

(43) Hesseltine, C. W.; Pidacks, C.; Whitehill, A. R.; Bohonos, N.; Hutchings, B. L.; Williams, J. H. Coprogen, a New Growth Factor for Coprophilic Fungi. *J. Am. Chem. Soc.* **1952**, *74* (5), 1362.

(44) Pidacks, C.; Whitehill, A. R.; Pruess, L. M.; Hesseltine, C. W.; Hutchings, B. L.; Bohonos, N.; Williams, J. H. Coprogen, the Isolation of a New Growth Factor Required by Pilobolus Species. *J. Am. Chem. Soc.* **1953**, *75* (23), 6064–6065.

(45) Diekmann, H.; Zähner, H. Constitution and Catabolism of Fusigen to Delta-2-Anhydromevalonic Acid Lactone. *Eur. J. Biochem.* **1967**, *3* (2), 213–218.

(46) Moore, R. E.; Emery, T. N α-Acetylfusarinines: Isolation, Characterization and Properties. *Biochemistry* **1976**, *15* (13), 2719–2723.

(47) Maurer, P. J.; Miller, M. J. Microbial Iron Chelators: Total Synthesis of Aerobactin and Its Constituent Amino Acid, N6-Acetyl-N6-Hydroxylysine. *J. Am. Chem. Soc.* **1982**, *104* (11), 3096–3101.

(48) Raymond, K. N.; Carrano, C. J. Coordination Chemistry and Microbial Iron Transport. *Acc. Chem. Res.* **1979**, *12*, 183–190.

(49) Carrano, C. J.; Cooper, S. R.; Raymond, K. N. Coordination Chemistry of Microbial Iron

Transport Compounds. 11. Solution Equilibria and Electrochemistry of Ferric Rhodotorulate Complexes. *J. Am. Chem. Soc.* **1978**, *101* (3), 599–604.

(50) Schwarzenbach, G.; Schwarzenbach, K. Hydroxamate Complexes. I. The Stabilities of the Iron(III) Complexes of Simple Hydroxamic Acids and Desferriferrioxamin B. *Helv. Chim. Acta* **1963**, *46* (4), 1390–1400.

(51) Kiss, T.; Farkas, E. Metal-Binding Ability of Desferrioxamine B. *J. Incl. Phenom. Macrocycl. Chem.* **1998**, *32*, 385–403.

(52) Yoshida, I.; Murase, I.; Motekaitis, R. J.; Martell, A. E. New Multidentate Ligands. XXI. Synthesis, Proton, and Metal Ion Binding Affinities of N,N′,N″-Tris[2-(N-Hydroxycarbamoyl)Ethyl]-1,3,5-Benzenetricarboxamide (BAMTPH). *Can. J. Chem.* **1983**, *61* (12), 2740–2744.

(53) Miller, M. J. Syntheses and Therapeutic Potential of Hydroxamic Acid Based Siderophores and Analogues. *Chem. Rev.* **1989**, *89* (7), 1563–1579.

(54) Smith, H. J.; Meremikwu, M. M. Iron-Chelating Agents for Treating Malaria. *Cochrane Database Syst. Rev.* **2003**, No. 2.

(55) Liu, Z. D.; Hider, R. C. Design of Iron Chelators with Therapeutic Application. *Coord. Chem. Rev.* **2002**, *232* (1–2), 151–171.

(56) Widmer, J.; Keller-Schierlein, W. Metabolic Products of Microorganisms. 139. Synthesis in the Sideramine Series. Rhodotorulic Acid and Dimerum Acid. *Helv. Chim. Acta* **1974**, *57* (7), 1904–1912.

(57) Page, M. G. P. Siderophore Conjugates. *Ann. N. Y. Acad. Sci.* **2013**, *1277* (1), 115–126.

(58) Ji, C.; Juárez-Hernández, R. E.; Miller, M. J. Exploiting Bacterial Iron Acquisition: Siderophore Conjugates. *Future Med. Chem.* **2012**, *4* (3), 297–313.

(59) Halliwell, B. Protection against Tissue Damage in Vivo by Desferrioxamine: What Is Its Mechanism of Action? *Free Radical Biol. Med.* **1989**, *7* (6), 645–651.

(60) Modell, B.; Letsky, E. A.; Flynn, D. M.; Peto, R.; Weatherall, D. J. Survival and Desferrioxamine in Thalassaemia Major. *Br. Med. J.* **1982**, *284* (6322), 1081–1084.

(61) Mclaren, G. D.; Muir, W. A.; Kellermeyer, R. W.; Jacobs, A. Iron Overload Disorders: Natural History, Pathogenesis, Diagnosis, and Therapy. *Crit. Rev. Clin. Lab. Sci.* **1983**, *19* (3), 205–266.

(62) Davies, M. J.; Donkor, R.; Dunster, C. A.; Gee, C. A.; Jonas, S.; Willson, R. L. Desferrioxamine (Desferal) and Superoxide Free Radicals. Formation of an Enzyme-

Damaging Nitroxide. *Biochem. J.* **1987**, *246* (3), 725–729.

(63) Lifa, T.; Tieu, W.; Hocking, R. K.; Codd, R. Forward and Reverse (Retro) Iron(III) or Gallium(III) Desferrioxamine E and Ring-Expanded Analogues Prepared Using Metal-Templated Synthesis from *Endo* -Hydroxamic Acid Monomers. *Inorg. Chem.* **2015**, *54* (7), 3573–3583.

(64) Emery, T.; Neilands, J. B. Contribution to the Structure of the Ferrichrome Compounds : Characterization of the Acyl Moieties of the Hydroxamate Functions. *J. Am. Chem. Soc.* **1960**, *82* (14), 3658–3662.

(65) Tor, Y.; Libman, J.; Shanzer, A. Biomimetic Ferric Ion Carriers. Chiral Ferrichrome Analogs. *J. Am. Chem. Soc.* **1987**, *109* (21), 6518–6519.

(66) Shanzer, A.; Libman, J.; Lazar, R.; Tor, Y.; Emery, T. Synthetic Ferrichrome Analogues with Growth Promotion Activity for Arthrobacter Flavescens. *Biochem. Biophys. Res. Commun.* **1988**, *157* (1), 389–394.

(67) Shanzer, A.; Libman, J. Synthetic Siderophores as Biological Probes. *Biol. Met.* **1989**, *2* (3), 129–134.

(68) Johnstone, T. C.; Nolan, E. M. Beyond Iron: Non-Classical Biological Functions of Bacterial Siderophores. *Dalton Trans.* **2015**, *44* (14), 6320–6339.

(69) Ramasamy, K.; Olsen, R. K.; Emery, T. N-Methylation of O-Benzyl N-(Alkoxycarbonyl) Alpha-Amino Acid Hydroxamate Derivatives. *J. Org. Chem.* **1981**, *46*, 5438–5441.

(70) Ramasamy, K.; Olsen, R. K.; Emery, T. Synthesis of a Retrohydroxamate Analogue of the Iron-Binding Ionophoric Peptide Ferrichrome. In *Peptides, structure and function: Eighth American Peptide Symposium*; 1983; pp 187–190.

(71) Emery, T.; Emery, L.; Olsen, R. K. Retrohydroxamate Ferrichrome, A Biomimetic Analogue of Ferrichrome. *Biochem. Biophys. Res. Commun.* **1984**, *119* (3), 1191–1197.

(72) Olsen, R. K.; Ramasamy, K.; Emery, T. Synthesis of Nα,Nδ-Protected Nδ-Hydroxy-L-Ornithine from L-Glutamic Acid. *J. Org. Chem.* **1984**, *49*, 3527–3534.

(73) Isowa, Y.; Takashima, T.; Ohmori, M.; Kurita, H.; Sato, M.; Mori, K. Synthesis of Rhodotorulic Acid. *Bulletin of The Chemical Society of Japan*. 1972, pp 1467–1471.

(74) Isowa, Y.; Ohmori, M.; Kurita, H. Total Synthesis of Ferrichrome. *Bull. Chem. Soc. Jpn.* **1974**, *47* (1), 215–220.

(75) Monzyk, B.; Crumbliss, A. L. Mechanism of Ligand Substitution on High Spin Iron(III) by Hydroxamic Acid Chelators. Thermodynamic and Kinetic Studies on the Formation

and Dissociation of a Series of Monohydroxamatoiron (III) Complexes. *J. Am. Chem. Soc.* **1979**, *101* (21), 6203–6213.

(76) Dhungana, S.; Heggemann, S.; Gebhardt, P.; Möllmann, U.; Crumbliss, A. L. Fe(III) Coordination Properties of a New Saccharide-Based Exocyclic Trihydroxamate Analogue of Ferrichrome. *Inorg. Chem.* **2003**, *42* (1), 42–50.

(77) Dhungana, S.; Harrington, J. M.; Gebhardt, P.; Möllmann, U.; Crumbliss, A. L. Iron Chelation Equilibria, Redox, and Siderophore Activity of a Saccharide Platform Ferrichrome Analogue. *Inorg. Chem.* **2007**, *46* (20), 8362–8371.

(78) Tor, Y.; Libman, J.; Shanzer, A.; Felder, C. E.; Lifson, S. Chiral Siderophore Analogs: Enterobactin. *J. Am. Chem. Soc.* **1992**, *114* (17), 6661–6671.

(79) Albrecht, M.; Osetska, O.; Abel, T.; Haberhauer, G.; Ziegler, E. An Enantiomerically Pure Siderophore Type Ligand for the Diastereoselective 1 : 1 Complexation of Lanthanide(III) Ions. *Beilstein J. Org. Chem.* **2009**, *5*, 78.

(80) Maurer, P. J.; Miller, M. J. Total Synthesis of a Mycobactin: Mycobactin S2. *J. Am. Chem. Soc.* **1983**, *105* (2), 240–245.

(81) White, C. J.; Yudin, A. K. Contemporary Strategies for Peptide Macrocyclization. *Nat. Chem.* **2011**, *3*, 509–524.

(82) Rodgers, S. J.; Lee, C. W.; Ng, C. Y.; Raymond, K. N. Ferric Ion Sequestering Agents. 15. Synthesis, Solution Chemistry, and Electrochemistry of a New Cationic Analogue of Enterobactin. *Inorg. Chem.* **1987**, *26* (10), 1622–1625.

(83) Ng, C. Y.; Rodgers, S. J.; Raymond, K. N. Ferric Ion Sequestering Agents. 21. Synthesis and Spectrophotometric and Potentiometric Evaluation of Trihydroxamate Analogues of Ferrichrome. *Inorg. Chem.* **1989**, *28* (11), 2062–2066.

(84) Lee, B. H.; Miller, M. J.; Prody, C. A.; Neilands, J. B. Artificial Siderophores. 2. Syntheses of Trihydroxamate Analogues of Rhodotorulic Acid and Their Biological Iron Transport Capabilities in Escherichia Coli. *J. Med. Chem.* **1985**, *28* (3), 323–327.

(85) Lee, B. H.; Miller, M. J.; Prody, C. A.; Neilands, J. B. Artificial Siderophores. 1. Synthesis and Microbial Iron Transport Capabilities. *J. Med. Chem.* **1985**, *28* (3), 317–323.

(86) Evers, A.; Hancock, R. D.; Martell, A. E.; Motekaitis, R. J. Metal Ion Recognition in Ligands with Negatively Charged Oxygen Donor Groups. Complexation of Fe(III), Ga(III), In(III), Al(III), and Other Highly Charged Metal Ions. *Inorg. Chem.* **1989**, *28*

(11), 2189–2195.

(87) Enyedy, A.; Csoka, H.; Farkas, E. A Comparison between the Chelating Properties of Some Dihydroxamic Acids , Desferrioxamine B and Acetohydroxamic Acid. *Polyhedron* **1999**, *18*, 2391–2398.

(88) Motekaitis, R. J.; Murase, I.; Martell, A. E. New Multidentate Ligands XII: Chelating Tendencies of N,N'-Ethylenediaminediacetic-N,N'-Diacethydroxamic Acid. *J. Coord. Chem.* **1971**, *1*, 77–87.

(89) Santos, M. A.; Bento, C.; Esteves, M. A.; Farinha, J. P. S.; Martinho, J. M. G. Iron Release Mechanism in a Trihydroxamate Siderophore Analogue. Kinetics and Effect of PH. *Inorganica Chim. Acta* **1997**, *258* (1), 39–46.

(90) Matsumoto, K.; Suzuki, N.; Ozawa, T.; Jitsukawa, K.; Masuda, H. Crystal Structure and Solution Behavior of the Iron(III) Complex of the Artificial Trihydroxamate Siderophore with a Tris(3-Aminopropyl)Amine Backbone. *Eur. J. Inorg. Chem.* **2001**, *6*, 2481–2484.

(91) Matsumoto, K.; Ozawa, T.; Jitsukawa, K.; Einaga, H.; Masuda, H. Crystal Structure and Redox Behavior of a Novel Siderophore Model System: A Trihydroxamato-Iron(III) Complex with Intra- and Interstrand Hydrogen Bonding Networks. *Inorg. Chem.* **2001**, *40* (2), 190–191.

(92) Kreutzer, A. G.; Salveson, P. J. Standard Practices for Fmoc-Based Solid-Phase Peptide Synthesis in the Nowick Laboratory. 1–22.

(93) Bergeron, R. J.; Stolowich, N. J.; Kline, S. J. Synthesis and Solution Dynamics of Agrobactin A. *J. Org. Chem.* **1983**, *48*, 3432–3439.

(94) Ho, C. Y.; Strobel, E.; Ralbovsky, J.; Galemmo, Robert A., J. Improved Solution- and Solid-Phase Preparation of Hydroxamic Acids from Esters. *J. Org. Chem.* **2005**, *70*, 4873–4875.

(95) Yale, H. L. The Hydroxamic Acids. *Chem. Rev.* **1943**, *33* (1), 209–256.

(96) Gao, X.-A.; Wang, X.-X.; Yan, H.; Li, J.; Yan, R.-L.; Huang, G.-S. An Efficient Method for the Preparation of Hydroxamic Acids. *J. Indian Chem. Soc.* **2013**, *90*, 381–385.

(97) Karunaratne, V.; Hoveyda, H. R.; Orvig, C. General Method for the Synthesis of Trishydroxamic Acids. *Tetrahedron Letters*. 1992, pp 1827–1830.

(98) Koshti, N. M.; Jacobs, H. K.; Martin, P. A.; Smith, P. H.; Gopalan, A. S. Convenient Method for the Preparation of Some Polyhydroxamic Acids: Michael Addition of Amines to Acrylohydroxamic Acid Derivatives. *Tetrahedron Lett.* **1994**, *35* (29), 5157–5160.

(99) Bonaccorsi, F.; Giorgi, R. A Convenient Large Scale Synthesis of O-Benzylhydroxylamine. *Synth. Commun.* **1997**, *27* (7), 1143–1147.

(100) Karakurt, A.; Dalkara, S.; Özalp, M.; Özbey, S.; Kendi, E.; Stables, J. P. Synthesis of Some 1-(2-Naphthyl)-2-(Imidazole-1-Yl)Ethanone Oxime and Oxime Ether Derivatives and Their Anticonvulsant and Antimicrobial Activities. *Eur. J. Med. Chem.* **2001**, *36* (5), 421–433.

(101) Saczewski, J.; Hudson, A. L.; Rybczynska, A. 2-[[(Aryl)Methoxy]Imino]Imidazolidine Derivatives With Potential Biological Activities. *Acta Pol. Pharm.* **2009**, *66* (Copyright (C) 2014 American Chemical Society (ACS). All Rights Reserved.), 671–679.

(102) Wrigglesworth, J. W.; Cox, B.; Lloyd-Jones, G. C.; Booker-Milburn, K. I. New Heteroannulation Reactions of N-Alkoxybenzamides by Pd(II) Catalyzed C-H Activation. *Org. Lett.* **2011**, *13* (19), 5326–5329.

(103) Ahuja, P.; Husain, A.; Siddiqui, N. Essential Aminoacid Incorporated GABA-Phthalimide Derivatives: Synthesis and Anticonvulsant Evaluation. *Med. Chem. Res.* **2014**, *23* (9), 4085–4098.

(104) Aronov, O.; Horowitz, A. T.; Gabizon, A.; Fuertes, M. A.; Perez, J. M.; Gibson, D. Nuclear Localization Signal-Targeted Poly(Ethylene Glycol) Conjugates as Potential Carriers and Nuclear Localizing Agents for Carboplatin Analogues. *Bioconjug. Chem.* **2004**, *15* (4), 814–823.

(105) Frecentese, F.; Sosic, A.; Saccone, I.; Gamba, E.; Link, K.; Miola, A.; Cappellini, M.; Cattelan, M. G.; Severino, B.; Fiorino, F.; Magli, E.; Corvino, A.; Perissutti, E.; Fabris, D.; Gatto, B.; Caliendo, G.; Santagada, V. Synthesis and in Vitro Screening of New Series of 2,6-Dipeptidyl-Anthraquinones: Influence of Side Chain Length on HIV-1 Nucleocapsid Inhibitors. *J. Med. Chem.* **2016**, *59* (5), 1914–1924.

(106) Abualreish, M. J. A.; Abdein, M. A. The Analytical Applications And Biological Activity of Hydroxamic Acids. *J. Adv. Chem.* **2014**, *10* (1), 2117–2125.

(107) Sever, M. J.; Wilker, J. J. Visible Absorption Spectra of Metal-Catecholate and Metal-Tironate Complexes. *Dalton Trans.* **2004**, 1061–1072.

(108) Gorden, A. E. V.; Xu, J.; Raymond, K. N.; Durbin, P. Rational Design of Sequestering Agents for Plutonium and Other Actinides. *Chem. Rev.* **2003**, *103*, 4207–4282.

(109) Jacques, V.; Desreux, J. F. Complexation of Thorium(IV) and Uranium(IV) by a Hexaacetic Hexaaza Macrocycle: Kinetic and Thermodynamic Topomers of Actinide

Chelates with a Large Cavity Ligand. *Inorg. Chem.* **1996**, *35*, 7205–7210.

CHAPTER FOUR

ETHYLENEDIAMINE POLYHYDROXAMIC ACID LIGAND DESIGN FOR F-ELEMENT COORDINATION

4.1 Hydroxamic acid introduction

The synthetic saga of understanding the complexities of hydroxamic acid chemistry began in 1869 with H. Lossen's discovery of the reaction between ethyl oxalate and hydroxylamine, producing oxalohydroxamic acid (Scheme 4.1, A). Later work by W. Lossen demonstrated the existence of multiple tautomers of hydroxamic acids, through the production of three products from the reaction of hydroxylamine and benzoyl chloride: benzohydroxamic acid, benzoyl benzohydroxamate, and dibenzoyl benzohydroxamate. These products could only have been produced through the presence of multiple intermediates, suggesting the existence of three possible tautomers of the hydroxamic acid product.[1,2] Later, in 1872, W. Lossen discovered what is now known as the Lossen Rearrangement through the pyrolysis of N-(benzoyloxy)benzamide to phenyl isocyanate (Scheme 4.1, B).[2] The majority of early work on hydroxamic acids focused on understanding their complex structural chemistry, however, the lack of understanding of the structural forms of hydroxamic acids in solution led to a significant issue with fully understanding the possible binding modes present.[3] Their biological and medicinal potentials were not heavily investigated until the latter half of the 1900s, when multiple classes of hydroxamic acid-containing siderophores, naturally occurring small molecules that aid in the bacterial metabolism and transportation of iron(III), were isolated and studied for biological uses.[4–6]

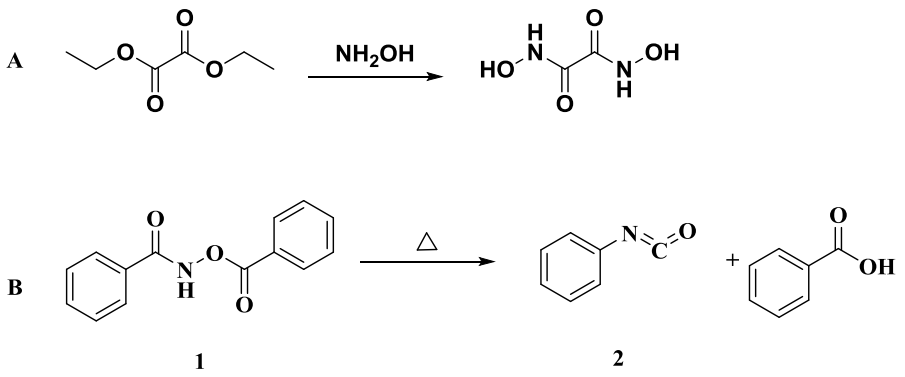

Scheme 4.1: A) Reaction of ethyl oxalate and hydroxylamine to form oxalohydroxamic acid. B)Lossen rearrangement of N-(benzoyloxy)benzamide (1) to phenyl isocyanate (2) and benzoic acid.

In early work, the differentiation between *N*- and *O*-acylated hydroxylamines (Figure 4.1) was not possible due to the lack of spectrophotometric analysis tools. However, through the use of infrared analysis, a difference in carbonyl stretch was noted for each form, 1670-1640 cm^{-1} and 1760-1730 cm^{-1} respectively. Solid state analysis of acetohydroxamic acid further pointed to the existence of the *N*-acylated product, more commonly known as the hydroxamic acid. The use of UV, IR, ESR, mass and NMR have all pointed to the hydroxamic acid being the dominant form, both in solid state and solution. Direct proof of the hydroxamic acid was further obtained using 2D NMR (^{15}N and ^{1}H) to show the N-H correlation. Thermodynamically, the hydroxamic acid is preferred. The kinetically *O*-acylated product has been shown to quickly rearrange to the other form.[7]

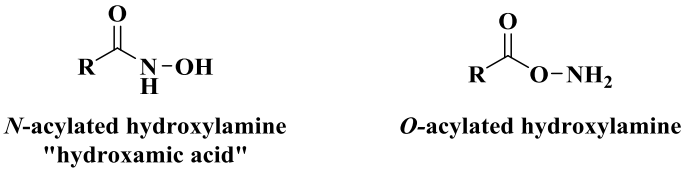

Figure 4.1: Structures of *N*- and *O*-acylated hydroxylamine

Hydroxamic acids are known to exist in two distinct forms, the keto (D) and enol (E) form, through the transfer of a proton between oxygen atoms (Scheme 4.). The keto form is believed to predominate in solid and solution state.[2,7–9] The ambiguity of the anionic form has been an issue throughout the study of the hydroxamic acids. Plapinger studied the UV-vis shift of various hydroxamic acid derivatives in an attempt to clarify the structure of the anionic form in solution. He noted both a red and blue shift for benzohydroxamic acid anions, but only a single shift for both *O*- and *N*-methylhydroxamic acids (red and blue, respectively). From this observation, Plapinger hypothesized that at least two anionic forms exist, with the possibility of a third form. He attributed the blue shift to form A and the red shift to form B and/or C (Scheme 4.2).[8] Later IR studies of benzohydroxamic acid by Steinberg further confirmed the existence of multiple anionic forms in solution through the isolation of forms A and B (Scheme 4.2). However, an inability to neither confirm nor deny the existence of form C led him to conclude that the third form could exist, but in a much lower concentration, where [A] ≈ [B] >>> [C] (Scheme 4.2).[2,9]

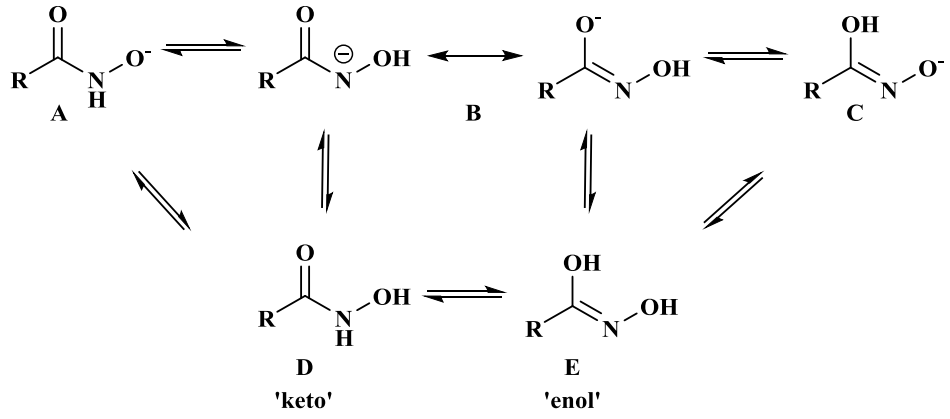

Scheme 4.2: A-C) Possible anionic forms of hydroxamic acids, D) keto and E) enol protonated forms.[2,9]

Hydroxamic acids are weakly acidic, primarily due to the OH group (pKa 8-9). They are weaker acids than their corresponding carboxylic acids (pKa 4-5), but more acidic than the

amides (pKa 20-22).[10,11] Early literature primarily insisted the acidity was strictly from the hydroxyl group (e.g. Scheme 4.2, A),[2,7,12,13] with few exceptions suggesting the presence of an N-anionic tautomer (e.g. Scheme 4.2, B, left).[8,13] This weakly acidic nature can be attributed to suppression of the basicity of the amine group via a resonance structure that leads to a partial double-bond character for the nitrogen (e.g. Scheme 4.2, B, right and E), a phenomenon also noted in amides.[14] Exner and Böhm used gas phase calculations to show the destabilizing inductive effect from the hydroxyl group allows for higher acidity of the nitrogen atom. A computational study by Exner in 2003 suggested that resonance was responsible for one half of the acidity of hydroxamic acids, compared to one-third in amides and one-quarter in carboxylic acids. The acidity of the nitrogen atom is strengthened by electron-withdrawing substituents.[15] The acidity of the compound was further suggested to not only come from the anionic form, but also from the negative inductive effect of the hydroxyl group, leading to a higher negative charge on the nitrogen atom.[16]

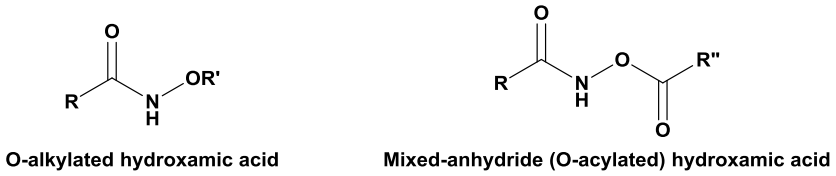

Figure 4.2: (Left) alkylation product, (Right) acylation product.

Alkylation of hydroxamic acids selectively leads to the *O*-alkylated product due to the α-effect, which leads to increased nucleophilicity of the hydroxyl oxygen atom due to the presence of the lone pair electrons on the nitrogen atom (Figure 4.2, left). Mixed anhydride hydroxamic acids can be synthesized through acylation, giving the *O*-esters (Figure 4.2, right).[3,7] When heated, or in the presence of strong base, hydroxamic acids are known to go through the Lossen Rearrangement when in contact with an alkylating agent, where they rearrange into

isocyanates.[2,7,17,18] However, Hoshino has shown evidence of a self-propagated Lossen rearrangement in base without the need of the alkylating agent.[17,18] Hydroxamic acids can also undergo acid and base-catalyzed hydrolysis, leading to the corresponding carboxylic acids.[19,20]

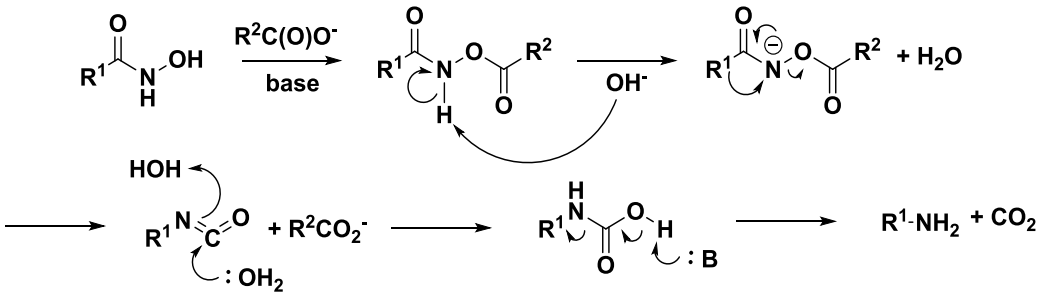

Scheme 4.3: Mechanism of base-mediated Lossen rearrangement

4.2 Hydroxamic acid ligands

Hydroxamic acids are capable of acting as mono- or bidentate ligands through the oxygen atoms, but can also act as monodentate ligands through the nitrogen atom, if unsubstituted.[6,21] The loss of a proton from the hydroxy group, followed by a ring closing by the carbonyl allows for the formation of a stable five-membered metallocycle during metal coordination.[14] Some metal-HA complexes are highly colored and have been used in the spectrophotometric and gravimetric analysis of the involved metals.[14,21,22] Due to neutral charge of many hydroxamate-metal complexes, they can be extracted from aqueous systems by most immiscible organic solvents.[14,23,24]

At low pH, a 1:1 ligand-to-metal complex is typically formed, with increasing L:M ratios as the pH increases. For example, in highly acidic solutions, hydroxamic acids form 1:1 complexes with iron(III), creating a deeply purple solution in aqueous media. As the pH increases, the 2:1 complex forms, followed by the 3:1 near a neutral pH, slowly turning the solution to a red-orange

color.[11,25] This behavior of increasing L:M stoichiometry with pH is typical for acidic groups capable of metal coordination, such as carboxylic acids. The pKa values can vary from 7-11, depending on the presence of groups with negative or positive inductive effects, such as halides or alkyl groups, respectively. The negative inductive effect decreases the pka value, while the positive inductive effect increases the pka value.[22]

4.3 Hydroxamic acids and actinides

Discovery of the potential of the *f*-elements in the late 19th and early 20th centuries instigated the beginning of the nuclear age, leading to the formation of many industries, including nuclear weapons, energy and radiopharmaceuticals.[26–28] While some actinides exist naturally, for example, thorium and uranium, others such as plutonium have largely been introduced into the environment by human means. As the demand for actinide use increased, so did their unwanted presence in the environment. An increased demand further pressured the actinide mining industry, requiring more efficient mining methods.[28] The complex chemistry of the actinides complicates the development of selective removal methods, particularly due to their wide range of oxidation states and the competitive environments they typically need to be removed from.[27]

Many approaches have been studied for the selective removal of actinides from various environments such as nuclear fuel waste, environmental water samples, and the human body.[27] The reprocessing of nuclear waste utilizes liquid extraction and various ligands to aide in the separation of uranium and plutonium from the other fission products present at the end of the fuel cycle. The PUREX process, developed during the Manhattan Project, is still the primary process used worldwide. It uses tributyl phosphate to help separate uranium and plutonium into an organic phase out of a nitric acid solution.[28] Environmental remediation and mining techniques have studied the use of highly coordinating ligands containing carboxylates and hydroxamates,

but selectivity issues lead to the inability to sufficiently separate only the target metal(s) from solutions containing other naturally occurring metals such as iron. The same issues exist with the selective removal of actinides from the body without the removal of biologically necessary metal ions.[27,29,30]

Siderophores, biological iron(III) scavengers, have often been used as the basis for actinide ligand design due to the similar charge/ionic radius ratio between iron(III) and plutonium(IV).[26,27,31,32] Ferrichrome, the first isolated and characterized siderophore, contains three hydroxamate binding moieties, making it a strong chelator of the ferric ion. Hydroxamates have a long history as potent actinide ligands, due the ability to accommodate the high coordination numbers of actinides through multidentate binding.[27,32,33]

Several factors contribute to the stable complexes formed by hydroxamic acids and actinides. The hard acidic nature of the early actinide metals gives a tendency to preferentially bind hard, oxoligands such as the hydroxamic acids.[26] A small bite angle allows for higher coordination numbers.[27,34] The small bite angle also allows for the formation of a stable five-membered ring when coordinated to the actinides. This both increases stability and selectivity of the hydroxamic acid actinide complexes.

Ligand examples (Waste management, radiopharmaceuticals, chelation therapy, mining/environmental)

Simple hydroxamic acids, such as aceto- (Figure 4.3, AHA) and formohydroxamic acid (Figure 4.3, FHA) were investigated early in actinide research for their ability to increase selective removal of metals during fuel waste reprocessing.[35] Both molecules were found to be effective stripping agents for tetravalent actinides, Pu(IV) and Np(IV). FHA was specifically

shown to allow the selective retainment of Pu(IV) and Np(IV) in an aqueous nitric acid solution, while U(VI) was removed by a tributylphosphate/kerosene organic extractant.[36] FHA has also been shown to quickly reduce Np(VI) to Np(V) while not affecting U(VI), allowing for the subsequent extraction of Np(V) in the aqueous solution.[34–39] The formation of hydroxylamine from the hydrolysis of hydroxamic acid in nitric acid contributes to the slower complexation and reduction of Pu(IV) to Pu(III).[36,37] At high nitric acid concentrations, U(VI) does not coordinate with formo- or acetohydroxamic acid, allowing for an effective separation of Np(VI) and Pu(IV) from U(VI).[36] Aromatic hydroxamates have also been investigated to improve the stability of the hydroxamates to hydrolysis at extreme pH (Figure 4.3, 1,2-HOPO).[34,40,41]

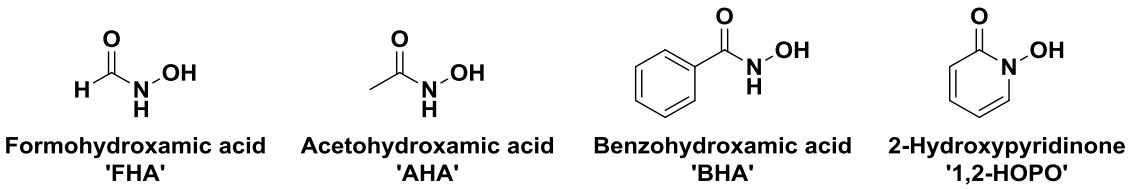

Figure 4.3: Structures of formohydroxamic acid, acetohydroxamic acid and benzohydroxamic acid

The retention of activity by the organic phase during reprocessing of irradiated nuclear fuel has been studied as a result of solvent degradation into metal coordinating by-products, such as hydroxamic acids.[42] Baroncelli and Grossi investigated the stability constants of benzohydroxamic acid (Figure 4.3, BHA) and metal isotopes present in nuclear fuel waste, ^{95}Zr, Fe(III), U(VI), U(IV), Th(IV), and Pu(IV). Overwhelmingly, benzohydroxamic acid was shown to preferentially bind ^{95}Zr in an acidic environment. In the presence of ^{95}Zr, a solution of the highly colored Fe(III)-benzohydroxamic acid complex was slowly decolorized as the Fe(III) was displaced by ^{95}Zr. The colored Fe(III) complex was not displaced by any other metal studied. However, at pH=0, benzohydroxamic acid was also an effective ligand for the coordination of

Fe(III) and Pu(IV). In the extraction process, investigators believed the formation of hydroxamic acids soluble in hydrocarbons would lead to the retention of activity in the aqueous phase through the coordination of isotopes such as ^{95}Zr and Pu(IV). The study focused on benzohydroxamic acid, which is insoluble in hydrocarbons, but the data led the authors to conclude that hydroxamic acids could hold potential as a way to selectively remove specific isotopes during the extraction process.[23,24]

The promising chelating behavior of hydroxamic acids with the actinides was mirrored by hydroxamic acid-containing siderophores, such as ferrichrome and desferrioxamine, which were investigated for medicinal use.[43–52] The development of polyhydroxamic acid ligands provided an array of chelating ligands for the *f*-elements. Examples such as BAMPTH,[53–55] EDTA-DX,[56] CYTROX,[57] and many other siderophore derivatives have been shown to be effective chelators of the *f*-elements.[27,40,54,58,59]

As discussed in Chapter 1, the field of polyhydroxamic acid ligands for chelation of the *f*-element is quite promising. However, a lack of consistent data and straightforward synthetic methods toward purified products has hindered the development of these ligands. However, the promising nature of these ligands begs for continued research into their development. A project was carried out to design a series of ligands based on the EDTA framework. By retaining an ethylenediamine backbone, while manipulating the hydroxamic acid sidearms (length, rigidity), a better understanding of the topology requirements for selective *f*-element chelation by a polyhydroxamic acid ligand could be gained.

In 1971, Motekaitis, Murase and Martell reported the synthesis of *N,N'*-ethylenediamine-*N,N'*-diacethydroxamic acid (EDTA-DX). Complexation with various divalent metals, Mg(II), Co(II), Ni(II), Cu(II), and Zn(II) was studied and compared to the constants of the corresponding

tetraamide EDTA derivative (EDDA) complexes. The stability constants were lower for the EDTA-DX ligand with each metal, with the largest discrepancy for the square planar Cu(II) complex (EDTA-DX K_{ML}=10.7, EDDA K_{ML}=16.2) due to a loss of basic amine interactions. However, the decrease was markedly smaller for the octahedral metals and an interaction with the hydroxamic acid amines was suggested.[56] The following year, Karlicek and Majer reported the synthesis of ethylenediamine-*N,N,N',N'*-tetraacetohydroxamic acid (EDTAHA) and its complexes with Fe(III) and Cu(II).

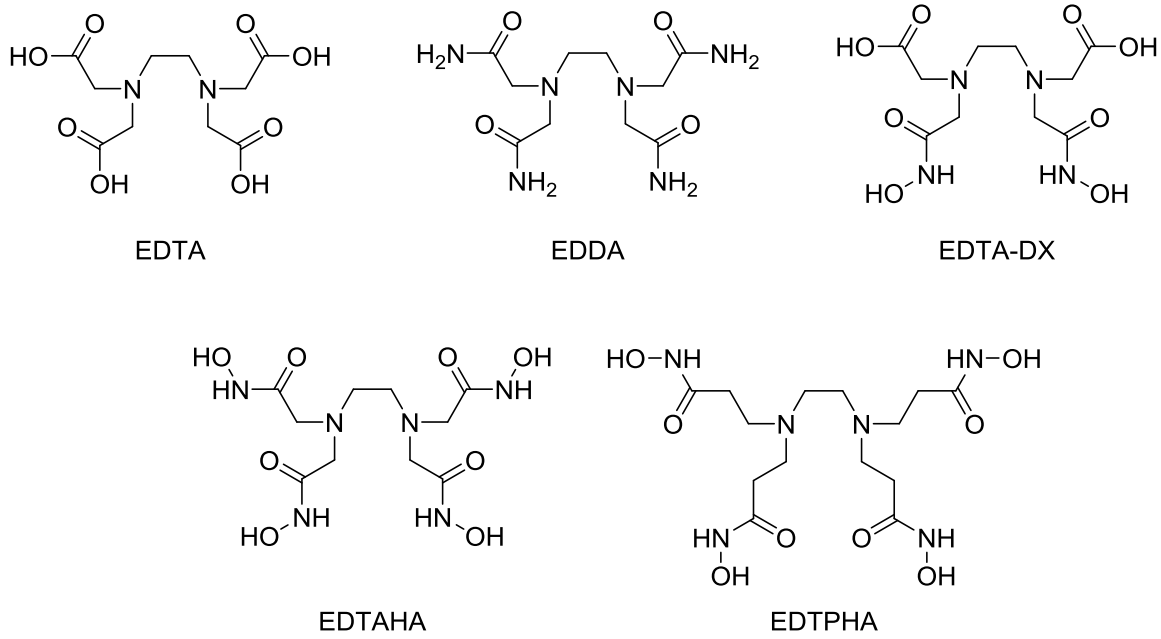

Figure 4.4. Structures of EDTA, EDDA, EDTA-DX, EDTAHA, and EDTPHA.

The main goal of this project was to synthesize a larger version of the EDTHA ligand for effective chelation of the *f*-elements. EDTA itself is too small to even encapsulate Fe(III) (leaving a coordinated water molecule on the iron) and is definitely too small for Ln(III)/An(III). Consequently, larger arms would be necessary to completely chelate the larger

lanthanide/actinide ions. Therefore, the first goal is the synthesis of the EDTPHA (see section below), which was successful and the stability constants of this ligand with a series of lanthanides is reported. Ultimately, this project could grow to a series of tetrahydroxamic acid ligands, such as ethylenediamine-*N,N,N',N'*-acethydroxamic acid (EDTHA), ethylenediamine-*N,N,N',N'*-propionohydroxamic acid (EDTPHA), ethylenediamine-*N,N,N',N'*-butyrylhydroxamic acid (EDTHA), and ethylenediamine-*N,N,N',N'*-benzodroxamic acid (EDTHA). This series could enable a systematic investigation of sidearm length and rigidity and the effect on complex stability with various metals (partial progress has been made toward completing the series of ligands). Two methods toward ligand synthesis were investigated, a divergent and convergent scheme. The target metals studied were La(III), Eu(III), and Lu(III), which allowed better understanding of trends across the lanthanide series. Stability constants were determined through potentiometric titrations.

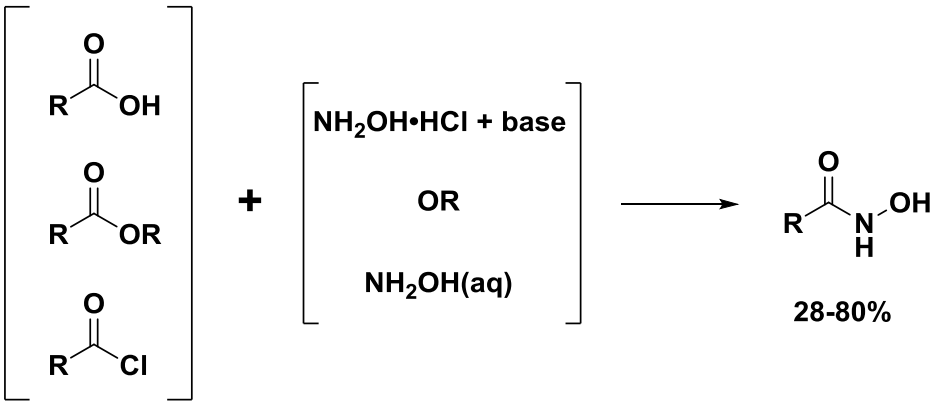

Scheme 4.4: Traditional synthetic routes toward monohydroxamic acids. Typically R in ester = CH_3.

4.4 EDTPHA synthesis

Traditional synthetic routes toward monohydroxamic acids involve the conversion of carboxylic acids, acid chlorides, or esters to the hydroxamate product through reaction with

hydroxylamine (Scheme 4.4).[2,60,61] However, low conversion yields and differentiation (both in characterization of the reaction progress and ultimately in purification) of the products from the starting materials, drastically complicate the synthesis of polyhydroxamic acids. Initially, a divergent approach was investigated for the synthesis of polyhydroxamic acid EDTA derivatives (Scheme 4.5). This "build-out" method allowed for the use of commercially available starting materials (*e.g.* EDTA, hydroxylamine HCl), but required difficult characterization and purification. The simultaneous conversion of four carboxylic acids to the corresponding hydroxamic acids proved unsuccessful (consistent with modest yields reported in the literature for conversions of single carboxylic acids to hydroxamic acids), so consequently, a convergent approach utilizing protected hydroxamine acids was utilized (Scheme 4.5). This "build-in" approached required more steps due to the synthesis of the hydroxamate-arm starting materials, but allowed for more straightforward purification and characterization. This approached eventually provided a successful route toward the synthesis of EDTPHA, allowing for study of the stability constants with several metals.

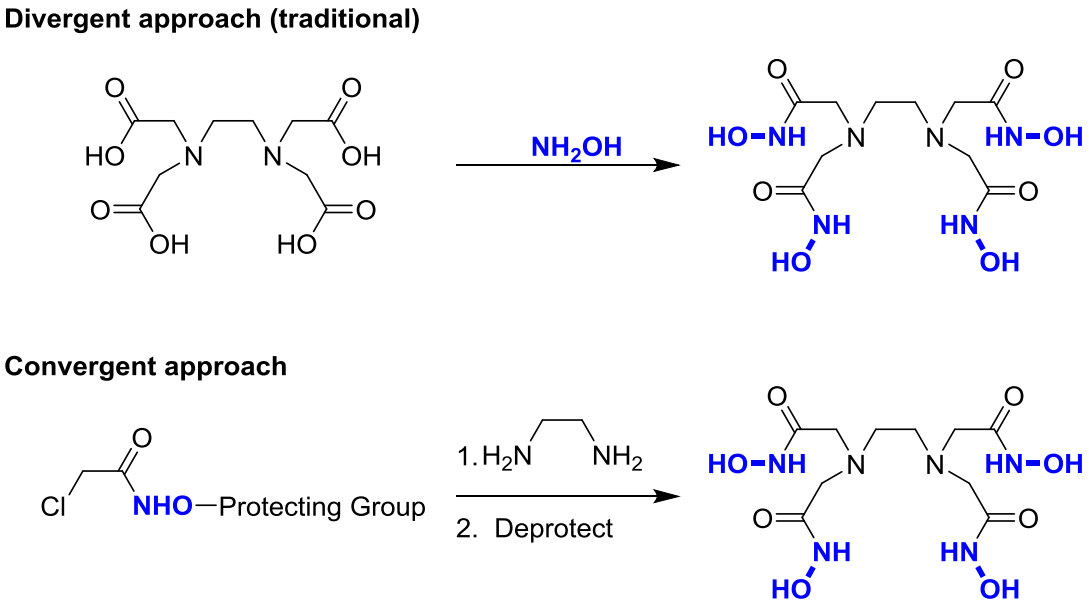

Scheme 4.5: Divergent and convergent routes toward polyhydroxamic acid EDTA derivatives. The hydroxylamine moieties of the hydroxamic acids are shown in blue to highlight the different stage at which the hydroxamic acid is put together.

Divergent "Build-out" Route

Karlicek and Majer employed the traditional divergent route for their reported EDTAHA ligand.[62] The authors reacted ethylenediamine-*N,N,N',N'*-tetramethylacetate with a methanolic solution of hydroxylamine in the presence of strong base. The product was isolated by precipitation with ether to give a pure, white solid. Several unsuccessful attempts were made to follow this reported method. The authors used 24 equivalents of base, and hydroxamates are known to decompose into carboxylates under strongly basic conditions.

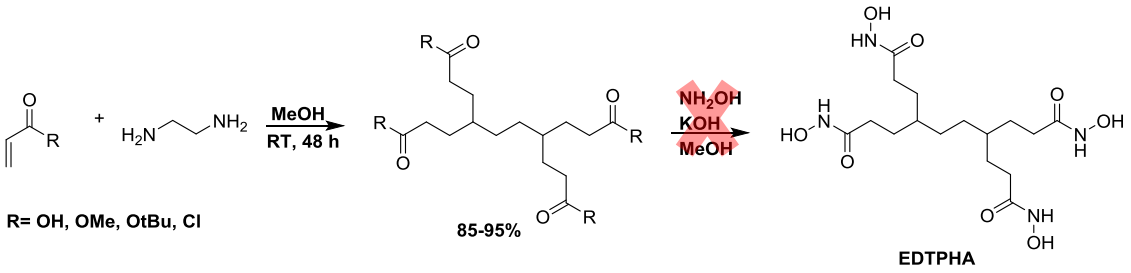

Scheme 4.6: Aza-Michael addition of methyl acrylate with ethylenediamine. Subsequent reaction with hydroxylamine did not lead to the hydroxamic acid product, but a mixture of EDTPHA and EDTP.

An aza-Michael addition of an acrylate starting material to an ethylenediamine backbone allowed for high yielding synthesis of EDTP (ethlyenediaminetatrapropionic acid) derivatives (Scheme 4.6). Methyl acrylate led to the methyl ester derivative of EDTP, which was then used in the same reaction scheme as reported by Karlicek and Majer and discussed in the previous paragraph. Due to the instability of aqueous hydroxylamine solutions, a fresh methanolic solution was made from hydroxylamine hydrochloride and potassium hydroxide. Cooling the solution allowed for removal of the resulting potassium chloride by filtration. The filtrate was then reacted with the methyl ester in the presence of excess potassium hydroxide. Excess hydroxylamine and potassium hydroxide were used (3eq/NHOH).

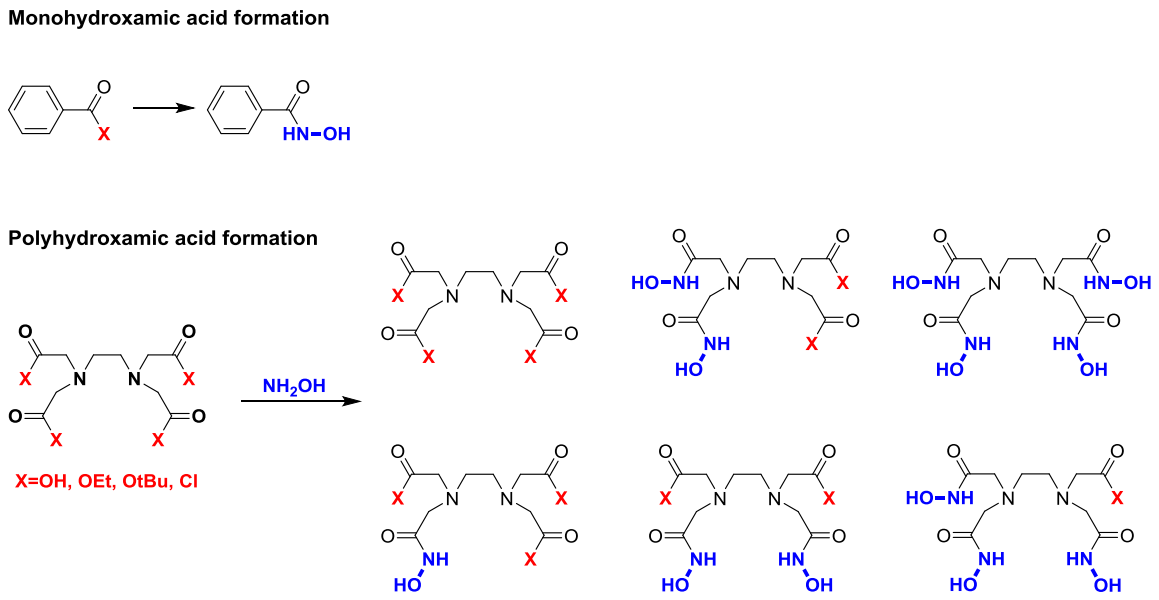

Scheme 4.7: Formation of monohydroxamic acids (top) and possible mixture of products formed during formation of polyhydroxamic acids (bottom). The starting groups (X), are highlighted in red and the desired hydroxamic acids are highlighted in blue. Most reactions led to mixtures of the desired hydroxamic acid products as well as starting materials and carboxylic acids (X=OH) in complex mixtures that

Conversion Problems

The simultaneous conversion of four ester groups to the corresponding hydroxamic acids proved unsuccessful. Characterization of the reaction was difficult due to a lack of identifying properties for complete conversion. The traditional iron(III) chloride test, which utilizes the distinct colors of hydroxamate-Fe(III) complexes for identification, was only able to identify the presence of hydroxamic acids, but not purity/progress of the reaction. Additionally there is overlap between carboxylate and hydroxamate features in infrared spectra, meaning IR spectroscopy is also only useful for confirming the presence of hydroxamic acids, not for demonstrating complete conversion. A small upfield shift in the ^{1}H NMR of the aliphatic protons was noted, but peaks representative of the EDTP sodium salt were present as well (Scheme 4.7).

Collectively, all the evidence suggested that while possible product formation was occurring, complete conversion was not occurring.

Hydroxamic acids are known to undergo acid and base-catalyzed hydrolysis, similar to the corresponding amides. With this knowledge, it is not surprising that products in Scheme 4.7 (particularly mixed ones containing carboxylates, i.e., X=OH) are able to form under the literature procedure. In the case of monohydroxamic acids, while the carboxylic acids may form, the mixture of products is much simpler and therefore, purification is much more straightforward (i.e., separating one product from one starting material). However, by attempting this conversion on multiple arms, many more species with very similar spectral properties as well as polarities are formed (Scheme 4.7), thereby complicating both characterization and purification.

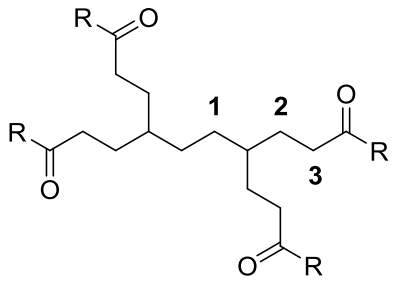

Figure 4.5: EDTP structure with relevant protons labeled. R = OH (EDTP), ONa (EDTP Na salt), NHOH (EDTPHA).

Optimization Attempts

Several factors in the reaction were varied in an attempt to optimize the product formation and minimize the side products. Two base/solvent systems were attempted, potassium hydroxide/methanol and potassium tert-butoxide/tert-butanol. ^{1}H NMR of both systems showed the growth of the sodium EDTP salt as well as what was believed to be the hydroxamic acid product (Figure 4.6). The EDTP structure produces three distinct peaks in the 2-3 ppm of ^{1}H

NMR, in D_2O. The ethylenediamine singlet (Figure 4.5, 1) and aliphatic triplet closest to the backbone (Figure 4.5, 2) do not appear to undergo a large shift between the EDTP sodium salt and EDTPHA. However, the triplet for the aliphatic protons closest to the changing functional group (Figure 4.5, 3) does shift between products, allowing for identification of the reaction products. In Figure 4.6, the peaks in red show the assumed EDTPHA peak, the peaks in blue show the EDTP sodium salt, and the purple peaks show the unaltered aliphatic triplet (Figure 4.5, 2). This initial study suggested the t-BuOK/t-BuOH system led to a higher ratio of EDTPHA/EDTP product; however, a mixture was still present. The bulk of the tert-butyl group was believed to hinder the basic hydrolysis of the hydroxamic acid.

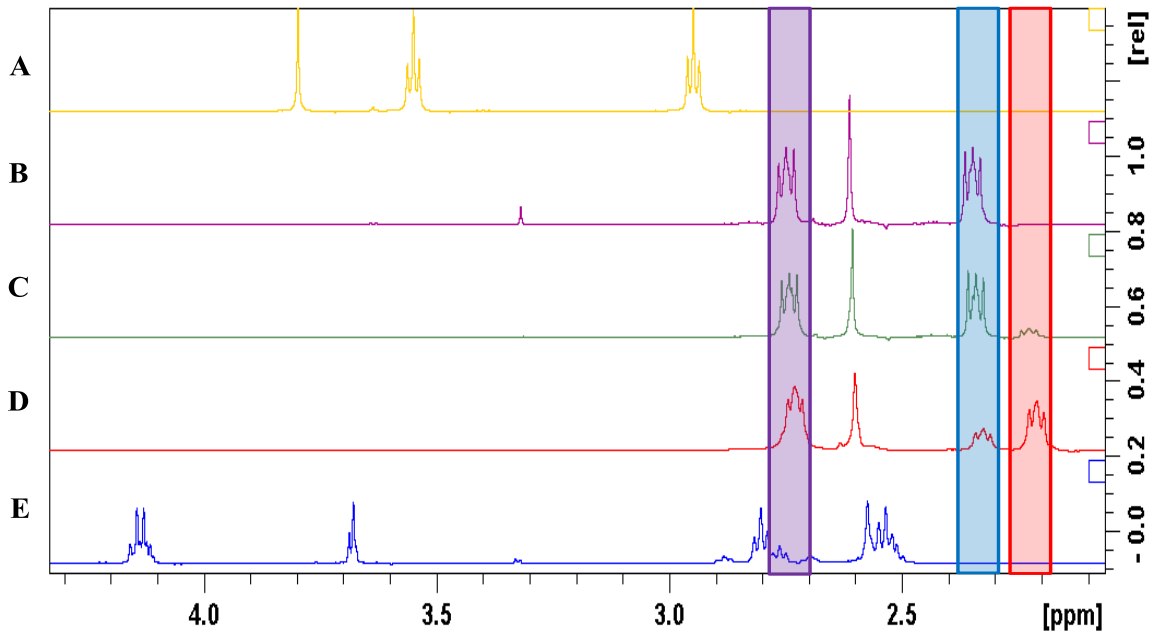

Figure 4.6: ^{1}H NMR of A) EDTP acidic, B) EDTP sodium salt, C) EDTPHA synthesis using NaOH/MeOH, D) EDTPHA synthesis using t-BuOK/t-BuOH, E) EDTP ethyl ester. All data were collected on a 500 MHz Bruker FT-NMR in D_2O. All reactions stirred at room temperature for 18 h in the presence of 3 eq base/arm. The blue box at 2.3-2.4 ppm demonstrates the presence of carboxylate arms in multiple synthetic conditions.

In an attempt to limit the hydrolysis products, the length of reaction time, along with amount of base in the system was varied. Three systems were tested, NaOH/MeOH (4eq base/arm), t-

BuOK/t-BuOH (4 eq base/arm), and t-BuOK/t-BuOH (2 eq base/arm). Reducing the base amount to 2 equivalents per arm led to no formation of EDTPHA after 18 hours (Figure 4.7, C). Between the base/solvent systems, NaOH/MeOH appeared to primarily form EDTPHA after 18 hours in the presence of 4 eq base/arm (Figure 4.7, A), in comparison to about 60% EDTPHA in the t-BuOK/t-BuOH system with the same amount of base (Figure 4.7 B). This contradicts the trend noted in Figure 4.7, but begins to show some of the difficulties with this system. The low freezing point of t-BuOH (~23°C) complicates processes such as filtration. For this reason, strict control over the concentration of the t-BuOH system was difficult and may have led to slight discrepancies in the results. Despite this, the NaOH/MeOH results with 4 eq base/arm were promising, so this system was used for the following study, which focused on the effect reaction time on product formation.

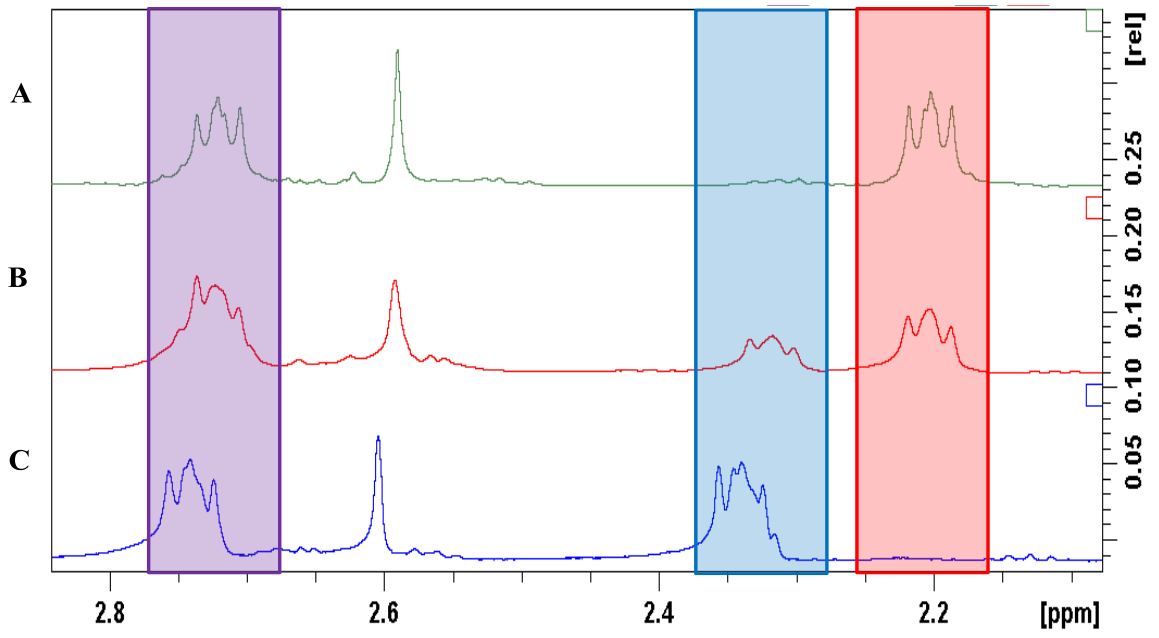

Figure 4.7: ^{1}H NMR of EDTPHA synthesis with varied base concentrations and base/solvent systems. A) NaOH/MeOH, 4 eq base/arm, B) t-BuOK/t-BuOH, 4 eq base/arm, C) t-BuOK/t-BuOH, 2 eq base/arm. All data were collected on a 500 MHz Bruker FT-NMR in D_2O. All reactions stirred at room temperature for 18 h.

The length of reaction time was varied in an attempt to isolate EDTPHA before the hydrolysis products began to form. The length of reaction was varied from 0-24 hours. Along with the aliphatic peaks, the methyl ester peak was also used for following the reaction progress. Figure 4.8 D appears to show a complete reaction, but the ester product was still present at this point. Despite this, the data suggests near complete conversion between 1-2 hours, with no formation of the carboxylic acid product until after 18 hours. This data shows the slow hydrolysis of the hydroxamic acid group during the basic reaction conditions.

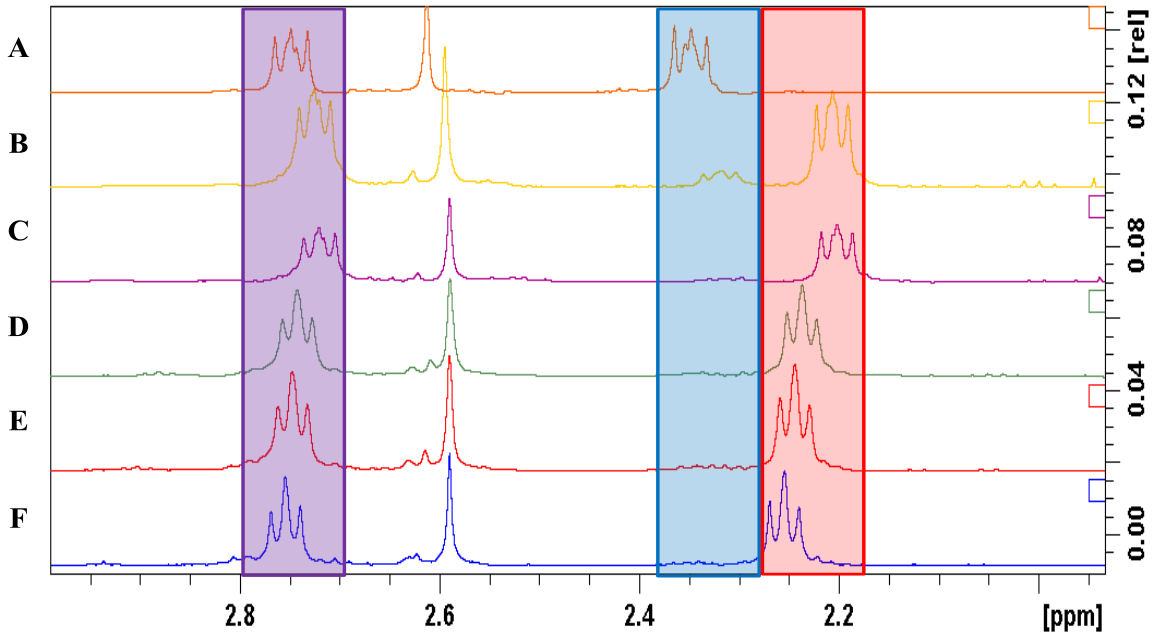

Figure 4.8: ^{1}H NMR of EDTPHA synthesis at different timepoints in NaOH/MeOH (4 eq base/arm) system. A) EDTP sodium salt, B) 24 hours, C) 18 hours, D) 2 hours, E) 1 hour, F) 0 hours. All data were collected on a 500 MHz Bruker FT-NMR in D_2O.

However, with a polyhydroxamic acid ligand, such as EDTPHA, this data does not fully represent the reaction products. As can be seen in Figure 4.6, a small shift of one aliphatic peak is the best indicator of product formation. Changes in mass between the possible products (Table

4.1) were small and difficult to characterize by MALDI-TOF. Often, due to the extreme basic conditions, the products could not be identified by MALDI-TOF. Additionally, both hydroxamates and carboxylates are known to break apart even under the relatively mild ionization conditions of MALDI-MS (losing hydroxylamine or water, respectively). Thin-layer chromatography was not useful other than for the identification and loss of the starting material.

Table 4.1: ^{1}H NMR shifts (D_2O) and masses of EDTP derivatives. The structure can be seen in Figure 4.4.

R=	A (ppm)	B (ppm)	C (ppm)	Mass (g/mol)
ONa	2.347	2.748	2.612	436.08
OH	2.947	3.549	3.797	348.15
NHO^-	2.222	2.741	2.610	404.20
NHOH	2.851	2.656	2.365	408.20
NHOBntBu	2.171	2.533	2.235	993.34

To provide more characteristic differences between starting materials and products, the tert-butyl ester derivative of EDTP was synthesized through the reaction of tert-butyl acrylate and ethylenediamine. However, this route experienced the same issues as the methyl ester starting material. An additional attempt to remove the tert-butyl group by trifluoroacetic acid followed by activation of the hydroxamates by 1-ethyl-3-(3-dimethylaminopropyl)carbodiimide hydrochloride (EDC) or dicyclohexylcarbodiimide (DCC) and subsequent reaction with hydroxylamine was hindered by difficulties removing the TFA counteranion, which prevented activation of the carboxylate.

Convergent "Build-in" Route

Due to the difficult characterization and purification of the many possible products from the divergent strategy, a new method was developed to avoid these issues. Several papers published by Gopalan, Koshti and coworkers discuss the use of *O*-protected hydroxylamines for the synthesis of polyhydroxamic acid ligands.[63–65] These papers report the use of *O*-benzyl hydroxylamine for the synthesis of the ligand, followed by hydrogenation in mild conditions (5% Pd/C, room temperature/pressure).

Initially, *O*-benzyl hydroxylamine was bought from a commercial source and reacted with acryloyl chloride to provide an *O*-protected hydroxamic acid acrylate for subsequent use in an aza-Michael addition (Scheme 4.8). Both reactions were straightforward, but required purification by column chromatography, leading to an overall yield of 14%. The final hydrogenation step was carried out via balloon hydrogenation with 10% Pd/C in methanol. However, after two weeks, with constant resupplying of the hydrogen balloon, a mixture of partially-deprotected products (0-4 benzyl groups) was present. The lengthy hydrogenation conditions began to lead to degradation of the ligand, rather than removal of the benzyl groups. Additionally, degradation of the Pd catalyst would definitely occur over two weeks, further diminishing possible reaction.

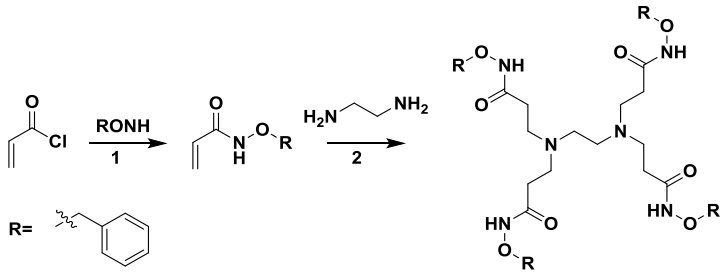

Scheme 4.8: 1) Synthesis of *O*-protected hydroxamic acid acrylate followed by 2) aza-Michael addition to ethylenediamine.

The removal of multiple benzyl groups simultaneously appeared to be experiencing the same issues as the divergent route discussed above. A slow reaction time suggested the need for a protecting group that is cleaved more easily. Gaunt and coworkers reported the effect of substitution of the benzyl groups on rate of deprotection by hydrogenation in esters (not hydroxamates). The report stated that the addition of an electron withdrawing group, such as CF_3 would slow hydrogenation, while an electron donating group, such as tert-butyl, methyl, or methoxy, would increase the rate.[66] To investigate if this was a viable option for cleaner reaction conditions, two additional *O*-benzyl hydroxylamines were synthesized (Scheme 4.9). The route was first tested by synthesizing *O*-benzyl hydroxylamine (R = H in Scheme 4.9) and comparing the product to the commercially available compound.

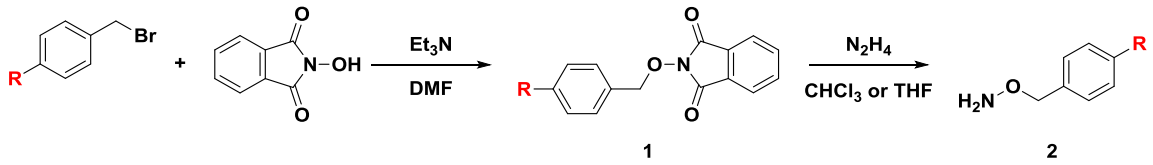

Scheme 4.9: Synthesis of *O*-protected hydroxylamine via phthalimide protection of a benzyl bromide, followed by deprotection of the phthalimide by hydrazine.

Table 4.2: Yields for *O*-protected hydroxylamine synthesis (Scheme 4.9).

R =	1 Yield (%)	2 Yield (%)
H	**83**	**24**
Me	**81**	**86**
t-Bu	**88-93**	**90-95**

The reaction of a benzyl bromide with *N*-hydroxyphthalimide was high yielding and only required precipitation of the product with water. The subsequent deprotection of the phthalimide

group was carried out by refluxing in chloroform or tetrahydrofuran in the presence of excess hydrazine. The resulting phthalazine was removed by filtration and the product purified through extraction. The deprotection step was higher yielding for the methyl and tert-butyl benzyl groups than for the unsubstituted benzyl. The highest yielding product was the *O*-tert-butyl benzyl hydroxylamine, so this was used for subsequent syntheses.

Using the same method shown in Scheme 4.8, an *O*-tert-butyl benzyl hydroxamic acid acrylate was formed and added to ethylenediamine using aza-Michael addition. This reaction provided a slightly better overall yield of 33%. The tert-butyl benzyl protected compound underwent balloon hydrogenation with 10% Pd/C at room temperature. Although the deprotection of the tert-butylbenzyl protecting group was faster and more complete than that of the unsubstituted benzyl protecting group, it was still not complete using near-atmospheric pressure balloon hydrogenation.

Ligand deprotection

Balloon hydrogenation provides an atmosphere of around 60 psi hydrogen. Briefly, an attempt was made to utilize the departmental Parr hydrogenation system, which should have been capable of providing a pressures up to ~200 psi. However, the age and lack of care for this instrument left it in a state of disrepair which did not provide a closed, pressurized system (consequently it both leaked hydrogen and could occasionally spark). Finally, a system was created which could provide 1000+ psi of hydrogen. The custom setup utilized a Parr pressurized vessel (Figure 4.9) to conduct the reaction in. Swagelok connectors and tubing allowed for straightforward and safe pressurizing of the system. Each reaction was purged multiple times to remove unwanted oxygen. Once pressurized, the reaction was stirred until complete.

Figure 4.9: Parr pressurized vessel utilized for high-pressure hydrogenation at room temperature.

The tert-butyl benzyl protected product was hydrogenated with 10% Pd/C in methanol at 1000 psi overnight. After removal of the Pd by filtration through a celite column, the methanol was evaporated by nitrogen and then a white solid was precipitated by diethyl ether. This white product was hygroscopic and formed a deep purple solution upon addition of small test quantities to $FeCl_3$. ^1H NMR of this solid suggested a clean product. However, to determine the presence of unwanted side products, TLC and an $FeCl_3$ stain were used (Figure 4.10). By staining the TLC plate with $FeCl_3$, the distinct colored Fe(III)-hydroxamic acid complexes could provide a characterization method. Only the benzyl protected starting material, along with any partially deprotected products were UV-active. All compounds interacted with the iodide stain, which did

not indicate the identification of the products. The $FeCl_3$ stain only formed colored spots with hydroxamic acid-containing products. Characterization of hydroxamic acids by this method has not previously been reported.

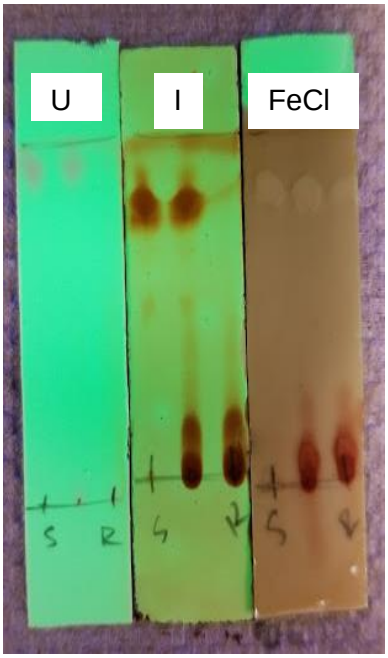

Figure 4.10: Characterization of EDTPHA by thin-layer chromatography (TLC). Left) UV light, no stain, Middle) Iodide stain, Right) $FeCl_3$ stain. S is the protected ligand before hydrogenation and R is the white solid collected by ether precipitation.

TLC of the white solid from ether precipitation appeared to show two colored spots at the baseline. However, the ^1H NMR only contained one set of peaks in the aliphatic region, suggesting only one product was present. The two spots in TLC could be from different conformations of the deprotected ligand caused by hydrogen bonding in solution. Elemental analysis of this product did not match calculated values. The results showed the possible presence of various solvent molecules (water, ether, methanol). In an attempt to remove these solvent molecules, the product was dried in a vacuum oven at 50°C and vacuum over the weekend.

Unfortunately, this degraded the hydroxamic acid units, most likely due to the added heat. As shown in Schemes 4.1 and 4.3, hydroxamic acids are capable of undergoing a Lossen arrangement when heated. The elemental analysis of multiple samples was consistent with ~12.5% decomposition of hydroxamic acid into carboxylic acid while heating under vacuum.

During characterization of the white solid from the initial deprotection, MALDI-TOF was attempted. While the fully deprotected ligand could not be identified by this method, metal complexes were able to be formed and identified. The Ln(III) series was coordinated with the white solid and characterized by MALDI-TOF (Figure 4.11). Lanthanide(III) oxides were mixed with the product in water and dried on the MALDI plate. A clear trend of coordination is seen across the series. Initially, the masses appeared to not agree with coordination by EDTPHA. However, a report from 1969 showed the loss of hydroxylamine during mass spectrometry.[67] With this in mind, the masses observed agree with an ML_2 complex and the loss of hydroxylamine.

Figure 4.11: MALDI-TOF results of EDTPHA coordination with Ln_2O_3 series. Nd(III) and Tb(III) not shown but fit within the trend.

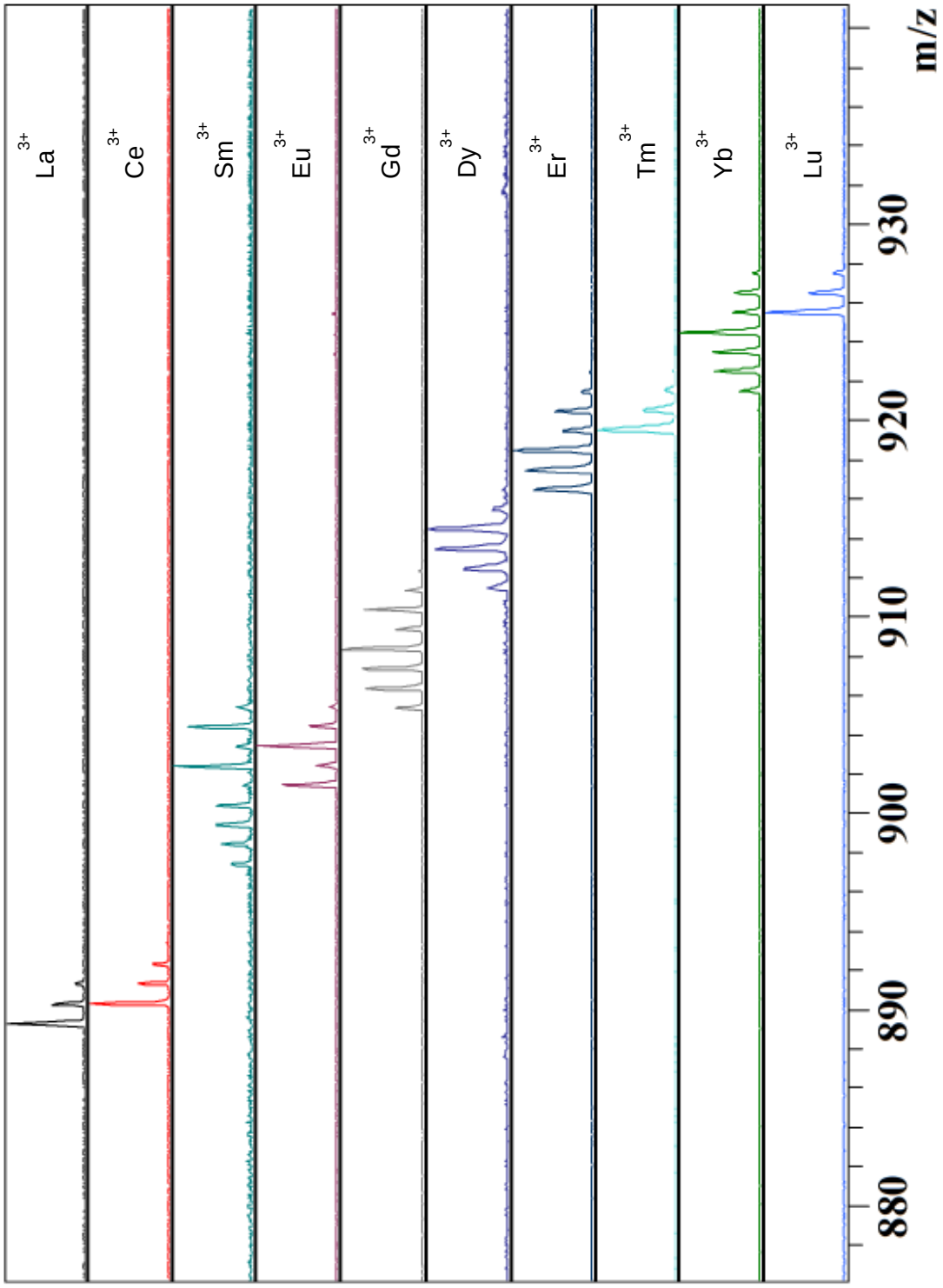

Additionally, the yield of this reaction was unreasonably low (<10%). When the filtrate from the ether precipitation was characterized, evidence of the fully protected ligand was observed. When the hydrogenation was carried out for an additional 24 hours, decomposition of the product began to occur. Increasing the Pd/C catalyst from 10% to 20% did not appear to have an effect on conversion progress. Due to the strong chelating properties of the hydroxamic acid moiety, all glassware was acid-washed to remove any residual Fe(III). However, during hydrogenation, the Pd(0) catalyst is oxidized to Pd(II), before being regenerated as Pd(0). If, as the benzyl groups were removed, the deprotected hydroxamic acids were capable of chelating the Pd(II) generated during hydrogenation, this would provide an explanation for the lack of complete deprotection. Loss of the catalyst during the reaction would prevent further reaction for occurring, thus explaining why only partial deprotection or low yielding full protection occurred.

By changing the solvent to 30% acetic acid/methanol and increasing the Pd catalyst to 30%, quantitative deprotection of the ligand was managed after four hours at 300 psi. Removal of the methanol *in vacuo*, followed by lyophilization of the product to further remove the acetic acid results in a viscous, orange oil. Full removal of the acetic acid was not achieved, but through ^{1}H NMR, determination of the amount of acetic acid present could be achieved. A small ratio of tert-butyl toluene, which was produced by the hydrogenation, was also present in the final product, but could be quantified by ^{1}H NMR.

4.5 EDTHA, EDTBHA, EDTBnHA Synthesis

To fully investigate the effect of ligand topology on complex stability with various metals, several additional EDTA derivatives were targeted. The *O*-tert-butyl hydroxylamine developed for the EDTPHA synthesis was used for the synthesis of arms for addition to the ethylenediamine backbone. For EDTHA, chloroacetyl chloride was reacted with the *O*-protected hydroxylamine to

give chloroacetyl-*O*-tert-butylbenzyl-hydroxamic acid in excellent yield (96%). Chlorobutyrl chloride underwent the same reaction to produce chlorobutyryl-*O*-tert-butylbenzyl hydroxamic acid in quantitative yield. Both products were white, crystalline solids. The same reaction was used to produce 4-chloromethyl benzo-*O*-tert-butyl hydroxamic acid from 4-chloromethyl benzyl chloride.

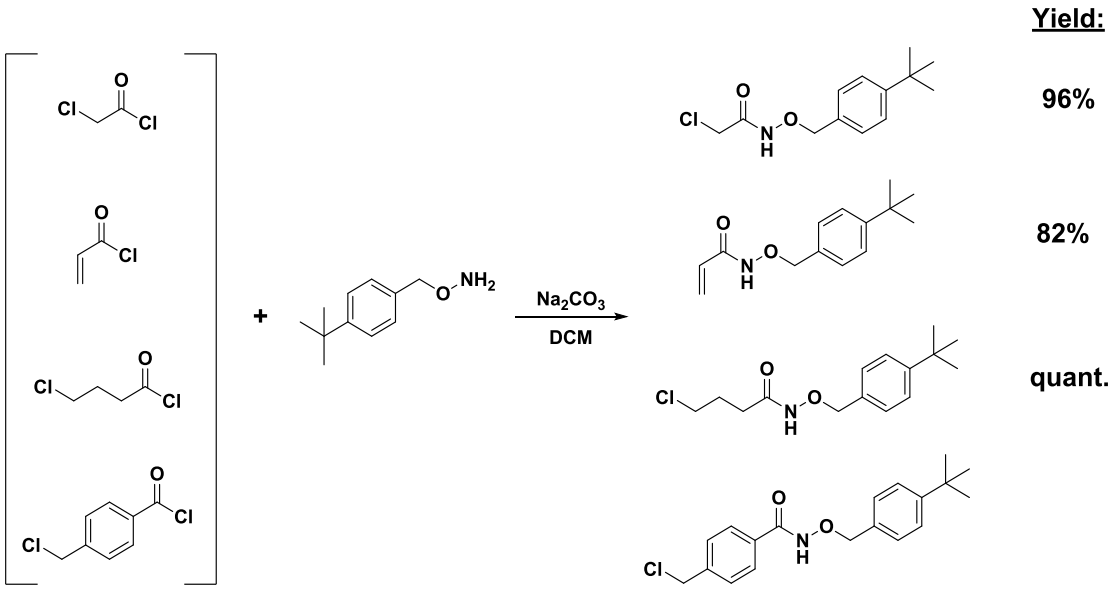

Scheme 4.10: Synthesis of arms containing *O*-tert butyl benzyl protected hydroxamic acids for (top to bottom) EDTHA, EDTPHA, EDTBHA, EDTBnHA.

The subsequent nucleophilic substitution of the alkyl chloride with the ethylenediamine backbone was the major roadblock for this route. To combat the low reactivity of the Cl^- ion, catalytic potassium iodide was added to the reaction. This addition led to a complicated mixture of compounds, including starting material. The oxidation of hydroxamic acids to nitrous acid by iodine, followed by hydrolysis to the carboxylic acid (Scheme 4.11) was reported by Kobashi and coworkers.[68] This report suggests that rather than speeding up reaction with ethylenediamine, the potassium iodide leads to the formation of unwanted products through the decomposition of the

starting material. In future work similar reactions could be performed using a bromide source to catalyze the S_N2 reactions of the relatively inert chloride.

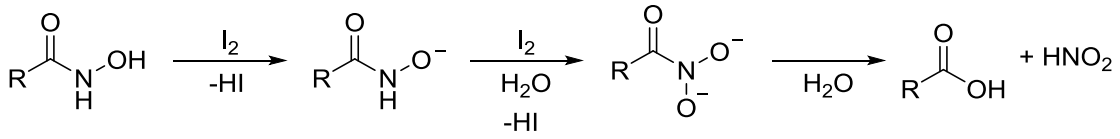

Scheme 4.11: Oxidation of hydroxamic acid by iodine, followed by hydrolysis to a carboxylic acid.[68]

Several attempts to change the reaction system for successful synthesis of EDTHA and EDTBHA were made. The acetyl arm was reacted with ethylenediamine in the presence of excess sodium carbonate for over a month. Evidence of product formation was seen by TLC; however the product could not be isolated and starting material was still present. Using triethylamine as the base instead led to a messier mixture of products and no evidence of product formation. The butyl arm appeared to cyclize during some synthesis attempts, preventing addition to the backbone.

The major issue with these reaction conditions was the possible formation of ligands with various amounts of arms. The desired ligand would have contained four arms, however, MALDI-TOF indicated the presence of the three-armed and five-armed products. To combat this problem, primarily the significant amount of under-reacted three-arm ligand, excess stoichiometric equivalents of the arm synthon were added to the reaction. Characterization did not indicate any improvement in terms of the percentage of desired product in the reaction mixture.

EDTBnHA was successfully synthesized by reacting the benzyl arm with ethylenediamine in the presence of sodium carbonate for one month. The product was isolated by recrystallization as a white solid. Deprotection of the hydroxamic acid groups was attempted by high-pressure hydrogenation in methanol with 10% Pd/C. After 18 hours, no deprotection was observed.

Solubility in methanol was limited, so the solvent was changed to ethanol. The change of solvent did not improve deprotection. Increasing the length of deprotection to over 48 hours did not lead to any change. When the deprotection was performed in 30% acetic acid/ethanol for four hours, evidence of deprotection was observed. However, full deprotection required a longer reaction time.

4.6: Stability constant determination

Potentiometric titrations were performed to study of the effect of changing the carboxylates in EDTP to hydroxamates (EDTPHA). In all cases titrations are performed by dissolving species (either a ligand or a ligand and a metal ion at various ratios) in buffered acidic media and then titrating with base. The potential of the solution is monitored with a pH electrode and is plotted as a function of the volume of base added. A model is generated to account for the protons arising from ligands deprotonating, metal-aquo ligands deprotonating, etc., and the model is refined to match the data. From ligand titrations, the pKa of each proton (referred to as protonation constants below) can be determinedwithin the pH range of the titration, and metal-ligand titrations yield a stability constant, similar to a K_a from simpler systems but accounting for the number of metal ions, ligands, and protons.

Protonation constants allow for understanding of the acidic nature of these ligands. Stability constants with La(III), Eu(III) and Lu(III) were determined to study the formation of complexes with EDTP and EDTPHA. Stability constants measure the extent of formation of a complex in relation to other components of the system at equilibrium. Higher stability constants represent a higher percentage of that complex as one of many possible species in the system.

Protonation constants

The first titrations performed were to determine the protonation constants of EDTA and the formation constants for EDTA-Fe(III). These were done to show agreement with literature values and validate the methods being used. The blind fit of the data matched the literature values well enough to not require subsequent manipulation of the data. EDTP protonation constants were determined and compared to literature values.[69,70] The values for this work were corrected for activity using the Davies equation (Equation 1), where γ is the activity coefficient, z is the charge of the complex and I is the ionic strength of the system. Without the activity correction, the values were comparable to the literature values. Corrections were performed to account for the ionic strength of the system. Corrections lowered the values slightly; however, they are still within an acceptable range. The protonation constants are defined in Equations 2-11.

$$-Log(\gamma) = 0.51z\left(\frac{\sqrt{I}}{1+\sqrt{I}} - 0.30I\right) \quad (1)$$

EDTP has six protons; however in the pH range of the system, only five protonation constants could be determined. The first four values ($logK_{HL}$-$logK_{H4L}$) represent dissociation of the protons from the carboxylate groups and the last two values ($logK_{H5L}$ and $logK_{H6L}$) represent dissociation of the ammonium backbone protons.[71] The protonation constants fall within expected values for polycarboxylate ligands, such as EDTA.

Titration data for EDTPHA (Figure 4.5) has not been published. The closest literature comparison is the 1972 report of EDTAHA (Figure 4.4) by Karlicek and Majer.[62] These values were used to initially build a model to compare the EDTPHA titration data to. Refinement of the values to match the data led to the values listed in Table 4.2. The ligand concentration was varied

(0.5-1.2 mM) to confirm the values. These values were used for modelling the metal complexation titrations with La(III), Eu(III), and Lu(III).

$$H_6L^{6+} \leftrightarrow H_5L^{5+} + H^+ \quad (2)$$

$$H_5L^{5+} \leftrightarrow H_4L^{4+} + H^+ \quad (3)$$

$$H_4L^{4+} \leftrightarrow H_3L^{3+} + H^+ \quad (4)$$

$$H_3L^{3+} \leftrightarrow H_2L^{2+} + H^+ \quad (5)$$

$$H_2L^{2+} \leftrightarrow HL^{+} + H^+ \quad (6)$$

$$HL^{+} \leftrightarrow L + H^+ \quad (7)$$

$$L \leftrightarrow L^{-} + H^+ \quad (8)$$

$$L^{-} \leftrightarrow L^{2-} + H^+ \quad (9)$$

$$L^{2-} \leftrightarrow L^{3-} + H^+ \quad (10)$$

$$L^{3-} \leftrightarrow L^{4-} + H^+ \quad (11)$$

Table 4.3: The protonation constants of EDTP and EDTPHA (*I* = 0.1 M $NaClO_4$, T = 25°C).

	EDTA		**EDTP**		**EDTAHA**	**EDTPHA**
LogK_n	Literature[71]*	Literature[70,71]	Literature[69]	This work	Literature[62]	This work
L^{3-}	10.21±0.04	9.74	9.43±0.04	8.80±0.5	11.1±0.1	11.5±0.05
L^{2-}	6.20±0.04	6.25	6.12±0.06	5.91±0.4	10.6±0.1	10.4±0.1
L^{-}	2.77±0.04	4.29	4.17±0.07	4.00±0.3	7.23±0.02	9.33±0.1
L	2.02±0.05	3.30	3.40±0.07	3.27±0.3	6.67±0.03	10.9±0.1
HL^{+}	1.31±0.10	2.98	2.90±0.07	2.72±0.2	6.05±0.05	9.89±0.2
H_2L^{2+}					5.55±0.05	9.09±0.1
H_3L^{3+}						8.89±0.2
H_4L^{4+}						9.53±0.1
H_5L^{5+}						7.75±0.3
H_6L^{6+}						7.55±0.2

All data determined by potentiometric titrations. *0.1 M KNO_3

Karlicek and Majer only reported six protons, the four hydroxamate (OH) groups and the two backbone ammonium protons. This set of protons was initially used but did not allow the model to accurately predict the behavior of the data, as can be seen in Figure 4.13, which shows the observed data (blue line) versus the calculated data (red line) with six protons. Figure 4.14 shows the fit of the data (blue line) to the model (red line) with ten protons and refinement of the values.

The model requires the assumption that the hydroxamate amino groups are all protonated in H_6L^{6+} (Figure 4.12). The resonance of the hydroxamate anion (Scheme 4.2) explains why the first eight protonation constants are nearly the same. The constants most likely represent an average of the loss of the two protons from each hydroxamate and the effect of the resonance structures. The speciation diagram of the base titration of EDTPHA is shown in Figure 4.15. The diagram shows the relatively low formation of L^-, HL^+, H_3L^{3+}, and H_5L^{5+}. further confirming the nearly simultaneous loss of both protons from each hydroxamate group. The data fits the 10H model across varying ligand and acid concentrations, verifying the validity of the model (Figure 4.16).

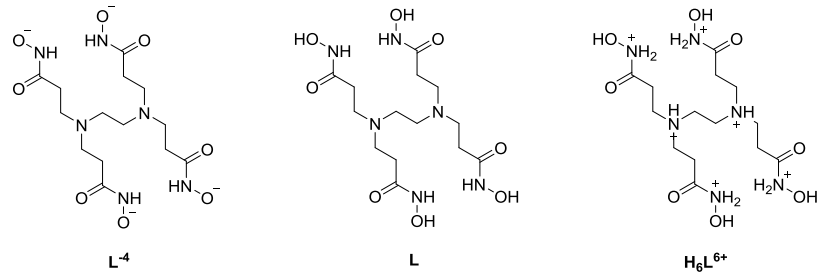

Figure 4.12: Example suggested protonation states for EDTPHA ligand in 10 proton model (Table 4.3).

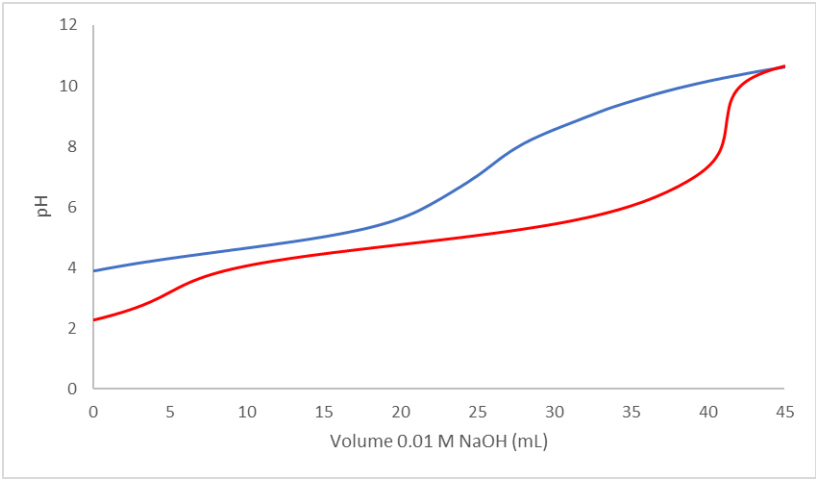

Figure 4.13. Calculated (red) and observed (blue) pH of base titration of EDTPHA in 0.1 M $NaClO_4$ with six protons in the model.

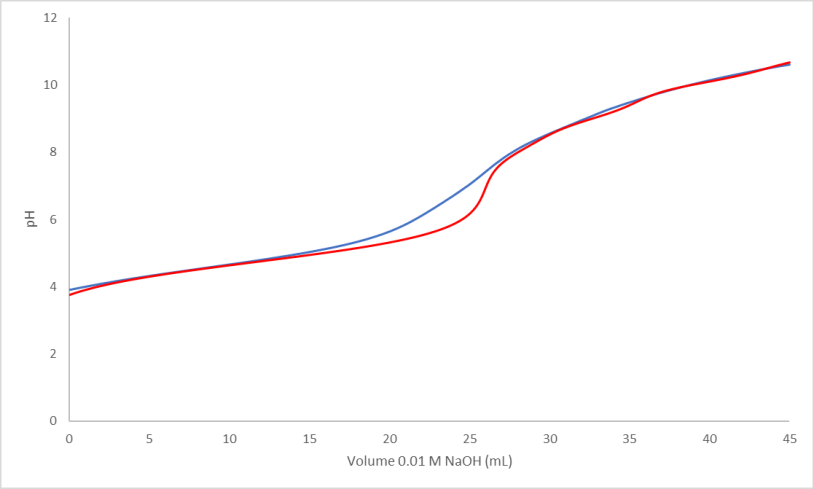

Figure 4.14. Calculated (red) and observed (blue) pH range of base titration of EDTPHA in 0.1 M $NaClO_4$ with ten protons in the model.

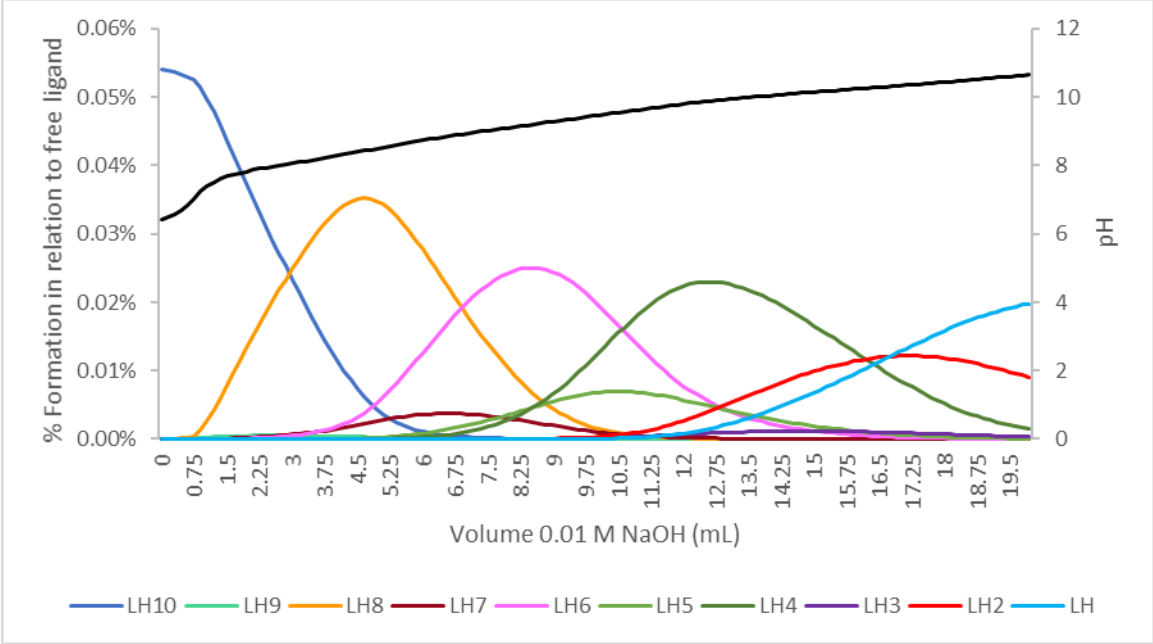

Figure 4.15. Speciation diagram for base titration of EDTPHA. Only a pH range of 7-11 (black line) is shown.

Comparison of the stability constants of coordination with La(III), Eu(III) and Lu(III) allowed for direction comparison of the chelation ability of EDTP and EDTPHA. The choice of metals also allowed for understanding of the general trend across the lanthanide series. The use of perchlorate salts of the metals avoided the presence of coordinating anions in the system.

However, the EDTPHA solution did have acetic acid present in a high enough concentration (a consequence of the final deprotection and the ligand's decomposition under sufficient vacuum and heat to remove all the acetic acid) that it had to be accounted for in the model. Fortunately, the acetic acid-Ln(III) coordination did not compete with the ligand.

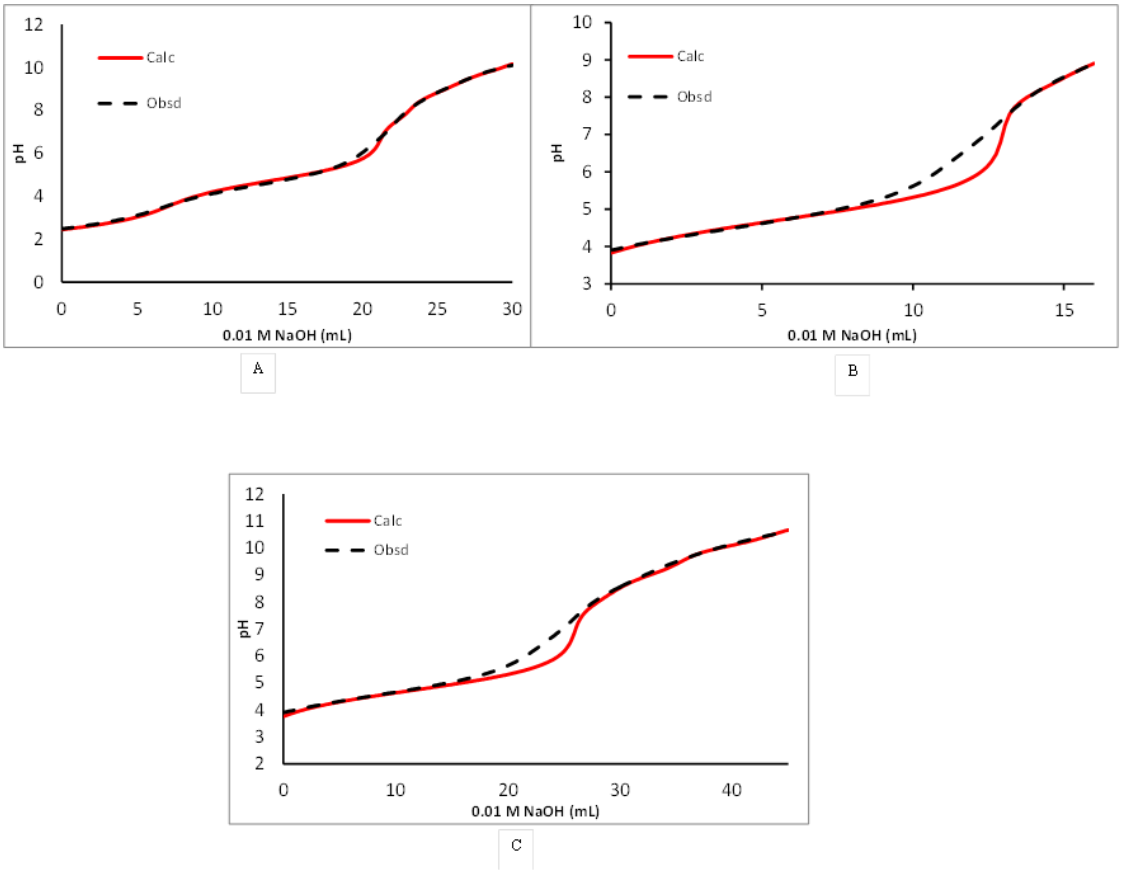

Figure 4.16. EDTPHA protonation trials with varying conditions. (A) EDTPHA (0.475 mM), AcOH (7.125 mM), H^+ (15.4 mM), titrate 30 mL 0.01 M NaOH. (B) EDTPHA (0.475 mM), AcOH (7.125 mM), H^+ (11.25 mM), titrate 16 mL 0.01 M NaOH. (C) EDTPHA (1.9 mM), AcOH (45 mM), H^+ (28.5 mM), titrate 45 mL 0.01 M NaOH.

Table 4.4. Stability constants for EDTP with La(III), Eu(III), and Lu(III) (I = 0.1 M $NaClO_4$).

Logβ	La(III)	Eu(III)	Lu(III)	
$M(OH)^{2+}$	-8.64[1]	-7.76	-7.61	
$M(OH)_2^{+}$	-11.6[1]	-15.8	-11.6	
$M(OH)_3$	-20.3[1]	-21.4	-14.5	
ML^{-}	11.6±0.9	10.3±1.0		This work
MLH	16.4±1.6	19.0±0.9	23.4±2.1	This work
	14.0[2]	14.3[2]	14.0[2]	
MLH_2	25.2±2.1	25.2±1.5	27.6±0.9	This work
	19.4[2]	19.7[2]	19.1[2]	
MLH_3	33.8±0.6	27.9±1.4	29.7±2.7	This work
	22.6[2]	22.7[2]	22.3[2]	
ML_2	20.9±0.8	15.6±0.8	21.0±0.2	This work
ML_2H	26.7±2.0	24.0±1.1	29.3±1.1	This work
ML_2H_2	29.6±2.6	33.4±0.6	35.6±2.9	This work

(1) LLNL Database.[72] (2) Ref 69 (I = 0.1 M $NaClO_4$)

The stability constants of EDTP with the lanthanide series have been reported.[69] However, the authors only reported the existence of ML species and not possible ML_2 species. Additionally, the authors ignored the lanthanide hydrolysis products, despite the pH range of 3-12, which could allow for the formation of insoluble hydroxide complexes. Modeling the data with the reported ML, MLH, MLH_2, and MLH_3 complexes did not lead to a good fit. However, the suggested complex structure from Hietapelto and coworkers (Figure 4.17) leaves room for the formation of the ML_2 species. Addition of ML_2 species (including ML, MLH, and ML_2H) and refining the data allowed for fitting of the data and determination of the stability constants.

The stability constants determined in this work are drastically different from the reported values, most likely due to the inclusion of the ML_2 species. Without identification of the species during titration, these constants cannot be considered definitive; however, the model provides the best fit of the data, suggesting a possible speciation of the system. The large error for MLH_2 and MLH_3 are due to the low relative formation of these complexes in the system. The primary complex formed is the ML_2 complex.

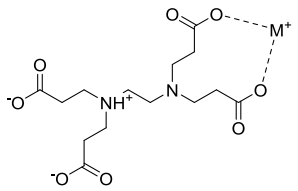

Figure 4.17. Suggested ML structure of EDTP-Ln(III) complex.[69]

Modeling the speciation of EDTPHA with the lanthanides was much more complicated. Karlicek and Majer reported stability constants of EDTAHA with Fe(III) and Cu(II).[62] Other polyhydroxamate ligands have been studied with other metals, including La(III), Th(IV) and U(VI).[54,63,73] Figure 1.3 shows some of the reported polyhydroxamate ligands that have been reported. However, there have not been any stability constants for EDTPHA reported. The model for the studied system was built using the constants from Table 4.4 as a starting point. Additionally, constants reported for H_4CDTMAHA (Figure 1.3, VI) were considered. The authors reported possible MLH_4 with Th(IV) and $M_2L_2H_4$ with Fe(III).[73]

According to the modeled data, the metals remain coordinated by acetic acid until around pH 6, when the ligand begins to coordinate them. Between pH 6.4 and 7.3, the primary complex is MLH_8, then MLH_6 (pH 7.3-8.5), then MLH_4 (pH 9.4-9.2), then MLH_2 (pH 9.2-10.3) and finally ML_2 (pH 10.3+). The major complexes follow the dissociation of the protons from the hydroxamate arms. Definitive determination of the speciation would require mass spectrometry to understand what complexes are present in the system.

Table 4.5. Stability constants for EDTPHA with La(III), Eu(III), and Lu(III) (I = 0.1 M $NaClO_4$).

Logβ	La(III)	Eu(III)	Lu(III)
ML^-	15.0±0.03	18.1±1.9	15.5±0.08
MLH	26.3±1.8	27.9±2.2	26.2±0.7
MLH_2^+	38.3±1.3	38.3±1.1	37.3±0.2
MLH_3^{+2}	47.4±1.3	47.7±0.9	47.0±0.3
MLH_4^{+3}	56.6±0.4	56.8±0.4	56.3±0.2
MLH_5^{+4}	64.4±0.001	65.0±0.6	65.0±0.3
MLH_6^{+5}	73.6±0.2	73.8±0.07	73.8±0.2
MLH_7^{+6}	81.2±0.3	81.2±0.4	81.6±0.2
LMH_8^{+7}	88.3±0.5	88.6±0.4	88.6±0.3
ML_2^{-5}	23.7±0.8	26.2±1.4	21.9±1.7
ML_2H^{-4}	32.9±1.3	32.1±1.3	31.6±0.3
$ML_2H_2^{-3}$	44.5±0.6	45.1±1.6	42.5±0.9
$ML_2H_3^{-2}$	54.7±0.7	56.6±1.2	53.3±0.6
$ML_2H_4^-$	64.8±0.2	66.0±1.1	63.5±0.3
$M_2L_2H_2$	56.1±0.1	56.9±0.7	56.7±0.4
AcOH	4.78±0.04	4.67±0.02	4.73±0.07
$MAcO^{+2}$	1.85[1]	1.85[1]	1.85[1]
$M(AcO)_2^+$	5.01[1]	5.01[1]	5.01[1]
$M(AcO)_3$	8.82±0.7	9.18±1.1	10.2±1.2

(1) NIST Database 46.[74]

The best comparison of the chelating ability of EDTP and EDTPHA is the LH_2 stability constants. The $\log\beta_{ML2}$ values for EDTPHA are higher than the corresponding EDTP constants, signifying stronger complex formation by EDTPHA. The metal complexation undergoes the same trend as EDTP, with the metal fully coordinated by the ligand by about pH 7. The primary complexes cycle through MLH_8, MLH_6, MLH_4, MLH_3, MLH_2 and finally ML_2.

The $\log\beta_{ML}$ constants are also higher for EDTPHA than EDTP. The EDTPHA values are in the range for what has been reported for EDTA with *d*-block metals and lanthanides ($\log\beta_{ML}$~18).[74] For the best possible comparison, titrations of EDTAHA with the lanthanides would be necessary. These titrations would allow for an understanding of not only the effect of including the hydroxamate groups, but also extending the arms by one carbon. However, the

reported data for EDTPHA provides an insight into the promising chelating ability of this decadentate ligand. Final refinements of the data are underway and will give more insight into the EDTPHA coordination system.

4.7. Conclusions

Ligand design for the *f*-elements has been driven by the need for highly selective ligands capable of forming stable complexes in complex environments. The unique chemistry of the hydroxamic acid functional group, as seen in the interaction of siderophores with environmental Fe(III), led to attempts to utilize them in the design of *f*-element ligands. The bidentate nature of hydroxamic acids allowed for coordination of larger metals with high coordination numbers (e.g. *f*-elements). Many literature examples exist studying the effectiveness of mono- and polyhydroxamic acid ligands for coordination of the lanthanides and actinides. While there is much promise in the reports, the big downfalls of hydroxamic acids are the difficult synthesis, characterization and purification of the group. This downfall required the development of a straightforward route toward the synthesis of polyhydroxamic acid ligands.

A route toward the synthesis of polyhydroxamic acid ligands utilizing *O*-protected hydroxylamines and acrylate starting materials has been developed. The use of *O*-protected hydroxylamines circumvents the difficult characterization and purification of traditional hydroxamic acid synthesis. This route was used to synthesize a tetrahydroxamic acid EDTA derivative, EDTPHA. The tetrabenzyl-protected ligand was synthesized through the aza-Michael addition of *O*-protected hydroxamic acid acrylate and ethylenediamine. The benzyl groups were removed under pressure (300 psi) in the presence of Pd/C and acetic acid.

Potentiometric titrations were used to study and compare the solution thermodynamics of EDTPHA and the carboxylate derivative, EDTP. Stability constants were determined for both ligands with La(III), Eu(III), and Lu(III). For both ligands, the data suggests the dominant metal complex in solution is the ML_2 complex. Overall, the stability constants were higher for EDTPHA than EDTP, suggesting a positive impact on complex stability from the addition of the hydroxamic acid functional group. The stability constants of EDTPHA with the lanthanides that were studied were similar to EDTA, while the EDTP constants were several orders of magnitude lower than EDTA. These promising results suggest that EDTPHA could be equally as effective as EDTA for coordination of the *f*-elements. The slightly lower values of EDTPHA suggest that the propyl hydroxamate arms may have created a binding pocket too large for the lanthanides. In this case, a smaller ligand, EDTHA, must be studied to better understand the topology effects on coordination of the target metals. With optimization, this ligand design could hold potential for the use in the selective coordination of the lanthanide and actinides.

4.8. Future directions

Ligand design

For better understanding of the effects of the inclusion of hydroxamic acids into an ethylenediamine backbone, a full series of EDTA derivatives must be studied. EDTA is too small for Fe(III) and allows for the coordination of a solvent molecule with the metal core when fully coordinated. When the target metal is the larger *f*-elements, the smaller ligand size becomes a major issue for complex stability. While the inclusion of hydroxamic acids will increase the coordination sites of the ligand, from hexadentate to decadentate, they would be unable to fully coordinate a large metallic core if the ligand backbone is too small. The ultimate goal for the project is to study the effect of the arm length of the ligand on the complex stability with the *f*-

elements. Future ligands to be synthesized should include the acetyl arm (EDTHA), butyl arm (EDTBHA) and benzyl arm (EDTBnHA) for study of ligand preorganization as well as arm length. The hydroxamic acid-containing arms have all been synthesized in high yield. However, the final addition of the arms to the ethylenediamine backbone was not accomplished. Once this chemistry has been worked out, a full series of ligands will be able to be studied. Additionally, the ligands should be compared to their carboxylate counterparts, EDTA, EDTBA, and EDTBnA to further understand the effects of the hydroxamic acid arms.

The straightforward and highly successful use of the acrylate starting material used for the synthesis of EDTPHA in and aza-Michael addition for the synthesis of a polyhydroxamic acid ligand holds a lot of potential for the creation of novel polyhydroxamic acid ligands. For example, initial attempts were made to add the acrylate arm to 1,4,7,10-tetraazacyclododecane (cyclen). This synthesis has been published,[57] but no work with metals was published. The preorganized backbone might provide a positive impact on the coordination of metals due to the lower entropic requirement of coordination. The acrylate arm could be added to a variety of amines through the aza-Michael addition reaction, leading to a new group of polyhydroxamic acids for study with the *f*-elements.

Solution thermodynamics

The reported titration data was determined by potentiometric titrations. The suggested models were determined computationally. For further confirmation of the speciation of the systems, mass spectrometry must be carried out at varying pH and concentrations. This study will determine which species are present at different points of the titration. Additionally, the stability constants with other metals, such as thorium(IV) and plutonium(IV) would allow for further investigation of the effectiveness of EDTPHA for the coordination of the *f*-elements. The distribution constants

of metals with EDTPHA would give further insight into the complex stability of the ligand with various metals in competitive environments. This experiment would also show the effectiveness of the ligand at separating metals in liquid-liquid extraction.

Once synthesized, the full series of ligands would need to be studied with all metals in order to optimize the ligand design. Each polycarboxylate and polyhydroxamate ligand would need to be compared to fully understand the topology effects of the inclusion of the hydroxamic acid group.

4.9. Experimental – Synthetic methods

Chemicals: *N*-hydroxyphthalimide and triethylamine were obtained from Chem-Impex. 4-t-Butylbenzyl bromide was obtained from Oakwood Chemicals. Hydrazine monohydrate and acryloyl chloride were obtained from Beantown Chemicals. Chloroacetyl chloride was obtained from Alfa Aesar. 4-Chlorobutyryl chloride was obtained from EMD Millipore. 4-Chloromethyl benzoyl chloride was obtained from TCI. All solvents were obtained from BDH. All chemicals were used without further purification.

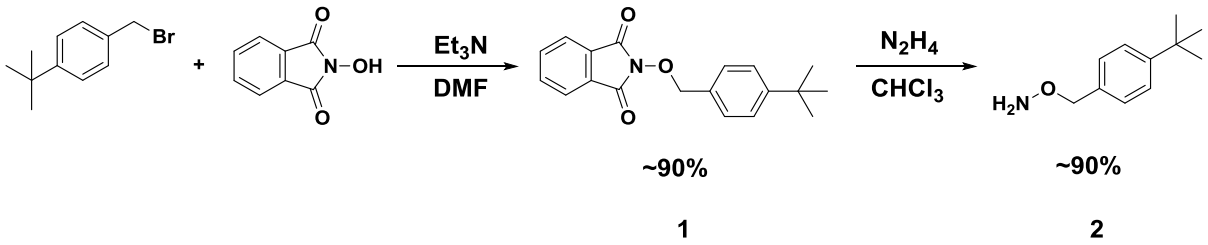

Scheme 4.12. Synthesis of *O*-tert butyl benzyl hydroxamic acid.

Synthesis of *O*-tert butyl benzyl hydroxamic acid: (**1**) Minimal N,N-dimethylformamide (300 mL) was used to dissolve *N*-hydroxylphthalimide (1 eq, 24.4 g) in a round-bottom flask, resulting in a yellow solution. Slowly, triethylamine (1 eq, 20.9 mL) was added to the reaction, which

turned the reaction mixture dark red. 4-t-butylbenzyl bromide (1 eq, 27.5 mL) was then added. After less than a minute, the reaction began to lighten, as solid began to form. The reaction was stirred at room temperature under ambient conditions. After 48 hours, enough solid was present to give the reaction an orange hue. The volume was doubled with deionized water, precipitating the product as a white solid, which was collected by vacuum and dried (43.4 g, 94%). ^{1}H NMR (500 MHz, DMSO): 7.19-7.17 δ (d, *J* = 10.25 Hz, 2 H), 6.86-6.84 δ (d, *J* = 10.25, 2 H), 3.73 δ (s, 2 H), 1.50 δ (s, 9 H). ^{13}C NMR (500 MHz, DMSO): 156.6 δ, 156.3 δ, 129.5 δ, 129.4 δ, 129.0 δ, 128.9 δ, 126.4 δ, 126.3 δ, 115.5 δ, 67.0 δ, 45.9 δ, 44.6 δ, 28.4 δ, 27.7 δ.

(**2**) Hydrazine monohydrate (10 eq, 130 mL) was slowly added to a solution of **1** (1 eq, 41.4 g) in chloroform (400 mL). The reaction mixture was stirred under reflux. Hydrazine was added every eight hours, three times for a total of 30 eq. After 24 hours, the reaction was cooled and the product extracted into dichloromethane three times, then dried over anhydrous sodium sulfate. The solvent was removed under reduced pressure, resulting in a viscous, colorless liquid (23.5 g, 98%). ^{1}H NMR (500 MHz, DMSO): 7.37-7.33 δ (t, *J* = 8.31 Hz, 2H), 7.26-7.22 δ (t, *J* = 8.31), 4.53 δ (s, 2H), 1.28 δ (s, 9H). ^{13}C NMR (500 MHz, DMSO): 150.28 δ, 135.71 δ, 128.31 δ, 125.35 δ, 77.18 δ, 34.69 δ, 31.63 δ.

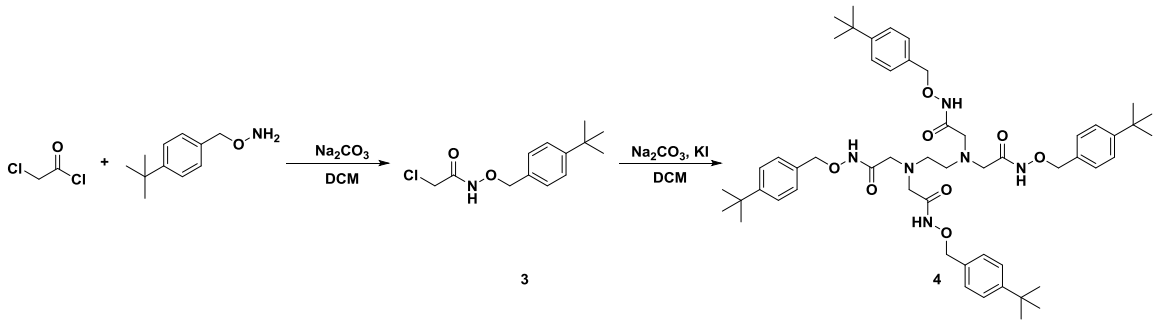

Scheme 4.13. EDTPHA synthesis.

Synthesis of EDTAHA: (3) Synthesis: 2 (1 eq, 17.9 g) and sodium carbonate (2 eq, 21.1 g) were cooled to 0°C in dichloromethane (200 mL). Chloroacetyl chloride (1 eq, 7.9 mL) was slowly added by addition funnel. More dichloromethane was added to aid stirring as a white solid began to form. The reaction was stirred at room temperature under ambient conditions for 4 hours. The reaction was filtered and the solvent was removed from the filtrate under reduced pressure, resulting in a white solid. The product was recrystallized in methanol, producing colorless, crystalline plates. (24.4 g, 96%). ^{1}H NMR (500 MHz, DMSO): 1.280 (s, 9.5 H), 3.964 (s, 1.7 H), 4.777 (s, 2.0 H), 7.317-7.333 (d, 1.9 H), 7.403-7.419 (d, 2.0 H), 11.470 (0.94 H). ^{13}C NMR (500 MHz, DMSO): CNMR (500 MHz, DMSO): 31.11, 34.35, 40.33, 76.67, 125.15, 128.85, 132.72, 150.91, 163.18.

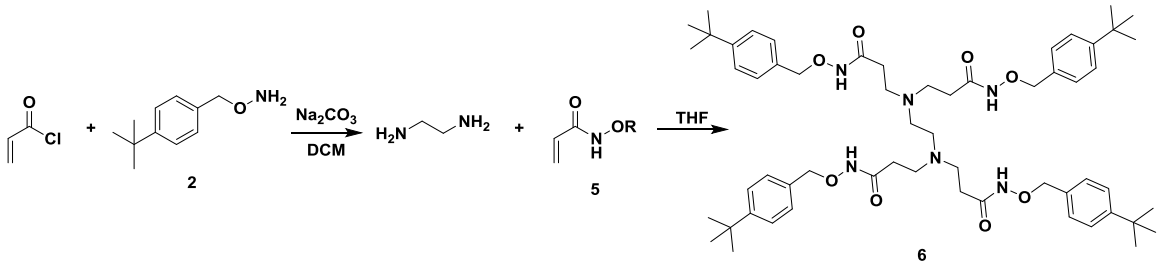

Scheme 4.14. EDTPHA synthesis.

Synthesis of EDTPHA: (5) 2 (1 eq, 3.1 g), sodium carbonate (2 eq, 3.6 g), and dichloromethane (100 mL) were cooled to 0°C in an acid-washed round-bottom flask. Acryloyl chloride (1 eq, 1.4 mL) was added over 30 minutes by addition funnel. More dichloromethane was added to aid stirring after the immediate formation of a white solid. The reaction was stirred at room temperature for 24 hours. The reaction mixture was then purified by extraction. The product was extracted into dichloromethane three times and dried over anhydrous sodium sulfate. The product was further purified through flash column chromatography (0-5% methanol/dichloromethane). Solvent was removed under reduced pressure, resulting in a pale, yellow oil (2.3 g, 58%). ^{1}H

NMR (500 MHz, $CDCl_3$): 1.310 (s, 9.15 H), 4.911 (br s, 1.7 H), 5.677 (br s, 0.77 H), 6.002 (br s, 0.50 H), 6.331-6.370 (br d, 0.82 H), 7.309-7.323 (d, 1.9 H), 7.383-7.400 (d, 2.0 H).

(**6**) **5** (4.1 eq, 10.5 g) and ethylenediamine (1 eq, 0.73 mL) were dissolved in minimal tetrahydrofuran (100 mL) in an acid-washed round-bottom flask. The reaction was stirred under reflux for 72 hours. After cooling, the solvent was removed under reduced pressure to give a yellow oil. The product was purified through column chromatography. The pure product was a white, crystalline solid (3.6 g, 31% yield). ^{1}H NMR (500 MHz, DMSO): 7.27-7.26 δ (d, *J* = 8.25 Hz, 1.4 H), 7.10-7.09 δ (d, *J* = 8.25 Hz, 1.4 Hz), 3.18 δ (s, 4 H), 2.66-2.63 δ (t, *J* = 7.50 Hz, 8 H), 2.43 δ (s, 4 H), 2.26 δ (s, 2.2 H), 2.11-2.08 δ (t, *J* = 7.50 Hz, 8 H), 1.91 δ (s, 28 H), 1.26 δ (s, 7 H). ^{13}C NMR (500 MHz, DMSO): 172.5 δ, 168.7 δ, 134.6 δ, 129.0 δ, 125.4 δ, 49.9 δ, 49.1 δ, 31.7 δ, 30.6 δ, 21.6 δ, 20.9 δ.

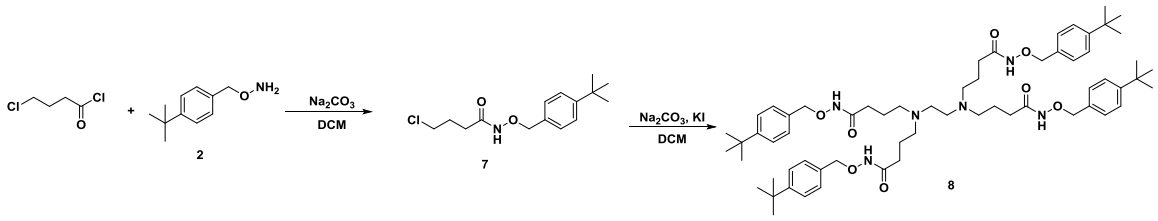

Scheme 4.15. EDTBHA synthesis.

Synthesis of EDTBHA: (7) 2 (1 eq, 12.6 g), sodium carbonate (2 eq, 14.9 g), and dichloromethane (300 mL) were cooled to 0°C in an acid-washed round-bottom flask. 4-Chlorobutyryl chloride (1 eq, 9.9 g) was added. More dichloromethane was added to aid stirring after the immediate formation of a white solid. The reaction was stirred at room temperature for 24 hours. Solvent was removed *in vacuo*, resulting in a white solid (20.0 g, quant.). ^{1}H NMR (500 MHz, DMSO): 11.02 δ (s, 1 H), 7.40-7.39 (d, *J* = 7.98 Hz, 2 H), 7.32-7.30 δ (d, *J* = 7.98 Hz, 2

H), 4.74 δ (s, 2 H), 3.62-3.59 δ (t, *J* = 6.60 Hz, 2 H), 2.12-2.10 δ (t, *J* = 6.60 Hz, 2 H), 1.96-1.92 δ (m, *J* = 6.94 Hz, 2 H), 1.28 δ (s, 9 H).

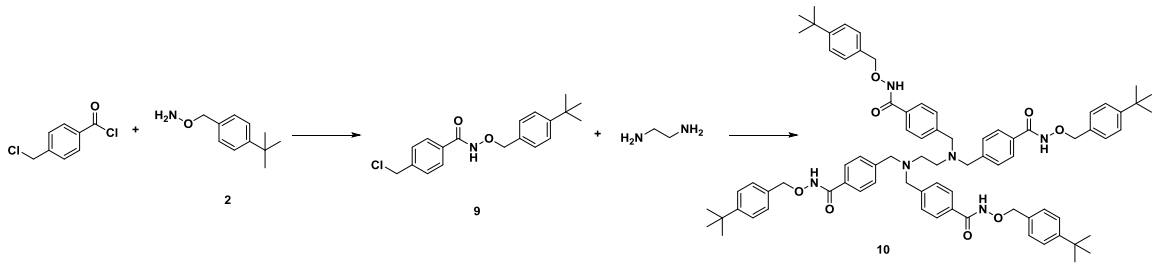

Scheme 4.16. EDTBnHA synthesis.

Synthesis of EDTBnHA: (9) 2 (1 eq, 10.8 g)was cooled to 0°C in a mixture of dichloromethane (150 mL) and Na_2CO_3 (2 eq, 12.8 g). While the mixture was stirring, 4-chloromethylbenzoyl chloride (1 eq, 11.4 g) in dichloromethane (100 mL) was slowly added dropwise. A white solid formed immediately, requiring more dichloromethane for stirring. The reaction was stirred at room temperature overnight. The solid was removed by filtration and the solvent removed from the filtrate under reduced vacuum. The resulting white solid was recrystallized in dichloromethane. The final product was a crystalline, white solid. ^{1}H NMR (500 MHz, DMSO): 7.77-7.75 δ (d, *J* = 9.13 Hz, 2 H), 7.53-7.52 δ (d, *J* = 9.13 Hz, 2 H), 7.43-7.41 δ (d, *J* = 9.13 Hz, 2 H), 7.38-7.37 δ (d, *J* = 9.13 Hz, 2 H), 4.89 δ (s, 2 H), 4.80 δ (s, 2 H), 1.28 δ (s, 9 H). ^{13}C NMR (500 MHz, DMSO): 150.8 δ, 141.1 δ, 132.9 δ, 132.2 δ, 128.9 δ, 127.5 δ, 76.8 δ, 45.4 δ, 34.3 δ, 31.1 δ.

4.8. Experimental: Potentiometric titrations

Potentiometric titrations

General: All titrations were performed with an 836 Titrando equipped with an 800 Dosino autotitrator. An Orion 8102BNUWP Ross Ultra pH electrode was used to measure the change in potential during titrations. A NIST standardized 0.01 M NaOH solution was used. This solution was used to standardize 0.01 M HClO4 solutions made from the dilution of a 1 M solution from Fluka. All titrations were performed in a vessel jacketed by a water bath set to 25°C. The ionic strength was kept constant with 0.1 M $NaClO_4$ (EMD Chemicals). Protonation constants were determined by titrating a solution of the ligand in $NaClO_4$ with NaOH up to pH 12. The ligand concentrations were varied (0.5-1.5 mM) to further confirm the constants. Before each titration, the electrode was calibrated by an acid-base titration with standardized 0.01 M $NaClO_4$ and 0.01 M NaOH. The E_0 and slope factor values were obtained by analyzing the calibration data with GLEE3. Measurements were recorded every 0.15 mL and the probe equilibration time was 360 sec for the calibrations and 900 sec for the experiments. The models were built using HySS and literature values. All data was compared and refined with Hyperquad.[75] All metal solutions were made from perchlorate salts and were 0.03 M in 0.01 M $HClO_4$. The $\log K_{OH}$ value was set to -13.997 for all titrations.

Electrode calibration: 2 mL of 0.01 M $HClO_4$ in 28 mL 0.1 M $NaClO_4$ was titrated with 4 mL 0.01 M NaOH. The electrode equilibration time was set to 360 sec. The E_0 value was determined by analyzing the data with GLEE3.[76]

EDTA titrations: A 0.03 M EDTA solution was made by dissolving disodium EDTA (BDH, 2.2334 g) in 200 mL 0.1 M $NaClO_4$. A 0.03 M $Fe(ClO_4)_3$ solution was made by dissolving

$Fe(ClO_4)_3 \bullet H_2O$ (Beantown Chemical, 2.7734 g) in 200 mL 0.01 M $HClO_4$. Protonation constants were determined by base titrations of EDTA (0.5-1.5 mM) from pH 3-10. Stability constants for EDTA-Fe(III) complexes were determined by base titrations of mixtures of 1:1, 1:2, and 1:3 M:L. There were carried out from pH 3-10.

EDTP titrations: A 0.03 M EDTP solution was made by dissolving $EDTPNa_4(H_2O)_2$ (2.834 g) in 200 mL 0.1 M $NaClO_4$. To cover a pH range of 4-10, 0.01 M $HClO_4$ was added to the beginning of the titration to lower the pH. Stability constants for La(III), Eu(III) and Lu(III) and EDTP were all determined by base titrations of mixtures of 1:1, 1:2, and 1:3 M:L.

EDTPHA titrations: A 0.016 M EDTPHA solution was made by dissolving EDTPHA (0.162 g) in 25 mL 0.01 M $HClO_4$. Stability constants for La(III), Eu(III) and Lu(III) and EDTP were all determined by base titrations of mixtures of 1:1, 1:2, and 1:3 M:L.

(1) Lossen, W. The Benzoyl Derivatives of Hydroxylamine. *European J. Org. Chem.* **1872**, *161*, 347–362.

(2) Yale, H. L. The Hydroxamic Acids. *Chem. Rev.* **1943**, *33* (1), 209–256.

(3) Sandler, S. R.; Karo, W. Hydroxamic Acids. In *Organic Functional Groups Preparations Volume III*; Blomquist, A. T., Wasserman, H., Eds.; Academic Press: New York, 1989; pp 482–522.

(4) Neilands, J. B. A Crystalline Organo-Iron Pigment from a Rust Fungus (Ustilago Sphaerogena). *J. Am. Chem. Soc.* **1952**, *74*, 4846–4847.

(5) Emery, T.; Neilands, J. B. The Iron-Binding Centre of Ferrichrome Compounds. *Nature* **1959**, *183*, 1813–1814.

(6) Neilands, J. B. Hydroxamic Acids in Nature. *Science.* **1967**, *156* (3781), 1443–1447.

(7) Bauer, L.; Exner, O. The Chemistry of Hydroxamic Acids and N-Hydroxyimides. *Angew. Chemie* **1974**, *13* (6), 376–384.

(8) Plapinger, R. E. Ultraviolet Absorption Spectra of Some Hydroxamic Acids and Hydroxamic Acid Derivatives. *J. Org. Chem.* **1958**, *24*, 802–804.

(9) Steinberg, G. M.; Swidler, R. The Benzohydroxamate Anion. *J. Org. Chem.* **1965**, *30*, 2362–2365.

(10) Knapp, D. R. Nitrogen Functional Groups Other than the Amino Group. In *Handbook of Analytical Derivatization Reactions*; Wiley: New York, 1979; pp 350–372.

(11) Abualreish, M. J. A.; Abdein, M. A. The Analytical Applications And Biological Activity of Hydroxamic Acids. *J. Adv. Chem.* **2014**, *10* (1), 2117–2125.

(12) Exner, O.; Holubek, J. Acyl Derivatives of Hydroxylamine. XI. Study of Hydroxamic

Acids Dissociation by Means of UV-Spectroscopy. *Collect. Czech. Chem. Commun.* **1964**, *30*, 940–951.

(13) Exner, O.; Simon, W. Acyl Derivatives of Hydroxylamine. XII. Dissociation Constants of Hydroxamic Acids and Their Functional Derivatives. *Collect. Czech. Chem. Commun.* **1965**, *30*, 4078–4094.

(14) Agrawal, Y. K. Hydroxamic Acids and Their Metal Complexes. *Russ. Chem. Rev.* **1979**, *48* (10), 948–963.

(15) Böhm, S.; Exner, O. Acidity of Hydroxamic Acids and Amides. *Org. Biomol. Chem.* **2003**, *1*, 1176–1180.

(16) *Hydroxamic Acids - A Unique Family of Chemicals with Multiple Biological Activities*; Gupta, S. P., Ed.; Springer-Verlag: Meerut, India, 2013.

(17) Ohtsuka, N.; Okuno, M.; Hoshino, Y.; Honda, K. A Base-Mediated Self-Propagative Lossen Rearrangement of Hydroxamic Acids for the Efficient and Facile Synthesis of Aromatic and Aliphatic Primary Amines. *Org. Biomol. Chem.* **2016**, *14*, 9046–9054.

(18) Hoshino, Y.; Okuno, M.; Kawamura, E.; Honda, K.; Inoue, S. Base-Mediated Rearrangement of Free Aromatic Hydroxamic Acids (ArCO–NHOH) to Anilines. *Chem. Commun.* **2009**, 2281–2283.

(19) Buglass, A. J.; Hudson, K.; Tillett, J. G. The Acid-Catalysed Hydrolysis and Protonation Behavior of Hydroxamic Acids. *J. Chem. Soc. B Phys. Org.* **1971**, 123–126.

(20) Berndt, B. C.; Fuller, R. L. The Kinetics and Mechanism of the Hydrolysis of Benzohydroxamic Acid. *J. Org. Chem.* **1966**, *31* (10), 3312–3314.

(21) Kakkar, R. Theoretical Studies on Hydroxamic Acids. In *Hydroxamic Acids: A Unique*

Family of Chemicals with Multiple Biological Activities; Gupta, S. P., Ed.; Springer-Verlag: Berlin, 2013; pp 19–53.

(22) Chatterjee, B. Donor Properties of Hydroxamic Acids. *Coord. Chem. Rev.* **1978**, *26* (3), 281–303.

(23) Barocas, A.; Baroncelli, F.; Biondi, G. B.; Grossi, G. The Complexing Power of Hydroxamic Acids and Its Effect on Behaviour of Organic Extractants in the Reprocessing of Irradiated Fuels II: The Complexes Between Benzohydroxamic Acid and Thorium, Uranium(IV) and Plutonium(IV). *J. Inorg. Nucl. Chem.* **1966**, *28*, 2961–2967.

(24) Baroncelli, F.; Grossi, G. The Complexing Power of Hydroxamic Acids and Its Effect on the Behaviour of Organic Extractants in the Reprocessing of Irradiated Fuels I: The Complexes Between Benzohydroxamic Acid and Zirconium, Iron(III) and Uranium(VI). *J. Inorg. Nucl. Chem.* **1965**, *27*, 1085–1092.

(25) Notari, R. E.; Munson, J. W. Hydroxamic Acids I: Factors Affecting the Stability of the Hydroxamic Acid-Iron Complex. *J. Pharm. Sci.* **1969**, *58* (9), 1060–1064.

(26) Kaltsoyannis, N.; Scott, P. *The F Elements*; Oxford University Press, 1999.

(27) Gorden, A. E. V.; Xu, J.; Raymond, K. N.; Durbin, P. Rational Design of Sequestering Agents for Plutonium and Other Actinides. *Chem. Rev.* **2003**, *103*, 4207–4282.

(28) Silverio, L. B.; Lamas, W. de Q. An Analysis of Development and Research on Spent Nuclear Fuel Reprocessing. *Energy Policy* **2011**, *39*, 281–289.

(29) Tian, G.; Teat, S. J.; Zhang, Z.; Rao, L. Sequestering Uranium from Seawater: Binding Strength and Modes of Uranyl Complexes with Glutarimidedioxime. *Dalton Trans.* **2012**, *41*, 11579–11586.

(30) Davies, R. V.; Kennedy, J.; McIlroy, R. W.; Spence, R. Extraction of Uranium from Sea Water. *Nature* **1964**, *203*, 1110–1115.

(31) Gopalan, A. S.; Jacobs, H.; Koshti, N. M.; Stark, P.; Huber, V.; Dasaradhi, L.; Caswell, W.; Smith, P. H.; Jarvinen, G. Synthesis and Evaluation of Polyhydroxamate Chelators for Selective Actinide Ion Sequestration. In *5th Annual WERC Technology Development Conference*; Las Cruces, NM, 1995; pp 77–98.

(32) O'Boyle, N. C.; Nicholson, G. P.; Piper, T. J.; Taylor, D. M.; Williams, D. R.; Williams, G. A Review of Plutonium(IV) Selective Ligands. *Appl. Radiat. Isot.* **1997**, *48* (2), 183–200.

(33) Whisenhunt, D. W.; Neu, M. P.; Hou, Z.; Xu, J.; Hoffman, D. C.; Raymond, K. N. Specific Sequestering Agents for the Actinides. 29. Stability of the Thorium(IV) Complexes of Desferrioxamine B (DFO) and Three Octadentate Catecholate or Hydroxypyridinonate DFO Derivatives: DFOMTA, DFOCAMC, and DFO-1,2-HOPO. Comparative Stability of The. *Inorg. Chem.* **1996**, *35* (14), 4128–4136.

(34) Veeck, A. C.; White, D. J.; Whisenhunt, D. W.; Xu, J.; Gorden, A. E. V.; Romanovski, V.; Hoffman, D. C.; Raymond, K. N. Hydroxypyridinone Extraction Agents for Pu(IV). *Solvent Extr. Ion Exch.* **2004**, *22*, 1037–1068.

(35) Carrott, M. J.; Fox, O. D.; Maher, C. J.; Mason, C.; Taylor, R.; Sinkov, S. I.; Choppin, G. R. Solvent Extraction Behavior of Plutonium (IV) Ions in the Presence of Simple Hydroxamic Acids. *Solvent Extr. Ion Exch.* **2007**, *25* (6), 723–745.

(36) Taylor, R. J.; May, I.; Wallwork, A. L.; Denniss, I. S.; Hill, N. J.; Galkin, B. Y.; Zilberman, B. Y.; Fedorov, Y. S. The Applications of Formo- and Aceto-Hydroxamic Acids in Nuclear Fuel Reprocessing. *J. Alloys Compd.* **1998**, *271–273*, 534–537.

(37) Taylor, R. J.; May, I. The Reduction of Actinide Ions by Hydroxamic Acids. *Czechoslov. J. Phys.* **1999**, *49*, 617–621.

(38) White, D. L.; Durbin, P. W.; Jeung, N.; Raymond, K. N. Specific Sequestering Agents for the Actinides. 16. Synthesis and Initial Biological Testing of Polydentate Oxohydroxypyridinecarboxylate Ligands. *J. Med. Chem.* **1988**, *31* (1), 11–18.

(39) Carrott, M. J.; Fox, O. D.; LeGurun, G.; Jones, C. J.; Mason, C.; Taylor, R. J.; Andrieux, F. P. L.; Boxall, C. Oxidation-Reduction Reactions of Simple Hydroxamic Acids and Plutonium(IV) Ions in Nitric Acid. *Radiochim. Acta* **2008**, *96* (6), 333–343.

(40) Gorden, A. E. V.; Xu, J.; Szigethy, G.; Oliver, A.; Shun, D. K.; Raymond, K. N. Characterization of a Mixed Salt of 1-Hydroxypyridin-2-One Pu(IV) Complexes. *J. Am. Chem. Soc.* **2007**, *129* (21), 6674–6675.

(41) Moore, E. G.; Jocher, C. J.; Xu, J.; Werner, E. J.; Raymond, K. N. An Octadentate Luminescent Eu(III) 1,2-HOPO Chelate with Potent Aqueous Stability. *Inorg. Chem.* **2007**, *46* (14), 5468–5470.

(42) Huggard, A. J.; Warner, B. F. Investigations to Determine the Extent of Degradation of TBP/Oderless Kerosene Solvent in the New Separation Plant, Windscale. *Nucl. Sci. Eng.* **1963**, *17* (4), 638–650.

(43) Halliwell, B. Protection against Tissue Damage in Vivo by Desferrioxamine: What Is Its Mechanism of Action? *Free Radical Biol. Med.* **1989**, *7* (6), 645–651.

(44) Modell, B.; Letsky, E. A.; Flynn, D. M.; Peto, R.; Weatherall, D. J. Survival and Desferrioxamine in Thalassaemia Major. *Br. Med. J.* **1982**, *284* (6322), 1081–1084.

(45) Mclaren, G. D.; Muir, W. A.; Kellermeyer, R. W.; Jacobs, A. Iron Overload Disorders: Natural History, Pathogenesis, Diagnosis, and Therapy. *Crit. Rev. Clin. Lab. Sci.* **1983**, *19*

(3), 205–266.

(46) Liu, Z. D.; Hider, R. C. Design of Iron Chelators with Therapeutic Application. *Coord. Chem. Rev.* **2002**, *232* (1–2), 151–171.

(47) Maurer, P. J.; Miller, M. J. Microbial Iron Chelators: Total Synthesis of Aerobactin and Its Constituent Amino Acid, N6-Acetyl-N6-Hydroxylysine. *J. Am. Chem. Soc.* **1982**, *104* (11), 3096–3101.

(48) Maurer, P. J.; Miller, M. J. Total Synthesis of a Mycobactin: Mycobactin S2. *J. Am. Chem. Soc.* **1983**, *105* (2), 240–245.

(49) Neu, M. P.; Matonic, J. H.; Ruggiero, C. E.; Scott, B. L. Structural Characterization of a Plutonium(IV) Siderophore Complex: Single-Crystal Structure of Pu-Desferrioxamine E. *Angew. Chem., Int. Ed.* **2000**, *39* (8), 1442–1444.

(50) Nigrovic, V.; Catsch, A. Incorporation of Radionuclides. Comparative Investigation of Deferrioxamine B and Diethylenetriaminopentaacetic Acid. *Strahlentherapie* **1965**, *128* (2), 283–287.

(51) Keith-Roach, M. J.; Buratti, M. V.; Worsfold, P. J. Thorium Complexation by Hydroxamate Siderophores in Perturbed Multicomponent Systems Using Flow Injection Electrospray Ionization Mass Spectrometry. *Anal. Chem.* **2005**, *77* (22), 7335–7341.

(52) Boukhalfa, H.; Reilly, S. D.; Neu, M. P. Complexation of Pu(IV) with the Natural Siderophore Desferrioxamine B and the Redox Properties of Pu(IV)(Siderophore) Complexes. *Inorg. Chem.* **2007**, *46* (3), 1018–1026.

(53) Yoshida, I.; Murase, I.; Motekaitis, R. J.; Martell, A. E. New Multidentate Ligands. XXI. Synthesis, Proton, and Metal Ion Binding Affinities of N,N′,N″-Tris[2-(N-Hydroxycarbamoyl)Ethyl]-1,3,5-Benzenetricarboxamide (BAMTPH). *Can. J. Chem.*

1983, *61* (12), 2740–2744.

(54) Evers, A.; Hancock, R. D.; Martell, A. E.; Motekaitis, R. J. Metal Ion Recognition in Ligands with Negatively Charged Oxygen Donor Groups. Complexation of Fe(III), Ga(III), In(III), Al(III), and Other Highly Charged Metal Ions. *Inorg. Chem.* **1989**, *28* (11), 2189–2195.

(55) Jarvis, N. V.; Hancock, R. D. Some Correlations Involving the Stability of Complexes of Transuranium Metal Ions and Ligands with Negatively Charged Oxygen Donors. *Inorganica Chimica Acta*. 1991, pp 229–232.

(56) Motekaitis, R. J.; Murase, I.; Martell, A. E. New Multidentate Ligands XII: Chelating Tendencies of N,N'-Ethylenediaminediacetic-N,N'-Diacethydroxamic Acid. *J. Coord. Chem.* **1971**, *1*, 77–87.

(57) Koshti, N.; Huber, V.; Smith, P.; Gopalan, A. S. Design and Synthesis of Actinide Specific Chelators: Synthesis of New Cyclam Tetrahydroxamate (CYTROX) and Cyclam Tetraacetonylacetone (CYTAC) Chelators. *Tetrahedron* **1994**, *50* (9), 2657–2664.

(58) Rosenthal, M. W.; Lindenbaum, A. Effect of Deferrioxamine B Methanesulfonate on Removal of Plutonium in Vitro and in Vivo. In *Proceedings of the Society for Experimental Biology and Medicine*; New York, 1964; Vol. 117, pp 749–750.

(59) Boukhalfa, H.; Reilly, S. D.; Smith, W. H.; Neu, M. P. EDTA and Mixed-Ligand Complexes of Tetravalent and Trivalent Plutonium. *Inorg. Chem.* **2004**, *43* (19), 5816–5823.

(60) Petrie, G.; Locke, D.; Meloan, C. E. Hydroxamic Acid Chelate Ion Exchange Resin. *Anal. Chem.* **1965**, *37* (7), 919–920.

(61) Reddy, A. S.; Kumar, M. S.; Reddy, G. R. A Convenient Method for the Preparation of

Hydroxamic Acids. *Tetrahedron Lett.* **2000**, *41*, 6285–6288.

(62) Karlicek, R.; Majer, J. Neue Komplexane XXIII. Athylediamin-N,N,N',N'-Tetraacethydroxamsaure. *Collect. Czech. Chem. Commun.* **1972**, *37*, 805–818.

(63) Gopalan, A. S.; Huber, V. J.; Zincircioglu, O.; Smith, P. H. Novel Tetrahydroxamate Chelators for Actinide Complexation: Synthesis and Binding Studies. *J. Chem. Soc., Chem. Commun.* **1992**, No. 17, 1266–1268.

(64) Gopalan, A. S.; Zincircioglu, O.; Smith, P. Minimization and Remediation of DOE Nuclear Waste Problems Using High Selectivity Actinde Chelators. *Radioactive Waste Management and the Nuclear Fuel Cycle*. 1993, pp 161–175.

(65) Koshti, N. M.; Jacobs, H. K.; Martin, P. A.; Smith, P. H.; Gopalan, A. S. Convenient Method for the Preparation of Some Polyhydroxamic Acids: Michael Addition of Amines to Acrylohydroxamic Acid Derivatives. *Tetrahedron Lett.* **1994**, *35* (29), 5157–5160.

(66) Gaunt, M. J.; Yu, J.; Spencer, J. B. Rational Design of Benzyl-Type Protecting Groups Allows Sequential Deprotection of Hydroxyl Groups by Catalytic Hydrogenolysis. *J. Org. Chem.* **1998**, *63* (13), 4172–4173.

(67) Bowie, J. H.; Hearn, M. T. W.; Ward, A. D. Hydroxamic Acids: III. Mass Spectra of Substituted Hydroxamic Acids and Cyclic Imides. *Aust. J. Chem.* **1969**, *22* (1), 175–184.

(68) Kobashi, K.; Sakaguchi, K.; Takebe, S.; Hosaka, K. A Colorimetric Method for the Determination of Hydroxamic Acid by Iodine Oxidation. *Anal. Biochem.* **1985**, *146* (1), 7–12.

(69) Hietapelto, V.; Anttila, R.; Rizkalla, E.; Lajunen, L. H. J. Complexation Thermodynamics of Lanthanoid(III) with Ethylenediaminetetrapropionic Acid (EDTP). *J. Alloys Compd.* **1995**, *225* (1–2), 312–315.

(70) Lajunen, L. H. J.; Kokkonen, P.; Knuutt, H.; Jokisaari, J. The Complex Formation Equilibria of Ethylenediaminetetrapropionic Acid (EDTP) with Some Divalent Transition Metal Ions in Aqueous NaClO4 Solutions.Pdf. *Acta Chem. Scand.* **1989**, *43*, 2–5.

(71) Gridchin, S. N. The Step Dissociation Constants of Ethylenediamine-N,N′-Diacetic-N,N′-Dipropionic and Ethylenediamine-N,N,N′,N′-Tetrapropionic Acids. *Russ. J. Phys. Chem. A* **2009**, *83* (1), 41–44.

(72) Delany, J. M.; Lundeen, S. R. *The LLNL Thermochemical Database UCRL-21658*; United States, 1991.

(73) Santos, M. A.; Rodrigues, E.; Gaspar, M. A Cyclohexane-1,2-Diyldinitrilotetraacetate Tetrahydroxamate Derivative for Actinide Complexation: Synthesis and Complexation Studies. *Dalton Trans.* **2000**, 4398–4402.

(74) Martell, A. E.; Smith, R. M.; Motekaitis, R. J. NIST Critically Selected Stability Constants of Metal Complexes Database. *NIST Ref. Database* **2004**, *46*.

(75) Gans, P.; Sabatini, A.; Vacca, A. Investigation of Equilibria in Solution. Determination of Equilibrium Constants with the HYPERQUAD Suite of Programs. *Talanta* **1996**, *43* (10), 1739–1753.

(76) Gans, P.; O'Sullivan, B. GLEE, a New Computer Program for Glass Electrode Calibration. *Talanta* **2000**, *51* (1), 33–37.

CHAPTER FIVE

FUTURE DIRECTIONS

Future Directions

Each project discussed in this work has been left open for future possibilities. The azamacrocyclic ligands are in need of more rigidity in the backbone to increase binding capabilities of the uranyl ion. Now that the monomer synthesis for the inclusion of hydroxamates in cyclopeptoid backbones has been worked through, large, complex polyhydroxamate ligands can be synthesized for the coordination of the tetravalent actinides. Additionally, the inclusion of catechols in cyclopeptoid backbones has been shown to be possible. With optimization, polycatecholate ligands can also be synthesized this way. Finally, a very promising tetrahydroxamate ligand, EDTPHA was synthesized and studied with several Ln(III) metals by potentiometric titrations. These preliminary studies must be expanded on to fully determine the speciation of the system at varying pH. Additional titrations with larger metals, such as Th(IV) and Pu(IV) would allow for understanding of how the decadentate ligand may interact with metals of higher coordination numbers. The efficiency of this ligand in the separation of the *f*-elements could be studied through the determination of the distribution coefficients of various metals. For the best results, the full series of ligands, EDTAHA, EDTPHA, EDTBHA and EDTBnHA must be studied and compared to their corresponding carboxylates to determine the effects of the hydroxamate inclusion and binding pocket size changes.

I sincerely hope to see this work contribute to the future of the field of ligand design for the *f*-elements.

Appendix A

Macrocyclic ligand NMR Data

Data presented here is discussed in Chapter two.

Figure A.1. 1,2-ethanediylbis(oxy-2,1-ethanedyl) bis(4-methylbenzenesulfonate) (500 MHz, ^{1}H NMR, DMSO).

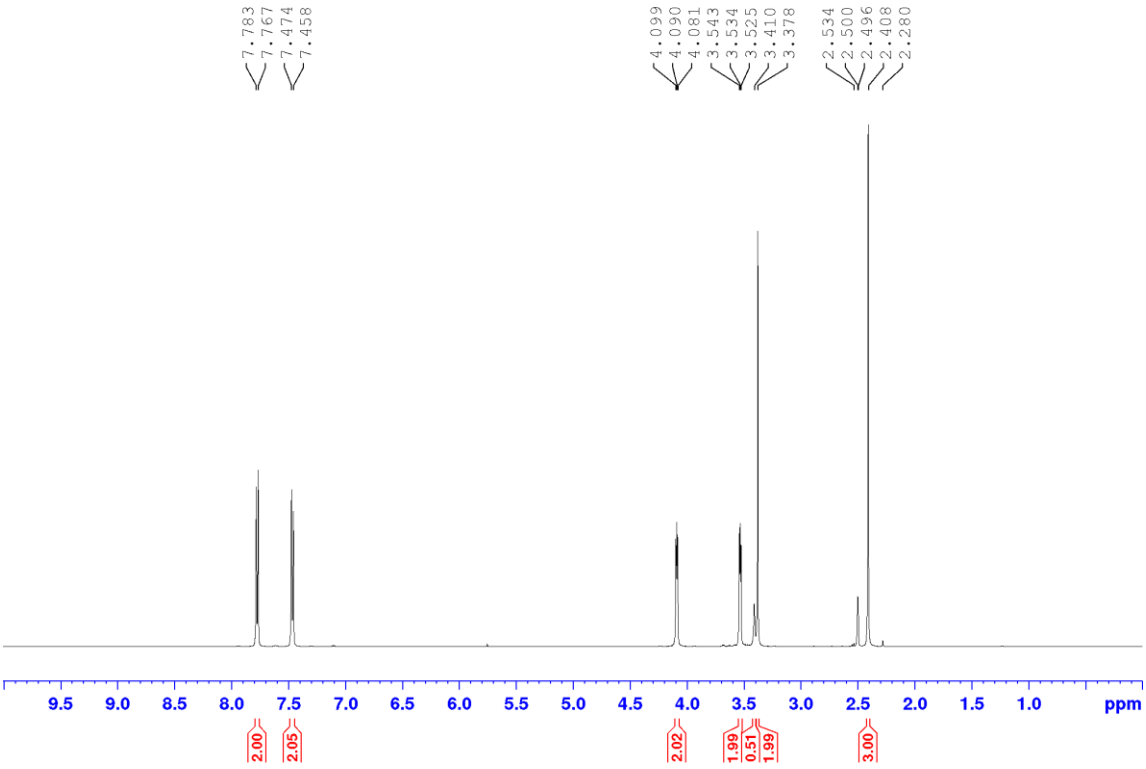

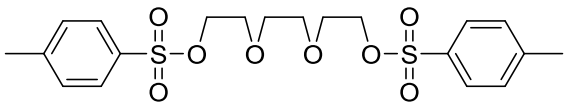

Figure A.2. 1,2-ethanediylbis(oxy-2,1-ethanedyl) bis(4-methylbenzenesulfonate) (500 MHz, ^{13}C NMR, DMSO).

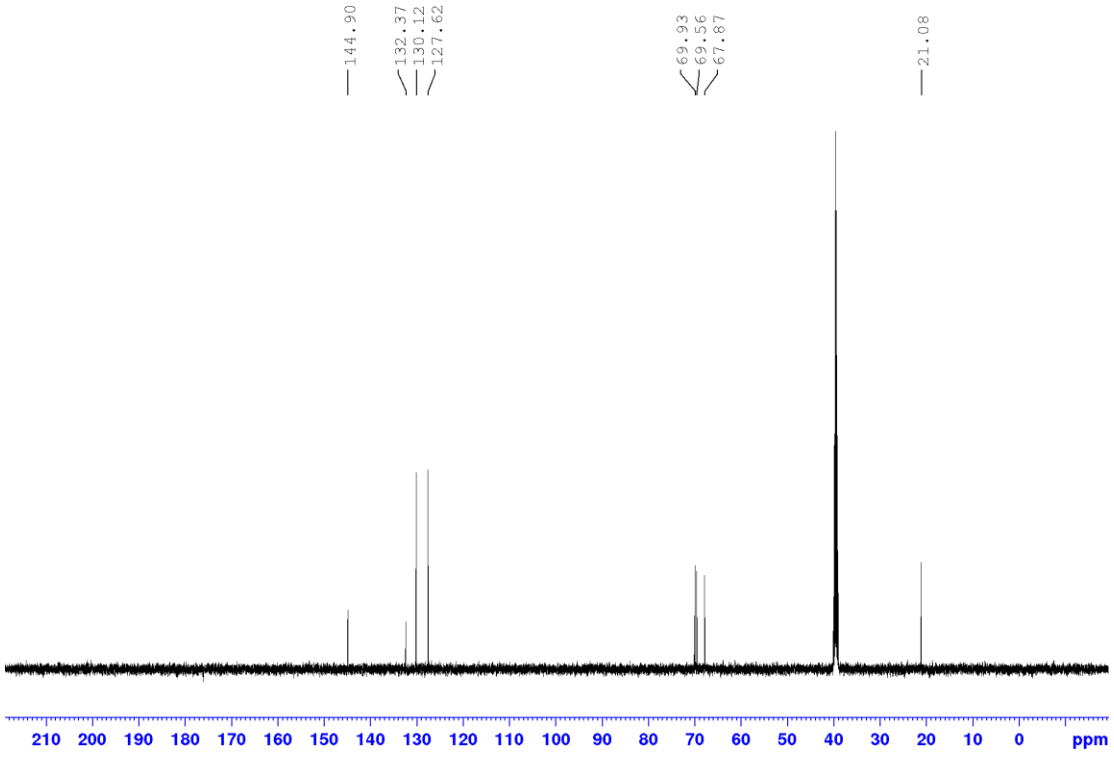

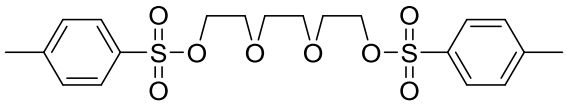

Figure A.3. 1,10-dibutane diamine-1,10-diaza-18-crown-6 (500 MHz, ^{1}H NMR, DMSO).

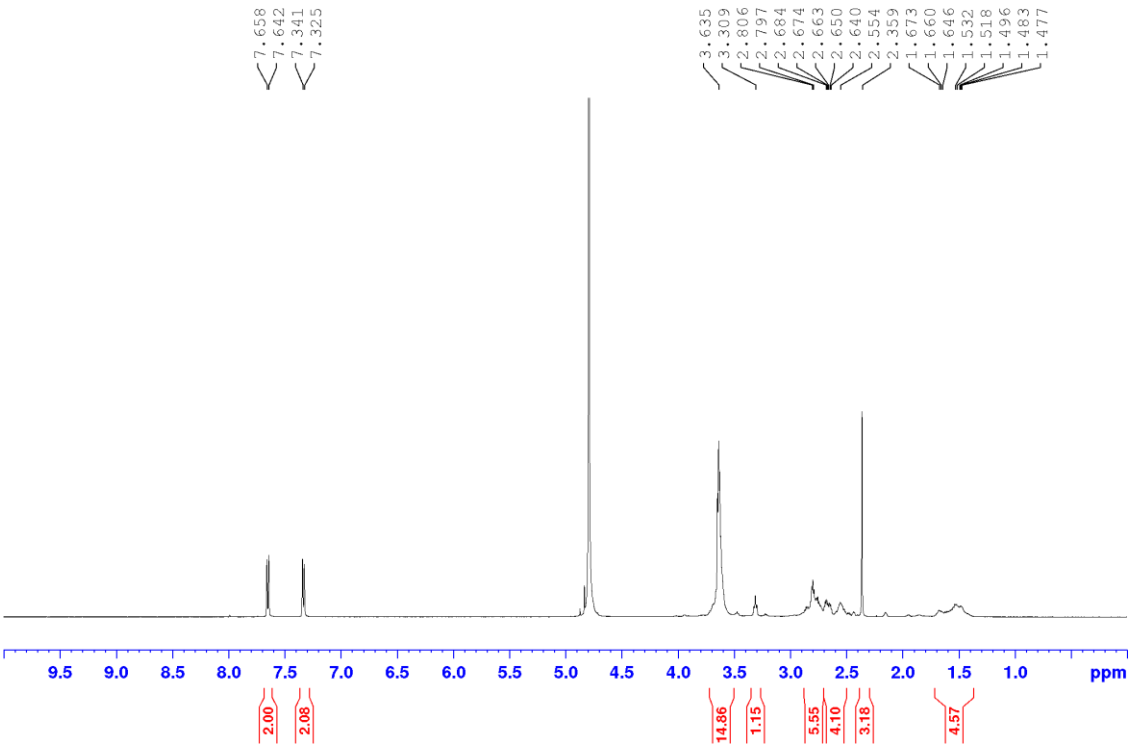

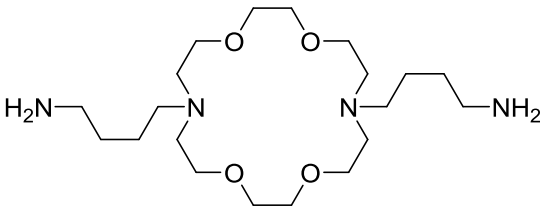

Figure A.4. 1,10-dibutane diamine-1,10-diaza-18-crown-6 (500 MHz, ^{1}H NMR, DMSO).

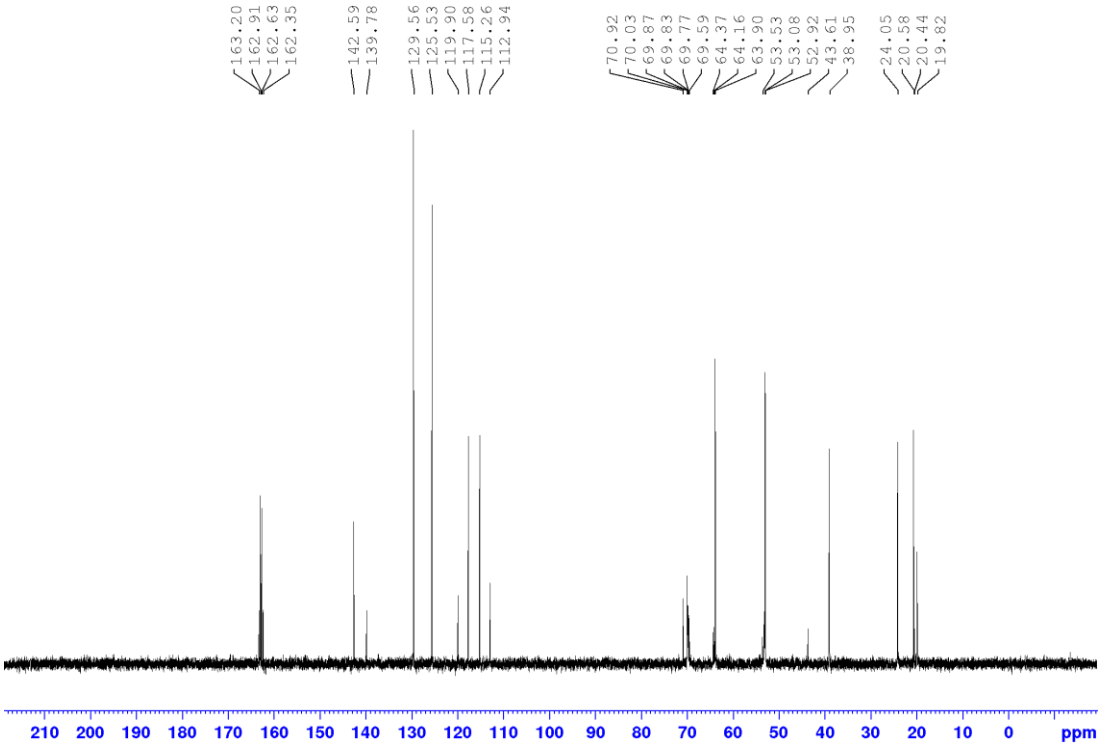

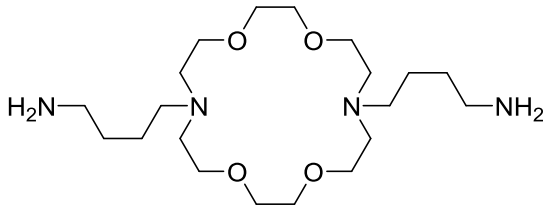

Appendix B

Cyclopeptoid monomer NMR data

Data presented here is discussed in Chapter three.

Figure B.1. Methyl 4-(aminomethyl)benzoate (500 MHz, ^{1}H NMR, D_2O).

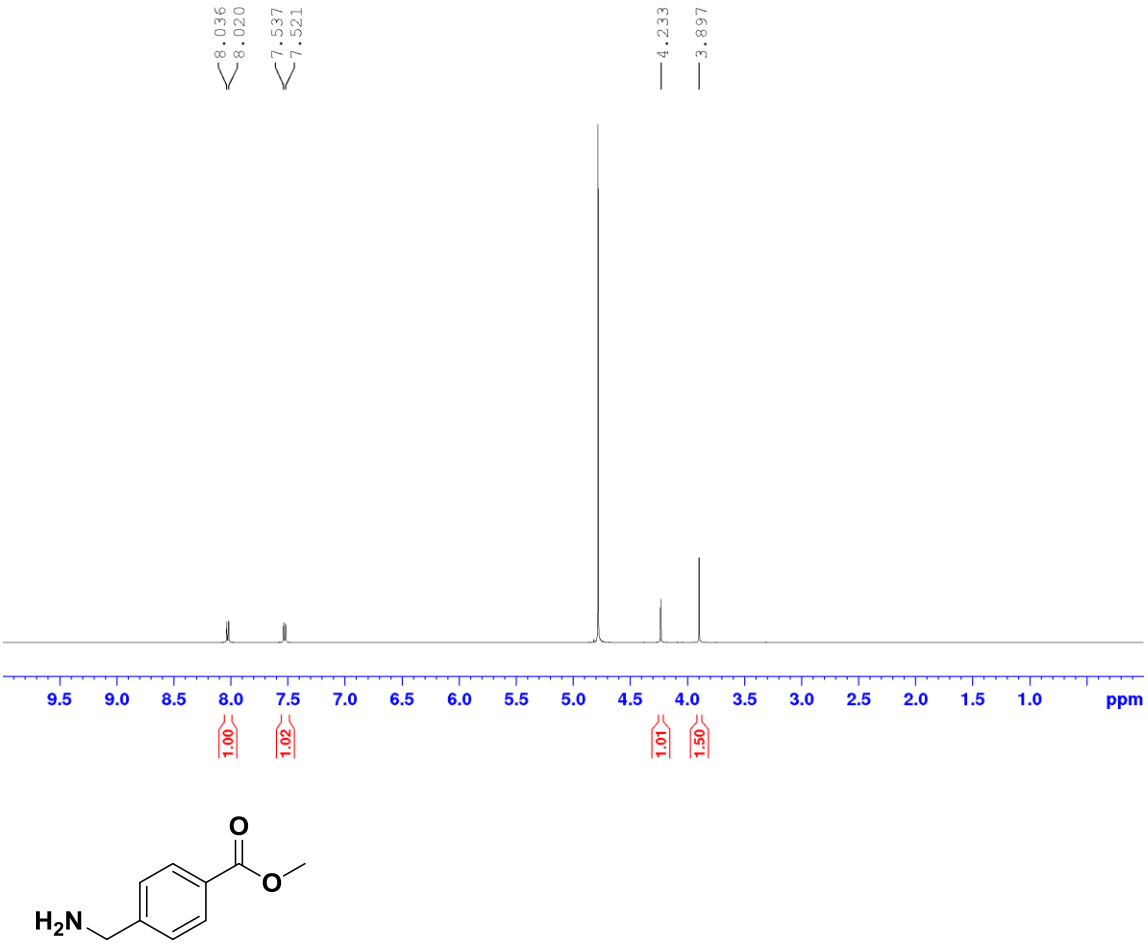

Figure B.2. Methyl 4-(aminomethyl)benzoate (500 MHz, ^{13}C NMR, D_2O).

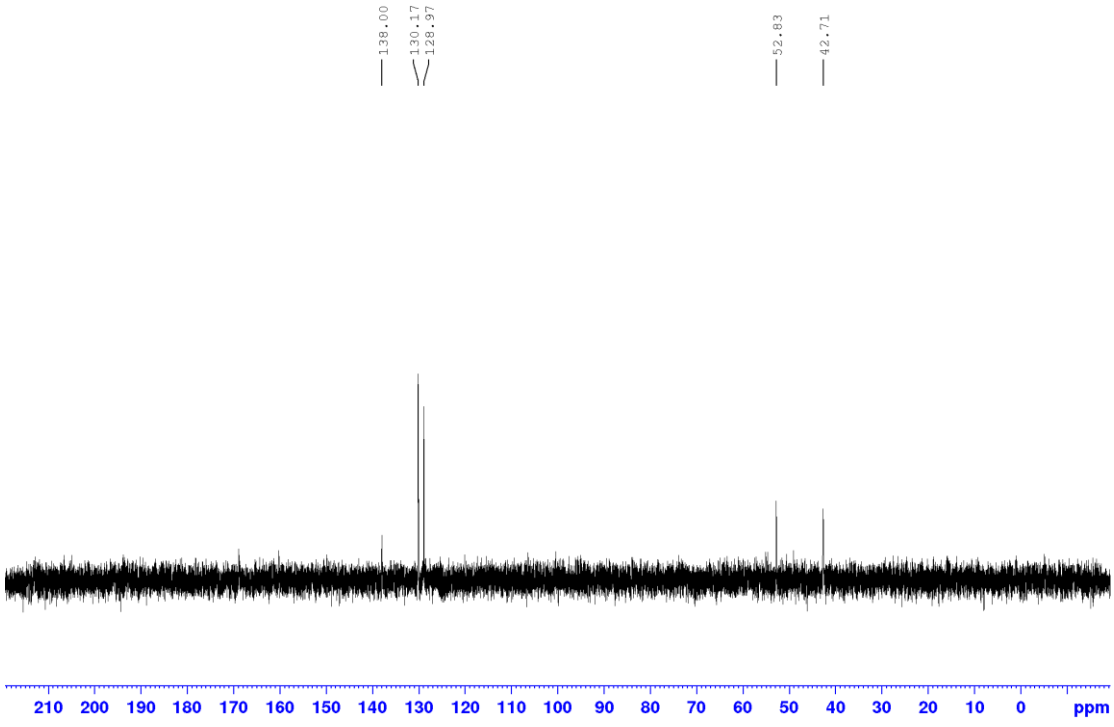

Figure B.3. Ethyl 4-(aminomethyl)benzoate (500 MHz, ^{1}H NMR, D_2O).

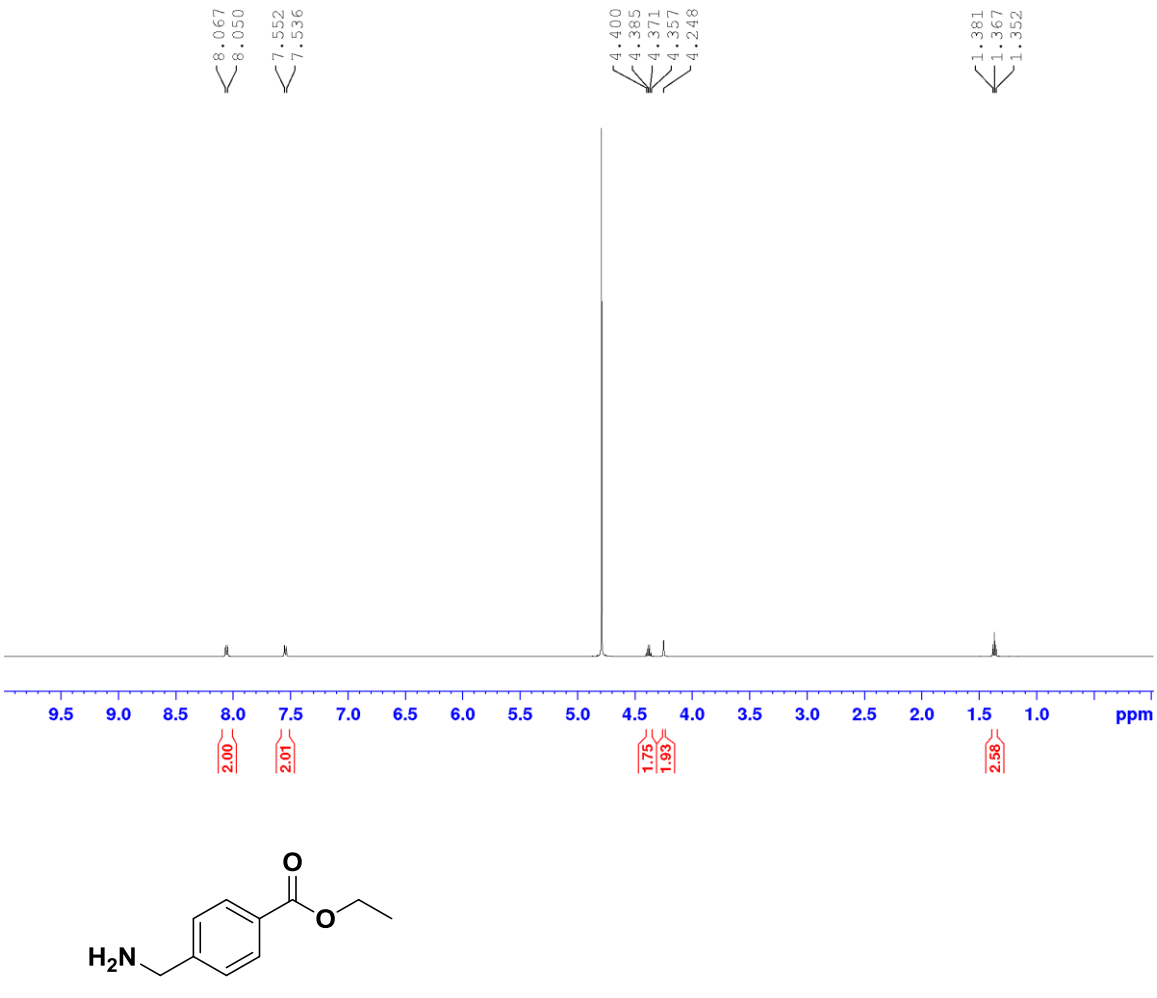

Figure B.4. NHS-activated 2,3-dihydroxybenzoic acid (500 MHz, ^{1}H NMR, DMSO).

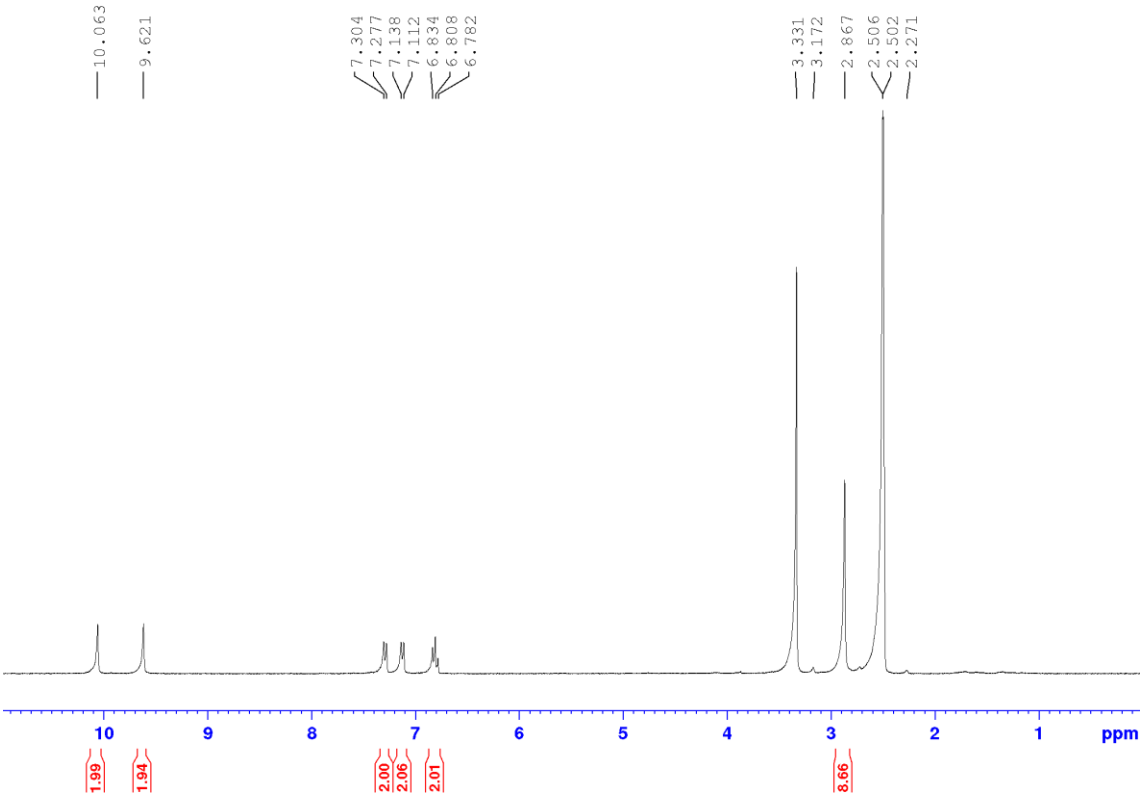

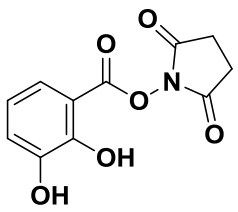

Figure B.5. Phthalimide-protected β-alanine (500 MHz, ^{1}H NMR, $CDCl_3$).

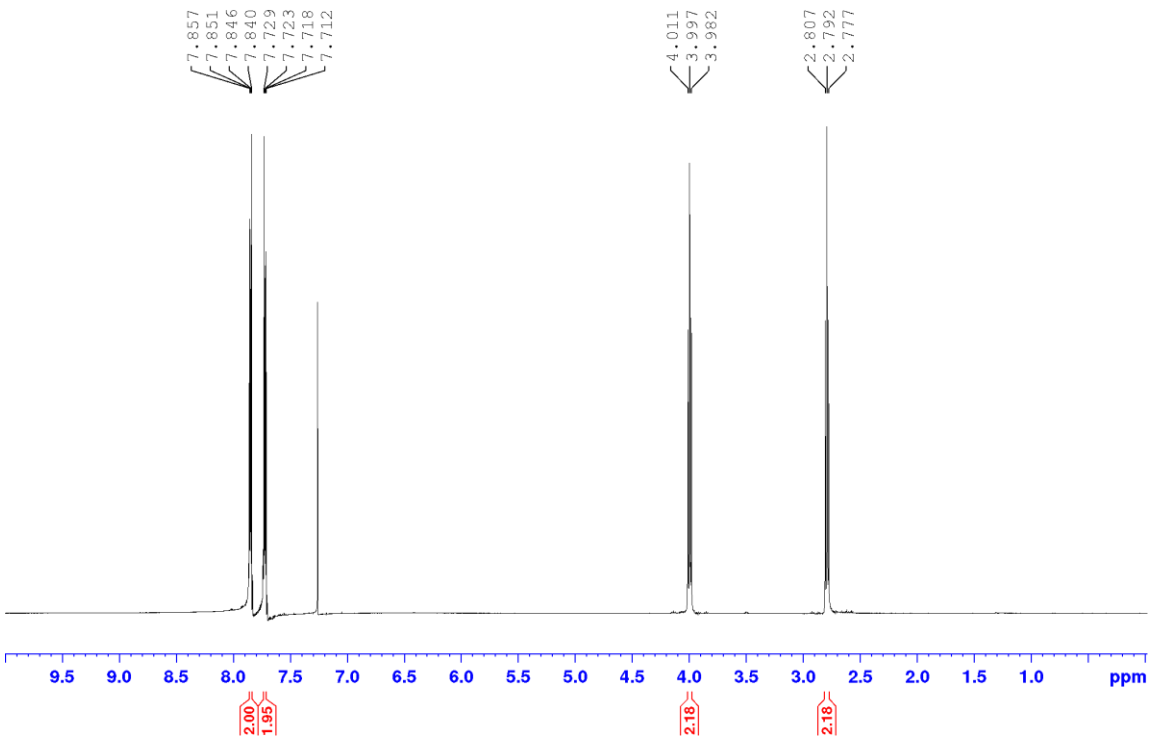

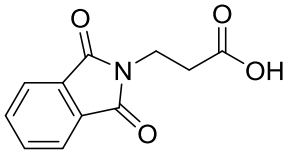

Figure B.6. Phthalimide-protected γ-GABA (500 MHz, ^{1}H NMR, $CDCl_3$).

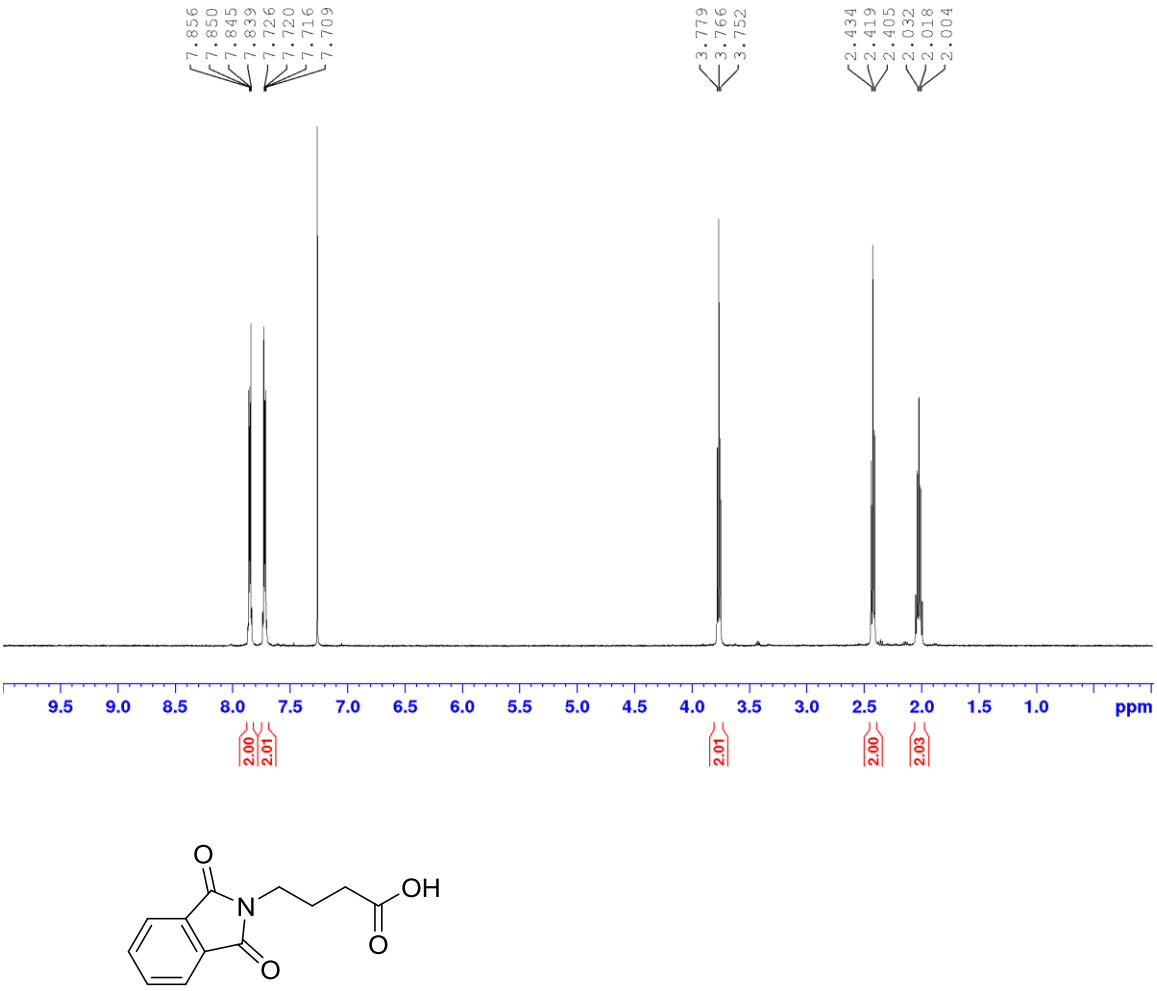

Appendix C

EDTA hydroxamate derivatives NMR data

Data presented here is discussed in Chapter four.

Figure C.1. Phth-NH-O-Bn-t-Bu (500 MHz, ^{1}H NMR, $CDCl_3$).

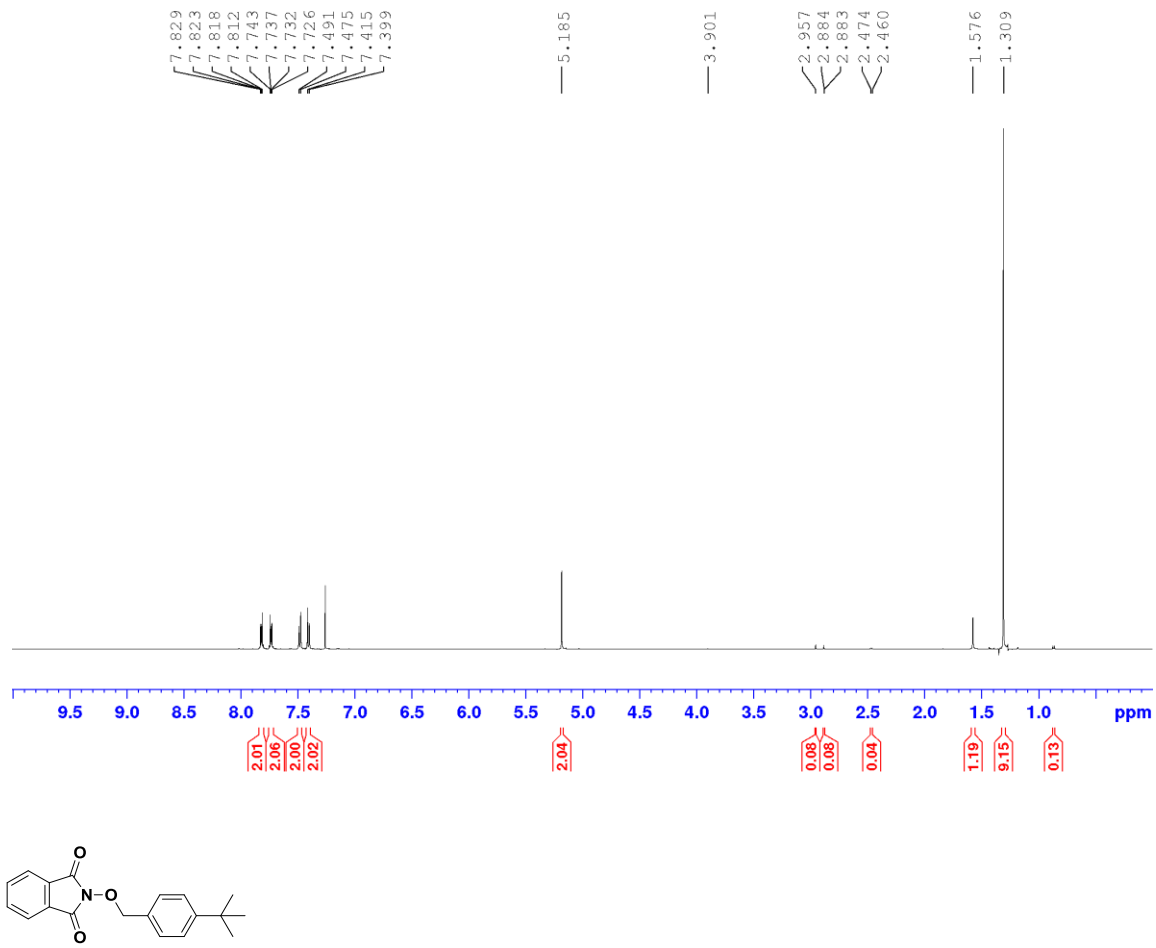

Figure C.2. Phth-NH-O-Bn-t-Bu (500 MHz, ^{13}C NMR, $CDCl_3$).

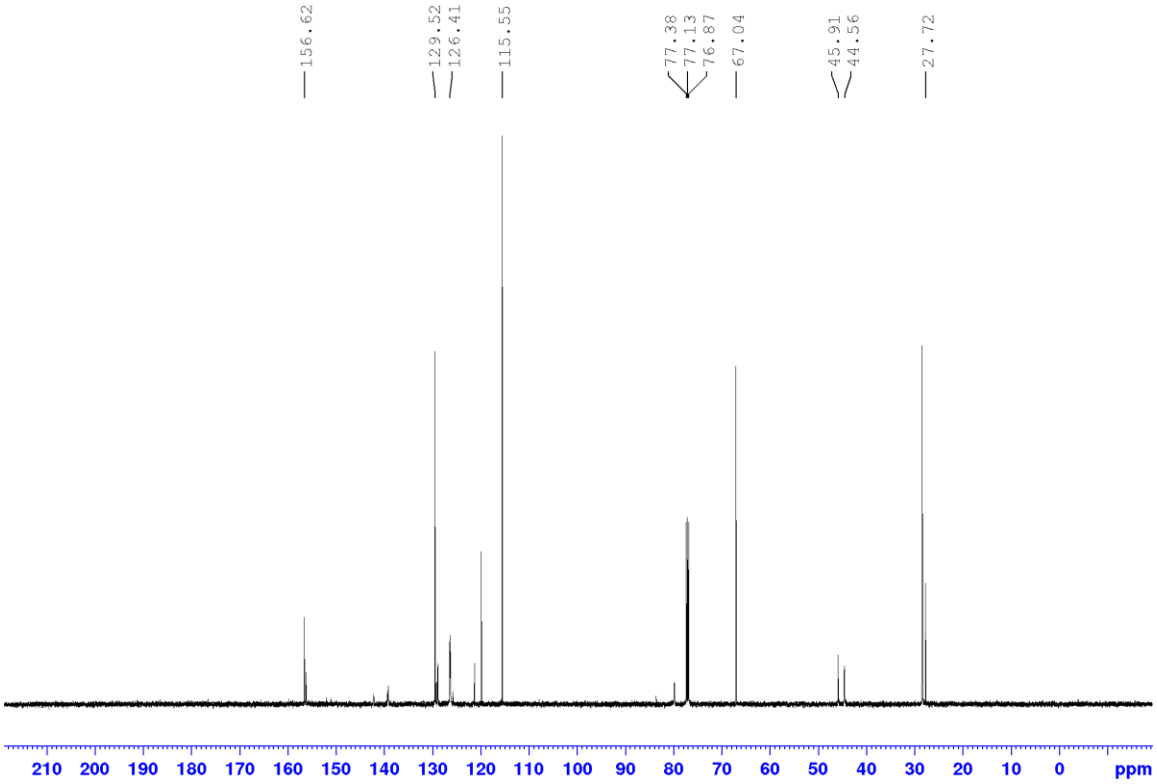

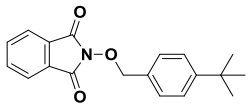

Figure C.3. *O*-tert-butylhydroxylamine (500 MHz, ^{1}H NMR, $CDCl_3$).

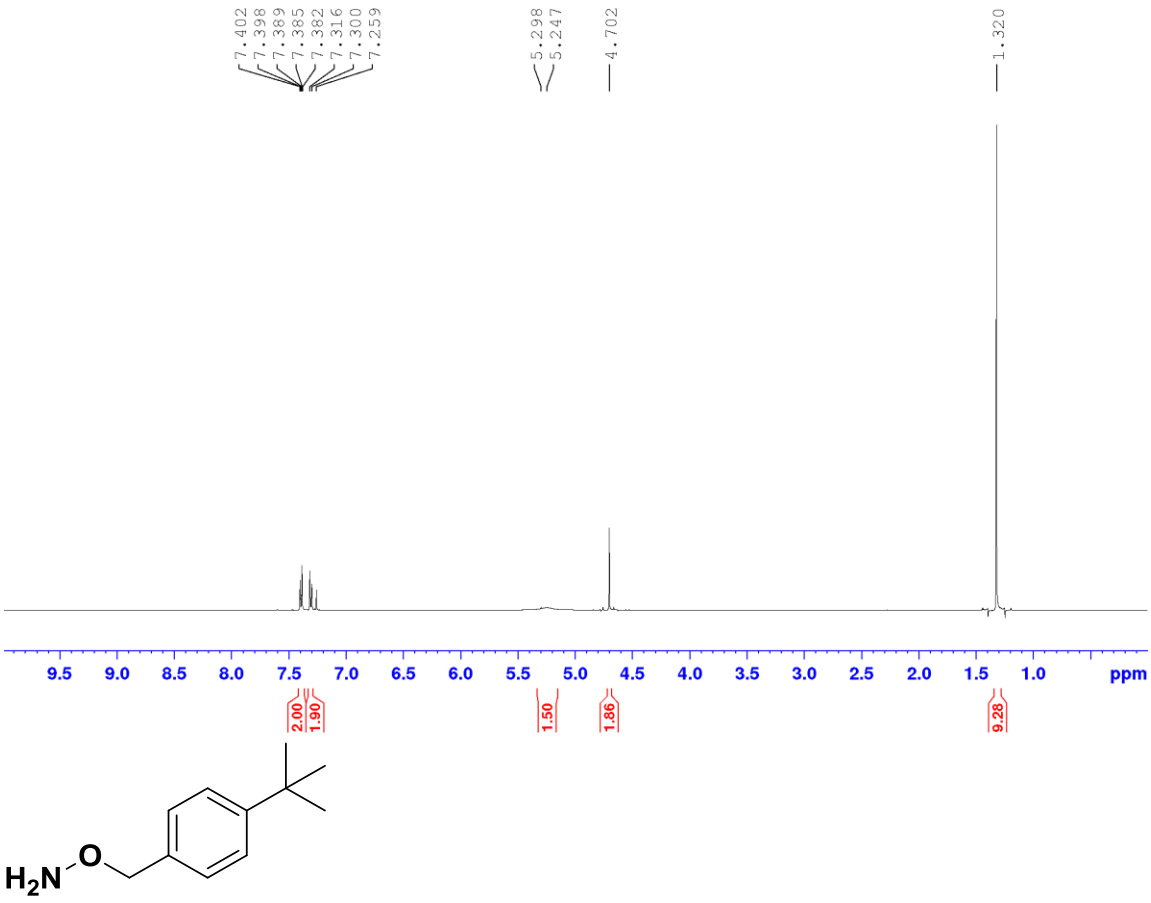

Figure C.4. *O*-tert-butylhydroxylamine (500 MHz, ^{13}C NMR, $CDCl_3$).

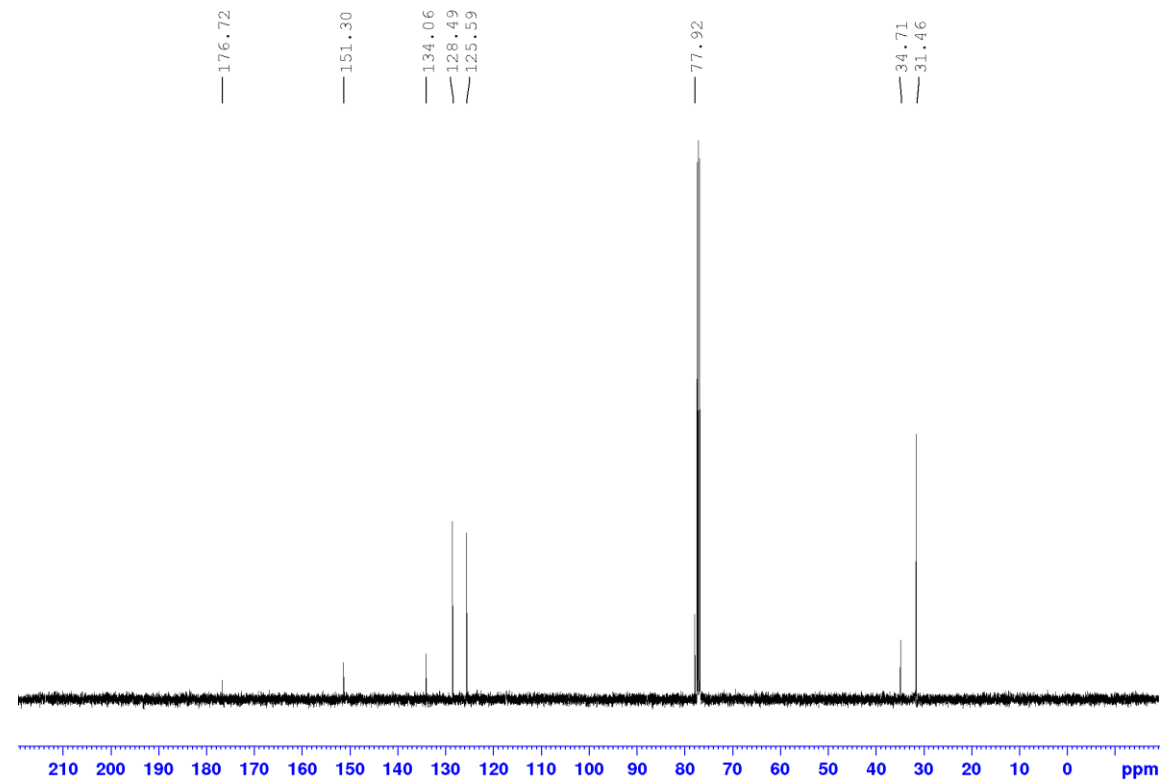

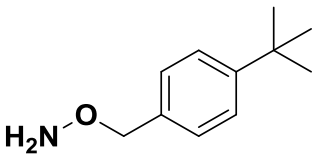

Figure C.5. EDTAHA arm (500 MHz, ^{1}H NMR, DMSO).

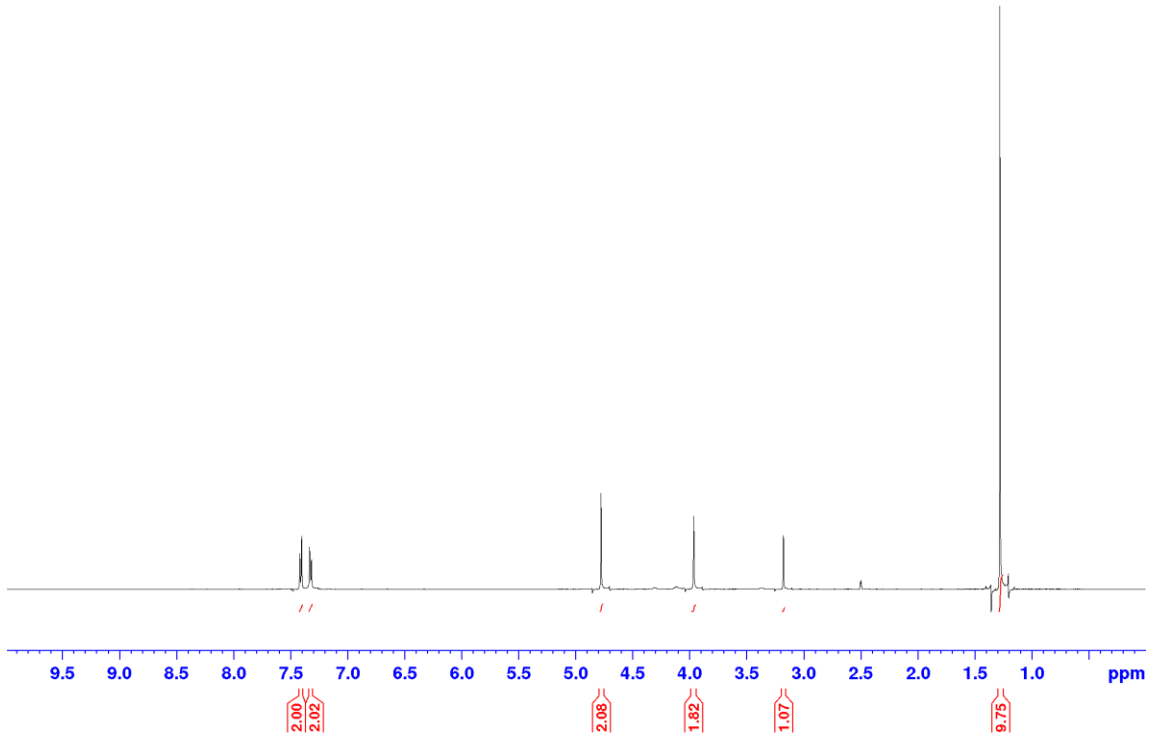

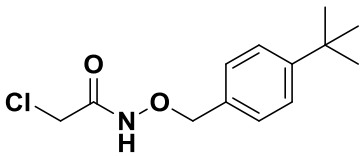

Figure C.6. EDTAHA arm (500 MHz, ^{13}C NMR, DMSO).

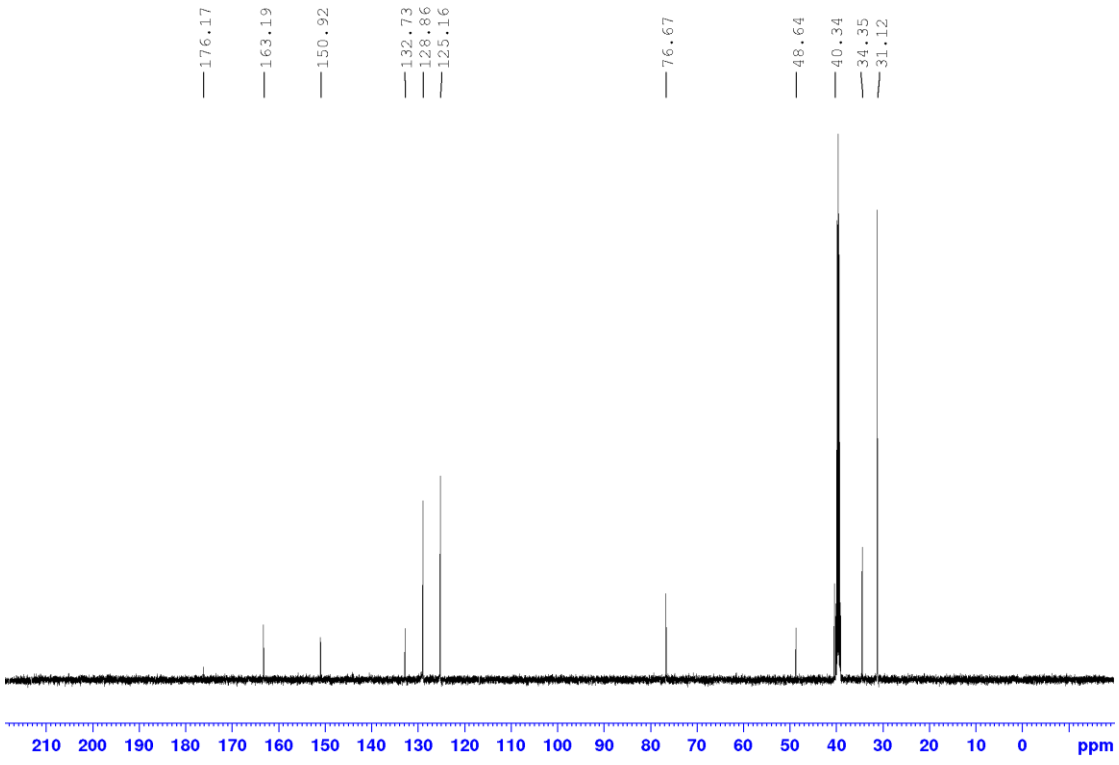

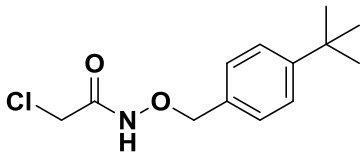

Figure C.7. EDTPHA arm (500 MHz, ^{1}H NMR, $CDCl_3$).

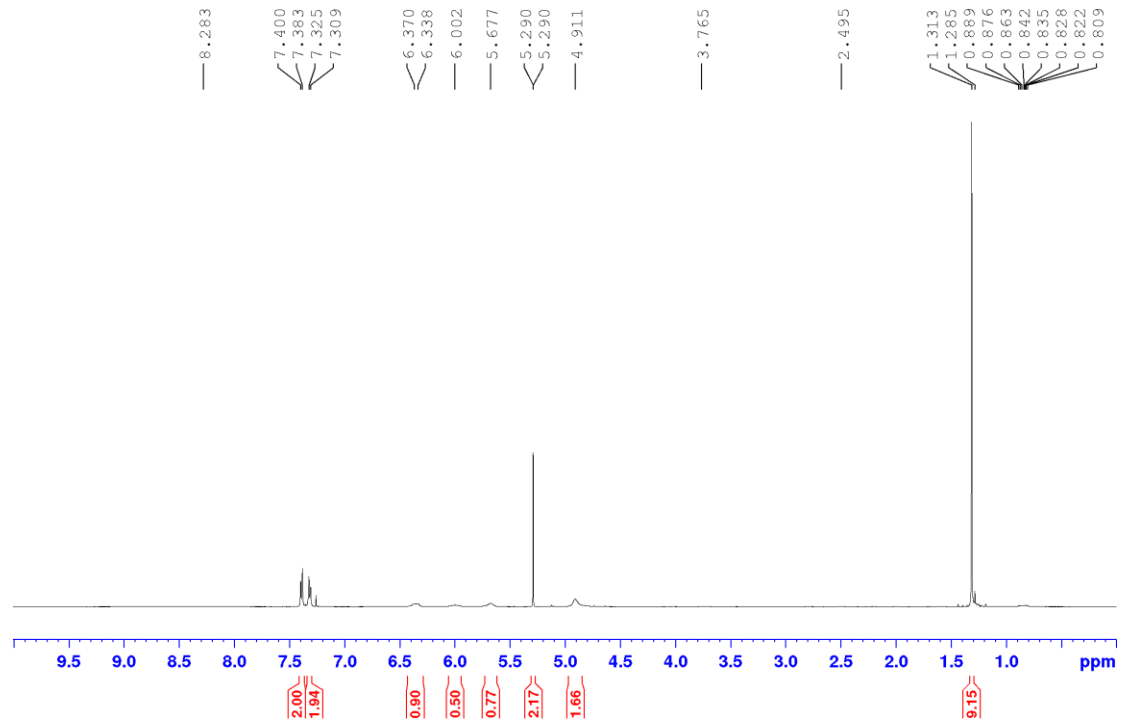

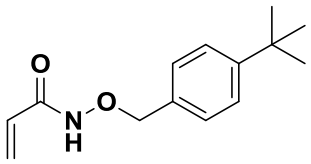

Figure C.8. EDTPHA arm (500 MHz, ^{13}C NMR, $CDCl_3$).

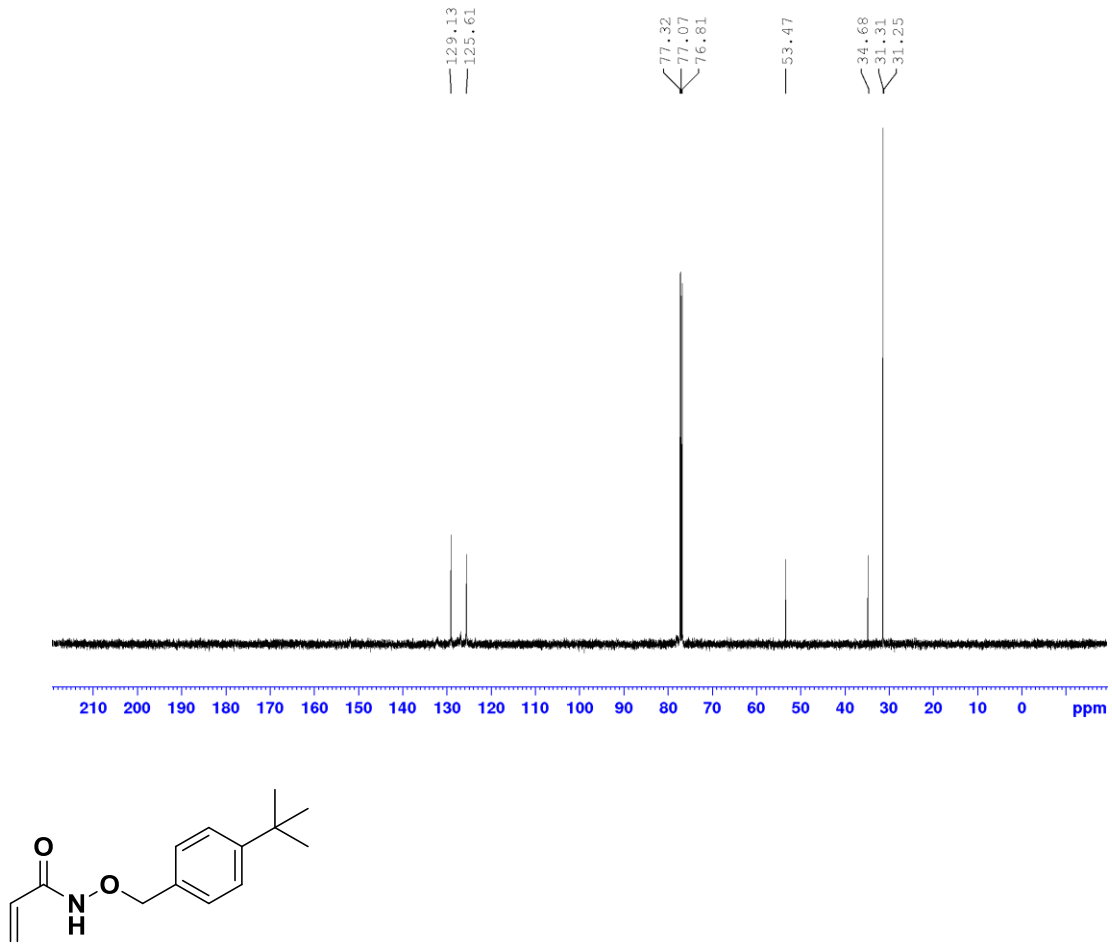

Figure C.9. EDTPHA, protected (500 MHz, ^{1}H NMR, DMSO).

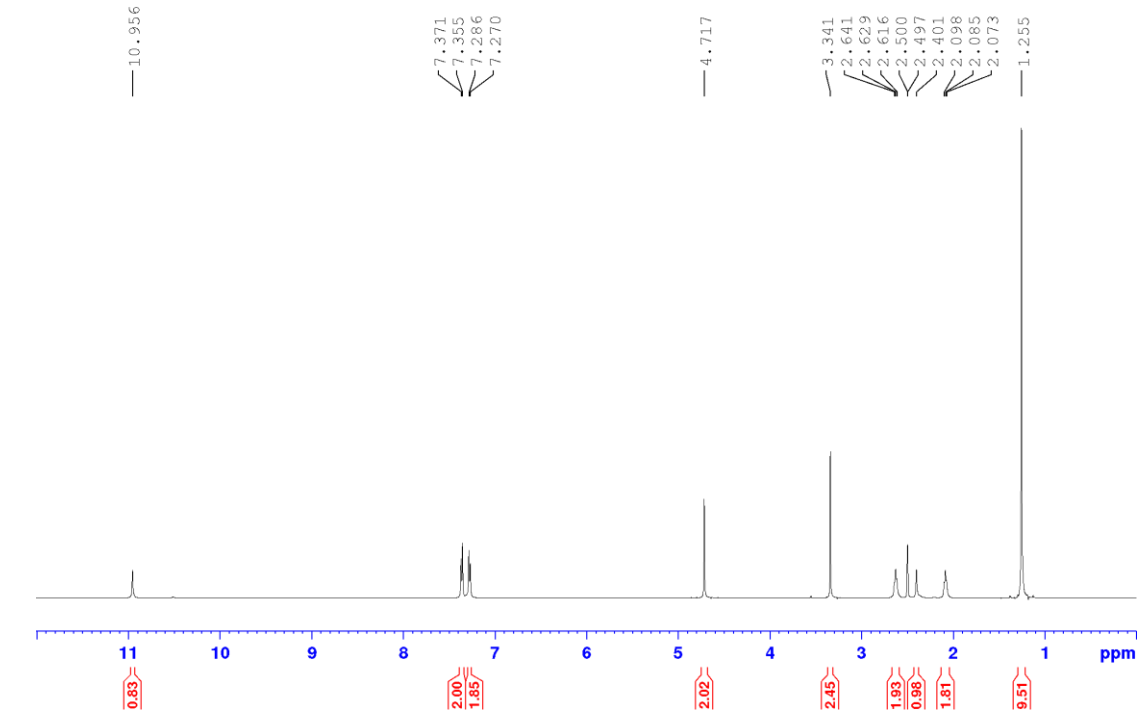

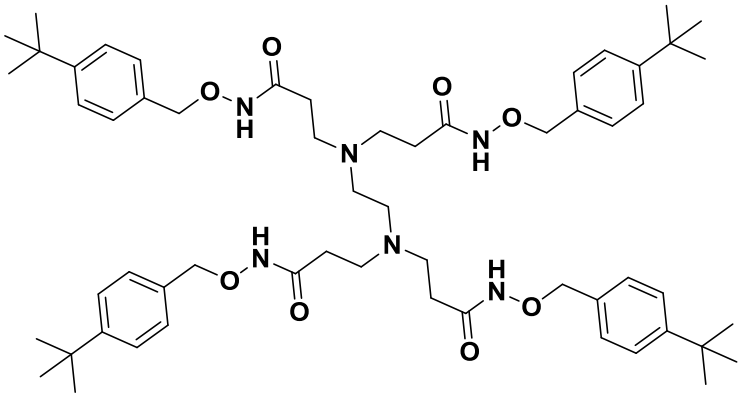

Figure C.10. EDTPHA, protected (500 MHz, ^{13}C NMR, DMSO).

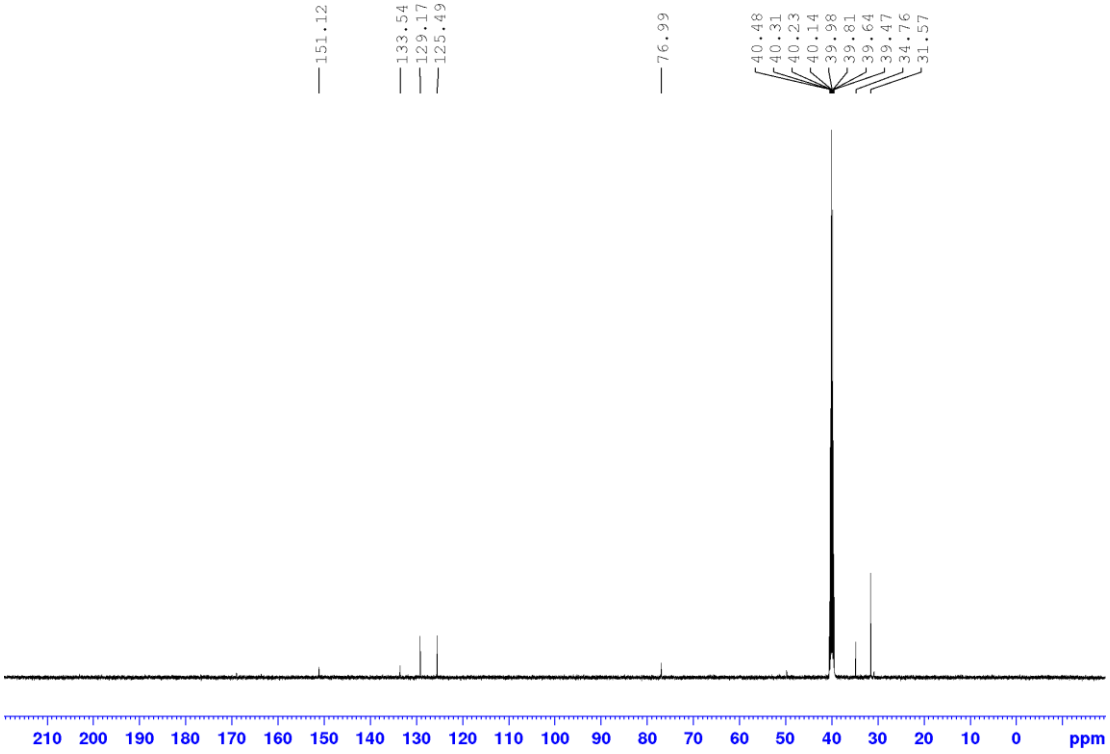

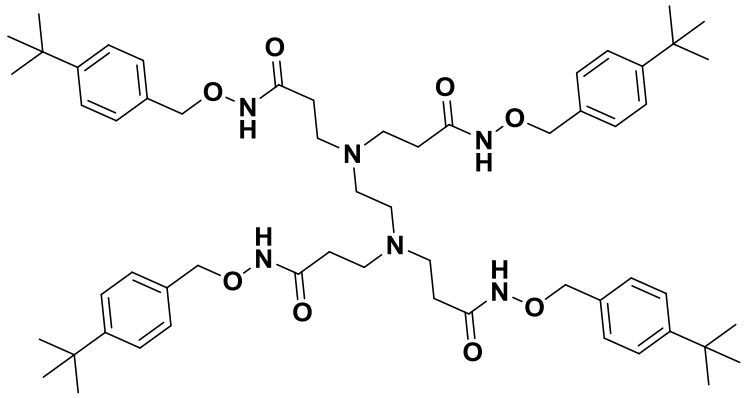

Figure C.11. EDTPHA, deprotecteed (500 MHz, ^{1}H NMR, D_2O)

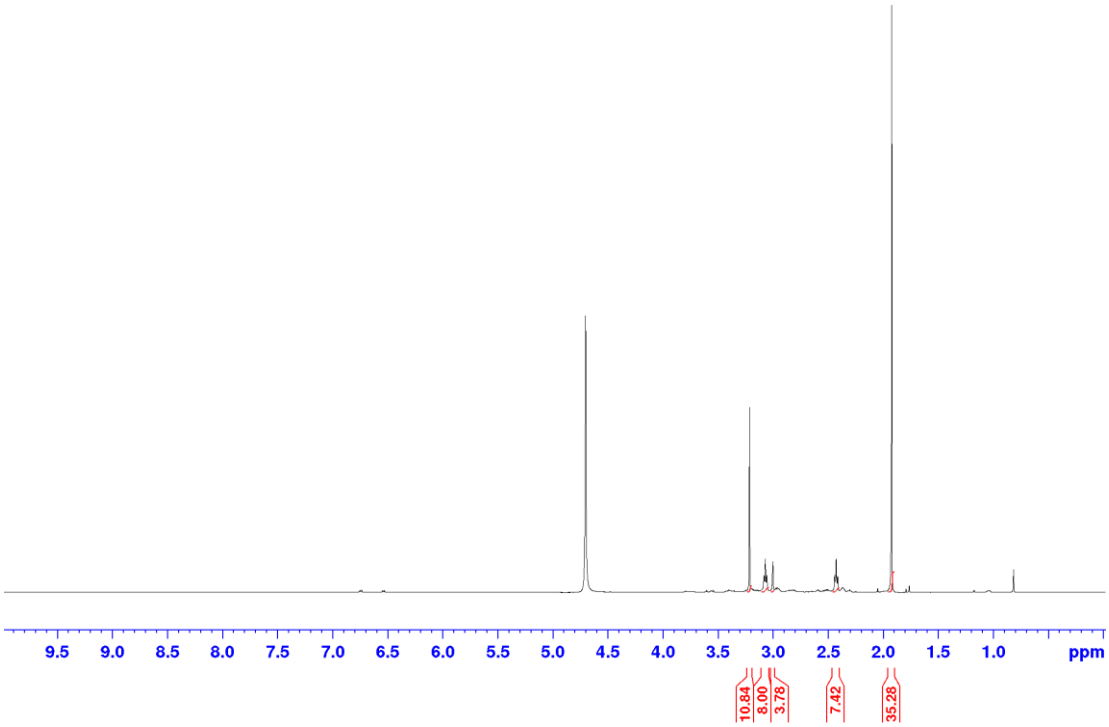

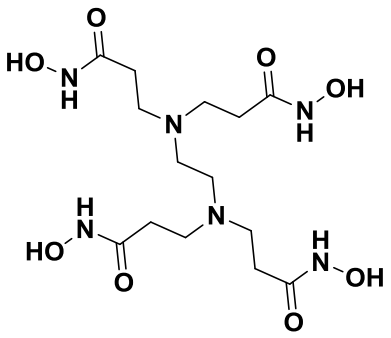

Figure C.12. EDTPHA, deprotected (500 MHz, ^{1}H NMR, D_2O).

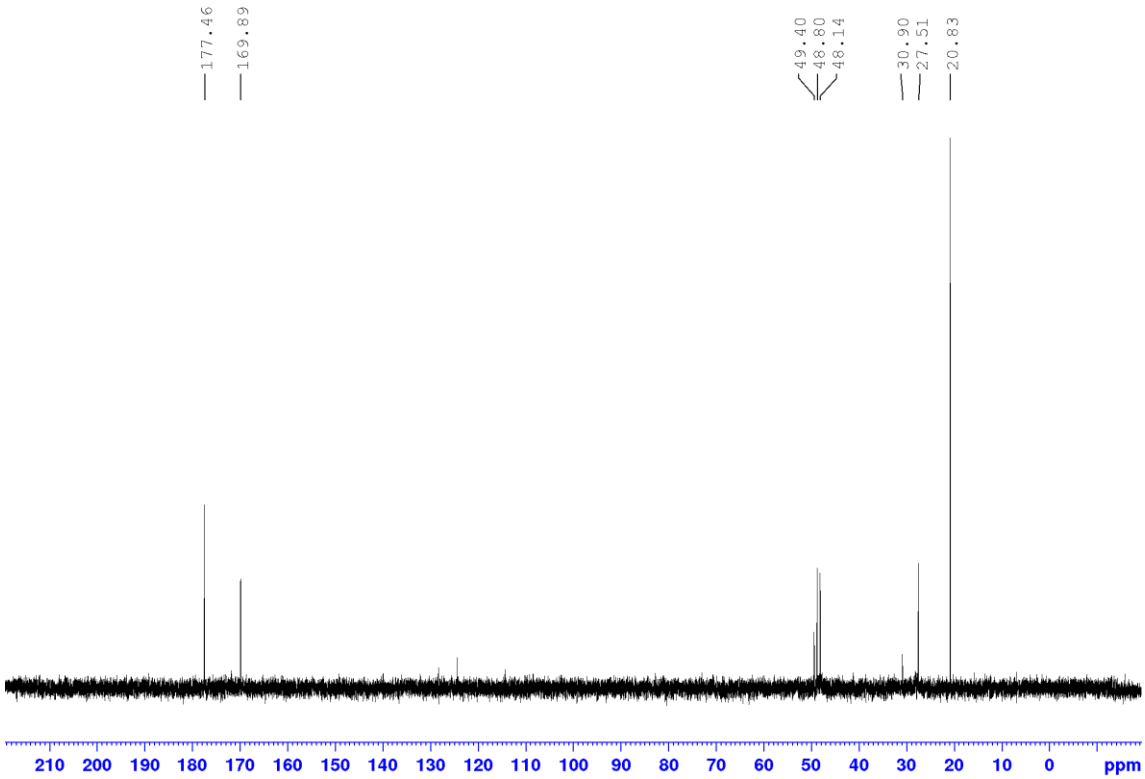

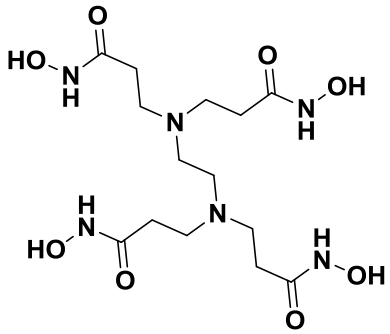

Figure C.13. EDTBHA arm (500 MHz, ^{1}H NMR, DMSO)

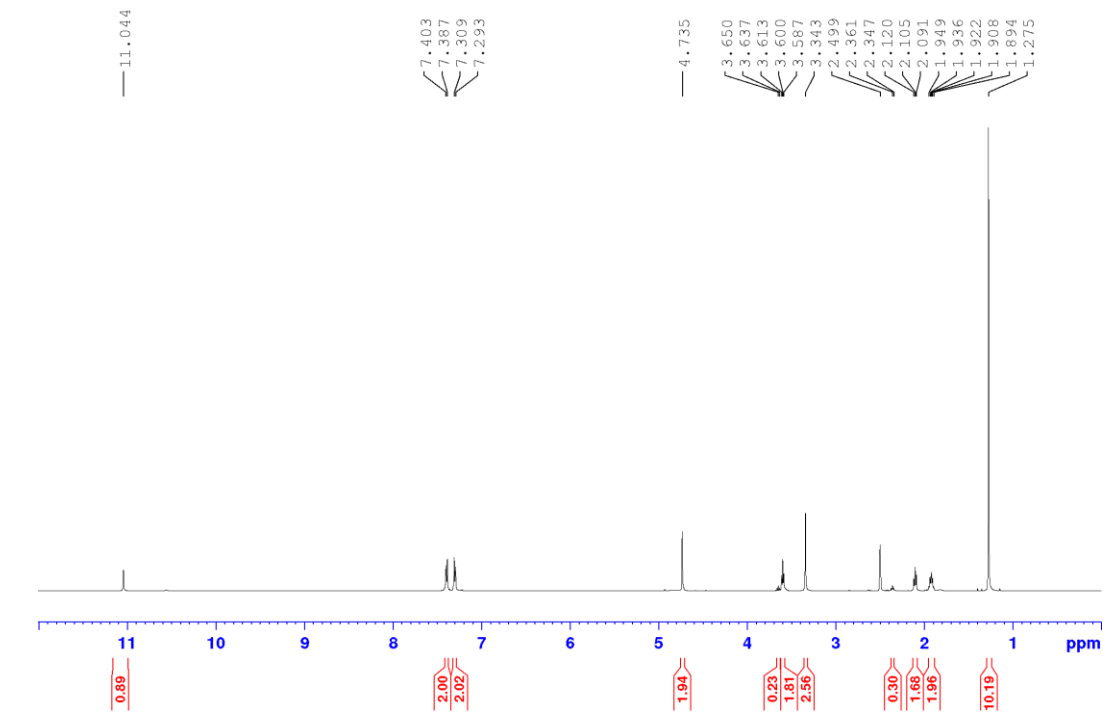

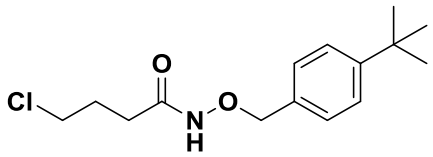

Figure C.14. EDTBnHA arm (500 MHz, ^{1}H NMR, DMSO).

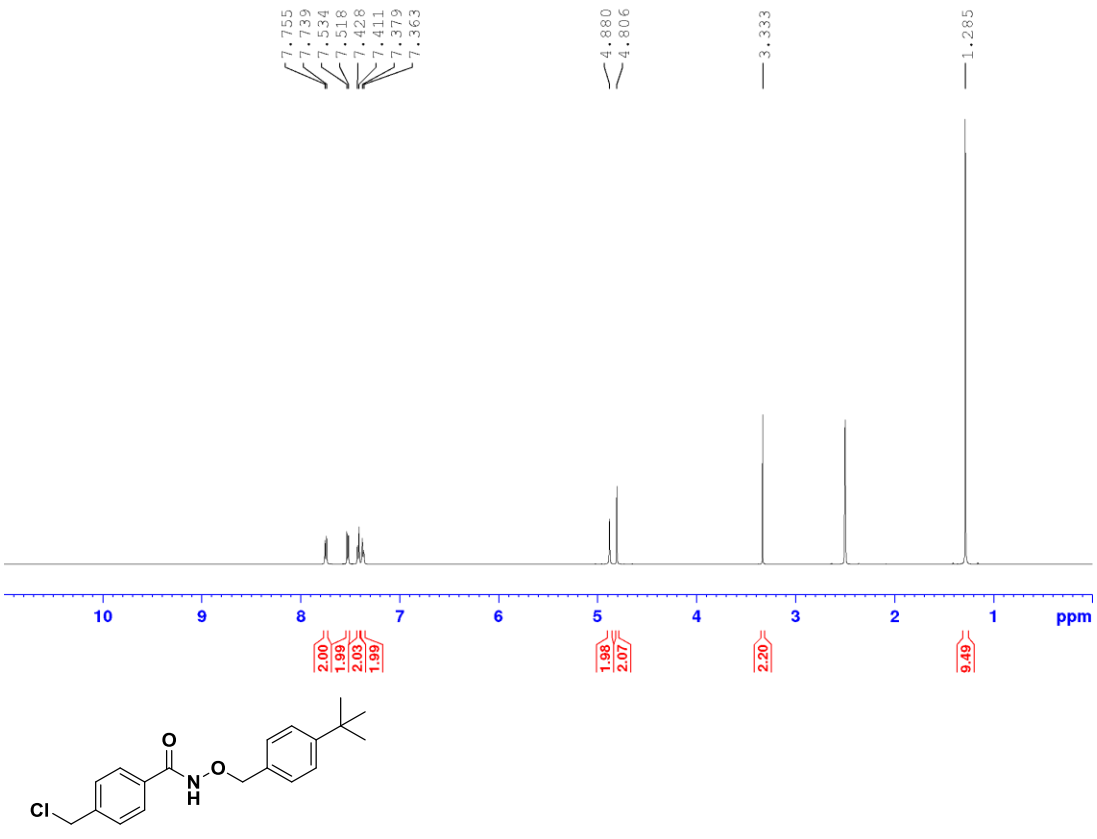

Figure C.15. EDTBnHA arm (500 MHz, ^{13}C NMR, DMSO).

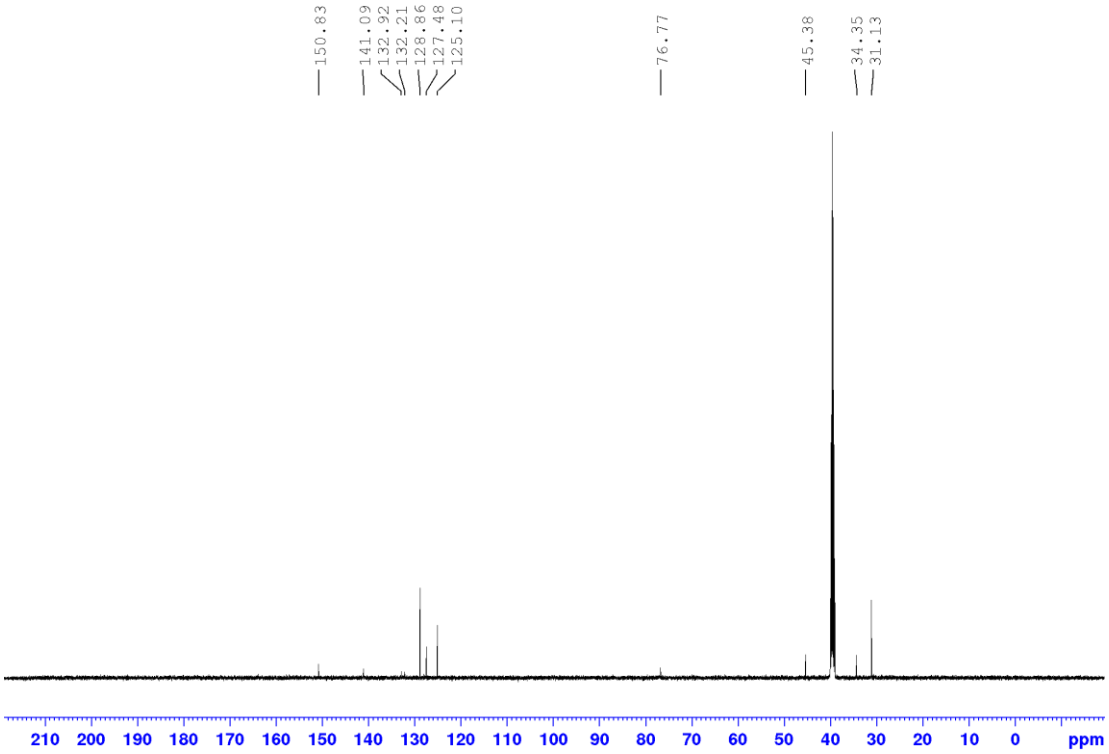

Figure C.16. EDTBnHA, protected (500 MHz, ^{1}H NMR, $CDCl_3$).

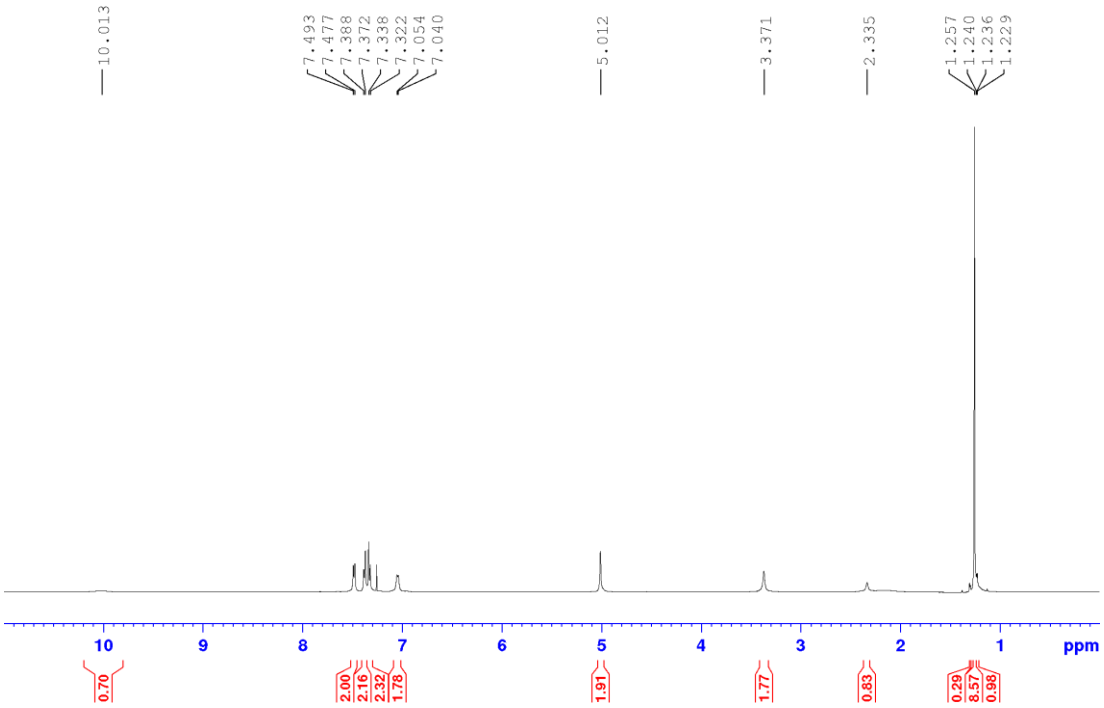

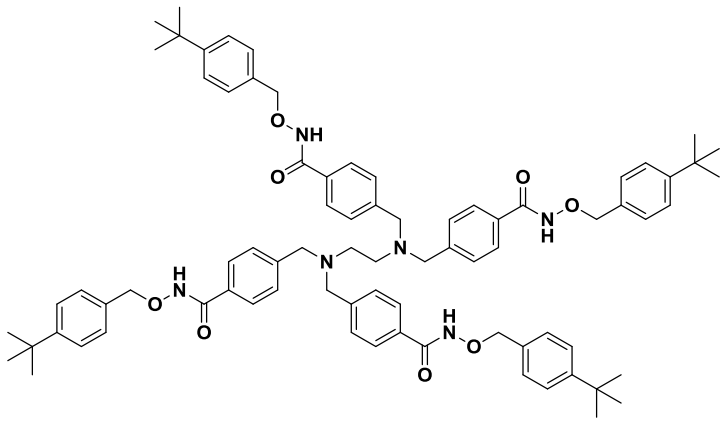

Figure C.17. EDTBnHA, protected (500 MHz, ^{13}C NMR, $CDCl_3$).